



University  
of Glasgow

Scott, Elizabeth Stephanie (2015) *Derivation of vascular endothelium from human embryonic stem cells: the roles of microRNAs in endothelial differentiation and commitment*. PhD thesis.

<http://theses.gla.ac.uk/6979/>

Copyright and moral rights for this thesis are retained by the author

A copy can be downloaded for personal non-commercial research or study

This thesis cannot be reproduced or quoted extensively from without first obtaining permission in writing from the Author

The content must not be changed in any way or sold commercially in any format or medium without the formal permission of the Author

When referring to this work, full bibliographic details including the author, title, awarding institution and date of the thesis must be given

# Derivation of vascular endothelium from human embryonic stem cells: the role of microRNAs in endothelial differentiation and commitment

Elizabeth Stephanie Scott  
BSc (Hons)

Submitted in the fulfilment of the requirements of  
the degree of Doctor of Philosophy in the College of  
Medical Veterinary and Life Sciences, University of  
Glasgow.

Institute of Cardiovascular and Medical Sciences,  
College of Medical, Veterinary and Life Sciences,  
University of Glasgow.



September 2015

© E.S. Scott 2015

## Authors Declaration

I declare that this thesis has been entirely written by myself and is a record of work performed by myself with the exception of qRT-PCR analysis of miR-143/145 expression after lentiviral modulation, which was performed by Dr Krishna Yalla. Triple transfection preparation of lenti-miR-483 was performed by Nicola Britton and the image of d7 RC9b cells during hematopoietic differentiation was provided by Alison Condie. The miRNA microarray screen was performed in collaboration with Dr David Mallinson at Sitemic Ltd., and analysis of results was performed with the aid of Dr Donald Dunbar. This thesis has not previously been submitted for a higher degree. This research was carried out at the Institute of Cardiovascular and Medical Sciences, University of Glasgow under the supervision of Professor Andrew H. Baker, Dr Joanne Mountford and Professor Graeme Milligan.

Elizabeth Scott

September 2015

## Acknowledgements

First and foremost, I would like to thank my supervisors Professor Andrew H Baker, Dr Joanne Mountford and Professor Graeme Milligan for all of the support, guidance and advice they have provided throughout my studies. In particular to Professor Baker for all of the opportunities which have been afforded to me during the last four years, and to Dr Mountford for all of her expertise and advice in terms of the stem cell culture and differentiation systems, without which many of the experiments would not have been possible.

Additionally, I would like to thank Sitemic Ltd. for allowing me to perform the miRNA microarray screen. In particular, thank you to Dr David Mallinson for his advice and assistance in the experimental design and running of the microarray, and to Dr Donald Dunbar for his assistance in the data analysis.

A massive thanks must go to everyone in the Baker group and on Level 4 of the BHF GCRC, in particular Nicola Britton for teaching me basic tissue culture skills and so many other techniques, Gregor Aitchison for all of his technical support (and banter!), Dr Raquel Garcia for helping with all my cloning and lentiviruses, Dr Laura Denby for providing four years of continuous support both in and out of the lab, Dr John Mercer for 3pm tea, Dr Ruth Mackenzie for being my work big sister and Wendy Beattie for educating me in many things non-lab related. A special thank you to Dr Peter Burton, who guided me through the first two years of my PhD, taught me everything he knew about hESC culture, and provided me with many a laugh and intellectual debate in TC.

I'd also like to thank all members of the Mountford group, Alison, Ange, Nik/Dave, John, Lamin, Emmanuel, Elaine, and Niove. Thanks for providing me with all the cells, reagents, advice, chat, cakes, chocolate and great reaction times, never again will I fall victim to 'two for flinching'. In particular, I'd like to thank Dr Scott Cowan, not only for his help with all things stem cell and flow cytometry related, but also for being my provider of coffees/beers/cups of tea/cereal bars/cakes, an amazing Olympics watching partner (still the best Saturday morning media changing session ever) and, most importantly, a great friend.

To all of the girls I've met during the last 4 years, Hollie, Clare, Jenny, Lesley, Caroline and Lisa, thanks for making me laugh every single day - even the ones when I was mainly crying - and for providing me with so many memories I know I will never forget. A special thanks to two people - Hannah Stepto and Josie Van Kralingen. Firstly to Hannah (the other half of my Liz and Hannah), thanks for being there every day from the very first. Your jokes and laughter have kept me coming to work even during the stressful times, and I know I've made a true friend for life. And to Josie, thanks for being an amazing friend and sometimes counsellor, letting me distract you from work with chat and always being available for a cup of tea and a piece of cake.

Thanks to my family, in particular my Mum, Dad and Brother Alex, who have always been there for me, kept me sane during all of the stressful times and reminded me that there is a life outside of science. Last but not least, thanks to Mikey. Thanks for listening to hours upon hours of practice presentations (even when you point out my misaligned graphs!), offering words of encouragement, and providing me with so much laughter. Without your love and support I definitely would not have made it this far.

## Table of Contents

Authors Declaration .....	2
Acknowledgements.....	3
List of Tables.....	9
List of Figures .....	10
List of Publications, Presentations and Awards .....	12
Summary .....	13
Abbreviations .....	16
Chapter 1 Introduction .....	24
1.1 Cardiovascular disease.....	25
1.2 Ischemic diseases.....	25
1.3 Peripheral arterial disease and critical limb ischemia .....	25
1.3.1 Current therapies.....	29
1.4 Strategies for vascular regeneration.....	30
1.4.1 Gene therapy.....	30
1.4.2 Cell therapies .....	32
1.5 Pluripotent Stem Cells.....	40
1.5.1 Human embryonic stem cells .....	40
1.5.2 Induced pluripotent stem cells .....	42
1.5.3 Regulation of pluripotency .....	43
1.6 Endothelial differentiation of pluripotent stem cells .....	46
1.6.1 <i>In vitro</i> differentiation of pluripotent stem cells to endothelium ..	46
1.6.2 <i>In vivo</i> development of the vasculature.....	49
1.7 MicroRNAs.....	51
1.7.1 miRNA biogenesis.....	52
1.7.2 miRNA function .....	56
1.8 Endothelial-associated miRNAs .....	57
1.8.1 miR-126 .....	58
1.8.2 miR-17-92 cluster.....	60
1.8.3 miR-210 .....	60
1.8.4 miR-10.....	61
1.8.5 miR-221 and -222 .....	62
1.8.6 Other notable pro- and anti- angiogenic miRNAs .....	62
1.9 miRNAs and pluripotent stem cells .....	67
1.9.1 Pluripotency-associated miRNAs .....	67
1.10 miRNAs and differentiation.....	70
1.10.1 miRNA regulation of hESC-EC differentiation .....	71

1.11	Control of pluripotency and differentiation by other regulatory non-coding RNAs.....	73
1.12	Project Aims .....	75
Chapter 2	Materials and Methods .....	76
2.1	General laboratory practice .....	77
2.2	General cell culture techniques.....	77
2.2.1	Culture of HEK293Ts .....	77
2.2.2	Human pluripotent stem cell culture .....	78
2.3	Differentiation of human pluripotent stem cells .....	79
2.3.1	Endothelial differentiation of hESC .....	79
2.3.2	MACSorting of hESC-ECs and further outgrowth.....	80
2.3.3	Differentiation of hESC to hemogenic endothelium .....	82
2.4	Functional analysis of hESC-ECs .....	84
2.4.1	Matrigel Tubule Assay.....	84
2.5	Gene and miRNA expression analysis .....	84
2.5.1	Extraction of total RNA from cells .....	84
2.5.2	Reverse transcription polymerase chain reaction (RT-PCR).....	86
2.5.3	mRNA and miRNA TaqMan® real-time PCR .....	87
2.5.4	miRNA microarray .....	93
2.6	Immunocytochemistry (ICC).....	95
2.7	Flow Cytometry.....	96
2.7.1	Fluorescence Activated Cell Sorting (FACS) .....	97
2.8	General DNA cloning techniques .....	98
2.8.1	Genomic DNA extraction .....	98
2.8.2	Polymerase chain reaction (PCR).....	98
2.8.3	Restriction digest .....	99
2.8.4	DNA gel electrophoresis .....	100
2.8.5	Dephosphorylation and ligation.....	101
2.8.6	Sequencing .....	102
2.8.7	Plasmid purification .....	102
2.9	Lentivirus production .....	105
2.9.1	Production of Lentivirus via triple transfection method.....	105
2.9.2	Concentration of Lentivirus .....	107
2.9.3	Calculation of lentiviral titre .....	107
2.10	Lentiviral transduction of hESCs .....	109
2.10.1	Monolayer transduction .....	110
2.10.2	Transduction of hESCs in suspension .....	110
2.11	Statistical analysis .....	110

Chapter 3 Development and characterisation of a direct hESC-EC differentiation protocol. ....	112
3.1 Introduction .....	113
3.2 Aims .....	115
3.3 Results .....	116
3.3.1 Development of a direct hESC-EC differentiation protocol .....	116
3.3.2 Characterisation of hESC-ECs generated via a direct hESC-EC differentiation protocol .....	119
3.3.3 Purification and expansion of CD144 <sup>+</sup> hESC-ECs.....	126
3.3.4 Tubule formation capacity of d14 CD144 <sup>+</sup> IVECs .....	128
3.3.5 Identification and characterisation of a CD326 <sup>low</sup> CD56 <sup>+</sup> progenitor population.....	129
3.3.6 Isolation and further characterisation of the CD326 <sup>low</sup> CD56 <sup>+</sup> population.....	135
3.4 Discussion .....	143
Chapter 4 Development and characterisation of an indirect hESC-EC differentiation protocol .....	150
4.1 Introduction .....	151
4.2 Aims .....	153
4.3 Results .....	154
4.3.1 Preliminary characterisation of adherent cells in a defined hematopoietic differentiation system .....	154
4.3.2 Multi-colour flow cytometry to identify HE populations within a defined hematopoietic differentiation system .....	161
4.3.3 Optimisation of an indirect hESC-EC differentiation protocol .....	168
4.3.4 Identification of a CD326 <sup>low</sup> CD56 <sup>+</sup> MP population during indirect hESC-EC differentiation .....	178
4.4 Discussion .....	181
Chapter 5 miRNA profiling and modulation during hESC-EC differentiation... ..	187
5.1 Introduction .....	188
5.2 Aims .....	190
5.3 miRNA microarray screen .....	191
5.3.1 Normalisation and Data Analysis .....	191
5.3.2 Experimental Design .....	191
5.3.3 Quality control .....	193
5.3.4 Differentiation Quality Control .....	195
5.4 Results .....	200
5.4.1 miRNA profiling - array .....	200
5.4.2 Modulation of miRNA during hESC-EC differentiation .....	227
5.4.3 Modulation of miRNAs in hESCs and hESC-EC differentiation .....	231
5.5 Discussion .....	242



Chapter 6	General Discussion.....	249
6.1	Discussion.....	250
6.2	Future perspectives .....	254
6.3	Concluding remarks .....	259
	List of References .....	261

## List of Tables

Table 1.1 - Current clinical trials using stem cells for the treatment of CLI. ....	37
Table 2.1 - Protocols for coating tissue culture plates with various matrices ...	78
Table 2.2 - Cytokine concentrations used on specific days of hESC-EC differentiation .....	80
Table 2.3 - Final concentration of cytokines in Stemline II medium on specific days of differentiation to hemogenic endothelium.....	83
Table 2.4 - List of gene expression TaqMan assays used. ....	90
Table 2.5 - List of miRNA TaqMan assays used. ....	90
Table 2.6 -TaqMan probes on custom TLDA cards used for gene expression analysis.....	93
Table 2.7 - Antibodies used for flow cytometric analysis. ....	97
Table 2.8 - Sequence of primers used for PCR amplification of miR-145, miR-143 and miR-143/145 cluster. ....	99
Table 3.1 - TLDA card analysis of d3 MP and NCFs during hESC-EC differentiation. ....	139
Table 4.1 - 2-colour flow cytometry antibody combinations. ....	156
Table 4.2 - 6-colour flow cytometry antibody panel. ....	161
Table 5.1 - Array samples and corresponding TapeStation gel labels.....	194
Table 5.2 - miRNAs differentially expressed between d3 CD326 <sup>low</sup> CD56 <sup>+</sup> and NCF samples. ....	213
Table 5.3 - Differentially expressed miRNAs and their changes in expression between d3 CD326 <sup>low</sup> CD56 <sup>+</sup> and NCF samples. ....	214

## List of Figures

Figure 1.1 - UK deaths by cause and gender. ....	27
Figure 1.2 - Atherosclerotic plaque formation. ....	28
Figure 1.3 - Derivation and potential uses of hiPSC. ....	43
Figure 1.4 -Pluripotency-associated transcription factors form an autoregulatory loop. ....	46
Figure 1.5 - MiRNA biogenesis .....	55
Figure 1.6 - miRNAs play an important role in the regulation of angiogenesis. ...	66
Figure 2.1 - Overview of MACSorting .....	81
Figure 2.2 - Plasmid map for pSFFV Lenti MCS. ....	106
Figure 3.1 - Preliminary analysis of H1 d7 hESC-ECs. ....	116
Figure 3.2 - Direct hESC-EC differentiation. ....	118
Figure 3.3 - Analysis of endothelial - associated surface markers during H9 hESC-EC differentiation. ....	120
Figure 3.4 - Analysis Tra1-60 expression during H9 hESC-EC differentiation. ...	121
Figure 3.5 - Gene expression analysis of direct hESC-EC differentiation.....	123
Figure 3.6 - hESC-EC differentiation in H1.....	125
Figure 3.7 - Sorting and further culture of CD144 <sup>+</sup> hESC-ECs .....	127
Figure 3.8 - Tubule formation capacity of d14 CD144 <sup>+</sup> IVECs. ....	128
Figure 3.9 - Identification of a previously published CD326 <sup>low</sup> CD56 <sup>+</sup> mesoderm progenitor population in direct hESC-EC differentiation. ....	131
Figure 3.10 - Analysis of mesoderm-associated genes during H9 and H1 hESC-EC differentiation. ....	132
Figure 3.11 - Co-expression of CD144 and CD326 or CD56 on d3, 5 and 7. ....	133
Figure 3.12 - CD144 staining of d3, 5 and 7 CD326 <sup>low</sup> CD56 <sup>+</sup> . ....	134
Figure 3.13 - FACSorting of CD326 <sup>low</sup> CD56 <sup>+</sup> progenitor populations.....	135
Figure 3.14 - Expression of pluripotency-, mesodermal- and endothelial-associated genes in FACSorted CD326 <sup>low</sup> CD56 <sup>+</sup> cells. ....	137
Figure 3.15 - Histograms of selected gene expression from TLDA card analysis. ....	140
Figure 4.1 - Schematic and morphological analysis of d7 and d10 of a defined hematopoietic differentiation protocol. ....	155
Figure 4.2 - d7 adherent and budding cells during hematopoietic differentiation. ....	156
Figure 4.3 - 2-colour flow cytometric analysis of HE markers in a defined hematopoietic differentiation system. ....	158
Figure 4.4 - 6-colour flow cytometric analysis of d7-10 adherent cells. ....	162
Figure 4.5 - CD235a/CD144 staining of d7-10 suspension cells. ....	165
Figure 4.6 - Gene expression analysis of suspension and adherent cells in a defined hematopoietic differentiation system. ....	167
Figure 4.7 - Schematic of indirect hESC-EC differentiation system.....	169
Figure 4.8 - Optimisation of a newly developed indirect hESC-EC differentiation system.....	171
Figure 4.9 -Average percentage of CD31 <sup>+</sup> CD144 <sup>+</sup> hESC-ECs .....	172
Figure 4.10 - Further analysis of surface marker expression in CD31 <sup>+</sup> CD144 <sup>+</sup> d7+3 cells. ....	172
Figure 4.11 - Gene expression profiling of generated hESC-ECs.....	174
Figure 4.12 - Analysis of pluripotency associated cell surface markers in H1 indirect hESC-EC differentiation. ....	175
Figure 4.13 - Indirect hESC-EC differentiation in H9 hESCs. ....	177

Figure 4.14 - Assessment of pluripotency markers in H9 indirect hESC-EC differentiation. ....	178
Figure 4.15 - Identification of CD326 <sup>low</sup> CD56 <sup>+</sup> MPs during hematopoietic and indirect hESC-EC differentiation. ....	179
Figure 5.1 - miRNA microarray experimental design. ....	192
Figure 5.2 - Schematic of comparisons performed ....	193
Figure 5.3 - Agilent TapeStation analysis of RNA quality. ....	194
Figure 5.4 - Typical TapeStation electropherogram. ....	195
Figure 5.5 - Flow cytometric analysis of hESC-EC differentiation samples used in microarray screen. ....	197
Figure 5.6 - FACS sorting of d3 CD326 <sup>low</sup> CD56 <sup>+</sup> MP cells for miRNA microarray. ..	199
Figure 5.7 - Principle component analysis. ....	201
Figure 5.8 - Microarray analysis of pluripotency-associated miRNAs. ....	203
Figure 5.9 - qRT-PCR validation of pluripotent-associated miRNA. ....	204
Figure 5.10 - Expression of miR-302a and -302b during indirect hESC-EC differentiation. ....	205
Figure 5.11 - Profile of endothelial-associated miRNAs during direct hESC-EC differentiation. ....	206
Figure 5.12 - miR-126 and -10a during indirect hESC-EC differentiation. ....	208
Figure 5.13 - Expression miR-181a, -181b and 99b ....	210
Figure 5.14 - miR-200c expression during direct hESC-EC differentiation. ....	211
Figure 5.15 - Microarray profiling of miR-143/145 cluster during hESC-EC differentiation. ....	217
Figure 5.16 - qRT-PCR for pri-miR-143 and -145 during direct hESC-EC differentiation. ....	218
Figure 5.17 - qRT-PCR validation of miR-143/145 cluster expression. ....	219
Figure 5.18 - qRT-PCR analysis of miR-143/145 expression during indirect hESC-EC differentiation. ....	220
Figure 5.19 - miR-483 stem loop expression. ....	222
Figure 5.20 - qRT-PCR validation of miR-483 expression during hESC-EC differentiation. ....	224
Figure 5.21 - miR-455 during direct hESC-EC differentiation. ....	226
Figure 5.22 - Transfection of pcDNA <sup>TM</sup> 3.3(+)-miR-143/145 constructs in 293s. ...	228
Figure 5.23 - GFP transduction of hESCs. ....	230
Figure 5.24 - miR-143/145 overexpression in HeLa cells. ....	232
Figure 5.25 - Preliminary testing of Lentiviral transduction - GFP expression on d3 of hESC-EC differentiation. ....	234
Figure 5.26 - Initial analysis of miR-143/145 overexpression. ....	236
Figure 5.27 - d7 CD31 <sup>+</sup> CD144 <sup>+</sup> and d3 CD326 <sup>low</sup> CD56 <sup>+</sup> populations after miR-143/145 overexpression. ....	237
Figure 5.28 - qRT-PCR analysis of miR-143/145 expression after viral transduction. ....	238
Figure 5.29 - Lenti-miR-483 transduction of HeLa cells. ....	239
Figure 5.30 - d7 CD31 <sup>+</sup> CD144 <sup>+</sup> and d3 CD326 <sup>low</sup> CD56 <sup>+</sup> populations after miR-483 overexpression. ....	241

## List of Publications, Presentations and Awards

Scott, E., Loya, K., Mountford, J., Milligan, G. & Baker, A. H. 2013. MicroRNA regulation of endothelial homeostasis and commitment-implications for vascular regeneration strategies using stem cell therapies. *Free Radic Biol Med*, 64, 52-60.

### Abstracts:

British Society for Gene and Cell Therapy (BSGCT) and British Society for Cardiovascular Research (BSCR) joint meeting.

University of Strathclyde, June 2015.

Derivation of Vascular Endothelium from Human Embryonic Stem Cells - The Role of miRNAs in Endothelial Commitment.

**E Scott**, P Burton, D Mallinson, G Milligan, J Mountford, AH Baker.

Poster communication

European Atherosclerosis Society (EAS)

SECC, Glasgow, March 2015.

Derivation to Vascular Endothelium from Human Embryonic Stem Cells - The Role of miRNAs in Endothelial Commitment.

**E Scott**, P Burton, D Mallinson, G Milligan, J Mountford, AH Baker.

Oral Communication

Scottish Cardiovascular Forum (SCF)

QMRI, University of Edinburgh, February 2015.

Derivation of Vascular Endothelium from Human Embryonic Stem Cells - The Role of miRNAs in Endothelial Commitment.

**E Scott**, P Burton, D Mallinson, G Milligan, J Mountford, AH Baker.

Rodger Wadsworth Memorial Prize oral presentation

### Awards:

3<sup>rd</sup> place Rodger Wadsworth Memorial Prize, SCF, awarded February 2015.

EAS Young Investigators Fellowship, awarded March 2015.

## Summary

With their unique ability to differentiate into any cell of the three germ layers (endoderm, ectoderm and mesoderm) and their capacity for unlimited self-renewal, pluripotent stem cells (PSC), including human embryonic (hESC) and induced pluripotent stem cells (hiPSCs), are thought to hold great potential as an unlimited source of functional, transplantable cells for a diverse range of scientific and clinical applications. Specifically, in the context of cardiovascular and ischemic diseases, it is believed that hESC-derived endothelial cells (hESC-ECs) may be used to stimulate angio- and vasculogenesis in ischemic tissues, therefore restoring blood supply to the affected area.

Despite the publication of numerous methods for the derivation of hESC-ECs, differentiation efficiency is often low, or protocols involve the use of cumbersome isolation techniques. Currently, mechanisms governing the commitment of pluripotent cells to this specific lineage remain poorly understood, although numerous studies have highlighted a role for microRNAs (miRNA; miR). miRNAs are short, non-coding RNAs, ~22 nucleotides in length, which act post-transcriptionally to control the expression of their specific mRNA targets. It was, therefore, hypothesised that specific miRNAs play crucial roles during hESC-EC differentiation and commitment. The aim of this study was to identify novel miRNAs with roles in early mesodermal and endothelial commitment, and their potential mechanisms of action, in two newly developed hESC-EC differentiation protocols. Identified miRNAs could then be modulated to drive hESCs toward an endothelial lineage, therefore, allowing for increased differentiation efficiencies.

In order to study the role of miRNAs during commitment of pluripotent cells to the endothelial lineage, two distinct hESC-EC differentiation systems were developed. The first was a direct system, whereby pluripotent cells were taken at d0 and differentiated directly to hESC-ECs. By d7 of direct differentiation, ~40% of cells were CD31<sup>+</sup>CD144<sup>+</sup> hESC-ECs, and this was coupled with a significant downregulation of pluripotent-associated genes and surface markers at this time point. Furthermore, it was demonstrated that CD31<sup>+</sup>CD144<sup>+</sup> hESC-ECs could be isolated and cultured for a further 7 days. Resultant d14 hESC-ECs were

~100% CD31<sup>+</sup>CD144<sup>+</sup> and were functional, demonstrated by their ability to form tubules on a Matrigel matrix.

The second method for hESC-EC generation was indirect, and was developed using a pre-existing hematopoietic differentiation system. *In vivo*, development of the hematopoietic and vascular systems are closely linked, with a number of publications demonstrating the existence of a bipotent progenitor population with the ability to generate both endothelial and hematopoietic lineages, known as hemogenic endothelium (HE). *In vitro* studies using hPSCs have also identified and characterised HE populations. Using the cell surface marker profiles defined during these studies, a CD31<sup>+</sup>CD144<sup>+</sup>CD235a<sup>-</sup>CD43<sup>-</sup>CD73<sup>-</sup> HE population was demonstrated to exist on d7 of hematopoietic differentiation. Optimisation was then performed, to drive HE cells toward an EC phenotype, and generate a second, indirect hESC-EC differentiation protocol. By d10 of indirect hESC-EC differentiation, cells formed a confluent monolayer, expressed endothelial markers CD144, CD31 and CD73, and were negative for hematopoietic and pluripotent-associated markers.

Profiling miRNAs involved in early stages of mesodermal and endothelial specification required identification of a progenitor population, indicating the beginning of lineage commitment. Using time course analysis, a CD326<sup>low</sup>CD56<sup>+</sup> mesoderm progenitor (MP) population was identified on d3 during direct hESC-EC differentiation, before the appearance of endothelial-associated markers, and coinciding with the peak in the expression of mesoderm-associated genes. Further characterisation was performed using fluorescence activated cell sorting (FACS), to isolate a pure CD326<sup>low</sup>CD56<sup>+</sup> MP samples, and TLDA card analysis, to examine the expression of 48 different genes. The existence of this population was also demonstrated in the indirect hESC-EC system, where CD326<sup>low</sup>CD56<sup>+</sup> MP cells were also present on d3 of differentiation, before the expression of hematopoietic- or endothelial-associated markers were detected.

Global analysis of changes in miRNA expression during direct hESC-EC was then performed using a miRNA microarray screen, using the previously characterised CD326<sup>low</sup>CD56<sup>+</sup> MP, as well as d0 pluripotent cells, the d3 negative cell fraction (NCF) and d7 hESC-ECs. Overall, it was observed that pluripotency-associated miRNAs, such as the miR-302 family, were significantly downregulated during

hESC-EC differentiation, with miRNAs associated with endothelial function and angiogenesis significantly upregulated as cells moved toward an endothelial phenotype. These findings were also validated in samples taken during indirect hESC-EC differentiation.

Direct comparisons between d3 CD326<sup>low</sup>CD56<sup>+</sup> MP and NCF samples were performed to identify novel miRNAs with potential roles in early mesoderm and endothelial commitment, and led to the identification of 56 differentially expressed miRNAs. Most interestingly, -3p and -5p strands of a number of miRNA stem loops, including miR-145 and miR-483, were found to be regulated in a similar manner during hESC-EC differentiation. Upon additional analysis, it was discovered that both strands of the miR-143 stem loop, transcribed in a cluster with miR-145, were also regulated in the same fashion. Therefore, the miR-143/145 cluster and miR-483 were chosen as miRNA candidates for further investigation.

Modulation of the miR-143/145 cluster and miR-483 was performed during direct hESC-EC differentiation. It was hypothesised that overexpression of these miRNAs would lead to increased differentiation efficiency, assessed via the percentage of CD31<sup>+</sup>CD144<sup>+</sup> hESC-ECs present on d7. Therefore, lentiviral vectors, for overexpression of these specific miRNAs, were produced and cells infected on d0 of differentiation. Although no significant differences were recorded when miRNAs were overexpressed in the system, there are a large number of studies which could still be performed in order to fully interrogate the roles of miR-143/145 and miR-483 in the differentiation and commitment of pluripotent cells to both mesodermal and endothelial lineages.

In summary, vast changes in global miRNA expression profiles during hESC-EC differentiation indicate an important role for these regulatory RNAs. Investigation was performed using two newly developed methods for hESC-EC generation and miRNAs were screened using microarray technology. Although the initial miRNA modulation studies were unsuccessful in increasing the efficiency of hESC-EC differentiation, further work must be completed in order to fully interrogate the roles of these specific miRNAs.



## Abbreviations

µg	Microgram
µM	Micromolar
acLDL	Acetylated low density lipoprotein
AGM	Aorta-gonad-mesonephros
Ago2	Argonaute protein 2
ANOVA	Analysis of variance
APC	Allophycocyanin
bFGF	Basic fibroblast growth factor
BM-MNC	Bone marrow mononuclear cell
BMP4	Bone morphogenic protein 4
bp	Base pair
BSA	Bovine serum albumin
BV421	Brilliant Violet 421™
CD	Cluster of differentiation
cDNA	Complementary deoxyribonucleic acid
CHD	Coronary heart disease
CLI	Critical limb ischemia
CM	conditioned medium

Ct	Cycle threshold
CVD	Cardiovascular disease
DCGR8	DiGeorge critical region 8
DMEM	Dulbecco's Modified Eagle's Medium
DMSO	Dimethyl sulfoxide
DNA	Deoxyribonucleic acid
ds	Double stranded
dsRBD	Double stranded RNA binding domains
EB	Embryoid body
EC	Endothelial cell
ECC	Embryonal carcinoma cell
EGM-2	Endothelial growth medium-2
EHT	Endothelial to hematopoietic transition
EMT	Epithelial to mesenchymal transition
eNOS	Endothelial nitric oxide synthase
EPC	Endothelial progenitor cell
EXPO5	Exportin 5
FACS	Fluorescence activated cell sorting
FBS	Foetal bovine serum

FCS	Foetal calf serum
FGF	Fibroblast growth factor
FITC	Fluorescein isothiocyanate
FN	Fibronectin
GMP	Good manufacturing practice
h	Hour
HC	Hematopoietic cell
HE	Hemogenic endothelium
hESC	Human embryonic stem cell
HGF	Hepatocyte growth factor
HIF-1 $\alpha$	Hypoxia-inducible factor 1 $\alpha$
hiPSC	Human induced pluripotent stem cell
HP	Hematopoietic progenitor
hPSC/hESC- EC	Human pluripotent/embryonic stem cell derived endothelial cells
HSC	Hematopoietic stem cell
HUVEC	Human umbilical vein endothelial cell
IC	Intermittent claudication
ICC	Immunocytochemistry

ICM	Inner cell mass
IGF2	Insulin-like growth factor 2
IMBX	3-isobutyl-1-methylxanthin
IPO8	Importin 8
IVEC	Immature vascular endothelial cell
IVF	<i>In vitro</i> fertilisation
Kb	Kilobase
kg	Kilogram
KOSR	Knockout serum replacement
L	Litre
Lenti	Lentivirus
LIF	Leukaemia inhibitory factor
lncRNA	long non-coding RNA
M	Molar (moles/L)
MACS	Magnetic activated cell sorting
MEF	Mouse embryonic fibroblast
MEM	Minimal essential medium
mESC	Mouse embryonic stem cell
MI	Myocardial infarction

min	Minute
miPSC	Mouse induce pluripotent stem cell
miRNA/miR	MicroRNA
mL	Millilitre
mM	Millimolar
MOI	Multiplicity of infection
MP	Mesoderm progenitors
mRNA	Messenger RNA
MSC	Mesenchymal stem cell
NCF	Negative cell fraction
ng	Nanogram
nM	Nanomolar
NO	Nitric oxide
nt	Nucleotide
Oct4	Octamer-binding transcription factor 4
PACT	Protein activator of pkt
PAD	Peripheral arterial disease
PBS	Phosphate buffered saline
PCR	Polymerase chain reaction

PE	Phycoerythrin
PerCP-Cy5.5	Peridinin-chlorophyll protein-cyanine 5.5
pri-miRNA	Primary microRNA
PSC	Pluripotent stem cell
qRT-PCR	Quantitative real time-polymerase chain reaction
RIN	RNA integrity number
RISC	RNA induced silencing complex
RLC	RISC loading complex
RNA	Ribonucleic acid
Rnase	Ribonuclease
rpm	Revolutions per minute
RQ	Relative quantification
rRNA	Ribosomal RNA
RT	Room temperature
RT-PCR	Reverse transcription-polymerase chain reaction
s	Second
SCF	Stem cell factor
SEM	Standard error of the mean
siRNA	Small interfering RNA

snoRNA	Small nucleolar RNA
Sox2	SRY-box 2
ss	Single stranded
SSEA3/SSEA4	Stage specific embryonic antigen 3/4
TF	Transcription factor
TLDA	Taqman Low Density Array
TNF- $\alpha$	Tumour necrosis factor- $\alpha$
TPO	Thrombopoietin
Tra1-60/Tra1-81	Tumour receptor antigen 1-60/1-81
TRBP	TAR RNA binding protein
UBC	Ubiquitin protein C
UTR	Untranslated region
v/v	volume/volume
VCAM-1	Vascular cell adhesion molecule 1
VEGF	Vascular endothelial growth factor
VEGFR2	Vascular endothelial growth factor receptor 2
VSMC	Vascular smooth muscle cell
vWF	von Willibrand factor

w/v            weight/volume

ZEB1            Zinc-finger E-box-binding homeodomain 1



# Chapter 1 Introduction

## **1.1 Cardiovascular disease**

Cardiovascular disease (CVD) is the leading cause of morbidity and mortality worldwide, with over 160,000 deaths caused by this in the UK alone in 2012 (BHF, 2014). The term CVD encompasses all diseases of the heart and circulatory system, including stroke, myocardial infarction (MI) and a variety of ischemic diseases, which in total cost the English National Health Service £6.9 billion in 2012, and amount to approximately 30% of total deaths in both male and females in the UK (Figure 1.1).

Although the numbers of people living with CVD has fallen in recent years, there is still need for the development of novel therapeutic strategies to relieve the burden on health services around the world.

## **1.2 Ischemic diseases**

A major cause of cardiovascular disease is the development of atherosclerosis, a disease characterised by the formation of plaques, causing narrowing, hardening and eventual occlusion of arteries. This often leads to ischemia in the affected tissues (Figure 1.2).

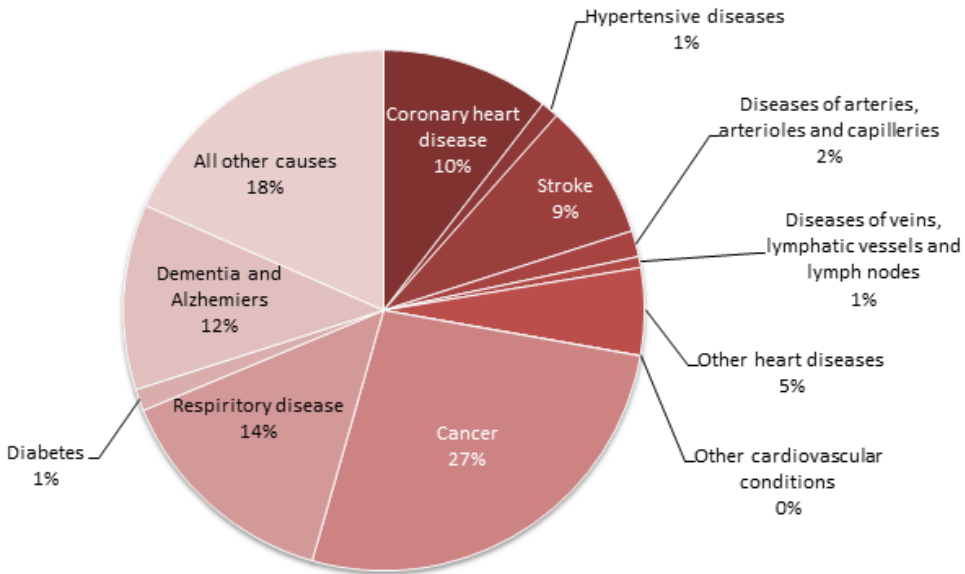
Ischemia is defined as a restriction in blood supply within a tissue. A restriction in blood supply results in insufficient supply of oxygen, nutrients and removal of degradation products, which can subsequently cause inhibition of tissue growth and cellular function, ultimately resulting in a death of affected cells and tissues. Depending on their location, ischemia induced by the formation of atherosclerotic plaques can result in various different disease pathologies, including coronary heart disease (CHD, a major cause of myocardial infarction), stroke (cerebral vasculature) and peripheral arterial disease.

## **1.3 Peripheral arterial disease and critical limb ischemia**

Peripheral arterial disease (PAD) is highly prevalent, thought to affect >25 million patients across Europe and North America (Raval et al., 2013). In 2012/13 in the UK alone almost half a million people were on the PAD register, equal to approximately 0.7% of the total population (BHF, 2014). Caused as a result of atherosclerotic plaque build-up in the systemic and peripheral

vasculature, therefore resulting in ischemia in tissues supplied by those vessels, symptoms include muscular pain in the leg during physical activity. Currently, there is no cure for PAD, and most treatment regimens rely on changes in the lifestyle of patients, such as increasing exercise levels, changes in diet and stopping smoking (Bendermacher et al., 2005, NHS Choices, 2012). If left untreated, however, PAD can lead to a plethora of other cardiovascular problems, such as myocardial infarction and stroke, as well as amputation of affected limbs.

### Female deaths by cause, 2012



### Male deaths by cause, 2012

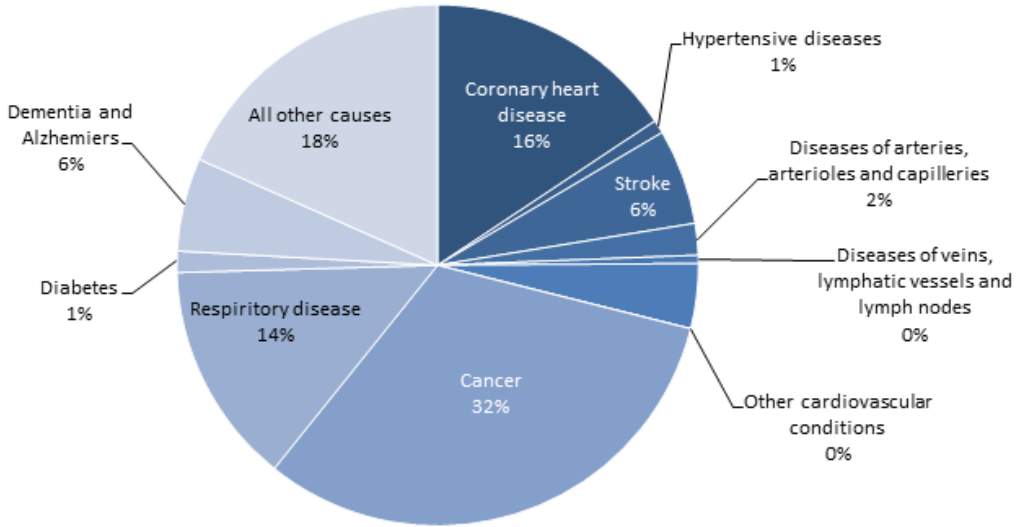


**Figure 1.1 – UK deaths by cause and gender.**  
 Charts showing female and male deaths in the UK in 2012 by cause. In total 28% (females) and 29% (males) of all deaths in the UK in 2012 were caused by cardiovascular diseases (Source: BHF, 2014).

The most common clinical manifestation of PAD is intermittent claudication (IC), characterised by exertion mediated pain in the lower limbs, caused through an inability to meet the demands of exercising skeletal muscle, due to inadequate blood flow. In the most serious cases, however, PAD can result in the development of critical limb ischemia (CLI). CLI is thought to affect approximately 1% of PAD sufferers, and develops as a consequence of chronic ischemia in the peripheral vasculature, and can lead to irreversible tissue damage and cell death. A reduced blood supply can result in a failure to meet basal metabolic requirements, causing CLI patients can present at clinic with severe pain during rest, ischemic ulceration or gangrene, and have a higher risk of other cardiovascular events, such as stroke and CHD (Subherwal et al., 2015). Large multicentre trials have shown that 25-30% of patients undergo major amputations (below or above knee) and up to 20% of patients die within the first year after presentation, with the limited amounts of longer-term data suggesting that mortality rates continue to rise after this time (Norgren et al., 2007, Powell, 2012).

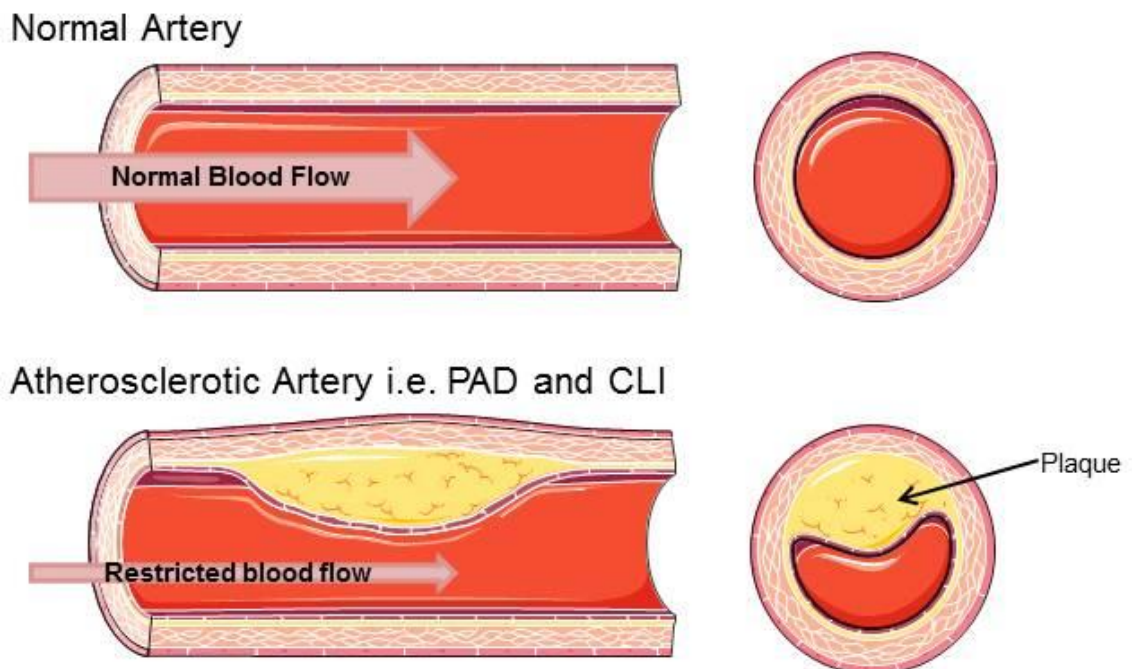


**Figure 1.2 – Atherosclerotic plaque formation.**

Diagram showing a normal artery (A) and an artery affected by the formation of an atherosclerotic plaque (B). The formation of these plaques causes hardening and narrowing of arteries, resulting in restricted blood flow to affected organs, tissues and limbs (NIH, 2014).

### 1.3.1 Current therapies

Current therapies for the treatment of CLI focus mainly on the prevention of major amputation, as well as relieving pain, increasing survival and improving the quality of life. Presently, the preferred treatment for patients with limb-threatening ischemia is revascularisation; the reestablishment of continuous in-line flow to the affected limb. This can be done in a number of ways, including surgical or endovascular revascularisation, or a hybrid, whereby a combination of these two therapies are used (Slovut et al., 2008).

The most common intervention strategy for CLI and symptomatic PAD is endovascular revascularisation, via the use of catheter-based therapies, such as balloon angioplasty and stenting. Originally, evidence that these strategies were leading to long term improvements in patient's health were lacking, and 1-year failure rates were high (Kalbaugh et al., 2006), although it had been claimed that some patients reported an improvement in symptoms, function and quality of life 1-year post procedure (Safley et al., 2007). More recently, however, innovations in technology and development of specialised therapeutic devices has improved clinical outcome, and has, therefore, led to increasing use of endovascular revascularisation strategies in the treatment of more advanced CLI (Thukkani et al., 2015).

Surgical revascularisation techniques may also be used to treat CLI, whereby bypass grafts are used to restore blood flow to ischemic limbs. This technique is particularly used in patients who have more complex lesions, and are therefore not suitable for catheter-based revascularisation techniques, and for younger patients with a longer life-expectancy, who require more durable revascularisation (Slovut et al., 2008). Although not the preferred therapy, an early study showed a limb-based patency in patients suffering CLI of 87.5% and 81.8% at 5 and 10 years post-intervention (de Vries et al., 1997). A meta-analysis of published studies, including one randomised control trial, comparing both endovascular and surgical revascularisation techniques, however, showed no significant differences in amputation-free survival and overall survival between the two groups (Bradbury et al., 2010, Jones et al., 2014).

Due to the varied clinical outcomes of these treatments, coupled with the fact that a large number of patients with CLI are considered ineligible for revascularisation using either surgical or endovascular-based techniques, the development of new treatments is paramount. In recent years, therefore, research has focused on the development of novel therapies. Vascular regenerative strategies, including gene and cell therapies, are thought to have great potential in this area, allowing for the potential generation of new vasculature and promotion of angiogenesis in affected limbs.

## **1.4 Strategies for vascular regeneration**

Regenerative medicine encompasses all strategies for the repair, replacement or regrowth of damaged or destroyed tissues and organs, including the use of biomaterials, or human genes, proteins or cells.

In PAD and CLI, early regenerative medicine strategies focused on the administration of angiogenesis-inducing growth factors, such as vascular endothelial growth factor (VEGF) or fibroblast growth factor (FGF) (Lederman et al., 2002, Henry et al., 2003). Angiogenesis is defined as the migration and proliferation of differentiated endothelial cells (ECs) in order to allow sprouting of new capillary branches from existing vessels, and stimulate the development and growth of new blood vessels in the affected tissue. Although early results from these trials were promising, and treatment using these factors was found to be safe, there were no lasting clinical effects when patients were treated with a single dose of VEGF, or when they were administered with two doses of FGF (Lederman et al., 2002, Henry et al., 2003). This may be due to insufficient doses - a very large amount of protein may be needed to have a significant effect, something which is unrealistic in a clinical setting.

### **1.4.1 Gene therapy**

Gene therapy has also been considered for the administration of a number of different angiogenic factors. Adenoviral vectors are largely used in gene therapy studies, however a number of high profile serious adverse events during clinical trials have led to major questions about the safety of these treatments (Marshall, 1999, Gansbacher et al., 2003). Another strategy, which has been

investigated in the setting of PAD and CLI, is the administration of naked plasmid DNA encoding angiogenic factors. These therapies aimed to increase the duration of transgene expression, when compared to injection of the proteins themselves, and the plasmids induce only a minimal immune response. Despite this, expression of the transgene remains low, as plasmids have low transfection efficiency and remain episomal (Raval et al., 2013).

The first case of administration of naked plasmid DNA, encoding for VEGF was reported almost 20 years ago (Isner et al., 1996), and although no definitive conclusions could be made from the study, results were optimistic. In 1998 a trial injecting a similar plasmid construct into 10 limbs of 9 patients suffering with CLI, showed an increase in VEGF expression in the injected limbs, possibly with an increase in therapeutic angiogenesis (Baumgartner et al., 1998). Since then, numerous clinical and pre-clinical studies have been performed, using a variety of VEGF family members and viral vectors. A Phase I clinical trial confirmed the safety of adenoviral-mediated delivery of VEGF cDNA to patients with PAD, although no conclusions could be drawn about efficacy due to the low numbers of participants in the trial (Rajagopalan et al., 2002). In 2012, a 10-year safety follow up on patients treated with injection of either an adenoviral vector containing a VEGF-encoding plasmid, or a plasmid/liposome combination, directly into an ischemic lower limb, confirmed the long-term safety of this approach, although there was no difference in Fontaine category (the scale used to clinically classify PAD) between the VEGF treatment groups and the control patients, possibly due to the low numbers of patients surviving to the 10-year follow up (Muona et al., 2012).

Currently, there are 22 known FGF ligands involved in angiogenesis (Murakami et al., 2008), and cardiovascular gene therapy trials have been performed using a number of these isoforms. The first clinical study of FGF-1 gene therapy showed significant improvements in wound healing, pain and transcutaneous oxygen pressure, after an intramuscular injection of a naked plasmid, encoding for the FGF-1 (NVFGF1) (Comerota et al., 2002). However, a large scale phase III clinical trial (TAMARIS) showed that there was no difference in major amputation or death between the active and placebo groups, when CLI patients, not suitable for revascularisation, were treated with eight intramuscular injections of either NVFGF1 or a placebo (Belch et al., 2011). Trials using a Sendai virus expressing



human FGF-2, which had previously been shown to significantly decrease in amputation rates in a mouse model through induction of endogenous VEGF expression, showed significant improvements of limb function (Masaki et al., 2002, Yonemitsu et al., 2013).

A number of gene therapy clinical trials, using other angiogenic factors, such as hypoxia-inducible factor-1 $\alpha$  (HIF-1 $\alpha$ ), hepatocyte growth factor (HGF) and developmentally regulated endothelial locus (Del-1), have also been performed in patients suffering with IC and CLI (Grossman et al., 2007, Powell et al., 2010, Creager et al., 2011). Although no significant safety issues were reported in any of these trials, results were mixed, with most studies finding no significant difference in primary end point between the treatment and placebo groups. Overall, strategies using angiogenic growth factors to treat PAD and CLI have been largely unsuccessful and, therefore, an increasing knowledge of stem and progenitor cells, and their potential clinical applications, has prompted a move towards cell-based therapies.

### **1.4.2 Cell therapies**

Currently, there are 34 clinical trials involving stem cell therapies in the treatment of CLI which have been registered at [clinicaltrials.gov](http://clinicaltrials.gov) (Table 1.1). Thus far, cell therapies results have been varied, with the majority of studies involving the transplantation or injection of autologous cell populations, broadly known as ‘adult stem cells’, including mesenchymal stem cells (MSC), bone marrow mononuclear cells (BM-MNC) and endothelial progenitor cells (EPC). Autologous cell types have an advantage in that they are derived from the patient themselves, reducing the risk of immune rejection.

MSCs originate in the stromal compartment of the bone marrow, where they make up only a small fraction of the total nucleated cells. Other sources of cells with mesenchymal potential have also been reported, for example adipose tissue and skeletal muscle (Jankowski et al., 2002, De Ugarte et al., 2003). These cells are described as multipotent, non-hematopoietic and fibroblast-like, possessing the ability to differentiate into a number of cell types, including bone, fat and cartilage (Liew et al., 2012). Although their cell surface marker profile has been debated (Lv et al., 2014), their broad potential in the field of regenerative

medicine is widely accepted, and because of this their safety profile has been well documented (Ankrum et al., 2010). In specific conditions, it has been shown that MSCs can differentiate directly into ECs, indicating a possible role for these cells in the treatment of ischemic diseases (Chen et al., 2009b). Indeed, in preclinical models of PAD and CLI, such as the murine model of hind limb ischemia, treatment of animals with ECs from MSCs, derived from numerous sources, perfusion rates of ischemic limbs were significantly higher in animals treated with the cells when compared to control animals (Kang et al., 2010, Lian et al., 2010). In clinical trials, however, results have been varied, and many trials have shown no significant improvement in secondary outcomes (Perin et al., 2011, Kirana et al., 2012) or have failed to publish their results (Table 1.1).

ClinicalTrials.gov Identifier	Phase	Patient Number	Cell Type(s)	Autologous/Allogeneic	Cell Number	Primary Outcome Measures	Status	Reference
<b>NCT01257776</b>	I & II	30	Adipose-derived MSCs	Autologous	Mid dose - $1 \times 10^6$ * weight (kg), Low dose - $0.5 \times 10^6$ * weight (kg)	Angiograph to assess neovasculargenesis; Major adverse events	Ongoing	ClinicalTrials.gov
<b>NCT02287974</b>	I & II	48 (estimated)	BM-MNCs; CD133 <sup>+</sup> EPCs; Bone marrow-derived MSCs	Autologous	150-250x10 <sup>6</sup> BM-MNCs; 2-7x10 <sup>6</sup> EPCs; 0.5x10 <sup>6</sup> Bone marrow-derived MSCs	Serious adverse events	Recruiting	ClinicalTrials.gov
<b>NCT01484574</b>	II	126 (estimated)	Bone marrow-derived MSCs	Allogeneic	High; Mid; Low	Relief of rest pain; Healing of ulcerations	Unknown	ClinicalTrials.gov
<b>NCT02477540</b>	I	10 (estimated)	Bone marrow-derived MSCs	Autologous	50x10 <sup>6</sup> cells/10mL x 2 injections	Ankle Brachial Pressure Index; Safety	Not yet recruiting	ClinicalTrials.gov
<b>NCT01745744</b>	I & II	33	Adipose-derived MSCs	Autologous	High dose - $1 \times 10^6$ * weight (kg), Low dose - $0.5 \times 10^6$ * weight (kg)	Numbers of adverse and serious adverse events	Ongoing	ClinicalTrials.gov
<b>NCT01867190</b>	I & II	24 (estimated)	CD34 <sup>+</sup> and CD45 <sup>+</sup> bone marrow-derived stem cells	Autologous	10x10 <sup>6</sup> CD45 <sup>+</sup> cells/mL; 5mL/min via intra-arterial infusion or 6 x 0.2mL intramuscular injections	Major amputations; persisting CLI; Safety	Recruiting	ClinicalTrials.gov
<b>NCT00913900</b>	I	10	CD133 <sup>+</sup> cells	Autologous	Not specified	Death or amputation	Terminated - adequate cells for minimum dose	ClinicalTrials.gov
<b>NCT01824069</b>	I & II	10	Adipose-derived MSCs	Autologous	$1 \times 10^6$ * weight (kg)	Safety	Unknown	ClinicalTrials.gov
<b>NCT00883870</b>	I & II	20	Bone marrow-derived MSCs	Allogeneic	Not specified	Adverse events; symptomatic relief	Completed	ClinicalTrials.gov

Table 1.1

ClinicalTrials.gov Identifier	Phase	Patient Number	Cell Type(s)	Autologous/Allogeneic	Cell Number	Primary Outcome Measures	Status	Reference
<b>NCT00371371</b>	I & II	160	BM-MNCs	Autologous	Not specified	Major amputations	Completed	(Teraa et al., 2015)
<b>NCT02145897</b>	I & II	60 (estimated)	Stromal vascular fraction (SVF); ex vivo expanded Adipose-derived MSCs	Autologous	SVF - not specified; MSCs - 2 x 1x10 <sup>6</sup> * weight (kg) cells, 1x intravenous, 1x intramuscular	Safety	Recruiting	ClinicalTrials.gov
<b>NCT00442143</b>	I	10	BM-MNCs	Autologous	Not specified	Transcutaneous oxygen pressure; 1st toe blood pressure; ankle blood pressure; wound healing; pain	Unknown	ClinicalTrials.gov
<b>NCT00616980</b>	I & II	28	CD34 <sup>+</sup> cells	Autologous	High dose - 1x10 <sup>6</sup> * weight (kg), Low dose - 0.1x10 <sup>6</sup> * weight (kg)	Safety; Rest pain; Ulcer healing; Functional improvement; Limb salvage	Completed	(Losordo et al., 2012)
<b>NCT01065337</b>	II	30	Bone marrow stem cells; CD90 <sup>+</sup> enriched bone marrow MSCs	Autologous	Not specified	Major adverse events; Wound healing; Ipsilateral replase	Completed	(Kirana et al., 2012)
<b>NCT01232673</b>	II	96	Bone marrow stem cells	Autologous	Not specified	Major limb amputation	Completed	(Prochazka et al., 2010)
<b>NCT00392509</b>	I & II	20	Bone Marrow Derived Aldehyde Dehydrogenase-Bright cells; Unfractionated BM-MNCs	Autologous	Not specified	Adverse events; Ankle-brachial systolic pressure index; transcutaneous oxygen valu; quality of life	Completed	(Perin et al., 2011)
<b>NCT01480414</b>	I & II	20	BM-MNCs	Autologous	Not specified	Side effect of cell injection	Completed	ClinicalTrials.gov

Table 1.1

ClinicalTrials.gov Identifier	Phase	Patient Number	Cell Type(s)	Autologous/Allogeneic	Cell Number	Primary Outcome Measures	Status	Reference
<b>NCT00523731</b>	I	6	Non-mobilised peripheral blood angiogenic cell precursors	Autologous	Not specified	Safety; Rest pain; Pain-free walking distance; Ulcer size; Gangrene; Perfusion improvements	Completed	(Mutirangura et al., 2009)
<b>NCT01584986</b>	II	22	Peripheral blood derived angiogenic cell precursors	Autologous	Not specified	Safety; Rest pain; Ulcer healing; Functional improvement; Limb salvage	Completed	(Murphy et al., 2011)
<b>NCT01049919</b>	Not specified	152	Bone marrow aspirate	Autologous	Not specified	Time to major adverse event	Ongoing	ClinicalTrials.gov
<b>NCT01483898</b>	III	41	ixmyelocel-T (patient specific multicellular therapy)	Autologous	Not specified	Amputation free survival	Unknown	ClinicalTrials.gov
<b>NCT00922389</b>	I & II	36 (estimated)	G-CSF mobilised peripheral blood-derived BM-MNCs	Autologous	Not specified	Adverse events; Laboratory parameters	Unknown	ClinicalTrials.gov
<b>NCT01245335</b>	III	210 (estimated)	Bone marrow aspirate	Autologous	Not specified	Amputation free survival	Ongoing	ClinicalTrials.gov
<b>NCT03454231</b>	II & III	38	BM-MNCs; Circulating CD14 <sup>+</sup> CD34 <sup>+</sup> cells	Autologous	Not specified	Safety; Adverse events; Changes in ischemic leg perfusion	Recruiting	ClinicalTrials.gov
<b>NCT01386216</b>	I	20	Bone marrow cell concentrate	Autologous	Not specified	Time to major amputation	Ongoing	ClinicalTrials.gov
<b>NCT01595776</b>	I & II	8	CD133 <sup>+</sup> EPCs	Autologous	Not specified	Contrast enhance ultrasound	Completed	ClinicalTrials.gov
<b>NCT01663376</b>	I & II	20	Adipose-derived MSCs	Autologous	3x10 <sup>8</sup> cells at 60 points in lower extremities	Major adverse events	Completed	(Lee et al., 2012)
<b>NCT00595257</b>	I & II	60	Bone marrow aspirate concentrate	Autologous	Not specified	Amputation free survival	Completed	ClinicalTrials.gov

Table 1.1

ClinicalTrials.gov Identifier	Phase	Patient Number	Cell Type(s)	Autologous/Allogeneic	Cell Number	Primary Outcome Measures	Status	Reference
<b>NCT01472289</b>	I & II	15	BM-MNCs	Autologous	Not specified	Safety; Limb salvage	Ongoing	ClinicalTrials.gov
<b>NCT00987363</b>	I & II	60	BM-MNCs	Autologous	High dose - $1 \times 10^9$ ; Intermediate dose - $5 \times 10^8$ ; Low dose $1 \times 10^8$	Number of adverse events; Arteriographic analysis	Completed	ClinicalTrials.gov
<b>NCT01408381</b>	II	38	BM-MNCs	Autologous	Intermediate dose - $5 \times 10^8$ ; Low dose $1 \times 10^8$	Adverse events	Completed	ClinicalTrials.gov
<b>NCT01558908</b>	I & II	15	Endometrial regenerative cells (ERC)	Autologous	$25 \times 10^6$ ; $50 \times 10^6$ ; $100 \times 10^6$ ERC	Safety; Adverse events	Unknown	ClinicalTrials.gov

**Table 1.1 – Current clinical trials using stem cells for the treatment of CLI.**

All data collected from clinicaltrials.gov, references given where trials published. MSC – mesenchymal stem cell, BM-MNC – bone marrow mononuclear cell, EPC – endothelial progenitor cell (<https://clinicaltrials.gov/>, search terms 'CLI' and 'stem cells', search performed July 2015).

As well as MSCs, studies have shown potential in the use of BM-MNCs for the treatment of vascular and ischemic diseases (Table 1.1). The term BM-MNCs is broad, and encompasses a number of different bone marrow-derived cell types, including hematopoietic cells such as lymphocytes, monocytes and hematopoietic stem cells, as well as MSCs. Studies have focused on using this entire fraction with the hypothesis that the presence of multiple progenitor cell types may work in synergy to promote regeneration in a variety of disease settings. Various studies have shown the possible angiogenic capacity of these cells in the treatment of CLI in the clinic (Matoba et al., 2008, Madaric et al., 2013), although this maybe in part due to the presence of MSCs in the BM-MNC fraction (Alvarez-Viejo et al., 2013). Indeed, a pilot study, comparing the treatment of type 2 diabetic patients suffering with CLI using either bone marrow-derived MSCs or BM-MNCs, demonstrated that patients treated with MSCs, suggested that MSC transplantation may be more effective than treatment with BM-MNCs. Although, results did show substantial improvements in patients, in terms of rest pain, pain-free walking time, ankle-brachial index, transcutaneous oxygen pressure and formation of new collateral vessels when examined using magnetic resonance angiography, for both treatment groups, suggesting both MSCs and BM-MNCs may make effective cell therapies (Lu et al., 2011). The recently published JUVENTAS trial (NCT00371371; Table 1.1), however, contradicted these results, showing no reduction in the major amputation rates in patients with severe CLI who underwent 3 intra-arterial infusions of BM-MNCs (Teraa et al., 2015). A recently published clinical study suggested that the efficacy of cell therapies could be improved if they were administered alongside gene therapies (Skora et al., 2015). Patients were intramuscularly injected with a solution containing BM-MNCs and a plasmid encoding VEGF<sub>165</sub>, directly into the ischemic lower limb. Although the primary objective of the study was to demonstrate the safety and feasibility of this combination, which was done so successfully, results also showed marginal improvements in the conditions of the patients.

A study, published in 1997, showed that another, distinct, small population of bone marrow derived cells can be isolated from peripheral blood, differentiate to endothelial cells *in vitro* and can contribute to vasculogenesis *in vivo* (Asahara et al., 1997, Shi et al., 1998). These cells were termed endothelial progenitor

cells (EPC) and, loosely defined, are any cell which retain the ability to form endothelial cells. Despite large numbers of both preclinical and clinical studies, the exact profile of these cells is still under debate. Asahara et al. described these cells as CD34<sup>+</sup>, and this profile was also used in a further study by Shi et al. in 1998 (Shi et al., 1998), where the endothelial potential of these cells was once again demonstrated comprehensively *in vitro* and *in vivo*. Since then, the presence of VEGFR2 (CD309; KDR) and CD133 on the surface of these cells (Gehling et al., 2000, Peichev et al., 2000), has also been demonstrated, and they have been isolated from a variety of sources, including umbilical cord blood and bone marrow (Eggermann et al., 2003). Other research has, however, questioned the accepted CD34<sup>+</sup>CD133<sup>+</sup>VEGFR2<sup>+</sup> profile, and Case et al. failed to get these cells to form ECs in culture, and instead demonstrated their ability to form haematopoietic precursor cells (Case et al., 2007). Preclinical studies showed increase blood flow recovery in an *in vivo* model of hind limb ischemia, compared to the control group, when animals were administered with human EPCs, which had been expanded *ex vivo* (Kalka et al., 2000), and recent clinical studies have also shown positive results, both in the safety and efficacy of these cells.

The efficacy of these cellular-based therapies does not always translate in clinical trials, and many studies fail to progress past phase I or II, as shown in Table 1.1. Cell survival may be low, and the estimated percentage incorporation of cells has been widely variable, for examples, some studies have shown EPCs located on the periphery of newly formed arteries, and not actually incorporated. This has led to speculation that MSC-, BMNC- and EPC-mediated vasculogenesis occurs almost entirely through paracrine mechanisms, via the secretion of angiogenic factors, such as VEGF (Kinnaird et al., 2004, Liang et al., 2014).

Although meta-analyses have shown that overall cell therapies have a beneficial effect in the reduction of amputations (Liu et al., 2012, Liu et al., 2015), clinical trials have shown varying degrees of success in terms of symptomatic relief and revascularisation. Although research and trials are continuing with ever increasing levels of specificity, research has also started to look at the use of pluripotent stem cell (PSC)-derived cells, in particular those derived from human embryonic (hESC) and induced pluripotent (hiPSC) stem cells, as a source of



functional, transplantable cells for the treatment of PAD and CLI, as well as a wide range of other ischemic diseases, including CHD and stroke. As of yet, no clinical trials have been registered for the use of these cells in CLI or PAD treatment (Table 1.1).

## 1.5 Pluripotent Stem Cells

Due to their unique ability to differentiate into any cell of the three germ layers (endoderm, ectoderm and mesoderm) and their capacity for unlimited self-renewal, hPSCs hold great potential for a number of diverse scientific and clinical applications, including pharmacology, toxicology and for the development of cellular-based therapies and regenerative medicine. Currently, there are 2 different types of pluripotent stem cells which have been described - embryonic stem cells (ESCs) and induced pluripotent stem cells (iPSCs).

### 1.5.1 Human embryonic stem cells

The first of the two pluripotent stem cell types to be identified and isolated, human ESCs (hESC) are important tools in the fields of developmental biology and regenerative medicine. Prior to the derivation of ESCs, embryonal carcinoma cells (ECC), isolated from teratocarcinomas formed after the implantation of early stage mouse embryos, were originally used as an *in vitro* model of the developing embryo (Martin, 1980). After a number of unsuccessful attempts, a breakthrough came in 1981 when ESCs were isolated from murine embryos (Evans et al., 1981, Martin, 1981), before they were isolated from non-human primate embryo's in 1995 (Thomson et al., 1995). In 1998 James A. Thomson used human embryos, produced by in vitro fertilisation (IVF), to isolate and culture the first human-derived ESCs (Thomson et al., 1998). The cells were obtained from the inner cell mass (ICM) of the blastocyst stage embryo, isolated by immunosurgery and cultured on irradiated mouse embryonic fibroblasts (MEF). Cells were grown as colonies and individual undifferentiated colonies were manually selected and dissociated into clumps until the cell line was established. Five different hESC lines were derived, two having a normal XX karyotype (H7 and H9) and 3 having a normal XY karyotype (H1, H13 and H14). These cells, generated in 1998, are still used in research today and are widely regarded as the 'gold standard' hESC lines.

Originally, hESC lines were cultured on MEF feeder layers, and in serum containing medium, in order to culture the cells whilst maintaining their undifferentiated state (Thomson et al., 1998). Using animal derived serum and cells to culture the hESCs, however, raised concerns about the transfer of non-human pathogens, and limits the potential use of these cells in a clinical setting. Therefore, efforts were made to advance the culture conditions to a clinically acceptable standard, and following good manufacturing practice (GMP). MEF feeder layers secrete a number of soluble factors required for the maintenance of pluripotency and, in mouse ESCs (mESC) culture, it was discovered that feeder layers could be replaced by the addition of leukaemia inhibitory factor (LIF) into the culture medium (Williams et al., 1988). LIF does not, however, have the same effect on hESC culture. The earliest feeder-free culture systems were established using Matrigel cell matrix and in MEF-conditioned medium (MEF-CM), containing the soluble factors secreted by MEFs to support pluripotency (Xu et al., 2001). Subsequently, Xu et al. were also able to show that hESCs can be maintained in serum replacement non-conditioned medium supplemented with basic fibroblast growth factor (bFGF), based on their expression of the receptors for a number of FGFs (Xu et al., 2005).

In addition to the original 5 lines, a large number of other hESC lines have now been generated. Between lines there exists considerable heterogeneity, with differences in gene expression signatures (Abeyta et al., 2004), differentiation propensity (Osafune et al., 2008) and population doubling time all demonstrated, possibly reflecting differences in derivation method and timing, initial culture conditions, or underlying genetics of the source embryos. Despite this, there are a number of criteria which any hESC line must meet (Hoffman et al., 2005). This includes expressing a number of pluripotency associated cell surface antigens and internal transcription factors such as stage specific embryonic antigens 3 and 4 (SSEA3; SSEA4), tumour receptor antigens 1-60 and 1-81 (Tra1-60; Tra1-81), octamer-binding transcription factor 4 (Oct4; encoded by the *Pou5f1* gene), Nanog, and SRY-box 2 (*Sox2*). Another definitive test of hESC pluripotency is often considered to be the ability to form derivatives of the three germ layers in immunocompromised mice *in vivo* (Allegrucci et al., 2007). Other properties these cells must possess include a capacity for indefinite self-renewal, and a normal karyotype.

Despite their promise, there are numerous caveats that must be addressed before such strategies can be considered for routine use clinically. Firstly, there are a number of ethical concerns, including the destruction of fertilised embryos, which must be taken into account when using these cells (de Wert et al., 2003). Secondly, ensuring all pluripotent cells are removed from the transplanted cell population is essential, as the presence of undifferentiated cells increases the potential of teratoma formation. Another caveat is their immunogenicity. In a similar way to tissue and organs, transplantation of hESCs is an allogeneic process, and rejection by the host is a very real prospect. Several studies have shown varying degrees of immune response elicited by these cells, with some reports even suggesting that hESCs are immune-privileged (Li et al., 2004, Drukker et al., 2006). Circumvention of rejection may be possible via the generation of hESC banks containing immunophenotyped lines, although this requires a large time and economic investment (Jacquet et al., 2013). It is estimated that generation of 150 hESC lines from random donors would only match 38% of the UK population (Taylor et al., 2005). Despite these safety concerns, however, the first clinical trials using hESC-derived cell types have commenced. A recently published trial, evaluating hESC-derived retinal pigment epithelium in the treatment of patients with age-related macular degeneration and Stargardt's macular dystrophy (Schwartz et al., 2015), provided evidence of safety, graft survival and possible biological activity.

### **1.5.2 Induced pluripotent stem cells**

One way in which to overcome the issue of hESC immunorejection is via the use of autologous cells. In 2007, Shinya Yamanaka and his team successfully reprogrammed both mouse (Takahashi et al., 2006) and human (Takahashi et al., 2007) adult fibroblasts to pluripotency by transduction of four defined factors; Oct4, Sox2, Klf4 and c-Myc. The pluripotent cells generated, known as induced pluripotent stem cells (iPSCs) are similar to hESCs in morphology, proliferation, surface antigens (SSEA3, SSEA4, Tra1-60 and Tra1-81) and gene expression (Oct4, Nanog, Sox2), and are able to produce cells from all 3 germ layers both *in vitro* and in *in vivo* teratoma formation assays. Although hESCs are still considered the 'gold standard' in terms of developmental biology, these cells have the potential to provide patient- and disease-specific autologous cells for transplantation. Additionally, iPSCs can be used as excellent *in vitro* models of disease. For

example, it has been demonstrated that iPSCs generated from patients with long QT syndrome type 2, a disease characterised by abnormal ventricular repolarisation, and subsequently differentiated to cardiomyocytes can be used to test drug potency and toxicity (Itzhaki et al., 2011, Matsu et al., 2011). Moreover, as the method of iPSC derivation does not require the use of human embryos, using these cells circumvents the ethical issues faced with the use of hESCs.

An overview of iPSC derivation and potential uses can be seen in Figure 1.3.

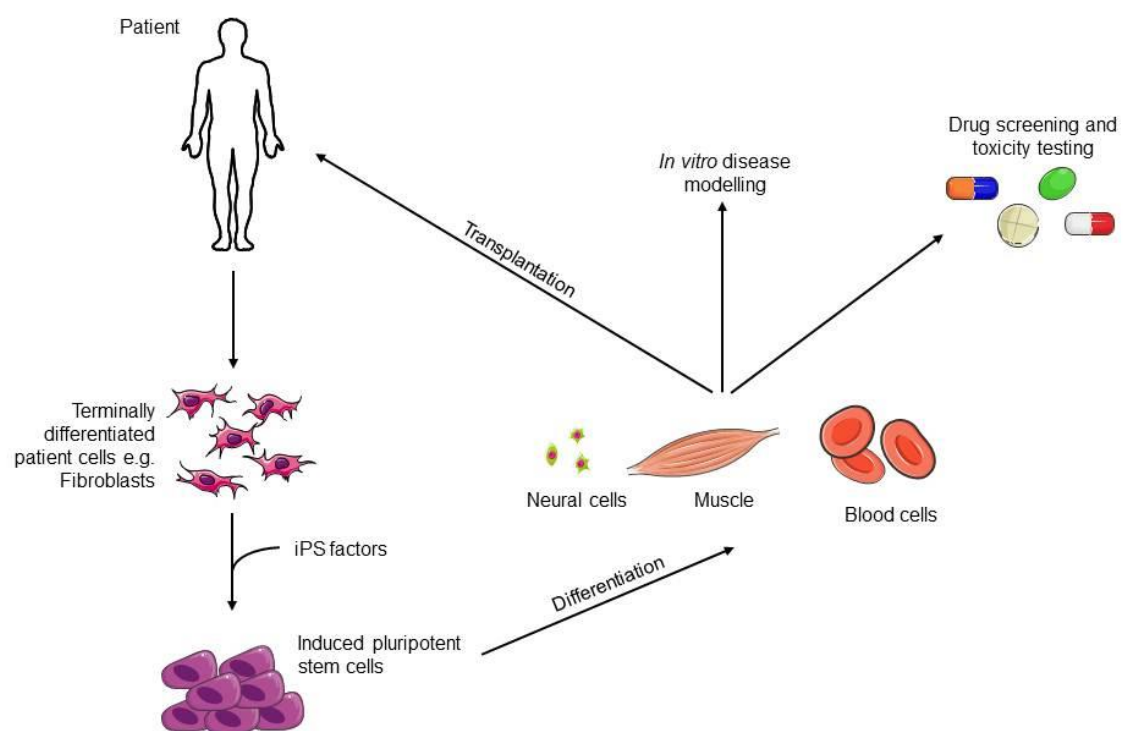


**Figure 1.3 – Derivation and potential uses of hiPSC.**

Human iPSC are generated via reprogramming of terminally differentiated adult cells e.g. fibroblasts, using a number of factors, including Oct4, Sox2, Klf4 and c-Myc. Once reprogrammed, they can be differentiated into any cell of the three germ layers. Differentiated cells then have a variety of uses including autologous cell therapies, *in vitro* disease modelling and drug screening.

### 1.5.3 Regulation of pluripotency

As stated previously, there are two main characteristics of pluripotent stem cells; their ability to self-renew indefinitely, and their pluripotency - the ability to generate cells from the mesoderm, ectoderm and endoderm. During *in vivo* development, pluripotency is a characteristic of the ICM of the preimplantation blastocyst, existing transiently. *In vitro*, however, these cells maintain their pluripotency indefinitely (section 1.5.1). Although well studied, the mechanisms governing pluripotency in these cells are still relatively poorly understood.

Thus far, research has identified a group of key transcription factors, playing essential roles in maintenance and control of pluripotency - Oct4, Sox2 and Nanog. Indeed, these factors are used in the reprogramming of somatic cells to a pluripotent state (section 1.5.2). Much of the original work was performed in mESCs, before the derivation of hESCs in 1998, with many of the mechanisms conserved between the two systems.

A member of the POU (Pit-Oct-Unc) transcription factor family and encoded by the *Pou5f1* gene, the role of Oct4 was first demonstrated during embryonic development in mice. *In vivo*, the expression of Oct4 mRNA and protein is restricted to pluripotent cells within the gastrulating embryo, and in germ cells (Rosner et al., 1990), and *in vitro* to ESCs (Okamoto et al., 1990), and was found to be rapidly downregulated during differentiation and specification of cells to specific germ layers (Okamoto et al., 1990, Pesce et al., 1998). Indeed, introduction of a homozygous Oct4<sup>-/-</sup> mutation results in peri-implantation lethality, and cells no longer progress to become mature ICM cells, revealing an essential role for Oct4 in the establishment of ICM pluripotency (Nichols et al., 1998). In hESCs *in vitro*, knockdown of Oct4 results in rapid changes in morphology, a marked reduction in growth rate and cell surface marker expression, including down regulation of SSEA3, SSEA4, and Tra1-60 (Hay et al., 2004, Matin et al., 2004). Cells deficient in Oct4 also show a clear upregulation of differentiation-associated markers, particularly genes associated with differentiation to trophoectoderm (Niwa et al., 2000, Matin et al., 2004), endoderm (Hay et al., 2004) and mesoderm (Rodriguez et al., 2007). Upregulation of Oct4 was also shown to induce changes in genes associated with mesodermal and endodermal differentiation (Niwa et al., 2000, Rodriguez et al., 2007), thus implying a critical amount of Oct4 is required to efficiently regulate pluripotency. Additionally, RNAi-induced silencing of Oct4 induced a change in >1000 genes, with both positive (e.g. pluripotency-associated TFs) and negative (e.g. mesoderm, endoderm and ectoderm-associated genes) regulation of different gene sets, many of which are implicated in the strict regulation of pluripotency (Babaie et al., 2007).

Oct4 interacts with other TFs, in order to activate and repress the expression of specific genes. One such protein, with which Oct4 can heterodimerise, is Sox2, a member of the SRY-related HMG box (Sox) family, which encodes transcription

factors with a single HMG DNA-binding domain. Similar to Oct4, Sox2 is expressed in the pluripotent cells in the developing embryo and in mESCs and hESCs *in vitro*. Inhibition of Sox2 expression results in embryonic lethality *in vivo*, as no ICM develops (Avilion et al., 2003), and in hESC in culture resulted in the loss of pluripotency, indicated by changes in morphology and surface marker expression (Fong et al., 2008). Furthermore, hESCs, in which Sox2 has been knocked down, are most likely to differentiate towards the trophectoderm, with significant upregulation in genes associated with this cell lineage (Adachi et al., 2010). Cells in which Sox2 was transiently overexpressed observed a very similar phenotype, suggesting that tight regulation of Sox2 is needed in order to maintain pluripotency.

The last of the three key transcription factors is Nanog. A homeodomain TF, Nanog was identified in mESCs, using *in silico* digital differentiation display, and found to be enriched in undifferentiated cells (Mitsui et al., 2003). mESC lacking Nanog acquired morphological changes, and differentiated towards extraendoderm lineages, and Nanog null embryos were epiblast deficient, showing that Nanog is essential for the maintenance of a pluripotent state (Mitsui et al., 2003). Hyslop et al. confirmed this in hESCs, whereby RNAi-mediated silencing of human Nanog induced activation of a number of extraembryonic endoderm associated genes such as GATA4 and GATA6, and trophoectoderm-associated genes (Hyslop et al., 2005). It was also shown that Nanog was expressed in the ICM of blastocyst stage pre-implantation human embryos, but not in some of the earlier-stage embryos, demonstrating a role for Nanog in the maintenance of pluripotency.

Most interestingly, genome-scale location analysis showed that main protein-coding and miRNA genes are targeted by all three of these transcription factors (Boyer et al., 2005). Oct4, Sox2 and Nanog were found to co-occupy the promoter region of 353 different genes, with binding sites occurring in close proximity. The three factors were found to regulate pluripotency by binding and transcriptionally activating genes with roles in pluripotency, including Oct4, Sox2, Nanog and STAT3, and binding and transcriptionally inactivating genes that promote development, such as HOXB1 and PAX6. The binding sites for the three TFs are in close proximity in co-occupied promoter regions, and the presence of Nanog was shown to increase the efficiency with which the Oct4-Sox2

heterodimer forms (Boyer et al., 2005, Rodda et al., 2005). Indeed, targeted down regulation of any one of these three factors results in a decrease in the expression of the other two. Thus, a synergy exists between these three factors, forming an autoregulatory loop (Figure 1.4), and working to regulate a large number of differentiation and pluripotency associated genes.

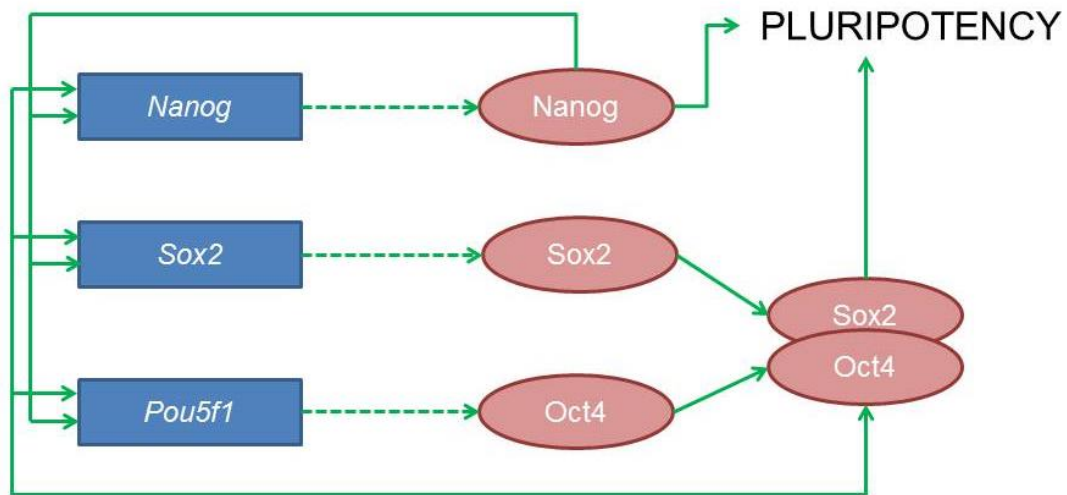


**Figure 1.4 –Pluripotency-associated transcription factors form an autoregulatory loop.** Schematic showing the autoregulatory function of the three main pluripotency-associated transcription factors. Blue boxes show genes, red circles show proteins/TFs, dotted arrows represent translation. Adapted from Boyer et al. (2005).

## 1.6 Endothelial differentiation of pluripotent stem cells

To date, there have been a large number of protocols published, demonstrating the ability of hESC and hiPSCs to differentiated into various cell types *in vitro*, including hepatocytes (Hannan et al., 2013), neural progenitors (Dhara et al., 2008), cardiomyocytes (Mummery et al., 2012) and smooth muscle (Cheung et al., 2011), and these have been extensively reviewed. However, in terms of vascular regeneration and stimulation of angiogenesis, hPSC-derived endothelial cells (hPSC-ECs) are thought to have the greatest potential, although methods of derivation still remain suboptimal.

### 1.6.1 *In vitro* differentiation of pluripotent stem cells to endothelium

Thus far, there have been a large number of publications describing protocols for the derivation of ECs from hPSCs, and these have been reviewed extensively (Descamps et al., 2012). Within this, there are two main approaches which have

been taken when generating hESC-ECs; 3D embryoid body (EB)-based culture systems and 2D monolayer culture systems.

Endothelial-associated genes, including Pecam-1 (CD31), VE-Cadherin (CD144) and CD34, are increased during spontaneous EB-based differentiation of hESCs (Levenberg et al., 2002). However, the efficiency of these differentiations is low, with only ~2% of cells expressing CD31 on their cell surface when analysed by FACS. Other studies showed that addition of VEGF into the system can increase the numbers of cells expressing CD31 and CD144 (Nourse et al., 2010), and although these cells can be isolated and cultured to obtain higher percentages of CD31<sup>+</sup> cells (Levenberg et al., 2002), more direct differentiation systems have been investigated to increase initial hPSC-EC generation efficiency.

3D EB-based direct differentiation protocols have been efficient in generating hESC-EC or hiPSC-ECs. These protocols are efficient, generating anywhere between 5-50% hPSC-ECs or hPSC-EC precursors in the first instance, before sorting and further culture to obtain cultures of 100% functional hPSC-ECs (Rufaihah et al., 2011, Costa et al., 2013, White et al., 2013). Rufaihah et al. used hiPSCs to generate cells which were positive for CD31, CD144, endothelial nitric oxide synthase (eNOS) and von Willibrand Factor (vWF), and were able to perform functionally as ECs in terms of acetylated low-density lipoprotein (acLDL) incorporation and tubule formation assays. When hiPSC-ECs were transplanted into a murine model of hind limb ischemia, there was a significant increase in both blood perfusion and capillary density, possibly as a result of detected higher levels of angiogenic cytokines, such as Angiopoetin-1 and VEGF-A and -C (Rufaihah et al., 2011). Another published EB-based EC differentiation assay involved the isolation of KDR<sup>+</sup> (CD309; VEGFR2) precursor cells on day 6 of differentiation. On day 6, approximately 44% of cells were positive for KDR, and only 12 or 13% of these expressed CD31 or CD144 respectively. When isolated cells were plated onto fibronectin (FN), cultured in endothelial medium, they exhibited a high proliferative capacity and after 14 days contained 97% or 93% CD144<sup>+</sup>CD31<sup>+</sup> cells when hESCs or hiPSCs were used respectively. Like the previous study, cells derived using this protocol displayed a cobblestone-like morphology, were functional in *in vitro* assays, and were able to form functional capillaries which linked with the endogenous circulatory system in a murine matrigel plug assay (White et al., 2013). Similarly, Costa et al. isolated



CD34<sup>+</sup>KDR<sup>+</sup> endothelial precursors on day 6 of an EB-based differentiation system, and continued their culture in a monolayer where, by day 12 of differentiation, cells uniformly expressed CD31, CD144, KDR, CD34 and other EC markers. Again, these cells were able to form tubules *in vitro* and incorporate acLDL, and the study also demonstrated a high degree of transcriptional similarity between hESC-ECs and post-natal ECs (Costa et al., 2013).

Recently, studies have focused on both increasing hESC-EC differentiation efficiency, i.e. the percentage of ECs generated, and scalability, i.e. the number of ECs generated. Although highly efficient, 3D EB-based culture systems are difficult to scale up to produce clinically relevant numbers of cells due to methods of EB formation, and because of this, monolayer-based protocols have also been investigated. An early 2D monolayer protocol used a co-culture system, whereby H9 hESCs were plated onto MEF and in hESC differentiation medium (Wang et al., 2007). Using this protocol, cells were shown to upregulate endothelial-associated CD31 and downregulate pluripotency-associated genes such as Oct4. However, the percentage of CD34<sup>+</sup> cells before selection was low (~5-10%), and the use of MEFs results in the inability of this protocol to be clinically transferrable. Kane et al. developed a fully defined, feeder- and serum-free 21 day monolayer-based protocol, yielding approximately 80% CD144<sup>+</sup>CD31<sup>+</sup> cells in the SA461 and SA121 hESC lines. These cells expressed high levels of endothelial-associated genes, and performed functionally in wound healing assays *in vitro* and in a murine model of hind limb ischemia *in vivo* (Kane et al., 2010). Recently, a method for simultaneous derivation of ECs and pericytes from hiPSCs was published (Orlova et al., 2014a, Orlova et al., 2014c). The protocol is a fully defined, monolayer-based protocol, allowing for easy large scale adaptation. Differentiation efficiency was consistent amongst different hPSC lines, including both hESC and hiPSC, with 10-30% of cells expressing CD31 (Pecam-1) and CD34, which were also shown to express comparable levels of other endothelial markers, including CD144 and CD309 (KDR; VEGFR2). The cells could be isolated and expanded, and analysis showed cells were able to perform functionally in an *in vivo* zebrafish xenograft model, and form interactions with pericytes - derived simultaneously - *in vitro*, promoting further differentiation of pericytes to smooth muscle cells. Furthermore, Patsch and colleagues also described a highly efficient monolayer-

based system for the derivation of ECs from hPSCs, which they developed alongside a protocol for VSMC differentiation (Patsch et al., 2015). Using two hESC lines (SA001 and Hues9) and two hiPSC lines, it was demonstrated that between 61.8% and 88.8% of generated cells were CD144<sup>+</sup>, when assessed by flow cytometry. Additionally, the CD144<sup>+</sup> cells also expressed other endothelial-associated cell surface markers, including CD31, KDR, CD34, CD105 and von Willibrand factor (vWF). The group also showed that the CD144<sup>+</sup> hPSC-ECs could be purified on day 6, using magnetic activated cell sorting (MACS), to obtain virtually pure (~96%) hPSC-EC cultures. Moreover, analysis of the transcriptional signature and metabolomics profiles revealed high levels of similarity between the generated CD144<sup>+</sup> hPSC-ECs and primary vascular cells.

Encouragingly, the studies described, using *in vivo* assays, showed largely positive results, with transplantation of hESC-ECs resulting in an increase in revascularisation and angiogenesis. These data are promising for the potential translation of these technologies into the clinic, as possible treatments for PAD and CLI.

### **1.6.2 *In vivo* development of the vasculature**

During embryonic development *in vivo* the vascular and hematopoietic systems are thought to be closely linked, with the first ECs originating from the lateral and posterior mesoderm, before migrating towards the yolk sac, where they differentiate into ECs and hematopoietic cells (HCs) (Medvinsky et al., 2011). The close relationship between the developing endothelial and hematopoietic systems led to the suggestions that they share a common mesodermal ancestor - the hemangioblast - and this common progenitor was observed *in vitro* in studies involving murine ESCs (Nishikawa et al., 1998). Another theory, however, suggests that the first hematopoietic stem cells (HSCs) are derived from ECs with hematopoietic potential, known as hemogenic endothelium (HE). *In vivo* studies have shown, using time lapse imaging in both mouse and zebrafish, that HCs originate from VE-Cadherin (CD144) expressing ECs in the dorsal aorta (Zovein et al., 2008, Bertrand et al., 2010, Boisset et al., 2010, Kissa et al., 2010). It has, however, been demonstrated that these two separate hypotheses can be merged to form a single linear developmental process, stating that hemangioblasts

generate HCs via the formation of intermediate hemogenic endothelial populations (Lancrin et al., 2009).

### 1.6.2.1 *In vitro* formation of hemogenic endothelium

As well as direct hPSC-EC differentiation systems, there have been a number of publications showing simultaneous derivation of ECs and hematopoietic cells through a common HE progenitor, mimicking conditions *in vivo*.

Originally, the Vodyanik group had demonstrated the ability of both hESCs and hiPSCs to differentiate to EC and hematopoietic cells simultaneously *in vitro* (Vodyanik et al., 2006, Choi et al., 2009). Cells were co-cultured with mouse bone marrow stromal cell line OP9 for 8 days, after which time both CD43<sup>+</sup> hematopoietic cells and CD31<sup>+</sup>CD43<sup>-</sup> ECs were detected. Recently, Choi et al. attempted to identify and classify HE populations present within the OP9 hPSC differentiation system (Choi et al., 2012). By day 5 of differentiation 3 distinct CD144<sup>+</sup> cell populations were identified; CD144<sup>+</sup>CD235a<sup>+</sup>CD43<sup>+</sup>CD41<sup>+</sup>, CD144<sup>+</sup>CD73<sup>+</sup> and CD144<sup>+</sup>CD73<sup>-</sup>CD235a<sup>-</sup>CD43<sup>-</sup>. All 3 of these subsets exhibited a similar endothelial phenotype, and were functional, capable of acLDL uptake. CD117 (c-Kit), a angiohematopoietic progenitor marker, was expressed at different levels in the different CD144<sup>+</sup> subpopulations, with the highest expression in the CD144<sup>+</sup>CD73<sup>+</sup> cells, the lowest in the CD144<sup>+</sup>CD235a<sup>+</sup>CD43<sup>+</sup>CD41<sup>+</sup> cells, and an intermediate level in the CD144<sup>+</sup>CD73<sup>-</sup>CD235a<sup>-</sup>CD43<sup>-</sup> cells. Further functional and phenotypic analysis allowed for their definition of the following EC populations; HE progenitors are CD144<sup>+</sup>CD73<sup>-</sup>CD235a<sup>-</sup>CD43<sup>-</sup>CD117<sup>intermediate</sup> with primary endothelial characteristics but can generate blood and endothelial cells, and CD144<sup>+</sup>CD73<sup>+</sup>CD235a<sup>-</sup>CD43<sup>-</sup> non-HE progenitors, which have all the functional and phenotypic characteristics of endothelial cells. Extensive functional characterisations of EC populations, including *in vivo* assays, were, however, not performed within this study.

The assay developed by Choi et al. involves co-culture with the OP9 mouse bone marrow stromal cell line, introducing an undefined factor into the system. Recently, a system, using fully defined conditions, generating both distinct hemogenic and arterial vascular endothelium has been published (Ditadi et al., 2015), although cells are cultured on feeders before being transferred to

Matrigel - an undefined cell matrix - 24 hrs prior to differentiation. In this protocol, a previously defined CD34<sup>+</sup>CD43<sup>-</sup> population, with the additional cell surface profile of CD31<sup>+</sup>CD144<sup>+</sup>KDR<sup>+</sup>CD117<sup>low</sup> and the ability to generate T-lymphoid, erythroid and myeloid cells (Kennedy et al., 2012), were isolated and cultured on Matrigel in hematopoietic supportive conditions. It was demonstrated that these cells underwent endothelial to hematopoietic transition (EHT) and formed CD45<sup>+</sup> hematopoietic cells, which were then able to undergo further definitive hematopoiesis. Definitive venous and arterial ECs were identified from the CD34<sup>+</sup>CD43<sup>-</sup> fraction as CD73<sup>hi</sup>CD184<sup>-</sup> and CD73<sup>med</sup>CD184<sup>+</sup> fractions respectively. Both of these cell types were shown to form functional vessels when transplanted into immunocompromised mice, subcutaneously in a Matrigel plug.

Combinations of direct and indirect differentiation systems are valuable tools for studying the mechanisms driving development of ECs *in vitro* and *in vivo*.

## 1.7 MicroRNAs

The historical central dogma of molecular biology explains that DNA codes for mRNAs, which in turn code for the specific amino acid sequences making up all of the proteins existing with a cell. Protein-coding genes, however, comprise only a very small fraction of the genome (Lander et al., 2001). A large portion of the remaining DNA codes for non-coding and regulatory RNAs, including ribosomal RNAs (rRNA), transfer RNAs (tRNA), small nucleolar RNAs (snoRNA), small interfering RNAs (siRNA), long-non coding RNAs (lncRNA) and microRNAs (miRNA; miR) - an extensively studied set of regulatory RNAs.

First discovered as regulators of development in *C.Elegans* (Lee et al., 1993, Lee et al., 2001), miRNAs have been shown to regulate a large number of important biological processes (Bartel, 2004). Existing as single stranded RNA molecules, approximately 22 nucleotides (nt) in length, miRNAs are non-coding RNAs, which exert post transcriptional control on the expression of their specific target messenger RNAs (mRNAs) (Wightman et al., 1993). It is hypothesised that there are over 1,000 miRNAs existing within the human genome, each one working to control the translation of a whole network of mRNAs. Since their discovery in 1993, large numbers of miRNAs and their functions in various processes have

been identified and described, with the current version of miRbase, the public repository for all published miRNA sequences, containing over 24,500 miRNA loci, processed to produce over 30,000 mature miRNA products from 206 different species (Kozomara et al., 2014). Patterns of miRNA expression are generally tissue specific, and dysregulation of miRNAs can lead to cellular dysfunction. Indeed, miRNAs have been implicated in a number of different diseases, including cancer (Iorio et al., 2012) and metabolic diseases (Rottiers et al., 2012), as well as CVD (Ono et al., 2011).

### 1.7.1 miRNA biogenesis

Although it was originally believed miRNAs would be transcribed by RNA polymerase III, in a similar fashion to other small RNAs such as tRNAs and the small nuclear RNA (snRNA) U6, it was subsequently discovered that miRNAs are transcribed in the nucleus by RNA polymerase II (Cai et al., 2004, Lee et al., 2004). This initial transcript is known as the primary miRNA (pri-miRNA), and contains an imperfect hairpin approximately 80nt in length, which in turn contains the mature miRNA sequence (Lee et al., 2002), flanked by single stranded RNA regions. It has also been demonstrated that multiple miRNA stem loops, existing in close proximity within the genome, may be transcribed together as one pri-miRNA (Mourelatos et al., 2002, Baskerville et al., 2005), known as a miRNA cluster. Recently, however, the existence of pri-miRNAs containing only a single miRNA has also been shown, suggesting that splicing may play a role in the uncoupling of clustered miRNAs previously thought to be co-transcribed and co-expressed (Ramalingam et al., 2014). Pri-miRNAs can be very large (>1kb) and can contain both a 5' cap and poly(A) tail, much like classical mRNAs.

Once transcribed, the pri-miRNA must undergo further processing in the nucleus. This processing is performed by Drosha, an RNase III type enzyme (Lee et al., 2003), along with its cofactor DiGeorge syndrome critical region gene 8 (DGCR8; known as Pasha in flies and worms) (Gregory et al., 2004, Han et al., 2004, Landthaler et al., 2004), a double stranded RNA binding protein, shown to play a major role in the recognition and binding of pri-miRNAs by this microprocessor complex. The DGCR8 protein contains two double-stranded RNA-binding domains (dsRBDs), which have previously been shown to bind the pri-

miRNA (Han et al., 2006). More recently, it has also been demonstrated that the DGCR8 protein also uses a heme-binding domain to directly bind pri-miRNAs at the basal and apical junction of the hairpin (Quick-Cleveland et al., 2014). Once bound, the Drosha-DGCR8 microprocessor complex cleaves the hairpin ~11nt from the ds-ssRNA junction (Zeng et al., 2005), resulting in a short miRNA precursor, with stem loop structure and ~70nt in length, termed pre-miRNAs. Cleavage of the pri-miRNA by Drosha results in a 2nt overhang on the 3' end of the stem loop, thereby allowing for recognition by exportin 5 (EXPO5) (Lee et al., 2002, Lund et al., 2004). EXPO5 binds pre-miRNAs, in the presence of its co-factor Ran-GTP, to allow for their export from the nucleus to the cytoplasm for further processing (Yi et al., 2003, Bohnsack et al., 2004).

Once in the cytoplasm, the pre-miRNAs are then bound by the RNA induced silencing complex (RISC)-loading complex (RLC), consisting of Argonaute protein 2 (Ago2), Dicer - another RNase III endonuclease (Grishok et al., 2001, Hutvagner et al., 2001, Knight et al., 2001) previously shown to be involved in generating small interfering RNAs (siRNAs) (Bernstein et al., 2001), and the cofactors TAR RNA binding protein (TRBP) and protein activator of ptk (PACT) (Chendrimada et al., 2005, Lee et al., 2006, MacRae et al., 2008).

Human Dicer (hDicer) recognises the 5' phosphate at the end of the pre-miRNA stem loop, as well as the 2nt overhang at the 3' end (Park et al., 2011, Feng et al., 2012). Once bound, Dicer cleaves both strands of the duplex, to produce an imperfect double-stranded mature miRNA duplex ~22nts in length. Dicer then dissociates from the complex, and the mature miRNA is transferred to the Ago2 protein and incorporated into the RNA-induced silencing complex (RISC), a process mediated by heat shock protein 90 (HSP90) in humans. The HSP90-Ago2 complex hydrolyses ATP, keeping the Ago2 in an open state to allow for the binding of the dsmiRNA molecule (Iwasaki et al., 2010, Johnston et al., 2010).

The dsmiRNA duplex is then unwound and a single strand of the duplex targeted for degradation. Although the mechanism behind this unwinding is still unclear, recent evidence suggests that the amino-terminal (N) domain of the Ago2 protein supports this step (Kwak et al., 2012). It was originally shown that the strand of the duplex containing the less stable 5' end was preferentially loaded into the Ago2 protein, with the other 'passenger' or 'star' (miRNA\*) strand

targeted for degradation (Khvorova et al., 2003). However, recent studies have shown important functional roles for these classical miRNA\* strands, suggesting that they are also actively incorporated into the RISC (Yang et al., 2011, Shan et al., 2013, Yang et al., 2013, Mitra et al., 2015). This has led to new nomenclature for miRNAs, with miRNA names suffixed with either -3p or -5p to denote their location within the pre-miRNA stem loop.

Recently, it has also been suggested that a number of miRNAs may be processed by Dicer-independent pathways. miR-451 was shown to be produced through an alternative pathway, whereby pre-miRNA-451 is recognised, loaded and cleaved directly by Ago2 (Cheloufi et al., 2010, Cifuentes et al., 2010, Yang et al., 2010). This yields a ~30nt precursor, which is then further processed to form the 23nt miR-451. The mechanism of this method of processing is still poorly understood, although recent data suggests a role for eIF1A, which may augment Ago2-mediated miRNA-guided RNAi and Dicer-independent miRNA biogenesis via direct interaction with Ago2 (Yi et al., 2015).

The classical miRNA biogenesis process is summarised in Figure 1.5.

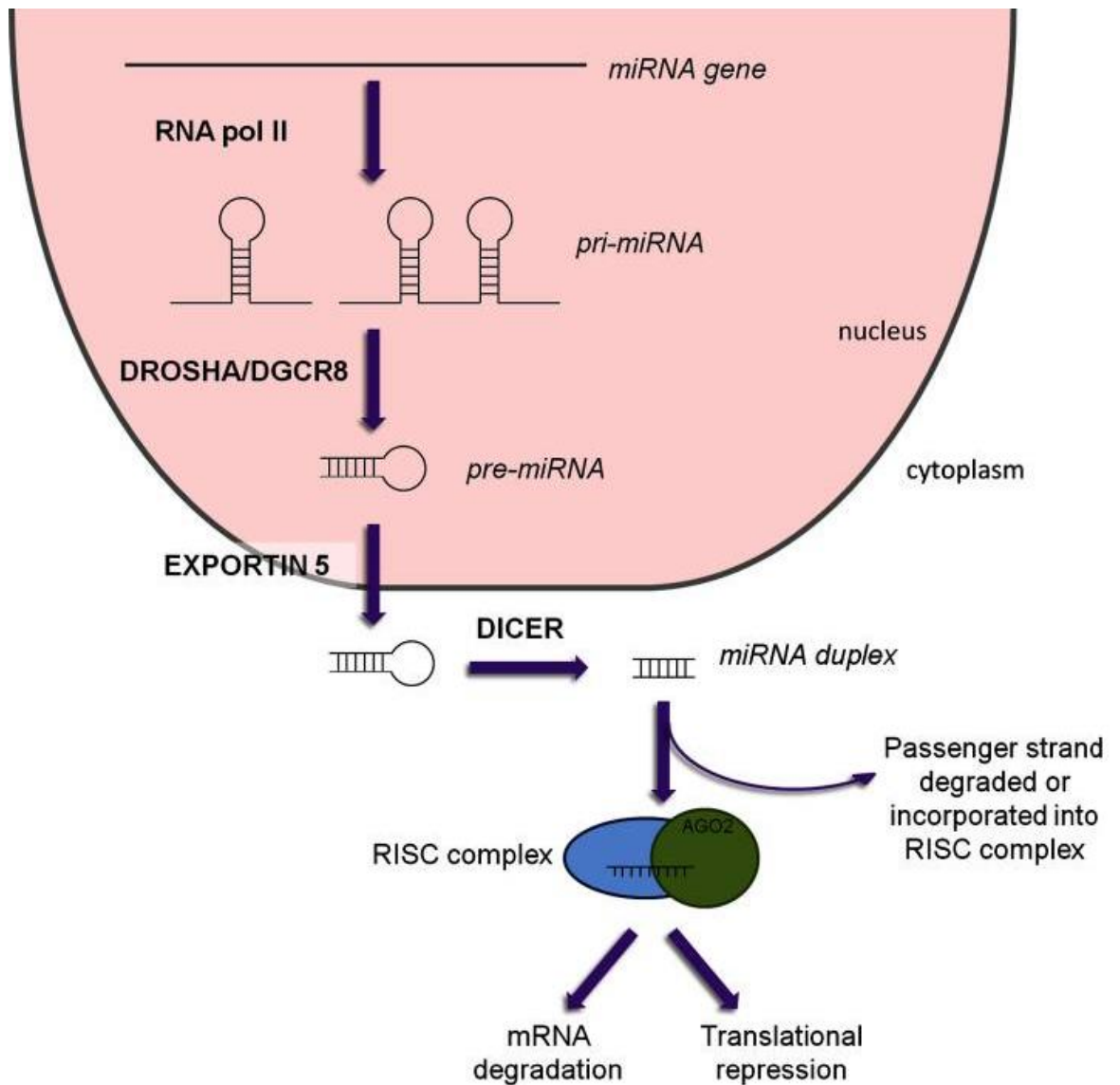


**Figure 1.5 – MiRNA biogenesis**

MiRNAs are transcribed in the nucleus and processed by Drosha and DCGR8 before being exported to the cytoplasm. Once in the cytoplasm pre-miRNAs undergo further processing by Dicer to form a double-stranded miRNA duplex. A single strand of this miRNA duplex is then incorporated into RISC, which then acts to inhibit mRNA expression, either by inhibition of translation or by targeting the mRNA for degradation (Grant et al., 2013).



### 1.7.2 miRNA function

Once incorporated into the RISC, miRNAs work to guide the Ago2 to specific target mRNAs. Often, the specific miRNA binding sites are located within the 3' untranslated region (UTR) of the gene, a phenomenon which was first observed in *C.Elegans*, when it was realised that the *lin-14* mRNA contained multiple conserved sites, which were complementary to the small RNA *lin-4* (Lee et al., 1993, Wightman et al., 1993). The binding of the miRNA to the mRNA target is determined by a region known as the miRNA 'seed' sequence - nucleotides 2-8 at the 5' end of the mature miRNA, which act to control target specificity (Lewis et al., 2003). Once bound the miRNA-RISC acts to control the expression of mRNAs in one of 2 ways; either inhibition of translation, or targeting of the mRNA for degradation (Guo et al., 2010), depending on the level of complementarity between the seed sequence and the binding site in the 3' UTR. In cases where the Watson-Crick base pairing between the miRNA seed and mRNA target sequence is perfectly complementary, Ago2 can catalyse mRNA cleavage. Other AGO proteins, which can also be incorporated into the RISC (Ago1, 2 and 4), do not possess this catalytic activity but can still be involved in miRNA-guided gene repression via the inhibition of translation. Recent studies have suggested that translational inhibition is the main form of repression at early time points, with mRNA degradation contributing more at later time points (Bethune et al., 2012).

As well as the Ago2 protein, miRNA-guided repression of mRNAs is mediated and assisted by a number of other proteins. The GW182 protein has been shown to directly interact with Ago proteins, via an N domain containing multiple glycine-tryptophan (GW) repeats. GW182 also contain a bipartite silencing domain (SD) within their carboxy-terminal and mid-regions. This SD has been shown to be required for efficient silencing and is thought to function through an interaction with poly(A)-binding protein C (PABPC), a protein which binds to the poly(A) tail at the 3' end of the target mRNA (Fabian et al., 2009, Zekri et al., 2009). This interaction has been proposed to induce silencing of the target mRNA in two different ways. Firstly, GW182 binding to PABPC inhibits the interaction of PABPC with the cap-binding complex, preventing circularisation of the mRNA, and therefore inhibiting translation. Recently, however, it has also been proposed that PABPC and the poly(A) tail may be involved in stimulating the

interaction between the Ago-GW complexes and the target mRNA, supported by evidence which shows gene silencing efficiency correlates with the length of the poly(A) tail and the number of PABPCs associated (Moretti et al., 2012). Although its main function is in the mediation of translational repression, it has also been hypothesised that GW182 may be involved in the destabilisation, and subsequent decay, of the target mRNA, via recruitment of the deadenylase CCR4-NOT complex (Behm-Ansmant et al., 2006, Wu et al., 2006, Piao et al., 2010).

Using both biochemical and proteomic approaches, further studies have also identified a number of proteins thought to interact with AGO proteins (Meister et al., 2005). Proteins can be indirectly associated with AGO proteins through binding to the same mRNA, subsequently affecting the miRNA-RISC binding and gene repression. One example of this is Importin 8 (IPO8). IPO8 was identified to be an AGO binding partner, and two distinct roles for this protein have subsequently been elucidated. Firstly, IPO8 was shown to be involved in the loading of Ago2-miRNA complexes onto target mRNAs in the cytoplasm (Weinmann et al., 2009). Secondly, IPO8 controls the import of mature miRNAs into the nucleus, via its association with Ago2 in the miRNA-RISC (Wei et al., 2014). Management of this import may suggest a role for IPO8 in the control of miRNA-guided repression of miRNA biogenesis.

While most miRNA-mediated gene repression is induced through binding to the 3' UTR of the target mRNAs, studies have also shown that miRNAs can bind to the 5' UTR or in coding regions in order to exert their effect (Lytle et al., 2007). Interestingly, it has also been shown that miRNAs can also upregulate their targets, for example miR-10a, which has been shown to bind to the 5'UTR of ribosomal protein mRNAs to enhance their translation (Orom et al., 2008). This data suggests more complex mechanisms of miRNA regulation than originally hypothesised.

## **1.8 Endothelial-associated miRNAs**

As an important component of the vascular wall, endothelial cells (EC) play a major role in maintenance of vascular integrity, particular with relation to

angiogenesis and wound repair post-injury, as well as in vasculogenesis during *in vivo* development and embryogenesis (Wang et al., 2008c).

As in most cell types, miRNAs have been implicated in EC function and proliferation, as well as in the regulation of angio- and vasculogenesis. Global reduction of miRNAs, via conditional knockdown of the miRNA processing Dicer using siRNAs *in vitro*, altered the expression of several important regulators of endothelial biology and angiogenesis including vascular endothelial growth factor receptor 2 (VEGFR2; KDR) and endothelial nitric oxide synthase (eNOS), as well as reducing proliferation and tubule formation capacity (Suarez et al., 2007). *In vivo*, Dicer silencing was also shown to reduce postnatal angiogenesis in response to angiogenic cytokines, such as VEGF (Suarez et al., 2008). Combined transient silencing of both Dicer and Drosha processing enzymes reduced the sprout forming and angiogenic properties of ECs, although only silencing of Dicer had significant effects on angiogenic potential *in vivo* (Kuehbacher et al., 2007). Several miRNAs have been identified to play a role in the regulation of function, proliferation and growth of vascular ECs (Jakob et al., 2012). These include miR-126, miR-10a, the let-7 cluster, the pro-angiogenic miR-17-92 cluster and the anti-angiogenic miR-221 and -222. MiRNAs identified to play key roles in the regulation of angiogenesis may be important therapeutic targets in the treatment of a range of ischemic diseases, as well as in the regulation of angiogenesis during cancer and tumour progression.

### **1.8.1 miR-126**

One of the most studied and extensively characterised EC miRNAs is miR-126, the -3p arm of the miR-126 stem loop. Early miRNA profiling studies found that miR-126 was enriched in tissues with a high vascular component, and expression patterns in zebrafish also showed the expression of miR-126 to be confined to the vascular system (Lagos-Quintana et al., 2002, Wienholds et al., 2005). Studies showed that miR-126 was expressed in primary human umbilical vein ECs (HUVEC), as well as in a number of EC lines (Harris et al., 2008, Wang et al., 2008c), and miR-126 was also found to be the most highly enriched miRNA in ECs generated from differentiating mESC (Fish et al., 2008). Generation of miR-126 null mice resulted in approximately 40% embryonic lethality, exhibiting a large number of vascular defects, including severe systemic oedema, haemorrhage

and vessel rupture, and knockdown in zebrafish using pri-miR-126-specific morpholinos resulted in compromised blood vessel integrity, haemorrhages and compromised endothelial tube formation. Taken together, this data suggested a role for miR-126 in the maintenance of endothelial and vascular integrity during development. Knockdown of miR-126 also resulted in a decrease in angiogenesis during *ex vivo* and *in vivo* assays. To exert its angiogenic effects, miR-126 was also shown to augment MAP kinase pathway activation in response to angiogenic factors such as FGF and VEGF *in vitro*, with knockdown of the miRNA resulting in a reduction in FGF and VEGF-mediated migration, possibly through defective reorganisation of the actin cytoskeleton (Fish et al., 2008, Wang et al., 2008c). It was subsequently demonstrated that miR-126 exerts its angiogenic effects through the targeting of the sprouty-related protein Spred-1 (Figure 1.6), a negative regulator of the Ras/MAP kinase pathway (Wakioka et al., 2001), and phosphoinositide-3-kinase regulatory subunit 2 (PIK3R2), a negative regulator of PI3 kinase (Ueki et al., 2003, Sessa et al., 2012). A role for miR-126 in the regulation of vascular inflammation has also been elucidated, via its targeting and repression of vascular cell adhesion molecule-1 (VCAM-1), an intercellular adhesion molecule expressed by ECs. VCAM-1 expression is upregulated during vascular inflammation, where it functions to mediate EC:leukocyte adhesion. Reduced expression of miR-126, in tumour necrosis factor- $\alpha$  (TNF- $\alpha$ ) stimulated ECs, increases the expression of VCAM-1, in turn enhancing leukocyte adherence and, ultimately, vascular inflammation (Harris et al., 2008).

MiR-126 is located within intron 7 of epidermal growth factor-like domain 7 (Egfl7), a gene which is highly expressed in ECs, and the expression of both strands of the miR-126 stem loop (miR-126-3p and -5p) mirrors the expression of Egfl7 (Harris et al., 2010). This suggested that miR-126 is processed from the pre-mRNA-Egfl7 transcript. A 5' region upstream of the Egfl7/miR-126 locus was then found to regulate expression of miR-126, and *in silico* analysis subsequently revealed two Ets binding sites (EBS) within this region. The Ets factors are a family of transcription factors, and several members, including Ets-1 and -2, have been shown to play important roles in vasculo- and angiogenesis (Dejana et al., 2007). Ets-1 and -2 were found to bind to the Egfl7/miR-126 5' region to activate transcription in ECs, therefore suggesting that these transcription

factors play an important role in the regulation of miR-126 expression and, therefore, the regulation of it angiogenic affects (Harris et al., 2010).

### **1.8.2 miR-17-92 cluster**

The miR-17-92 cluster, consisting of miR-17, -18a, -19a/b, -20a and -92a, has also been extensively studied in the context of ECs and angiogenesis. Originally, it was discovered that this cluster plays a role in the augmentation of tumour angiogenesis. Expression of this cluster was found to be upregulated in colonocytes co-expressing K-Ras and c-Myc, two proto-oncogenes. In this system the miRNAs target the anti-angiogenic thrombospondin-1 (Tsp1) and the related protein connective tissue growth factor (CTGF), to cause an increase in angiogenesis, and cells transduced with the miR-17-92 cluster formed larger, better-perfused tumours (Dews et al., 2006). In contrast to this, however, Doebele et al. demonstrated that the overexpression of individual members of the cluster, specifically miR-17, -18a, -19a and -20a, resulted in reduced angiogenic sprouting, whereas inhibitors of the same miRNAs caused an increase in angiogenesis *in vitro*, suggesting an anti-angiogenic role for this cluster (Doebele et al., 2010). This ties in with previous work showing that miR-92a targets several proangiogenic proteins, including integrin subunit alpha 5, to exert an anti-angiogenic effect, with overexpression of this miRNA blocking angiogenesis *in vivo* and *in vitro* (Bonauer et al., 2009). More recently, it was shown that histone deacetylase 9 (HDAC9) displays a proangiogenic affect, regulated through the transcriptional repression of the miR-17-92 cluster (Kaluza et al., 2013). Taken together, this data suggests a varied role for the miR-17-92 cluster in the context of EC function and angiogenesis.

### **1.8.3 miR-210**

Reduced miR-210 expression has been shown to inhibit EC growth and induce apoptosis, suggesting a proangiogenic role for this miRNA. In hypoxic conditions, it was found that the level of miR-210 was increased in HUVECs when compared to cells in normoxic conditions (Fasanaro et al., 2008). In normoxic ECs *in vitro*, overexpression of miR-210 simulated the formation of capillary-like structures on matrigel, and VEGF-mediated migration. Knockdown of this miRNA inhibited these same functions, and also inhibited cell growth and caused an increase in

apoptosis. *In silico* analysis revealed Ephrin-A3 (EFNA3), a gene post-transcriptionally downregulated by hypoxia, as a potential target for miR-210, and luciferase assays using the 3'UTR of the EFNA3 mRNA confirmed this. Downregulation of this gene was proven to be necessary for miR-210-regulated angiogenesis. Lou et al. further elucidated the mechanism of miR-210 and its role in angiogenesis by investigating the role of this microRNA in regulating angiogenesis in response to brain ischemic injury. miR-210 was significantly upregulated in adult rat ischemic brain cortexes *in vivo*, where the expression of Notch-1 signalling molecules, which facilitate the migration of endothelial cells, were also increased. Using lentiviral-mediated overexpression, it was shown that miR-210 activated the Notch signalling pathway, facilitating the migration of endothelial cells and inducing *in vitro* capillary formation (Lou et al., 2012). Recently, this has also been shown in the normal adult mouse brain, where overexpression of miR-210, using stereotactic injection of a lentiviral vector, increased neurogenesis and angiogenesis, associated with a local increase in the levels of VEGF (Zeng et al., 2014). Overall, data suggests that miR-210 could be used as a therapy, or a therapeutic target for the modulation of angiogenesis in the treatment of ischemic diseases. Indeed, miR-210 has been used as a therapy *in vivo* to enhance wound healing, and tissue repair, processes in which angiogenesis plays a key role (Kawanishi et al., 2014, Usman et al., 2015).

#### **1.8.4 miR-10**

Interestingly, it was also suggested that miR-10 may play a role in angiogenesis, after it was discovered that heparin, an anti-thrombotic drug, impairs angiogenesis through the inhibition of miR-10b, therefore inducing upregulation of its mRNA target HoxD10 (Shen et al., 2011). Indeed, further investigation showed an increase in the expression of miR-10a in CD144<sup>+</sup>VEGFR2<sup>+</sup> ECs generated from mESCs when compared to CD144<sup>-</sup>VEGFR2<sup>-</sup> non-ECs (Hassel et al., 2012). Knockdown of all four miR-10 isoforms (a-d) during zebrafish development resulted in an impairment in angiogenesis and the development of the intersegmental vessels, whereas overexpression lead to enhanced angiogenic potential *in vivo*. *In vitro* experiments demonstrated the direct targeting of the 3'UTR of Flt1, also known as VEGFR1, and its soluble splice variant sFlt1 by miR-10, with miR-10 depletion leading to an increase in Flt-1 expression both *in vivo*

and *in vitro*. Flt-1 binds VEGF and is thought to function to inhibit angiogenesis by sequestering VEGF to prevent binding to VEGFR2 (Hassel et al., 2012).

### 1.8.5 miR-221 and -222

Just as important as miRNAs with potential proangiogenic functions, miRNAs with anti-angiogenic functions may also be useful targets in the control of angiogenesis in a disease setting, such as in the regulation of tumour angiogenesis during cancer, as well as in cardiovascular and ischemic diseases. Similarly to those involved in the positive regulation of angiogenesis, anti-angiogenic miRNAs function via the targeting of an array of angiogenic-associated mRNAs, as previously described in section 1.8.2 (Figure 1.6).

Located intergenically, miR-221 and -222 are transcribed as a cluster, and have been shown to share an identical seed sequence. Both of these miRNAs have been described as anti-angiogenic, and were shown to regulate c-kit, the receptor for stem cell factor (SCF), at the protein level (Poliseno et al., 2006). SCF is an angiogenic factor, which has been shown to promote survival, migration and capillary formation of HUVECs *in vitro* (Matsui et al., 2004). Overexpression of miR-221 and -222 caused a reduction in survival, migration and capillary formation *in vitro* mediated through a reduction in the levels of c-kit. Another study showed that miR-221 and -222 regulate the expression of eNOS, with overexpression of these miRNAs inhibiting the increase in eNOS expression observed after Dicer knockdown (Suarez et al., 2007).

It has also been shown that miR-221 indirectly up-regulates GAX, a potential master regulator of EC angiogenic phenotype (Gorski et al., 1993), in order to inhibit angiogenesis (Chen et al., 2010). It was hypothesised that this upregulation was mediated through the downregulation of an intermediate protein, and this was subsequently discovered to be ZEB2, a zinc-finger nuclear factor which primarily acts as a transcriptional repressor (van Grunsven et al., 2003).

### 1.8.6 Other notable pro- and anti- angiogenic miRNAs

Similarly to miRNAs already mentioned, other angiogenesis-regulating miRNAs also function via the direct or indirect targeting of growth factors and their

receptors (Figure 1.6). One such miRNA is the proangiogenic miR-296, which was found to be upregulated when human brain microvascular ECs were treated with angiogenic factors, and also shown to be expressed at higher levels in primary highly angiogenic ECs derived from human brain tumours, when compared to normal brain endothelial cells (Wurdinger et al., 2008). In this context miR-296 was found to target hepatocyte growth factor-regulated tyrosine kinase substrate (HGS), a protein involved in the mediation of the degradation of a number of growth factor receptors, including platelet derived growth factor receptor  $\beta$  and VEGFR2, therefore increasing the levels of signalling by angiogenic factors (Takata et al., 2000, Ewan et al., 2006).

Moreover, miR-15b and -16, along with miR-20a and -20b, are also thought to exert their antiangiogenic effects via the targeting of VEGF (Hua et al., 2006). Although the study was performed in a human nasopharyngeal carcinoma cell line, all of four of these miRNAs were downregulated in response to hypoxia, in contrast to the concomitant upregulation of VEGF. As well as VEGF, other angiogenic factors were also found to be targets of all or some of these miRNAs, including COX2, c-MET and uPAR. These data suggest a role for these four miRNAs in the regulation of angiogenesis, and this has been supported by evidence in a number of other studies (Sun et al., 2013, Xue et al., 2015). In the same study which originally identified the previous four miRNAs (-15, -16, -20a and -20b), miR-378 was also shown to regulate the expression of VEGF (Hua et al., 2006), although not through direct binding to its predicted 3' UTR target sequence. Further studies showed a proangiogenic role for miR-378, through its propensity to cause an increase in cell survival and a decrease in apoptosis, in a similar way to miR-210 and the miR-17-92 cluster (Lee et al., 2007). In the U87 human cancer cell line, miR-378 was shown to target both Suppressor of Fused (SuFu) and Tumour Suppressor Candidate 2 (Fus-1), two tumour suppressor genes, to control blood vessel growth and tumour survival. These studies were all performed using cancer cell lines, however, and as stated previously, miRNA expression patterns and profiles are tissue and cell-type specific. The angiogenic-regulating behaviours of these miRNAs have not yet been recapitulated in the context of the vasculature and human ECs.

MiR-100, a miRNA expressed in both ECs and vascular smooth muscle cells (VSMCs), was also found to be downregulated during hypoxia, much like miR-15



and -16. *In vivo*, miR-100 was significantly downregulated after the induction of hind limb ischemia in mice, and it was found to control angiogenic sprouting and the proliferation of vascular cells *in vitro* (Grundmann et al., 2011). Mammalian target of rapamycin (mTOR), a gene previously demonstrated to be involved in angiogenesis and proliferation of ECs in response to hypoxia (Humar et al., 2002), was found to be a direct target of miR-100 (Wang et al., 2008a) and this was confirmed in the context of ECs, indicating a role for this miRNA in the negative regulation of EC angiogenesis. More recently, this has also been shown in the context of graft-versus-host disease (GvD), whereby miR-100 antagonism increased neovascularisation and, therefore, increased disease severity (Leonhardt et al., 2013).

A global knock out of miRNA processing enzymes in human ECs also lead to the identification of miR-27b and let-7f as possible proangiogenic miRNAs (Kuehbacher et al., 2007). Knockdown of Dicer and Drosha processing enzymes lead to a reduction in the expression of these two miRNAs, shown to be highly expressed in ECs, and treatment of cells with selective inhibitors of miR-27b and let-7f caused a decrease in sprout forming capacity. *In silico* analysis revealed Tsp1, an antiangiogenic protein also shown to be a target of the miR-17-92 cluster (Section 1.8.2), as a predicted target of let-7f. Dicer and Drosha knockdown caused a significant increase in the levels of Tsp1, although specific knockdown of let-7f only triggered a small increase in the levels of Tsp1, confirming that this antiangiogenic protein may be a shared target of a number of important proangiogenic miRNAs.

Finally, GAX, previously shown to be indirectly regulated by the antiangiogenic miR-221 (Section 1.8.5), was verified as a direct target of miR-130a. As stated previously, GAX has been implicated in the inhibition of angiogenesis in vascular ECs, and suppression of this gene by miR-130a suggests a role in the positive regulation of angiogenesis for this miRNA. In the same study, a genome wide search for other genes containing at 3' UTR miR-130a binding site also identified another antiangiogenic homeobox gene, HOXA5, enhancing the proposal that miR-130a may play an important role in the regulation of the angiogenic phenotype in vascular ECs (Chen et al., 2008b).

Taken as a whole, the studies and findings reported show a significant role for miRNAs in the control of vascular EC function and angiogenic phenotype. Utilising knowledge gained from these studies may be critical in the development of novel therapies, not only for the treatment of ischemic diseases, such as PAD, CLI, CHD and stroke, but also in the context of cancer and regulation of tumour angiogenesis. It is now essential to elucidate exact mechanisms of action, in order to determine crucial signalling pathways and whether it is preferable to directly target key miRNAs, or the pathways which they regulate.

The function and mechanisms of a number of angiogenesis-regulating miRNAs are summarised in figure 1.4.

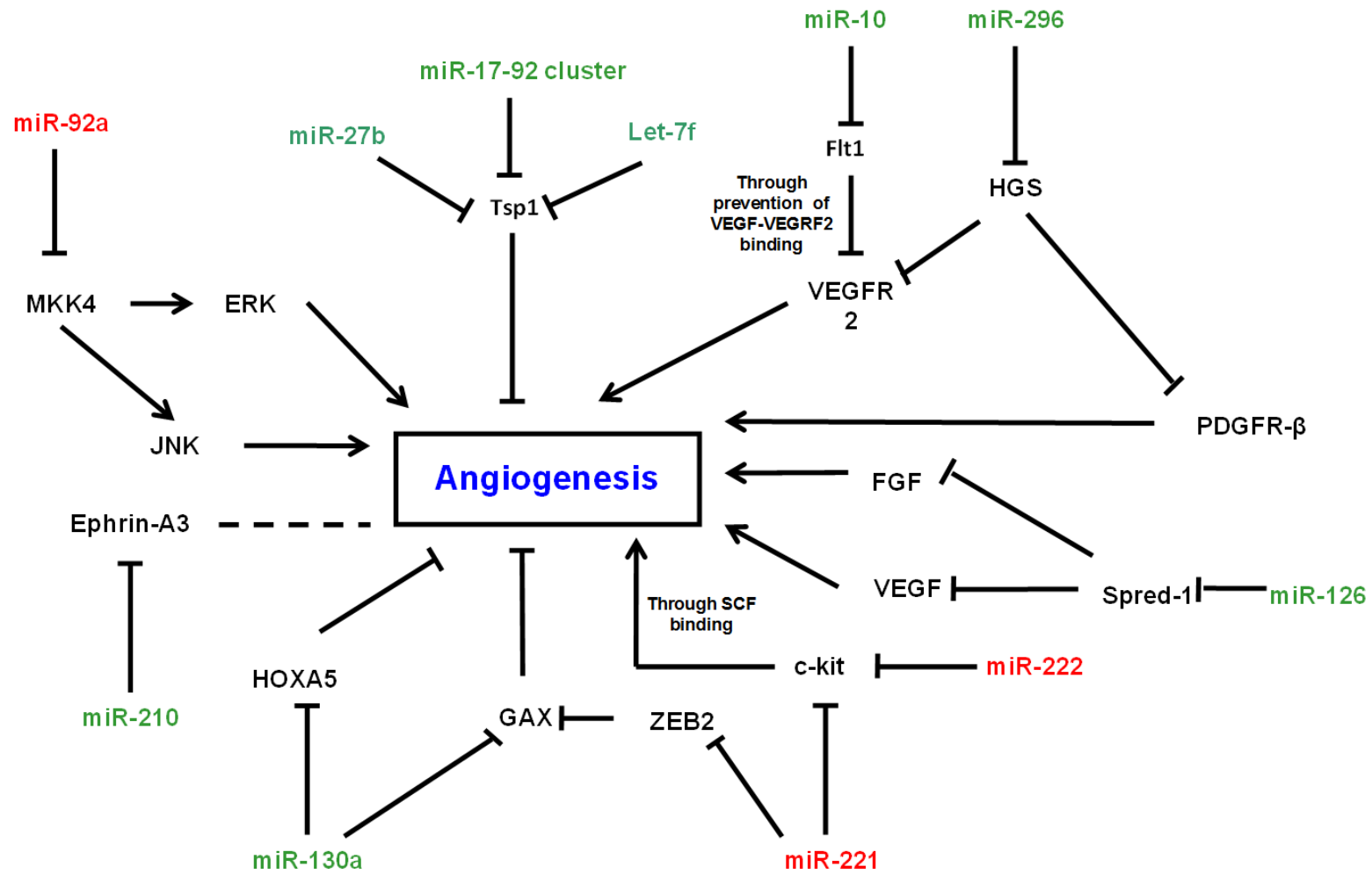


**Figure 1.6 – miRNAs play an important role in the regulation of angiogenesis.**

A summary of published miRNAs, and their mRNA targets, involved in the regulation of angiogenesis. Antiangiogenic miRNAs are shown in red and pro-angiogenic miRNAs in green. (Scott et al., 2013)

## 1.9 miRNAs and pluripotent stem cells

MiRNAs are essential for vertebrate development. Indeed, the discovery of the original miRNAs in *C.elegans* demonstrated a role in early embryonic development and developmental timing (Lee et al., 1993, Wightman et al., 1993). Dicer-1 depletion in the developing zebrafish embryo using targeted morpholinos, resulted in developmental arrest with a decrease in miRNA accumulation after 1 week (Wienholds et al., 2003). Knockout of this processing enzyme in murine embryos was similar, and resulted in embryonic lethality (Bernstein et al., 2003). Profiling of both mouse and zebrafish embryos also showed that miRNAs are differentially expressed throughout embryonic development, signifying their importance during development, lineage specification and maintenance (Wienholds et al., 2005, Mineno et al., 2006).

The integral role played by miRNAs in embryonic development, has implicated them in both regulation of pluripotency and differentiation of PSCs. Since their discovery, many studies have probed the function of these short non-coding RNAs in both ESCs and iPSCs, with the hope of finding master regulators of the pluripotent phenotype and in commitment to specific lineages, with the prospect of driving *in vitro* PSC reprogramming and differentiation.

### 1.9.1 Pluripotency-associated miRNAs

MiRNAs, along with other TFs, signalling pathways and epigenetic changes, are involved in a complex network, acting to control both pluripotency and differentiation in hPSCs. Early profiling studies used both mESC and hESC lines to identify miRNAs expressed in pluripotent conditions, with data showing a distinct set of miRNAs, enriched in these cells, unlike any other adult tissue or cell line (Houbaviy et al., 2003, Suh et al., 2004, Stadler et al., 2010).

Specifically expressed at high levels in hPSCs, the miR-302 cluster is located on chromosome 4, contains 10 miRNA sequences, all located within a ~700bp region; -3p and -5p forms of miR-302a, -302b, -302c, -302d and -367. Four of the eight miR-302 (miR-302a, -b, -c and -d) members in this cluster are highly homologous in their mature forms, with the greatest levels of sequence similarity existing at the 5' end - the location of the miRNA 'seed' sequence.

Homology in this region suggests the existence of a number of shared target mRNAs (Suh et al., 2004). When tested in a number of different hESC cell lines, the miR-302 cluster was shown to be consistently down-regulated during early differentiation, in a similar manner to pluripotency-associated genes, such as Oct4 (Stadler et al., 2010). Analysis of the miR-302 promoter region revealed binding sites for 3 pluripotency-associated TFs, Oct4, Sox2 and Nanog, and it was subsequently discovered that Oct4/Sox2 function as transcriptional activators of the miR-302 cluster. Inhibition of the miR-302 cluster in hESCs using anti-miRs resulted in an increase in cells in the G<sub>1</sub> phase of the cell cycle, a phenomenon observed in differentiated cell types. This affect was shown to be mediated through the translational repression of Cyclin D1 by the miR-302 cluster, a protein expressed at low levels in hESCs (Card et al., 2008). Oct4 and miR-302 also work together to regulate the activity of NR2F2 (COUP-TFII), a member of the NR2F, COUP-TF, nuclear orphan receptor family of transcription factors. NR2F2 is silenced transcriptionally by Oct4 and post-transcriptionally by miR-302 in hPSCs. However, when Oct4 and miR-302 levels decline during hPSC differentiation, NR2F2 becomes transcriptionally activated and in turn acts to transcriptionally repress Oct4 expression, thus reducing the levels to miR-302, providing positive feedback for the tight regulation of pluripotency and differentiation within these cells (Rosa et al., 2011). Most recently, Zhang et al. showed that in addition to its roles in cell cycle control, the miR-302 cluster also works to regulate apoptosis in hESCs (Zhang et al., 2015). These affects were mediated through the targeting and down regulation of BNIP3L/Nix (a BH3-only proapoptotic gene), and upregulation of BCL-xL, preventing apoptosis in these cells.

The murine homolog of the miR-302 cluster (miR-302), however, has a much lower abundance in mES cells. In these cells, it is the miR-290 cluster, a 2.2kb region encoding 6 miRNA stem loops (miR-290, -291, -292, -293, 294 and -295), which is highly expressed (Houbaviy et al., 2003). In human cells, the miR-371-373 cluster (containing miR-371, -372 and -373) is homologous to the mouse miR-290 cluster and, similarly, is expressed at high levels in pluripotent hESCs (Suh et al., 2004, Stadler et al., 2010). Yet, unlike miR-302 and miR-290, it was discovered that this cluster of miRNAs were expressed at lower levels in hiPSCs than in hESCs, suggesting that robust expression of this cluster may not be

critical for pluripotency (Wilson et al., 2009). Both miR-372 and -373 possess the same 'seed' sequence as the miR-302 family, suggesting shared targets for these miRNAs. The 'seed' sequence in many pluripotency-associated miRNAs appears near identical and, in fact, comprehensive profiling suggests the miRNA signature in hESCs is dominated by one 'seed' sequence (Laurent et al., 2008).

Numerous profiling studies have observed high expression of the miR-17 family in pluripotent hESC, while they were rapidly down-regulated in response to various differentiation cues (Suh et al., 2004, Stadler et al., 2010). Encompassing miR-17, -18a, -18b, -20a, -20b and -93, the miR-17 family possess the same, or a very similar, conserved pluripotent seed sequence, and are contained within 3 paralogous clusters in the genome; the miR-17-92, miR-106a-92 and miR-106b-25 clusters, all located on different chromosomes (Hayashita et al., 2005).

In particular, the miR-17-92 cluster has been shown to play a possible role in self-renewal. Comprising miR-17, -18a, 19a/b, -20a and -92a, the miR-17-92 cluster is expressed in a number of cancers, as well as in pluripotent hESCs, where expression is controlled by c-Myc. In the presence of c-Myc, the expression of the miR-17 cluster is increased, resulting in a decrease in expression of one target, E2F1, therefore tightly regulating c-Myc mediated proliferation (O'Donnell et al., 2005). Smith et al. confirmed the regulation of the cluster by c-Myc in pluripotent cells, and demonstrated a role for the miR-17-92 cluster in cell cycle control in murine iPSCs, via the regulation of a number of cell cycle control genes such as Rb2/p30 (Wang et al., 2008b, Smith et al., 2010).

Indeed, miRNAs are such potent regulators of pluripotency that numerous studies have demonstrated their ability to reprogram both mouse and human cells to pluripotency to generate iPSCs. Particularly, studies have focused on the use of the miR-302 cluster. Originally, it was shown that this cluster of miRNAs, when over expressed in human skin cancer cells, was able to reprogram the cells to an ES-like pluripotent state (Lin et al., 2008). Further studies showed that transfecting miR-200c, miR-302 and miR-369 family double stranded (ds) mature miRNAs in combination allowed for efficient reprogramming of mouse and human adipose stromal cells (ASCs) and human dermal fibroblasts (HDFs) (Miyoshi et al., 2011). In both of these studies showed increases in the pluripotency markers in

the transfected cells, and an ability to differentiate into multiple cell lineages. Hu et al. also demonstrated that reprogramming efficiency was greatly increased when miR-302 was used alongside four other factors (Oct4, Klf4, Sox2 and C-Myc) in human ASCs, although this study was unable to produce iPSCs using miR-302 alone (Hu et al., 2013). miRNA reprogramming methods do not require vector-based gene transfer and could, therefore, hold significant potential for future applications in biomedical research, regenerative medicine and cell therapies.

## 1.10 miRNAs and differentiation

Pluripotent stem cell differentiation is governed by a complex network of genes, signalling pathways and non-coding RNAs. In particular, miRNAs have been implicated in hESC differentiation *in vitro* (Bar et al., 2008). Knock down of the miRNA processing enzyme Dicer has been shown to have a significant effect on the ability of mESCs to differentiate *in vivo* and *in vitro* (Kanellopoulou et al., 2005, Murchison et al., 2005).

Studies have also identified a number of specific miRNAs highly expressed during differentiation of pluripotent cells, and playing vital roles in both unspecific and specific differentiation and lineage commitment. In 2009, miR-145, a smooth muscle cell associated miRNA expressed at very low levels in pluripotent cells, was identified as a regulator of general differentiation. Exerting its effects through its ability to bind and suppress the expression of the pluripotency factors Oct4, Sox2 and Klf4, knockdown of miR-145 in differentiating hESCs resulted in a significant reduction in differentiation (Xu et al., 2009). Additionally, it was also shown that Oct4 binds to the promoter region of miR-145 during pluripotency to repress its expression, forming a double negative feedback loop. Upon differentiation the miR-145 promoter is derepressed and miR-145 is upregulated, allowing for the downregulation of pluripotency factors.

In mESCs, the miR-17 family members, miR-17-5p, miR-20a, miR-93 and miR-106a are differentially expressed during differentiation, as well as *in vivo* in the developing mouse embryo (Foshay et al., 2009). Modulation of miR-93 and miR-20 *in vitro* demonstrated a role for this family of miRNAs in differentiation to specific germ layers, with miR-93 having possibly the most potent effect. Subsequently, it was shown that this family of miRNAs bind the 3' UTR of STAT3

during ESC differentiation, a mechanism possibly conserved between species. STAT3 is expressed at high levels in pluripotent cells, although it is not necessary for self-renewal. It is, therefore, likely that downregulation of this gene by the miR-17 family is needed for the onset of differentiation.

### 1.10.1 miRNA regulation of hESC-EC differentiation

Specifically, differential expression of various miRNAs has been documented during hESC-EC differentiation. Silencing of the Dicer processing enzyme during hESC-EC differentiation *in vitro* was shown to significantly decrease the percentage of cells positive for two endothelial markers, VE-Cadherin (CD144) and Pecam-1 (CD31), 10 and 14 days post-induction of differentiation (Kane et al., 2012).

It has also been reported that there is an increase in the expression of angiogenesis-associated miRNAs (e.g. miR-126, miR-210, let-7f) during a 10 day hESC-EC differentiation protocol, coinciding with an increase in endothelial-associated genes and an increase in the angiogenic abilities of the cells both *in vitro* and *in vivo* (Kane et al., 2010). Although it has previously been shown that miR-126 does not contribute towards endothelial lineage commitment during differentiation, despite its wide functional role in ECs (Fish et al., 2008). Anti-angiogenic miRNAs, such as miR-221 and -222, were also shown to be downregulated in these differentiated hESC-derived ECs (Kane et al., 2010). Furthermore, when the miRNA-ome of these differentiated cells was studied in more detail, miR-181a, -181b and -99b were observed to be expressed at significantly higher levels in hESC-ECs than in pluripotent hESCs (Kane et al., 2012). Modulation of their expression *in vitro* significantly increased percentage of cells expressing Pecam-1 and VE-cadherin, as well as inducing a significant increase in the production of nitric oxide (NO). Transplantation of hESC-derived ECs overexpressing miR-181b or miR-99b, were shown to significantly improve therapeutic angiogenesis in an *in vivo* mouse model of peripheral ischemia. Mechanisms of action and identification of targets of these miRNAs were not elucidated during this study, although a role for miR-181a in vascular development, through its targeting of Prox-1, had previously been described (Kazenwadel et al., 2010). MiR-181b has also been reported to be expressed in



vascular endothelium, with a possible role in EC activation and vascular inflammation (Sun et al., 2012).

Due to their previously defined role in endothelial cell function and neovascularisation, as well as their high expression in hESCs, it was also hypothesised that the miR-17-92 cluster may play a role in endothelial differentiation and commitment. Treguer et al. used mESCs and miPSCs to study the expression of this cluster during differentiation. Although all miRNAs in the cluster were expressed at high levels in undifferentiated cells, it was discovered that they are differentially regulated during differentiation. miR-17, -18, -19 and -20 were upregulated during mESC-EC differentiation, whereas miR-92a was downregulated during differentiation (Treguer et al., 2012). Antagomir inhibition of the individual members of the cluster, however, did not appear to have any effect on mESC-EC differentiation, suggesting these individual miRNAs are not essential for differentiation.

Two miRNAs, miR-200c and -150, were also shown to play a role in endothelial lineage specification and differentiation, both during hESC-EC differentiation and during chick embryo vasculogenesis. Knock down of these miRNAs caused a decrease in the levels of endothelial associated genes in mixed cell populations *in vitro*, as well as impairment in blood vessel formation or vasculogenesis in an *in vivo* chick embryo model. It was discovered that the 3' UTR of the transcriptional repressor zinc-finger E-box-binding homeobox 1 (ZEB1) contained two highly conserved binding sites for miR-200c and one highly conserved binding site for miR-150, and it was subsequently confirmed that this gene is a shared target of the two miRNAs (Luo et al., 2013). ZEB1 was shown to directly repress the transcriptional activity of a number of EC specific genes, including CD144, endothelial nitric oxide synthase (eNOS) and Von Willebrand factor (vWF). Taken together, this suggested that both miR-150 and -200c regulate the expression of endothelial-associated genes during hESC-EC differentiation via the targeting and repression of ZEB1.

Other studies in murine stem cells have also suggested roles for specific miRNAs in EC commitment and differentiation from ESCs, including miR-10, which has been shown to be upregulated during specification of mESC to mesoderm (Hassel et al., 2012). Experiments in miPSCs have also suggested a role for miR-21 in the

regulation of endothelial lineage differentiation, through the control of transforming growth factor  $\beta$ 2 (TGF $\beta$ 2) (Di Bernardini et al., 2014). In this study phosphate and tensin homolog (PTEN) was identified as a direct target of miR-21. During differentiation to ECs, PTEN is inhibited by miR-21, therefore resulting in an increase in the phosphorylation of Akt, which in turn induces TGF $\beta$ 2 to drive EC differentiation, hypothesised to occur possibly through the activation of Twist1 (Xue et al., 2012).

Novel miRNAs, with no identified role in EC function, have also been recognised as having a potential role in hESC-EC differentiation and commitment. During hESC-EC differentiation, miR-6086 and -6087 were shown to downregulate the expression of CD144 and endoglin respectively (Yoo et al., 2012), and miR-5739 was shown to potentially regulate the expression of endoglin within the same system (Yoo et al., 2011b).

Although a large number of miRNAs have been identified as being differentially regulated, in the context of hESC-EC differentiation and EC lineage commitment, exact mechanisms for many still remain unknown. Changes in expression of specific miRNAs may, however, be a consequence of differentiation, rather than a cause. Distinguishing between these phenomena, and identifying key miRNAs with roles in hESC-EC differentiation, may be crucial in the development of regenerative therapies.

### **1.11 Control of pluripotency and differentiation by other regulatory non-coding RNAs**

Recently, another genre of non-coding RNAs, long non-coding RNAs (lncRNA) have been implicated in hESC differentiation (Klattenhoff et al., 2013) and control of pluripotency (Wang et al., 2013, Lin et al., 2014). Much larger than miRNAs, lncRNAs are classified as non-coding RNAs >200 nts in length, and recent studies have identified large numbers of lncRNAs contained within mammalian genomes (Guttman et al., 2009, Derrien et al., 2012), although biological functions have only been elucidated for a select few. Similarly to mRNAs, they are transcribed by RNA polymerase II, are spliced, polyadenylated and have a 5' cap, although, unlike mRNAs, they lack protein coding potential.

The functions and mechanisms of lncRNAs, are still widely under investigation. Whereas miRNAs mainly function through binding to the 3' UTR of target genes, lncRNAs can function through a variety of different mechanisms. They can be nuclear or cytoplasmic, and their location is associated with their mechanism of action. Most nuclear lncRNAs function via the guiding of chromatin modifiers to specific genomic loci, whereas cytoplasmic lncRNAs have various functions, including modulation of translational control (Carrieri et al., 2012, Yoon et al., 2012) and modulation of mRNA stability. Most interestingly, lncRNAs can act as a competing endogenous control RNA (ceRNA) or miRNA sponge (Poliseno et al., 2010), suggesting lncRNAs work in synergy with miRNAs, adding extra levels of regulation in the control of cell phenotype and function by non-coding RNAs.

Numerous lncRNAs have been identified with potential roles in the control and regulation of pluripotency. Originally identified to modulate reprogramming during the derivation of hiPSCs (Loewer et al., 2010), the large intergenic non-coding RNA RoR (Regulator of Reprogramming) was found to act as an endogenous miRNA sponge to regulate the pluripotency-associated genes Oct4, Nanog and Sox2 (Wang et al., 2013). Wang et al. showed that linc-RoR binds miR-145, a key differentiation regulating miRNA, to prevent degradation of the critical pluripotency genes and regulate hPSC self-renewal. Additionally, a genome wide screen identified two novel lncRNAs (AK028326 and AK141205), directly controlled by the pluripotency factors Oct4 and Nanog, involved in the regulation of pluripotency and differentiation in mESCs (Sheik Mohamed et al., 2010). TUNA, another lncRNA, was also discovered to control pluripotency and differentiation towards neural lineages in mESCs (Lin et al., 2014).

In terms of cardiovascular development and differentiation, Klattenhoff et al. identified Braveheart, a lncRNA expressed in pluripotent mESCs. Braveheart was found to be critical for cardiovascular lineage commitment, specifically in promotion of cardiac cell fate, via the regulation of a number of cardiovascular-related transcription factors, including Mesp1 (Klattenhoff et al., 2013). Recently, RNA sequencing analysis of transcripts differentially regulated in specific populations during hESC-EC differentiation, including pluripotent hESCs, mesoderm committed cells, early cardiovascular progenitors, committed vascular progenitors and vascular endothelial cells, identified three specific lncRNAs, each with specific roles in governing pluripotency, cardiovascular

commitment and endothelial cell identity; *TERMINATOR*, *ALIEN* and *PUNISHER* respectively (Kurian et al., 2015).

Collectively, data from miRNA and lncRNA studies shows a vital role for non-coding RNAs in pluripotent cells, both in the regulation of pluripotency and the control of differentiation and commitment to specific lineages.

## 1.12 Project Aims

The aims of this thesis were to generate and characterise protocols for the derivation of hESC-ECs, therefore allowing for identification and investigation of differential expression of miRNAs within the system, and in-depth probing of their mechanisms of action. Gaining insight into these mechanisms would allow us to understand how miRNAs drive commitment of pluripotent cells towards specific lineages, with particular focus on mesoderm and vascular endothelium. Specifically, these aims included:

1. To develop, optimise and characterise differentiation protocols for the derivation of endothelial cells from hESCs.
2. To identify miRNAs differentially regulated throughout hESC-EC differentiation.
3. To modulate miRNA expression during hESC-EC differentiation, thereby allowing for the elucidation of functional role(s) of specific miRNAs.

## **Chapter 2    Materials and Methods**

## 2.1 General laboratory practice

Laboratory reagents and equipment were of the highest commercially available standard. All chemicals, unless otherwise stated, were purchased from Sigma-Aldrich, Dorset, UK. Hazardous chemicals were handled and disposed of in compliance with Control of Substances Hazardous to Health (COSHH) guidelines. Laboratory coats, nitrile powder-free gloves and fume hoods were used where appropriate.

## 2.2 General cell culture techniques

All cell culture was performed in standard biological safety class II vertical laminar flow cabinets under sterile conditions. Cabinets were cleaned before and after use with 1% virkon and 70% ethanol. Cells were cultivated in a humidified incubator at 37°C with a constant atmosphere of 5% CO<sub>2</sub>.

### 2.2.1 Culture of HEK293Ts

Human Embryonic Kidney (HEK) 293T cells (ATCC, Teddington, UK) were cultured as a monolayer in 150 cm<sup>2</sup> vented-cap cell culture flasks (Corning, Poole, UK) and maintained in Minimum Essential Media (MEM), supplemented with 10% foetal calf serum (FCS), 100 µg/mL penicillin, 100 µg/mL streptomycin, 2 mM L-Glutamine (all Gibco, Paisley) and 1 mM sodium pyruvate (Sigma). Cell culture medium was replenished every 2-3 days, or in line with cell growth and cells were passaged when 70% confluent to avoid over growth.

To passage, culture medium was removed and cells were washed with PBS. 2-3 mL 1x citric saline was then added to each flask, and cells were incubated at 37°C, 5% CO<sub>2</sub> for 2-3 min. When the majority of cells had lifted from the bottom of the flask, an equal volume of serum-containing cell culture medium was added in order to neutralise the reaction. Cells were then collected and pelleted by centrifugation at 1,500 rpm for 5 mins. The supernatant was then discarded and cells were resuspended in an appropriate volume of fresh culture medium before they were distributed amongst flasks.

For virus preparation (section 2.9.1) HEK293Ts were passaged at a ratio of 1:2 24 hours prior to triple transfection of lentivirus producing plasmids.

When cells were needed at specific densities, e.g. titration of lentivirus particles (section 2.9.3), cells were counted using a haemocytometer prior to seeding in appropriate cell culture vessel.

## 2.2.2 Human pluripotent stem cell culture

Human embryonic stem cells (hESCs) were cultured as a monolayer in feeder- and serum-free conditions, with media replaced every 24-48 hours. This study focused on the use of 2 different hESC lines; the original Wisconsin lines H1 and H9 (Thomson et al., 1998) (WiCell, Madison, USA) Cells were tested for Mycoplasma using MycoAlert™ Mycoplasma detection kit (Lonza) and routinely and independently tested for karyotypic abnormalities.

### 2.2.2.1 Maintenance and passage of hESCs

H1 and H9 hESC lines were maintained in StemPro® hESC SFM culture medium (Life technologies), a medium specialised for the growth and expansion of hESCs and consisting of DMEM/F12 with GlutMAX™ medium, 1x StemPro® hESC supplement and 1.8% bovine serum albumin (BSA). Medium was then further supplemented with 0.1 mM 2-mercaptoethanol (Gibco, Paisley) and 20 ng/mL basic fibroblast growth factor (bFGF). When confluency reached 80-90%, cells were passaged mechanically using the StemPro® EZPassage tools (Invitrogen). EZPassage tools create a grid-like pattern of hESC cell colonies, which can then be lifted and transferred to new tissue culture vessels at a split ratio of 1 in 6. Tissue culture vessels were pre-coated with either CELLstart™ (Life Technologies) or recombinant Vitronectin (Life Technologies), protocols for coating plates are shown in table 2.1.

Matrix	Volume	Concentration	Incubation time	Incubation Temperature
CELLstart	750µL/well	N/A	2hr	37°C
Recombinant Vitronectin	0.5-1mL/well	5µg/mL	1hr	Room temperature
Gelatin	2mL/well	0.1% Solution	1hr	Room temperature

**Table 2.1 – Protocols for coating tissue culture plates with various matrices**

### 2.2.2.2 Cryo-preservation and recovery of cells

Cells were treated as described in section 2.2.2.1. Culture medium containing small colonies, produced from the use of the StemPro® EZPassage tool, was added, at a ratio of 1:1 (v/v), to a 'freezing medium' mixture. The 'freezing medium' comprised 60% cell culture medium, 30% knock out serum replacement (KOSR) and 10% dimethyl sulfoxide (DMSO). 1 mL of the mixture, containing cells and freezing medium mix, was then added to 1 cryovial. Cryovials were then placed in a Nalgene® Mr.Frosty freezing container, and placed at -80°C. The freezing container contains isopropanol (2-propanol), ensuring a critical 1°C/min cooling rate, required for successful cryopreservation of cells. Cells were subsequently transferred to liquid nitrogen tanks for long term storage.

For recovery from liquid nitrogen, cells were thawed quickly in a water bath at 37°C, before being immediately transferred to a 15 mL flacon. 10 mL pre-warmed culture medium was then added, dropwise. Cells were then centrifuged at 1,200 rpm for 3 min, and resuspended in culture medium containing 10µM Y-27632, a rho-kinase inhibitor shown to improve stem cell survival (Watanabe et al., 2007). Culture medium was replaced the next day to remove remaining Y-27632.

## 2.3 Differentiation of human pluripotent stem cells

### 2.3.1 Endothelial differentiation of hESC

Endothelial differentiation of hESC was performed using an embryoid body (EB)-based method. On d0, hESCs (90-100% confluent, 8 days post-passage) were taken to single cell suspensions using StemPro® Accutase (Life Technologies) or TrypLE Select™ (Gibco, Paisley). Cells were counted and 10,000 cells placed into each well of the inner 60 wells of a Corning® 96-well clear round bottom ultra-low attachment microplate (Corning), or 96-well clear round bottom microplate coated with 5% pluronic F-127 (Sigma-Aldrich) (Ungrin et al., 2008), with 100 µL Stemline II medium (Sigma), supplemented with BMP4, Wnt3a (both R&D Systems), Activin A, VEGF (both Peprotech) and Y-26732 (Millipore) at concentrations shown in Table 2.2. To coat plates with 5% pluronic F-127, 50 µL solution was added to each well and plates were incubated at room temperature for 30 min, before being removed prior to the addition of cells (Table 2.1).



Day	Media	Cytokine Concentration				
		BMP4	VEGF	Wnt3A	Activin A	Y-26732
0	Stemline II	10ng/mL	10ng/mL	10ng/mL	5ng/mL	10 $\mu$ M
2	Stemline II	40ng/mL	60ng/mL	20ng/mL	10ng/mL	N/A
3-7	LONZA-EBM2 with EGM-2 bullet kit	N/A	50ng/mL	N/A	N/A	N/A

**Table 2.2 – Cytokine concentrations used on specific days of hESC-EC differentiation**

2 days after EB formation 16.6  $\mu$ L of Stemline II medium, supplemented with BMP4, VEGF, Activin a and Wnt3A, was added to each well in the 96-well plate, giving final cytokine concentrations shown in Table 2.2. On d3, EBs were collected, washed in PBS and resuspended in 3mL Endothelial Growth Medium-2 (EGM-2, Lonza) containing 50 ng/mL VEGF. The EGM-2 medium used is produced from the addition of the EGM-2 bullet kit to the Endothelial Basal Medium-2 (Lonza), without the addition of the VEGF and FBS components. EBs were transferred into 6-well plates coated with 0.1% gelatin (Sigma). Medium was then changed (2 mL LONZA EGM-2 with 50 ng/mL VEGF) every 2 days until appropriate analysis time point was reached. Some earlier differentiations were performed using 6-well ultra-low attachment dishes (Corning) and StemPro® EZPassage tools for EB formation (as described in hematopoietic differentiation, section 2.3.3).

### 2.3.2 MACSorting of hESC-ECs and further outgrowth

After 7 days of endothelial differentiation, CD144<sup>+</sup> cells were sorted using magnetic activated cell sorting (MACS), in order to allow for further culture of hESC-ECs (Figure 2.1). MACS was performed as follows, using commercially available microbeads, columns, magnets and holders from Miltenyi Biotec. Media was removed and cells were washed briefly with PBS, before dissociation to single cells using TrypLE Select™. Once collected, single cells were resuspended in MACS buffer; PBS, pH 7.2, 0.5% bovine serum albumin (BSA), passed through a 40  $\mu$ m nylon mesh (Fisherbrand) to ensure removal of cell clumps, and counted to determine total cell number. Cells were then centrifuged at 300 x g for 5 min, and the resulting pellet resuspended in 80  $\mu$ L of MACS buffer per 10<sup>7</sup> total cells.

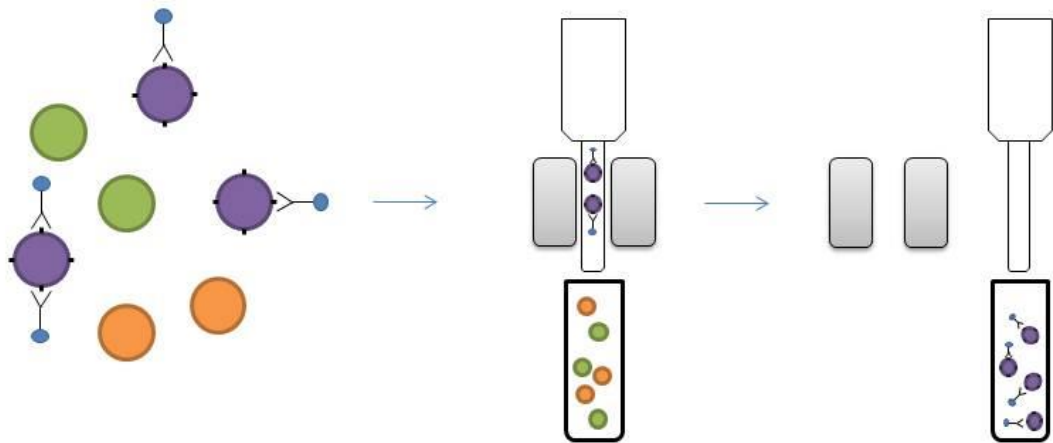


**Figure 2.1 – Overview of MACSort**

Cells were magnetically labelled using MACS microbeads conjugated antibodies, before being passed through a column within a magnetic field. Labelled cells will bind to the column, and those which are unlabelled will pass through. Labelled cells were then be collected by removal of the column from the magnetic field (Adapted from Miltenyi Biotec).

20  $\mu\text{L}$  of CD144 microbeads, per  $10^7$  total cells, was then added and the mixture incubated at  $4^\circ\text{C}$  for 15-30 min. Cells were then washed using 1-2 mL MACS buffer and centrifuged at  $300 \times g$  for 5 min, to remove any excess or unbound CD144 microbeads, and the resulting pellet resuspended in 500  $\mu\text{L}$  MACS buffer. A cell separation column (LS column) was placed in a MidiMACS™ separator and prepared for use by rinsing with 3 mL MACS buffer. The MidiMACS™ separator contains a powerful permanent magnet which applies a high-gradient magnetic field to a MACS column, allowing for cells labelled with even small amount of magnetic microbeads to bind to the column (Figure 2.1). Once the column was prepared, the cell suspension was then applied to the column and the flow through collected. The column was washed 3 times with 3 mL MACS buffer, the flow through collected and combined with that from the cell suspension. This flow through contains CD144<sup>-</sup> cells from the mixture, as they are unlabelled and have therefore been unable to bind to the MACS column. To collect the CD144<sup>+</sup> cells, the column was removed from the MidiMACS separator and the magnetically labelled cells were flushed out using 5 mL MACS buffer.

Flow cytometry was performed to ensure efficient purification of CD144<sup>+</sup> cells. Sorted cells were then plated onto gelatin coated 6-well tissue culture plates at a density of  $1 \times 10^5$  cells per well and cultured for a further 7 days in LONZA EGM-2 media with FBS component added and supplemented with 50ng/mL VEGF.

### 2.3.3 Differentiation of hESC to hemogenic endothelium

Differentiation of cells to early hemogenic endothelium was performed using the first 10 days of a defined serum- and feeder-free EB-based hematopoietic differentiation protocol (Mountford lab). On d0 EBs are formed by removing medium from the wells and washing cells in PBS. 3 mL/well Stemline II medium (Sigma-Aldrich), supplemented with BMP4, VEGF, Activin A, Wnt3A and Inhibitor VIII, was added, and cells were cut into rough squares using a StemPro® EZPassage tool. Cells were then removed from the well and transferred to a Corning® 6-well ultra-low attachment plate (Corning) at a 1:3 ratio. A further 1.5 mL media, containing d0 cytokines, was then added to each well, resulting in a final volume of 3 mL/well. At d2, cells had formed EBs and a further addition of 0.5mL Stemline II medium, supplemented with BMP4, VEGF, Inhibitor VII, Wnt3A, Activin A, FGF $\alpha$ , SCF and  $\beta$ -Estradiol, was made. On d3 cells were collected and dispersed, using Tryple Select. Single cells were then resuspended in Stemline II medium, counted, and seeded at  $2 \times 10^5$  cells per well in a standard 6-well plate, in 3 mL/well Stemline II medium, with appropriate cytokines added. A further 0.5 mL media, supplemented with specific cytokines, was added on day 5, before a complete media change was then performed on d7. On day 9, a final addition of 0.5 mL media and cytokines was made, before cells were harvested for analysis on d10. Stemline II medium was used for all stages of differentiation, and concentrations of all cytokines added are shown in table 2.3.

Day	Media	Cytokine Concentration											
		BMP4	VEGF	Wnt3A	Activin A	Inhibitor VIII	FGF $\alpha$	SCF	$\beta$ -Estradiol	IGF2	TPO	Heparin	IBMX
0	Stemline II	10ng/mL	10ng/mL	10ng/mL	5ng/mL	2 $\mu$ M	-	-	-	-	-	-	-
2		20ng/mL	30ng/mL	10ng/mL	5ng/mL	2 $\mu$ M	10ng/mL	20ng/mL	0.4ng/mL	-	-	-	-
3		20ng/mL	30ng/mL	-	-	-	10ng/mL	30ng/mL	0.4ng/mL	10ng/mL	10ng/mL	5ng/mL	50 $\mu$ M
5		20ng/mL	30ng/mL	-	-	-	10ng/mL	30ng/mL	0.4ng/mL	10ng/mL	10ng/mL	5ng/mL	50 $\mu$ M
7		20ng/mL	30ng/mL	-	-	-	10ng/mL	30ng/mL	0.4ng/mL	10ng/mL	10ng/mL	2.5ng/mL	50 $\mu$ M
9		10ng/mL	15ng/mL	-	-	-	5ng/mL	15ng/mL	0.2ng/mL	5ng/mL	5ng/mL	1.25ng/mL	25 $\mu$ M

**Table 2.3 – Final concentration of cytokines in Stemline II medium on specific days of differentiation to hemogenic endothelium.**

## **2.4 Functional analysis of hESC-ECs**

### **2.4.1 Matrigel Tubule Assay**

Growth-factor reduced Matrigel™ (BD Biosciences) was thawed overnight at 4°C. Once thawed, 75 µL Matrigel™ was added to each well of a 96-well cell culture dish, ensuring an even spread across the surface and removing any bubbles. Plates were then incubated at 37°C for ≥30 min to ensure setting of the matrix.

hESC-ECs were taken to a single cell suspension using TryPLE select and resuspended in Lonza EGM-2 medium supplemented with 50 ng/mL VEGF. 75 µL medium containing  $2 \times 10^4$  cells was added to each well, and cells were incubated for 24 h at 37°C and 5% CO<sub>2</sub>. After 24 h cells were removed from the incubator and assessed for their ability to form tubules. Cells were imaged using an EVOS® XL Core Cell Imagine System (Life Technologies).

## **2.5 Gene and miRNA expression analysis**

### **2.5.1 Extraction of total RNA from cells**

Extraction of total RNA, including miRNA, from cultured cells was performed using the Qiagen miRNeasy mini kit, with as per manufacturer's instructions. An on-column DNase treatment was also performed during the extraction via the use of the accompanying RNase-free DNase Set (Qiagen).

Culture medium was removed and cells were washed using PBS. For one well of a 6 well plate, 700 µL QIAzol lysis reagent was added to the cells, either directly on the plate, or after dissociation using TrypLE Select™. Samples were homogenised by pipetting up and down using, and the lysate transferred to a 1.5 mL microcentrifuge tube. Lysates were then either directly processed or stored at -80°C until required.

When required, cell lysates were placed at RT for 5 min, before the addition of 140 µL chloroform. Samples were mixed and incubated at RT for a further 3 min, before being centrifuged at 12,000 x g at 4°C for 15 min. Centrifuging the sample allows for separation into three different phases; an upper, aqueous phase, containing total RNA, a middle interphase, containing DNA and a lower,

organic phase, containing proteins. The aqueous phase was then removed and transferred to a new 1.5 mL microcentrifuge tube. 1.5 volumes of 100% ethanol was added to each sample and mixed thoroughly. Samples were then transferred to RNeasy spin columns, and centrifuged at 8,000 x g for 15 s, and the flow through discarded. This allows total RNA to bind to the column, whilst phenol and other contaminants are efficiently washed away. 350 µL RWT buffer was then added and columns were centrifuged again at 8,000 x g for 15 s at RT.

At this stage an on-column DNase digest was performed, allowing for removal of any contaminating genomic DNA in the sample. To do this, DNase was prepared according to manufacturer's instructions and 10 µL of enzyme mixed with 70 µL RDD buffer per sample. 80 µL of the DNase/RDD buffer mix was then added to directly onto each column and left to incubate for 15 min at RT. After 15 min, a further 350 µL of RWT buffer was added and columns were centrifuged for 15 s at 8,000 x g at RT.

Samples were then washed twice with 500 µL RPE buffer, the first with a 15 s spin and the second with a 2 min spin, both at 8,000 x g at RT. RNeasy spin columns were then transferred to clean 2 mL collect tubes and centrifuged at full speed for 1 min. This spin ensures removal of residual ethanol and avoids carryover of buffer RPE which may interfere with downstream reactions. Total RNA was then eluted by passing 30-50 µL nuclease-free water through the spin column for 1 min at 8,000 x g. The eluate was then collected and passed through the column again to obtain an optimal RNA yield.

RNA concentration was determined using a NanoDrop 1000 spectrophotometer (Thermo Scientific), and samples stored at -80°C until required.

#### **2.5.1.1 RNA quality control**

Quality control of RNA was performed using the Agilent® 2100 Bioanalyser or Agilent 2200 TapeStation instrument.

The Aligent® 2100 Bioanalyser is used to measure the quality of RNA, via the calculation of an RNA integrity number (RIN), calculated based on the presence or absence of degradation productions within the sample. This was used to test

RNA samples before analysis using TLDA card (see section 2.5.3.1), samples with a RIN value of 7 or more are deemed of a high quality. For analysis using the Agilent® bioanalyser, 1 µL of RNA was used for each sample. First, the Agilent gel was prepared by centrifuging 550 µL of gel matrix through a spin column at 1500 x g for 10 min. Once passed through the column, 65 µL of the matrix was transferred to a new Eppendorf, and 1 µL of RNA 6000 Nano dye concentrate was added and mixed well. The mix was then centrifuged at 13,000 x g for 10 min. An RNA 6000 nano chip was then placed into the chip priming station, and 9 µL of the gel-dye mix was added to the specified well, and spread evenly through the chip using the 1 mL syringe attached to the chip priming station. A further 9 µL of gel-dye mix was then added to two other wells on the nano chip. 5 µL of RNA 6000 Nano marker was then added to all wells, including the 12 sample wells and the ladder well. 1 µL of sample was added to each sample well, with a maximum of 12 samples per chip, and 1 µL of RNA ladder added to the marked 'ladder' well. The chip was then vortex mixed for 60 s at 2400 rpm, before being inserted into the Agilent® 2100 bioanalyser and immediately run.

For miRNA microarray (section 2.5.4) RNA quality control was performed using an Agilent® 2200 TapeStation, following the standard operating procedures at Sismic Ltd. Similarly to the Agilent® 2100 Bioanalyser system, this instrument provides a readout of RNA quality, via the calculation of a RIN value. Briefly, all reagents were allowed to equilibrate to room temperature and vortex mixed before use, and RNA samples thawed on ice. 5 µL sample buffer was added to 1 µL of sample RNA, or RNA ladder. All samples were vortex mixed for 1 min at 2,000 rpm, and briefly centrifuged, before samples were then denatured. To do this, tubes were heated to 72°C for 3 min, followed 2min incubation on ice. Samples were then loaded into the Agilent® 2200 TapeStation and analysis was performed.

## **2.5.2 Reverse transcription polymerase chain reaction (RT-PCR)**

In order to analyse cellular gene and miRNA expression levels, cDNA (complementary DNA) must first be created from total RNA.

For gene expression analysis, cDNA was generated using TaqMan® Reverse Transcription Reagents (Life technologies). Each reaction contained 200-1000 ng

RNA (consistent within experiments), and the following reagents: 1x reverse transcription buffer, 5.5 mM MgCl<sub>2</sub>, 0.5 mM of each dNTP, 2.5 μM random hexamers, 0.4 U/μL RNase inhibitor enzyme and 1.25 U/μL Multiscribe™ Reverse Transcriptase. Nuclease-free H<sub>2</sub>O was then added to give a final reaction volume of 20 μL, and samples were put through the following temperature cycle in a thermal cycler: 10 min at 25°C to allow for annealing of primers, 30 min at 48°C for reverse transcription, and 5 min at 95°C to inactivate the reverse transcriptase. Samples were then removed from the thermal cycler and placed at -20°C until required.

When performing miRNA analysis, cDNA was generated using the TaqMan® miRNA Reverse Transcription kit (Life Technologies). Reactions contained 5ng total RNA, and the following reagents: 1 x reverse transcription buffer, 0.25 U/μL RNase inhibitor, 3.33 U/μL Multiscribe™ Reverse Transcriptase, 1 mM of each dNTP (all provided with the kit), 1 x TaqMan® miRNA reverse transcription primers (provided with TaqMan® assays, Life Technologies). H<sub>2</sub>O was then added to make a final reaction volume of 7.5 μL. Synthesis was then performed using the following thermal cycling conditions: 16°C for 30 min to allow for the binding of the miRNA primers, 42°C for 30 min for the reverse transcription, and 85°C for 5 min to allow for inactivation of the reverse transcription enzyme. Samples were then removed from the thermal cycler and stored at -20°C until required. Reverse transcription of an endogenous control miRNA (RNU48) was also performed, in order to allow for normalisation of changes in miRNA expression.

Non-template controls (NTC), whereby H<sub>2</sub>O was added to in the place of RNA, were performed for each experiment. For the miRNA RT-PCR, one NTC was performed for each miRNA primer used.

### **2.5.3 mRNA and miRNA TaqMan® real-time PCR**

Quantitative real time-PCR (qRT-PCR) is a technique which can be used for the quantification of a specific mRNA or miRNA within a sample. TaqMan® qRT-PCR assays are labelled with a 5' fluorescent reporter dye, such as VIC or FAM, and a quencher molecule at the 3' end. When the TaqMan® probe is intact, fluorescence released from the 5' dye is transferred to the 3' quencher molecule



by a phenomenon known as fluorescence resonance energy transfer (FRET). However, during the amplification process, if the target sequence is present in the sample, the probe anneals and the quencher is cleaved via the action of the *Taq* DNA polymerase - present in the reaction mixture. The *Taq* polymerase enzyme contains a 5' nuclease domain, which allows degradation of DNA bound to the target, downstream of DNA synthesis. This results in the degradation of the TaqMan® probe, and cleavage of the 3' quencher molecule, therefore preventing FRET and allowing for the detection of the reporter fluorophores. The strength of the fluorescence is increased with each amplification cycle, and is relative to the amount of a specific mRNA or miRNA within a sample. The fluorescence signal can be normalised to that of a reference or 'housekeeping' gene - a gene which should maintain relatively stable expression levels throughout a sample set. This allows for comparison of expression levels between samples. For gene expression analysis, Ubiquitin protein C (UBC) was selected as a stable housekeeping gene using a human endogenous control array and, unless otherwise stated, was used as a reference gene throughout the studies. GAPDH was used during TLDA card analysis. RNU48 was used as an endogenous control for all miRNA expression experiments.

For mRNA expression, qRT-PCR was performed using TaqMan® Gene Expression assays and TaqMan® Universal Master Mix II (both Life Technologies) in accordance with the manufacturer's instructions. Reactions were performed in 384-well plates, and contained 1 x Taqman® assay (5 µL), and 1 x TaqMan® master mix (0.5 µL), as well as 1.5 µL cDNA (section 2.5.2) and 3 µL nuclease-free H<sub>2</sub>O - giving a total reaction volume of 10 µL.

miRNA expression qRT-PCR was performed using TaqMan® miRNA RT-PCR probes (provided in same assay as reverse transcription primers), and TaqMan® Universal Master Mix II in accordance with the manufacturer's instructions. Each reaction contained 5 µL TaqMan® mastermix, 0.5 µL miRNA probe, 3.83 µL nuclease-free H<sub>2</sub>O and 0.67 µL cDNA from miRNA reverse transcription, and were performed in 384-well plates.

Both mRNA and miRNA expression was measured using ABI Prism Applied Biosystems 7900HT sequence detection system. Samples were subject to 10 min at 95°C to allow for denaturing, before undergoing 40 cycles of denaturing at

95°C for 15 s, followed by 60 s at 60°C for primer and probe annealing and primer extension.

Data was then analysed using the comparative  $C_T$  method, also known as  $2^{-\Delta\Delta C_T}$  method (Livak et al., 2001). The number of cycles taken for the reporter dye emissions to reach a specific level is known as the cycle threshold ( $C_T$ ). The  $\Delta C_T$  is the difference between the  $C_T$  of the gene of interest (GOI) and the  $C_T$  of the housekeeper or reference gene, therefore allowing for expression to be normalised to total RNA content. The mean  $\Delta C_T$  of all biological replicates for the same GOI was calculated, and then used to calculate the  $\Delta\Delta C_T$ , which shows the difference in gene expression between a sample and control or non-treatment group.  $2^{-\Delta\Delta C_T}$  is then used to calculate the fold increase or decrease in gene expression between a sample and the control group, whose value is equal to 1.

Gene name	Alternative name	Assay ID
UBC		Hs01871556_s1
GAPDH		Hs02758991_g1
PECAM-1	CD31	Hs00169777_m1
CDH5	VE-Cadherin; CD144	Hs00901463_m1
POU5F1	Oct4	Hs00999632_g1
NANOG		Hs04399610_g1
SOX2		Hs01053049_s1
T	Brachyury	Hs00610080_m1
MESP1		Hs01001283_g1
MIXL1		Hs00430824_g1
SPN	CD43	Hs01872322_s1

Table 2.4 – List of gene expression TaqMan assays used.

miRNA	Alternative names	miR Base Identifier	Assay number
miR-10a-5p	miR-10a	MIMAT0000253	000387
miR-126-3p	miR-126	MIMAT0000445	002228
miR-143-3p	miR-143	MIMAT0000435	002249
miR-143-5p	miR-143*	MIMAT0004599	002146
miR-145-3p	miR-145*	MIMAT0004601	002149
miR-145-5p	miR-145	MIMAT0000437	002278
miR-302a-3p	miR-302a	MIMAT0000684	000529
miR-302b-3p	miR-302b	MIMAT0000715	000531
miR-451a	miR-451	MIMAT0001631	001141
miR-483-3p	-	MIMAT0002173	002339
miR-483-5p	-	MIMAT0004761	002338
RNU48	-	-	001006

Table 2.5 – List of miRNA TaqMan assays used.

### 2.5.3.1 TaqMan® Low Density Array cards (TLDA)

TaqMan® Low Density Array (TLDA) cards use the same chemistry as previously described for TaqMan® qRT-PCR (section 2.5.3), but allow for higher throughput screens. In this format, lyophilized TaqMan® assays are stored on 384-well microfluid cards, therefore allowing for a large number of reactions to be performed with relatively low amounts of sample. Cards allow for a maximum of 8 samples to be run simultaneously, for up to 48 different genes. For each sample, 30-1000 ng DNA (consistent between experiments) was diluted into 55  $\mu\text{L}$  nuclease-free  $\text{H}_2\text{O}$  and added to 55  $\mu\text{L}$  TaqMan® master mix. 100  $\mu\text{L}$  of this mixture was then added directly to one port of on the TLDA card. Cards were then centrifuged to ensure even distribution of sample cDNA between wells, and data was collected using the ABI Prism Applied Biosystems 7900HT sequence detection system.

Data was then analysed using the  $2^{-\Delta\Delta\text{CT}}$  method as previously described (section 2.5.3). Details of assays on custom TLDA cards are given in Table 2.6.

This technology, in the form of a human endogenous control array (Life Technologies), was also used to help identify UBC as a suitable housekeeper gene for gene expression analysis studies.

Gene name	Protein name	Alternative name	Assay ID
18S	18S ribosomal RNA		Hs99999901_s1
ACTC1	Alpha actin		Hs00606316_m1
AFP	Alpha-fetoprotein		Hs00173490_m1
B2M	Beta-2 microglobulin		Hs99999907_m1
BMP4	Bone morphogenic protein 4		Hs00370078_m1
CDX2			Hs00230919_m1
CER1	Cerberus		Hs00193796_m1
CGA	Chorionic gonadotropin alpha		Hs00174938_m1
CXCR4			Hs00607978_s1
CYP26A1	Cytochrome P450 26A1		Hs00175627_m1
DES	Desmin		Hs00157258_m1
DKK1	Dickkopf-related protein 1		Hs00183740_m1
FN1	Fibronectin		Hs00277509_m1
FOXA2	Forkhead box protein A2	HNF-3B	Hs00232764_m1
FOXC1	Forkhead box C1		Hs00559473_s1
FZD5	Frizzled-5		Hs00258278_s1
GAPDH	Glyceraldehyde 3-phosphate dehydrogenase		Hs99999905_m1
GATA2	GATA binding protein 2		Hs00231119_m1
GATA4	Transcription factor GATA-4		Hs00171403_m1
GATA6	Transcription factor GATA-6		Hs00232018_m1
GDF15	Growth differentiation factor 15		Hs00171132_m1
GJA1	Gap junction alpha-1 protein	Cx43	Hs00748445_s1
GSC	Goosecoid		Hs00418279_m1
HAND1	Heart- and neural crest derivatives-expressed protein 1		Hs00231848_m1
HNF1B	Hepatocyte nuclear factor 1 homeobox B	TCF2	Hs00172123_m1
INS	Insulin		Hs00355773_m1
ISL1	Insulin gene enhancer protein ISL-1	ISLET1	Hs00158126_m1
ITGB5	Integrin beta-5		Hs00609896_m1
KDR	Kinase insert domain receptor	CD309; VEGFR2; FLK1	Hs00911700_m1
MESP1	Mesoderm posterior 1 homolog		Hs00251489_m1
MIXL1			Hs00430824_g1
MSX1	Msh homeobox 1		Hs00427183_m1
MYL2	Myosin regulatory light chain 2	MLC-2	Hs00166405_m1
NANOG			Hs02387400_g1
NES	Nestin		Hs00707120_s1
NKX2-2	Homeobox protein Nkx-2.2		Hs00159616_m1
NKX2-5	Homeobox protein Nkx-2.5		Hs00231763_m1
PAX6	Paired box protein Pax-6	AN2	Hs00240871_m1

PDX1	Pancreatic and duodenal homeobox 1	IPF1	Hs00426216_m1
PECAM1	Platelet endothelial cell adhesion molecule	CD31	Hs00169777_m1
POU5F1	POU domain, class 5, transcription factor	OCT4	Hs00742896_s1
SNAI1	Zinc finger protein SNAI1	SNAIL	Hs00195591_m1
SOX17	SRY (Sex determining Y)-Box 17		Hs00751752_s1
SOX2	SRY (Sex determining Y)-Box 2		Hs00602736_s1
SOX7	SRY (Sex determining Y)-Box 7		Hs00846731_s1
SST	Somatostatin		Hs00174949_m1
T	Brachyury		Hs00610080_m1

**Table 2.6 –TaqMan probes on custom TLDA cards used for gene expression analysis.** GAPDH, 18S and B2M were used as housekeeper genes.

## 2.5.4 miRNA microarray

Total RNA extraction was performed using the Qiagen miRNeasy mini kit, as described in section 2.5.1. Concentration and quality control of collected RNA was determined using the NanoDrop and Agilent® 2200 TapeStation respectively. The TapeStation platform allows for a read out of RNA quality as given by the RIN value, to ensure data collected was of the highest quality, RNA was tested to ensure RIN values of >7 (see section 5.3.3). All RNA samples were then diluted to the working concentration of 50 ng/μL. Before running on the array, samples were also randomised to ensure equal distribution of biological replicates between microarray slides.

Samples were then processed for analysis. To do this, two kits were used; the miRNA Spike-In kit and the miRNA Complete Labelling and Hybridisation kit (both Agilent Technologies). The miRNA Spike-In kit contains a mix of ten *in vitro* synthesised, polyadenylated transcripts in predetermined ratios. These transcripts hybridise to control probes on the Agilent microarray, and allow for distinguishing of significant biological data from processing errors. Two different Spike-In solutions are provided in the kit, and both are used in the analysis; the Labelling Spike-in, added during the labelling reaction, and the Hybridisation (Hyb) Spike-In, added during the hybridisation reaction. To prepare the Spike-In solutions, serial dilutions of both Spike-In mixtures were performed. Briefly, 2 μL of the Labelling Spike-In, prepared as per the manufacturer's instructions, was

added to 198  $\mu\text{L}$  of nuclease-free  $\text{H}_2\text{O}$  and mixed thoroughly. 2  $\mu\text{L}$  of this dilution was then added to 198  $\mu\text{L}$  nuclease-free  $\text{H}_2\text{O}$  and mixed thoroughly to give the working dilution of the Labelling Spike-In. This process was repeated with the Hyb Spike-In.

Once the Spike-In solutions were prepared, samples underwent Labelling and Hybridisation, performed using the aforementioned miRNA Complete Labelling and Hybridisation kit. 2  $\mu\text{L}$  of each RNA samples (100 ng total) was added to individual 1.5 mL microcentrifuge tubes and maintained on ice to avoid degradation. Samples were then dephosphorylated using the Calf Intestine Alkaline Phosphatase (CIP) enzyme. The CIP Master Mix was prepared as shown below and kept on ice until needed:

<u>Reagent</u>	<u>Amount per reaction (<math>\mu\text{L}</math>)</u>
10X Calf Intestinal Phosphatase Buffer	0.4
Labelling Spike-In	1.1
Calf Intestinal Phosphatase	<u>0.5</u>
<b>Total</b>	<b>2.0</b>

2  $\mu\text{L}$  CIP Master Mix was added to each sample tube and gently mixed by pipetting. Tubes were then incubated at 37°C for 30 min to allow for dephosphorylation. Samples then underwent denaturation using DMSO. 2.8  $\mu\text{L}$  DMSO was added to each sample, before incubation at 100°C for between 5-10 mins. Samples were transferred immediately to an ice-water bath, thus ensuring samples remain properly denatured, before moving immediately onto labelling of samples. Immediately prior to use, the Ligation Master Mix was prepared as described below:

<u>Reagent</u>	<u>Amount per reaction (<math>\mu\text{L}</math>)</u>
10X T4 RNA Ligase Buffer	1.0
Cyanine 3-pCp	3.0
T4 RNA Ligase	<u>0.5</u>
<b>Total</b>	<b>4.5</b>

After preparation, 4.5  $\mu\text{L}$  of Ligation Master Mix was added to each sample, gently mixed by pipetting and briefly centrifuged. Samples were then incubated for 2 h at 16°C to allow for efficient labelling.

Micro Bio-Spin P-6 Gel Columns (Bio-Rad) were then employed to purify labelled RNA samples. This allows for removal of DMSO and excess Cyanine 3-pCp from samples. Before use, columns were inverted several times to ensure resuspension of the settled gel and to remove any air bubbles. The tip of each column was removed, and columns were placed into a 2 mL collection tube. The green cap of each column was removed allowing the buffer, hydrating the Bio-Gel on the column, to drain through. Once evenly drained, flow through was discarded and tubes containing columns were centrifuged for 2 min at 1000 x g. Columns were then placed into a new 1.5 mL RNase-free microcentrifuge tube. 38.7  $\mu$ L of nuclease-free H<sub>2</sub>O was added to each sample, to give a total reaction volume of 50  $\mu$ L. All 50  $\mu$ L of sample was then carefully added to a column, ensuring the gel bed was not disturbed. Samples were then centrifuged at 1000 x g for 4 min, eluting the purified sample, which appears slightly pink. Columns were then discarded and samples kept on ice. Samples were then dried using a vacuum concentrator with heater. Before proceeding with the hybridisation reaction, it was ensured that all samples were completely dry.

Once all samples had undergone labelling, hybridisation was performed. Dried samples were resuspended in 17  $\mu$ L nuclease-free H<sub>2</sub>O, before the addition of 1  $\mu$ L Hyb Spike-In solution, 4.5  $\mu$ L 10x Gene Expression Blocking Agent and 22.5  $\mu$ L 2x Hi-RPM Hybridisation Buffer. Tubes were incubated at 100°C for 5 min and then transferred to ice for a further 5 min. Samples were then immediately loaded into one well of a gasket slide, in an Agilent SureHyb chamber base. Gasket slides were loaded with 8 samples, before the SurePrint G3 Human v16 miRNA 8x60K microarray slides were placed, active side down, onto the gasket slide, ensuring correct alignment of both slides. This was then clamped into place and each assembled chamber placed into an oven on a rotating rack. Samples were hybridised overnight (~20 h) at 55°C and 20 rpm. After hybridisation, slides were washed thoroughly, and placed into a slide holder. Slides were then processed using the Agilent C Scanner, and data was extracted using the Agilent Feature Extraction Software.

## **2.6 Immunocytochemistry (ICC)**

Media was aspirated and cells were washed with PBS. Ice cold 100% methanol was added and cells were placed at -20°C for 15 min. Methanol was aspirated



and cells were washed once again in PBS. For blocking, 750  $\mu$ L 10% normal goat serum (NGS) was added to each well of a 6 well plate and cells were incubated for 1 h at RT on a shaker. After incubation, cells were washed twice using PBS-Tween20 (PBS-T); 0.5 mL Tween-20 in 49.5 mL PBS. Primary antibodies were diluted in 1% NGS at a pre-optimised dilution, 1 mL primary antibody was added to each well and cells were incubated overnight at 4°C. The primary antibody was then removed and cells were washed 3 times in PSB-T. 800  $\mu$ L of the appropriate secondary antibody, diluted in 1% NGS, was then added to each well and cells incubated for 1 h at room temperature. Secondary antibodies were then aspirated and cells washed in PSB-T another 3 times. Once the last wash of PBS-T has been performed, cells were washed twice in PBS and all PBS was aspirated. Prolong gold with DAPI was then added to each well and a coverglass was applied, ensuring all bubbles were removed, before leaving the cells to set for 1 h at 4°C. Imaging was then performed using Zeiss Axiovert 200M.

## 2.7 Flow Cytometry

Cells were prepared for analysis by flow cytometry by dissociating to single cells using TrypLE Select™ (Gibco, Paisley). Cells were washed using PBS and resuspended in FACS sheath fluid (BD Biosciences) or in FACS buffer; 2 mM EDTA, 1% KOSR, PBS. Cells were counted and  $1 \times 10^5$  cells were transferred to a reaction tube. Antibodies were then added to each reaction tube, with amount varying with the conjugate used; 1  $\mu$ L allophycocyanin (APC) and brilliant violet 421 (BV421), 2  $\mu$ L phycoerythrin (PE), 3  $\mu$ L fluorescein isothiosyanate (FITC), APC-Cy7 and peridinin-chlorophyll proteins (PerCP)-Cy5.5. The antibody-cell mixture was incubated in the dark at 4°C for 30 min. Cells were washed with 2 x 3 mL FACS sheath fluid, and resuspended in 200  $\mu$ L of sheath fluid. Samples were then analysed using the BD Biosciences FACSCanto II with FACSDiva software and either a 2-laser (red - 633-nm, and blue - 488-nm) or 3-laser (red, blue and violet - 405-nm) configuration. Unstained and matched isotype control samples were used as negative controls and used to set gates for positive and negative populations, and 10,000 events were collected for each sample.

Compensation was performed using single-stained samples for each fluorophore and calculated using the FACSDiva software. For samples with GFP virus compensation set up was performed manually. For large, multi-colour

experiments, fluorescence minus one (FMO) controls were used to ensure compensation settings were correct.

Analysis of flow cytometry data was performed using FlowJo analysis software (Tree Star). Antibodies used for flow cytometry are shown in Table 2.7.

Target Antigen	Species Raised in	Conjugate	Supplier
SSEA3	Rat	Alexa fluor® 647	BD Biosciences
SSEA3	Mouse	PE	BD Biosciences
SSEA4	Mouse	APC	BD Biosciences
Tra1-60	Mouse	PE	BD Biosciences
CD56	Mouse	PE	BD Biosciences
CD326	Mouse	APC	BD Biosciences
CD326	Mouse	FITC	BD Biosciences
CD144	Mouse	PE	BD Biosciences
CD144	Mouse	APC	eBiosciences
CD31	Mouse	FITC	BD Biosciences
CD31	Mouse	PE	BD Biosciences
CD31	Mouse	APC	R&D Systems
CD43	Mouse	PE-Cy7	BD Biosciences
CD309	Mouse	PE	BD Biosciences
CD117	Mouse	PerCP-Cy5.5	BD Biosciences
CD117	Mouse	PerCP-eFlour® 710	eBiosciences
CD235a	Mouse	BV421	BD Biosciences
CD73	Mouse	APC	BD Biosciences

Table 2.7 – Antibodies used for flow cytometric analysis.

### 2.7.1 Fluorescence Activated Cell Sorting (FACS)

For FACS sorting, cells were prepared in the same way as described for flow cytometry (see above), with the addition of a step whereby cells were passed through a 40 µm cell strainer (Fisher) after resuspension, before staining. Cells were stained with APC-conjugated CD326 (EpCAM) and PE-conjugated CD56

(NCAM) antibodies (both BD biosciences). FACS sorting was performed using either BD Biosciences FACS Aria™ or FACS Aria III™. Cells for FACS sorting were gated for Live/Dead using 7-AAD, and sorting performed until  $\approx 1 \times 10^6$  cells were collected. Compensation was performed using single-stained samples.

## **2.8 General DNA cloning techniques**

Eukaryotic expression plasmids were employed to create miRNA overexpressing lentiviruses for hESC transduction. All plasmids used in this study encoded ampicillin resistance. Cloning of miRNA fragments into pcDNA3.3 was performed using the pcDNA™3.3-TOPO® TA Cloning Kit (Life Technologies).

### **2.8.1 Genomic DNA extraction**

Extraction of genomic DNA from cells was performed using the QIAamp DNA Mini and Blood Mini Kit (Qiagen) as per manufacturer's instructions. Briefly, cells were collected, pelleted and resuspended in 200  $\mu$ L PBS. 20  $\mu$ L proteinase K was then added to each sample, followed by 200  $\mu$ L of buffer AL and then pulse-vortexed for 15secs. Tubes were placed at 56 °C for 10 min before 200  $\mu$ L ethanol was added and samples were mixed again by pulse vortexing. This mixture was then added to a QIAamp Mini spin column and centrifuged at 6,000 x g for 1 min. The QIAamp Mini spin column contains a silica membrane onto which the DNA is adsorbed. The conditions of the lysate and during wash steps ensure removal of proteins and other contaminants from the column, whilst still allowing the binding of DNA. Samples were washed via the addition of 500  $\mu$ L buffer AW1 and centrifuged again at 6,000 x g for 1 min. A second wash was performed using 500  $\mu$ L buffer AW2 and centrifuging at 16,000 x g for 3 min, followed by a further centrifugation step of 16,000 x g for 1 min to remove any remaining contaminants. The spin column was then placed in a 1.5 mL Eppendorf and DNA was eluted using 50  $\mu$ L of nuclease-free H<sub>2</sub>O. Concentration of DNA was then measured using the Nanodrop and stored at -20 °C until required.

### **2.8.2 Polymerase chain reaction (PCR)**

Standard reaction mixes and thermal cycling protocols are shown below. Protocols were optimised when standard conditions were unsuccessful. PCR primers (shown in table 2.8) were designed using OligoPerfect™ Designer

(Invitrogen, Life Technologies) software and purchased from Eurofins. Reactions were performed using Platinum®Taq DNA Polymerase (Invitrogen, Life Technologies) as shown below:

Per reaction:

Reagent	Amount per reaction (µL)
10 x Buffer	5
10 mM dNTP mix	1
50 mM MgCl <sub>2</sub>	1.5
Primer mix (10 µM of F and R)	1
Betaine	5
Taq Polymerase	0.2
H <sub>2</sub> O	Up to 50µL total reaction volume

Thermal cycling conditions:

- 1: 95 °C for 2 min
  - 2: 95 °C for 30 s
  - 3: 55 °C for 30 s
  - 4: 72 °C for 1 min
  - 5: 72 °C for 10 min
  - 6: 12 °C forever
- ←  x30

Primer name	miRNA(s) to amplify	5' Addition	Primer sequence
miR-145 F	miR-145	ATGCCTCGAG	GAGCAATAAGCCACATCCG
miR-145 R	miR-145; miR-143/145 cluster	ATGCACGCGT	TCCAGGGACAGCCTTCTTC
miR-143 F	miR-143; miR-143/145 cluster	ATGCCTCGAG	TGGTCCTGGGTGCTCAAAT
miR-143 R	miR-143	ATGCACGCGT	ATGGACACACTGGGGTACACA

**Table 2.8 – Sequence of primers used for PCR amplification of miR-145, miR-143 and miR-143/145 cluster.**

A mix of 10µM of forward (F) and reverse (R) primers were used in each reaction.

### 2.8.3 Restriction digest

Restriction digests were performed as diagnostic tools, and for the insertion of specific DNA sequences (inserts) into plasmid backbones for expression. Reactions were performed using restriction endonucleases (all used in this study from New England Biosciences), in either a 20 µL reaction (for diagnostic

purposes) or in a larger, 250  $\mu$ L reaction for digestion and purification of plasmid or insert DNA.

Small 20  $\mu$ L reactions contained 500 ng DNA, 0.5  $\mu$ L of each specific restriction endonuclease, 0.2  $\mu$ L BSA, 2  $\mu$ L buffer (matched for the activity of each enzyme) and were made up to 20  $\mu$ L total volume using nuclease-free H<sub>2</sub>O. Samples were incubated at 37°C for  $\approx$ 2 h. DNA gel electrophoresis was performed to visualise DNA and assess digests.

For insertion of specific sequences into a plasmid backbone, both plasmid and insert were digested using the same restriction endonucleases to ensure the creation of compatible ends for ligation. 10  $\mu$ g of DNA was added to each restriction digest, with 2  $\mu$ L of each enzyme, 2.5  $\mu$ L BSA, 25  $\mu$ L of buffer and the total volume made to 250  $\mu$ L using nuclease free H<sub>2</sub>O. Samples were incubated overnight at 37°C. Purification was subsequently performed using DNA gel electrophoresis and gel extraction (section 2.8.4).

## **2.8.4 DNA gel electrophoresis**

Gel electrophoresis allows for the separation of DNA molecules based on size. An appropriate percentage agarose gel was chosen (0.8-2.5% w/v) based on fragment sizes and agarose was dissolved and electrophoresed in 1 x Tris-Borate EDTA (TBE) buffer (Gibco, Paisley). Ethidium bromide (1 ng/100mL) was added to molten agarose before gels were poured. Gels were run in BIO-RAD electrophoresis tanks and using a BIO-RAD Power Pac 300, at a constant voltage of 30-100 V. Samples were mixed with 6 x blue/orange loading dye and loaded onto the gel along with appropriate DNA marker ladders (100 bp or 1 Kb) (Promega, Southampton, UK). Bands were visualised using trans UV illumination on a ChemiDoc XRS+ Imaging System.

### **2.8.4.1 Gel extraction and purification**

In order to perform further ligation of digested plasmids and inserts, restriction endonuclease digested DNA was purified using gel extraction using the Wizard® SV Gel and PCR Clean-Up System (Promega, Southampton, UK). This kit is based on the ability of DNA to bind to silica membranes in the presence of chaotropic salts. Following electrophoresis, DNA bands were excised, placed in a 15 mL

falcon and 10  $\mu$ L Membrane Binding Solution was added per 10 mg of gel slice. Falcons were incubated at 65°C and vortexed until gel was completely dissolved. The dissolved gel mixture was then transferred to an SV Minicolumn in a collection tube, and incubated at room temperature for 1 min. columns were then centrifuged at 16,000 x g for 1 min. Flow through was discarded and this was repeated until all of the gel mixture had been passed through the column. 700  $\mu$ L of Membrane Wash Solution was then added and columns centrifuged at 16,000 x g for 1 min. This was repeated with 500  $\mu$ L of Membrane Wash Solution, with a longer 5 min centrifugation. Tubes were finally centrifuged at 16,000 x g for 1 min to remove any residual ethanol - present in the Membrane Wash Buffer. DNA was then eluted from the column using 50  $\mu$ L nuclease-free H<sub>2</sub>O, and centrifuging at 16,000 x g for 1 min. Eluate was collected and passed through the column again to ensure highest possible recovery.

### 2.8.5 Dephosphorylation and ligation

Dephosphorylation of plasmid DNA was performed in order to prevent circularisation during ligation. This was performed using Antarctic Alkaline Phosphatase (New England Biolab UK Ltd, Hertfordshire, UK), following the manufacturers' protocol. Briefly, 500 ng of plasmid DNA was added to 2  $\mu$ L Antarctic Phosphatase enzyme, 1  $\mu$ L 10 x Antarctic Phosphatase buffer and made up to 10  $\mu$ L total using nuclease free H<sub>2</sub>O. Reactions were incubated at 37°C for 15 min, followed by 10 min incubation at 65°C to deactivate the enzyme.

Ligation of inserts into dephosphorylated plasmid was performed using T4 DNA ligase (New England Biolabs UK Ltd, Hertfordshire, UK) as per manufactures' instructions. Reactions were performed at a variety of molar ratios to ensure successful ligation of inserts into plasmid backbone. Ratios of 1:1 and 1:3 of plasmid:insert were routinely used, with a negative control of 1:0. Molar ratios were calculated using the following equation:

$$\left( \frac{\text{ng of vector} \times \text{Kb of insert}}{\text{Kb of vector}} \right) \times \text{molar ratio} = \text{ng of insert}$$

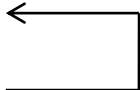
50 ng of dephosphorylated plasmid vector was added to each reaction, along with the calculated amount of insert DNA, 1  $\mu$ L T4 DNA ligase enzyme, 2  $\mu$ L 10 x

T4 ligase buffer were added to a 0.5 mL microcentrifuge tube and reaction made up to 20  $\mu$ L total using nuclease-free H<sub>2</sub>O. Samples were incubated at 16°C overnight. Ligation success was probed using restriction endonuclease digest (section 2.8.3) and sequencing (section 2.8.6).

## 2.8.6 Sequencing

Sequencing of cloned plasmids and inserts were routinely performed to check the cloning efficiency. DNA sequences were analysed using dideoxy sequencing.

300 ng of plasmid DNA was used in each sequencing reaction, along with 2 nM of forward or reverse sequencing primers, 0.5  $\mu$ L Ready Reaction Mix (Applied Biosystems, UK) and 3.5  $\mu$ L Sequencing Buffer. The reaction was then made up to a final volume of 20  $\mu$ L using nuclease-free H<sub>2</sub>O. Samples were then subject to 25 PCR cycles at the following conditions:

1: 96°C for 50 s		x25
2: 50°C for 20 s		
3: 60°C for 3 min		

The PCR products were then cleaned using CleanSEQ (Agencourt Bioscience Corporation, MA, USA) following the manufacturers' protocol. 20  $\mu$ L of sequencing products were then loaded into optically clear barcoded 96-well PCR plates for capillary electrophoresis, which was performed on a 48-capillary Applied Biosystems 3730 Genetic Analyser with 36 cm capillaries.

## 2.8.7 Plasmid purification

### 2.8.7.1 Transformation of competent bacteria

Successfully cloned expression plasmids were transformed into chemically competent bacteria. One Shot® TOP10 chemically competent *Escherichia coli* (*E. coli*) (Invitrogen, Life Technologies) were used as hosts in this study, and transformations were performed as per the manufacturer's instructions. A vial of One Shot® bacteria was thawed on ice. Once thawed, 1-5  $\mu$ L (10 pg-100 ng) of plasmid DNA was added, mixed gently and incubated on ice for 30 min. Cells were then heat-shocked in at water bath at 42°C for 30 s, before being removed and immediately incubated on ice for 2 min. 250  $\mu$ L of S.O.C medium was then

added, and the tube was shaken, horizontally, for 1 h at 200 rpm and 37°C in a shaking incubator. Varying amount of the plasmid-media mix was then spread onto pre-warmed Luria agar (Sigma) culture plates containing 100 µg/mL ampicillin, and incubated overnight at 37°C. Bacterial colonies were then selected and grown overnight in 10 mL Luria broth (LB), before they were screened using diagnostic restriction digests, DNA electrophoresis and plasmid sequencing (described in sections 2.8.3, 2.8.4 and 2.8.6).

#### **2.8.7.2 Small scale DNA purification**

Small scale DNA purification was performed using the PureLink® Quick Plasmid Miniprep Kit (Invitrogen, Life Technologies), and 2-3 mL transformed *E.coli* in LB medium from overnight culture. Bacteria were harvested by centrifugation at 6,000 x g for 5 mins, and the supernatant discarded. The cell pellet was then resuspended in 250 µL resuspension buffer R3 (50 mM Tris-HCl, pH 8.0; 10 mM EDTA) containing RNase A (100 µg/mL). 250 µL lysis buffer L7 (200 mM NaOH, 1% w/v SDS) was then added and the sample was mixed by inverting the tube until the mixture was homogenous. The mix was then incubated at room temperature for 5 min, and then centrifuged at 12,000 x g for 10 min. The supernatant was then loaded onto a spin column - a silica membrane column which selectively binds plasmid DNA - in 2 mL wash tube and centrifuged at 12,000 x g for 1 min. 500 µL of wash buffer W10 was added to the column, incubated at room temperature for 1 min and then centrifuged at 12,000 x g for 1 min. 700 µL of a second wash buffer W9 was then added to the column, and again centrifuged at 12,000 x g for 1 min. The flow through was discarded and the column was centrifuged again at 12,000 x g for 1 min to remove any remaining ethanol contamination. The spin column was transferred to a new 1.5 mL Eppendorf and plasmid DNA was then eluted from the column using 50 µL nuclease-free H<sub>2</sub>O. The water was added to the column, incubated for 1 min at room temperature, and then centrifuged at 12,000 x g for 2 min. DNA concentration was measured using the Nanodrop (Thermo Scientific) and stored at -20°C until required.

#### **2.8.7.3 Large scale DNA purification**

The PureLink® HiPure Plasmid Maxiprep Kit was used to perform large scale DNA purification. A 10 mL 'starter' culture, made using a single colony, was added to



a further 450-500 mL LB medium containing 100 µg/mL ampicillin and incubated overnight in a shaking incubator at 37°C and 170 rpm. Bacteria were first collected by centrifugation at 6,000 x g for 5 min at 4°C, in a Beckman Coulter Avanti J-26XP. All supernatant was discarded and the pelleted cells were resuspended in 10 mL resuspension buffer R3 (50 mM Tris-HCl, pH 8.0; 10 mM EDTA) containing RNase A (100 µg/mL) until homogenous. 10 mL lysis buffer L7 (0.2 M NaOH; 1% w/v SDS) was then added and mixed gently by inversion until the sample is thoroughly mixed and completely homogenous. The mixture was then incubated at room temperature for 5 min to ensure sufficient lysis, the SDS in the solution acts a detergent to disrupt the bacterial membrane and NaOH denatures chromosomal DNA and proteins. To neutralise the lysis, 10 mL precipitation buffer N3 (3.1 M potassium acetate, pH 5.5) was added, and the sample immediately mixed by inverting the tube until the mixture is homogenous. The precipitated lysate was then centrifuged at 20,000 x g for 20 min. The clarified supernatant was then added to a HiPure Column, pre-equilibrated using equilibration buffer EQ1 (0.1 M sodium acetate, pH 5.0; 0.6 M NaCl; 0.15% (v/v) Triton® X-100), and allowed to drain by gravity flow. The HiPure columns use an anion-exchange resin to bind DNA. The negatively charged phosphates on the backbone of the DNA will interact with the positive charges on the surface of the resin. Temperature, salt concentration and pH of solutions all influence the binding of the DNA. Once all of the clarified supernatant has passed through the column, 60 mL wash buffer W8 (0.1 M Sodium acetate, pH 5.0; 825 mM NaCl). The moderate salt conditions, which occur on the column during washing with W8, allow for plasmid DNA to remain bound, whilst RNA, proteins and other impurities are removed. Plasmid DNA was then eluted from the column using 15 mL elution buffer E4 (100 mM Tris-HCl, pH 8.5, 1.25 M NaCl). 10.5 mL isopropanol (2-propanol) was used to precipitate the DNA, before the mixture was centrifuged at 15,000 x g for 30 min at 4°C. The pelleted DNA was then washed in 4 mL 70% ethanol, and 4 x 1 mL aliquoted into 4 x 1.5 mL eppendorfs. Eppendorfs were centrifuged at full speed for 5 min at 4°C and all supernatant was removed. Pellets were then allowed to air dry, either on the bench top at room temperature, or at 37°C. Once dried, DNA pellets were combined in a total of 200 µL nuclease-free H<sub>2</sub>O and centrifuged at full speed for 1 min, to remove any remaining impurities. Finally, the supernatant was transferred to a clean 1.5 mL Eppendorf. DNA concentration

was measured using the Nanodrop (Thermo Scientific) and stored at  $-20^{\circ}\text{C}$  until required.

#### **2.8.7.4 Glycerol stocks**

700  $\mu\text{L}$  of overnight bacterial cultures were combined with 300  $\mu\text{L}$  glycerol solution for long term storage of successfully transformed bacterial cultures. The bacteria-glycerol mixture was then stored at  $-80^{\circ}\text{C}$ . Recovery of bacterial from these stocks was performed by thawing, followed by streaking for single colonies on ampicillin containing agar plates.

## **2.9 Lentivirus production**

Lentiviral vectors were second-generation, self-inactivation (SIN), HIV-1 based and produced as previously described (Demaison et al., 2002).

### **2.9.1 Production of Lentivirus via triple transfection method**

Lentiviral vectors were produced using a transient triple transfection protocol, whereby HEK293Ts were transfected with 3 different plasmids, required for viral production; the expression plasmid (pHR<sup>'</sup>SIN-cPPT-SFFV-MCS-WPRE; pSFFV Lenti MCS) containing the desired gene under the control of the spleen focus-forming virus (SFFV) promoter (a kind gift of Prof. Adrian Thrasher, Institute of Child Health, University College London, London, UK), a packaging plasmid (pCMV $\Delta$ 8.74) which contains Gag, Pol, Tat and Rev, and a plasmid encoding the enveloped of vesicular stomatitis virus (VSVg) (pMDG). Polyethylenimine (PEI; Sigma-Aldrich) was used as the transfection reagent. Lentivirus preparations were performed in batches of 6 or 12 T150 flasks and cells were prepared as previously described (section 2.2.1).

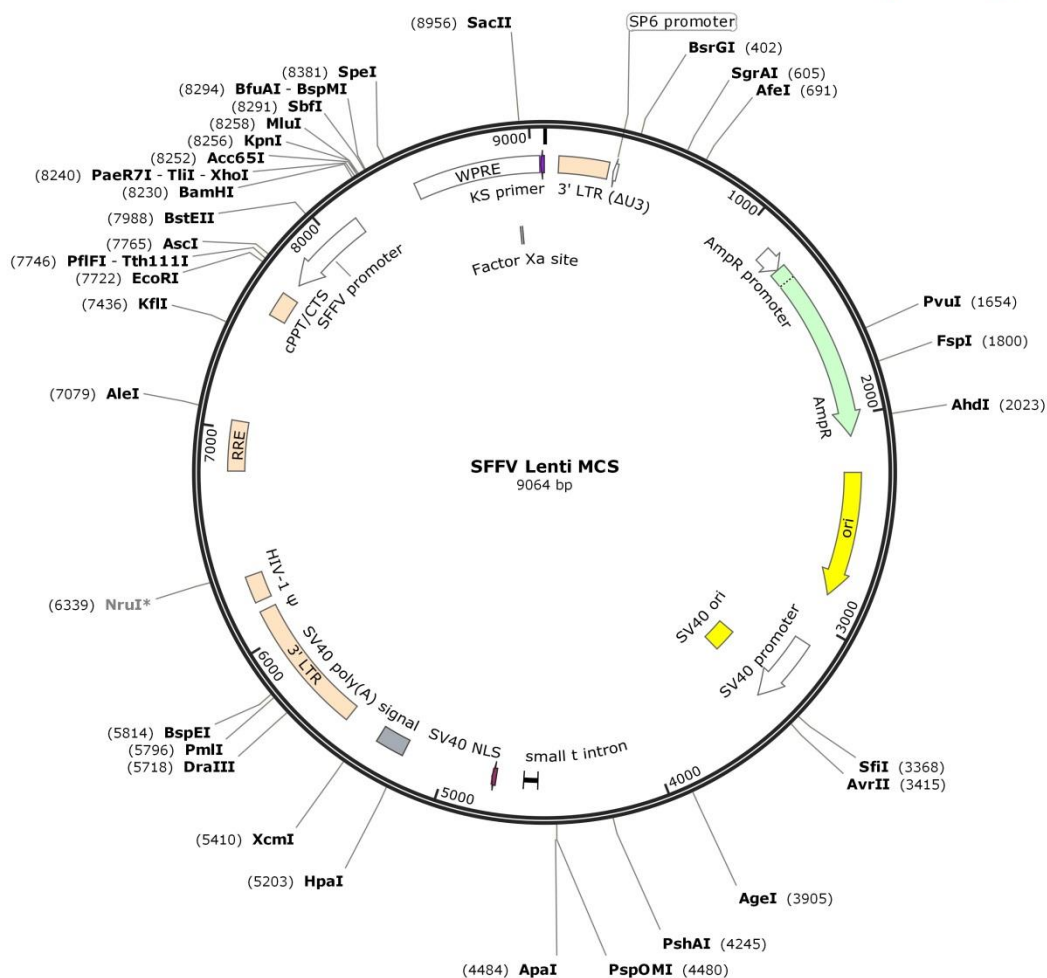


**Figure 2.2 – Plasmid map for pSFFV Lenti MCS.**

Plasmid map showing the sequence of the pSFFV Lenti MCS. Features are shown, as are unique restriction sites.

For each T150 flask, 2 mixes were prepared; one containing the 3 plasmids for transfection, and one containing the PEI. Each DNA mix contained 50  $\mu$ g expression plasmid, 17.5  $\mu$ g PMDG and 32.5  $\mu$ g pCMV $\Delta$ 8.74, in 5 mL Opti-MEM reduced serum medium with GlutaMAX™ supplement (Gibco, Paisley), and was filtered using a 0.22  $\mu$ m sterile filter. 5 mL Opti-MEM containing 1  $\mu$ L PEI was then sterile filtered and added directly to the DNA mixture. Tubes containing DNA and PEI were then incubated in a tissue culture cabinet, at room temperature, avoiding exposure to light, for 20 min. This allows for the formation of DNA:PEI complexes, which have endosomolytic activity, and are protected from lysosomal degradation.

Culture medium was removed from HEK293Ts and cells were gently washed with 5 mL Opti-MEM medium. This was then removed and 10 mL of medium containing DNA:PEI complexes were added to the flask. Cells were incubated for 4 h at

37°C and 5% CO<sub>2</sub>. After 4 h Opti-MEM was removed, replaced with 20 mL fresh complete culture medium (section 2.2.1) and cells were returned to the incubator. Lentiviral particles are produced and released into the medium by the cells after successful transfection of the 3 plasmids. Medium was collected after 48 h, replaced with 10 mL fresh complete culture medium and filtered using a 0.22 µm sterile filter unit. Cells were cultured for a further 24 h, when medium was collected, filtered and combined with the medium removed at 48 h.

### **2.9.2 Concentration of Lentivirus**

After collection, lentivirus was concentrated using ultracentrifugation. Briefly, media collected from triple-transfected cells was dispensed into Beckman 14 x 95 mm (14 mL) plastic tubes (Beckman Coulter), loaded into a SW-32.1 Ti rotor buckets and placed into the SW32 Ti rotor (Beckman Coulter). Ultracentrifugation was then performed at 23,000 rpm for 1 h at 4°C in an Optima L-80 XP Ultracentrifuge (Beckman Coulter). Supernatant was discarded and this process was repeated until all virus-containing medium had been used. Excess media was removed from all tubes before 100 µL Opti-MEM® reduced serum medium with GlutaMAX™ supplement (Gibco, Paisley) was added to each tube, and incubated for 1 h at 4°C. Pelleted lentivirus was then resuspended in the OptiMEM, and the virus was aliquoted and stored at -80°C until required.

### **2.9.3 Calculation of lentiviral titre**

The concentration of produced lentivirus, in particle infectious units per mL (PIU/mL), was determined using a TaqMan® qRT-PCR based method, which detects linear, double-stranded DNA pre-integration complexes as previously described (Butler et al., 2001). The sequence of the primers used was as follows; forward (F) - 5'-TGTGTGCCCGTCTGTTGTGT-3', reverse (R) - 5'-GAGTCCTGCGTCGAGAGAGC-3'. The probe used was FAM labelled with a TAMRA quencher, with the following sequence; 5'-(FAM)-CAGTGGCGCCCGAACAGGGA-(TAMRA)-3'.

HEK293T cells were cultured and seeded into a 12-well plate, at a density of 5x10<sup>4</sup> cells per well and left overnight. Lentivirus was serially diluted and added to each well at decreasing concentrations. Virus was allowed to transduce cells

for 72 h. After 72 h, cells were washed and 200  $\mu\text{L}$  PBS was added to each well. Cells samples in PBS were stored at  $-20^{\circ}\text{C}$  and underwent a freeze thaw prior to DNA extraction performed using the QIAamp Mini and Blood Mini kit as described in section 2.8.1. Concentrations of samples were determined using the Nanodrop and samples were diluted to 250  $\text{ng}/\mu\text{L}$  using nuclease-free  $\text{H}_2\text{O}$ .

To titrate samples, serial dilutions of the expression plasmid, used to make the lentivirus, were performed to generate a standard curve of  $1 \times 10^{13}$  to  $1 \times 10^4$  plasmid copies. To prepare the most concentrated standard, plasmid was diluted in nuclease-free  $\text{H}_2\text{O}$ , using the following calculation was performed:

1: Molecular weight of one copy of expression plasmid

$$\frac{\text{Size of plasmid (bp)} \times (\text{Size of 1 bp (660 Daltons)})}{\text{Avogadro's constant}} = \text{g per molecule}$$

Daltons = g/mole

Avogadro's constant =  $6.023 \times 10^{23}$  molecules/mole

2: Determine the copy number of plasmids in 1mL stock

$$\frac{\text{Concentration of stock plasmid (g/mL)}}{\text{g per molecule}} = \text{no. molecules per mL}$$

3: Preparation of top standard ( $1 \times 10^{13}$  copies)

$$\frac{\text{no. of molecules per mL}}{1 \times 10^{13}} = \text{initial dilution factor for top standard}$$

$$\frac{1000}{\text{initial dilution factor for top standard}} = \mu\text{L of plasmid stock needed to make 1mL } 1 \times 10^{13} \text{ standard}$$

A reaction master mix was prepared and 11.5  $\mu\text{L}$  was added to each well of a 384-well PCR plate, with each well containing the following:

2x TaqMan® Universal Master Mix	2 $\mu\text{L}$
Primer/Probe mix	3.125 $\mu\text{L}$
Nuclease-free $\text{H}_2\text{O}$	2.125 $\mu\text{L}$

1  $\mu\text{L}$  of DNA standard or DNA samples collected from lentiviral titre was added to each well, and reactions were performed in technical triplicate. The samples were then run on the ABI Prism Applied Biosystems 7900HT sequence detection system as previously described (section 2.5.3).

Titre was calculated by plotting cycle threshold (cT) values for standards, and solving the equation of the line for each virus titration sample. This generates a value of copies of plasmid DNA in each sample. The number of cells whose DNA would have been included in 250 ng DNA was also calculated:

concentration of DNA collected  $\times$  50  $\mu\text{L}$  = total ng DNA collected

$$\frac{\text{total ngDNA collected}}{\text{ng DNA in 1 } \mu\text{L}} \times 100 = \% \text{ of total DNA added for 250 ng}$$

$$\frac{5 \times 10^4}{\% \text{ of total DNA added for 250 ng}} = \text{no. cells used for 250 ng DNA}$$

The number of copies of plasmid DNA in each sample, plus the number of cells whose DNA was included in 250 ng were then used to calculate the number of copies of plasmid per cell:

Copies of plasmid in sample  $\times$  no. of cells used in 250 ng = copies of plasmid per cell

And this was subsequently used to calculate PIU/mL:

$$\text{copies of plasmid per cell} \times \left( \frac{\text{dilution factor of virus stock used} \times 1000}{\mu\text{L virus added to cells}} \right) = \text{PIU/mL}$$

## 2.10 Lentiviral transduction of hESCs

Unless stated, all viral infections were performed using a multiplicity of infection (MOI) of 10. The MOI describes the ratio of virus to cells, where an MOI of 10 is the addition of 10 viral particles per cell, and is calculated as follows:

$$\frac{\text{Cell no.} \times \text{MOI}}{\text{viral titre}} = \mu\text{L virus to add}$$

### **2.10.1 Monolayer transduction**

Titration of EGFP lentivirus was performed using a monolayer transduction protocol. hESCs were passaged enzymatically using TryPLE select (Gibco, Paisley) and plated out in 12-well tissue culture dishes, coated with CellStart matrix, at a density of  $1 \times 10^5$  cells per well and in the presence of Y-27632 (ROCK inhibitor). Cells were incubated overnight at 37°C and 5% CO<sub>2</sub>. Virus was then added to the culture medium at the correct MOI and incubated for a further 24 h. After 24 h virus containing medium was removed and replaced with fresh culture medium. Cells were cultured for a further 48 h, before they were harvested and analysed.

### **2.10.2 Transduction of hESCs in suspension**

Transduction of hESCs in suspension was performed for overexpression studies during hESC-EC differentiation. To do this, hESCs were taken to a single cell suspension using TryPLE Select as previously described. Cells were counted and added to 1 mL Stemline II medium in a 15 mL falcon. Virus was then added at the correct MOI and cells were incubated at 37°C for 30 min. Mixing was performed at intervals of 10 min to ensure a homogenous mixture of virus and cells.

After 30 min incubation cells were added to Stemline II containing d0 cytokines and hESC-EC differentiation was performed as previously described (2.3.1).

All viral transduction experiments were performed using the following negative controls; non-transduced, EGFP-pSFFV lentivirus and pSFFV-‘empty’ lentivirus, where pSFFV-‘empty’ contained the pSFFV expression plasmid without an insert.

## **2.11 Statistical analysis**

Unless stated, values are presented as mean  $\pm$  the standard error of the mean (SEM). qRT-PCR results are expressed as relative quantification (RQ) calculated

using  $2^{-\Delta\Delta CT}$  (see section 2.5.3), and error is expressed as RQ max and RQ min, determined by the calculation of RQ using  $\Delta\Delta CT \pm SEM$ .

Statistical analysis was performed using GraphPad Prism 5 Software (California, USA). Student's t-test was used to perform comparisons when 2 groups were present, or one-way analysis of variance (ANOVA), followed by a Tukey's post hoc t-test, in experimental conditions with more than 2 groups. In conditions where multiple readings were taken from the same sample set, paired or repeated measures tests were used. Statistical significance was accepted as  $p < 0.05$ .



## **Chapter 3    Development and characterisation of a direct hESC-EC differentiation protocol.**

### 3.1 Introduction

It has been suggested that hPSC-derived ECs, may hold the key to the development of a long term cell-based therapy for the treatment of a wide range of ischemic diseases, such as PAD, CLI, CHD and stroke. It is believed that these cells are able to stimulate angio- and vasculogenesis *in vivo*, and this has been demonstrated in a number of different publications, with cells generated using a variety of hPSC-EC differentiation protocols (Kane et al., 2010, Orlova et al., 2014a, Patsch et al., 2015).

Thus far, there have been a number of protocols published describing the generation of ECs from hPSCs; either hESCs (hESC-ECs) or hiPSCs (hiPSC-ECs), and these have been reviewed extensively (Descamps et al., 2012). Many early publications used undefined systems, containing serum-supplemented or conditioned medium (Levenberg et al., 2002) or co-culture with stromal cell lines, any of which make the protocol unsuitable for use in a clinical setting. Additionally, undefined culture can lead to introduction of unknown factors, thus making it difficult to study exact mechanisms and pathways involved in specific differentiation and culture systems. Therefore, studies have focused on the development of protocols using more defined conditions. Differentiation efficiency in many of these protocols has, however, been poor, with generation of <10% hPSC-ECs. Recently, a number of publications have demonstrated more efficient generation of these cells (Orlova et al., 2014a, Orlova et al., 2014c, Patsch et al., 2015). Development of efficient differentiation protocols is essential for the translation of any cell-based therapy, due to the large numbers of cells which may be needed for each treatment.

Gaining further understanding of mechanisms of both differentiation and commitment will allow for the development of more efficient protocols. Signalling pathways, molecules or non-coding RNAs involved in differentiation, may be manipulated in order to drive differentiation, and produce higher number of hPSC-ECs for potential transplantation. In order to study mechanisms of mesodermal and early endothelial commitment, and to determine the role of specific factors within this differentiation system, there has also been a focus on the identification of progenitor cell populations, existing within these *in vitro* hPSC-EC differentiation systems. Early mesodermal progenitor (MP) populations

are, thus far, poorly defined and various studies have suggested an array of cell surface marker profiles, describing these distinct populations (Evseenko et al., 2010, Drukker et al., 2012, Kurian et al., 2015).

One study, published in 2010, suggested that these MP cells can be described as cells negative for the cell surface marker epithelial cell adhesion molecule (EpCAM; CD326) and positive for neural cell adhesion molecule (NCAM; CD56), also known as CD326<sup>-</sup>CD56<sup>+</sup> (Evseenko et al., 2010). During early embryogenesis, epithelial-to-mesenchymal transition (EMT) plays an important role in gastrulation and lineage specification and, specifically, has been shown play a key role in the generation of mesoderm in several experimental organisms (Nakaya et al., 2008). Specifically, FGF, Wnt and TGF $\beta$  signalling, have been shown to contribute to mesoderm formation via EMT *in vivo* (Ciruna et al., 2001, Kemler et al., 2004, Ben-Haim et al., 2006). It was therefore, hypothesised that the earliest stage of mesoderm formation during hESC differentiation *in vitro* may also be associated with this process. CD56 had previously been shown to be upregulated during EMT in human epithelial breast carcinoma cells, and this upregulation was associated with a loss of E-cadherin and epithelial cell adhesion molecule (Lehembre et al., 2008). Similarly to epithelial cells, hESCs express adhesion molecules such as E-Cadherin and CD326, that may possibly play roles in the maintenance of hESC pluripotency (Lu et al., 2010). In hESC culture, CD326 is localised to Oct4 positive cells, and becomes downregulated during differentiation, with knockdown causing an increase in mesoderm-associated markers in pluripotent cells (Lu et al., 2010, Ng et al., 2010b). Evseenko et al. demonstrated that CD326<sup>-</sup>CD56<sup>+</sup> cells, occurring at day 3.5 of a general hESC-mesoderm differentiation protocol, represent a multipotent mesoderm-committed progenitor population, capable of differentiating towards hematopoietic, endothelial, mesenchymal, smooth muscle and cardiomyocyte lineages, whilst lacking the ability to differentiate to endo- or ectodermal lineages (Evseenko et al., 2010). These cells, herein known as mesoderm progenitors (MP), were described as possible precursors to previously described, more lineage-restricted, mesodermal progenitor cell types.

Experiments within this chapter were designed to develop and characterise an efficient hESC-EC differentiation protocol, generating immature vascular ECs directly from hESCs. Using the marker profile published by Evseenko et al., we

also wanted to probe early MP populations, existing within the direct hESC-EC differentiation system (Evseenko et al., 2010). Identified populations could then be used for investigation and interrogation of factors, mechanisms and pathways involved in hESC-EC commitment, thus allowing for manipulation of the system and the potential to increase differentiation efficiency by driving hESCs toward an EC phenotype.

## **3.2 Aims**

The aims of this chapter were as follows:

- To develop and characterise a direct hESC-EC differentiation protocol.
- To assess hESC-ECs produced using this newly developed direct hESC-EC differentiation protocol.
- To identify and characterise a multipotent MP cell population, existing within this direct hESC-EC differentiation system

### 3.3 Results

#### 3.3.1 Development of a direct hESC-EC differentiation protocol

Originally, a 6-well based differentiation protocol was developed for direct generation of hESC-ECs (Figure 3.1). In this protocol hESCs were taken at d0, and mechanically cut into clumps using a StemPro® EZPassage tool, before being transferred into a Corning Ultra Low Attachment 6-well cell culture plate in 3mL Stemline II media. On day 3, EBs were collected and dispersed using Tryple Select, before they were plated onto 0.1% gelatin in 2mL LONZA EGM-2 medium containing 50ng/mL VEGF. Although able to generate CD31<sup>+</sup>CD144<sup>+</sup> hESC-ECs at high efficiency (Figure 3.1), preliminary experiments suggested that the robustness of this protocol was poor, and reproducibility between experiments and hESC lines was low.

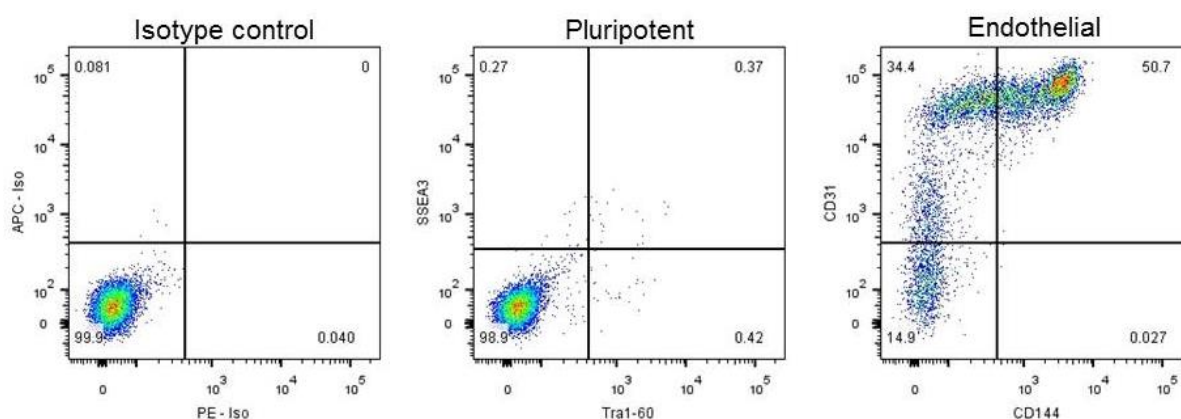


**Figure 3.1 – Preliminary analysis of H1 d7 hESC-ECs.**

H1 pluripotent hESCs were differentiated using a 6-well hESC EC differentiation protocol. Cells were harvested on d7, stained using antibodies against pluripotent (SSEA3, Tra1-60; centre) and endothelial (CD31, CD144; right) surface antigens. Dot plots show representative images.

Cytokines were added to the differentiation system at specific time points and concentrations as described in section 2.3.1. The cocktail of cytokines and growth factors given to cells in the differentiation medium, including BMP4, VEGF, Wnt3A and Activin A, were used to drive the cells towards a mesodermal fate. These specific factors, and their associated signalling pathways, have been implicated in development of the mesoderm or vascular system *in vivo* (Winnier et al., 1995, Dyson et al., 1997, Liu et al., 1999, Coultas et al., 2005), and have all been used extensively to recapitulate this phenomenon *in vitro* (Lindsley et al., 2006, Evseenko et al., 2010, Cerdan et al., 2012, Orlova et al., 2014c). Additionally, LONZA EGM-2 medium also contains a number of cytokines and

growth factors, including human Epidermal Growth Factor (hEGF), R3-Insulin-like Growth Factor-1, Ascorbic Acid, Hydrocortisone and human Fibroblast Growth Factor-Beta (hFGF- $\beta$ ), which support the maturation and expansion of hESC-ECs after d3.

To increase the levels of reproducibility between experiments, changes were made in the method used to create the EBs. Previously, EBs had been formed using mechanically cutting the cells into clumps, before transferring into ultra-low attachment 6 well plates, in the presence of Y-27632, a Rho kinase inhibitor. Optimisation involved standardising the size of the EBs, by using a spin EB protocol to form them in 96-well round-bottom tissue culture plates coated with 5% Pluronic F-127 (Ungrin et al., 2008). Cells were counted, and each EB was formed from 10,000 cells (Figure 3.2B). Unlike in previous versions of the differentiation protocol, d3 cells were not dispersed, and instead EBs were collected, washed and plated directly onto gelatin, where cells were cultured to allow outgrowth from the EB (Figure 3.2B). Once optimised, the newly developed 96-well direct differentiation protocol was then characterised.

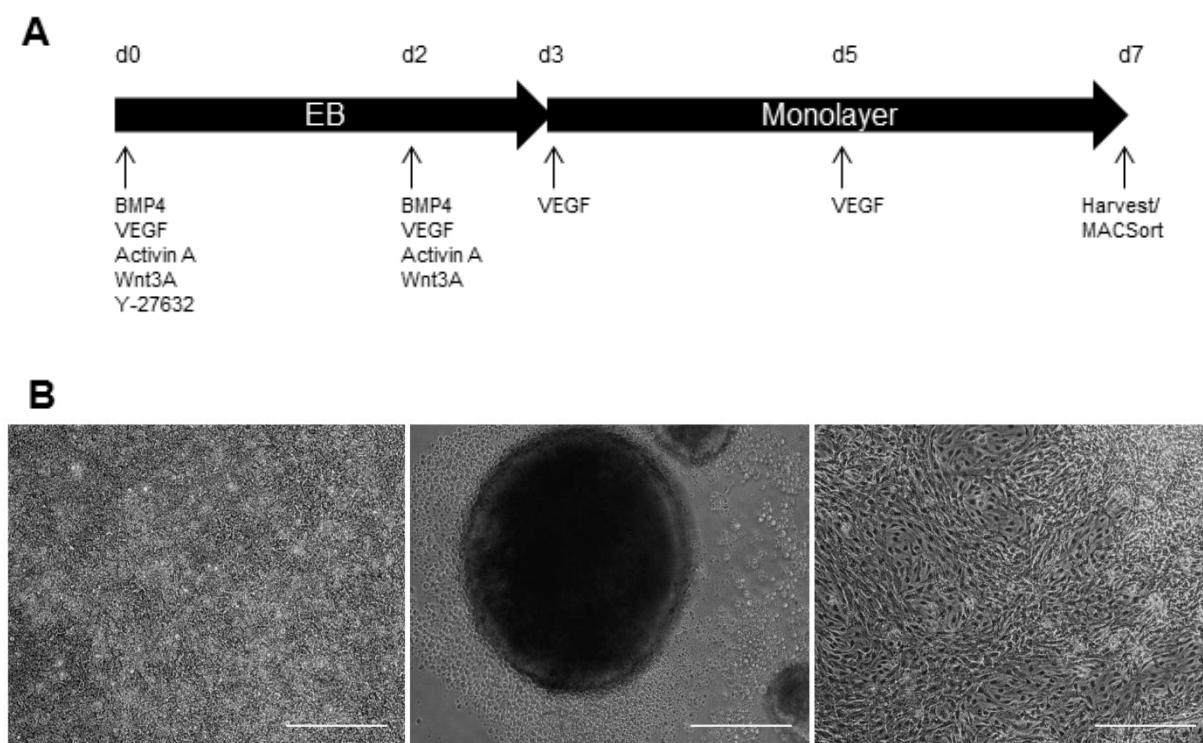


**Figure 3.2 – Direct hESC-EC differentiation.**

Pluripotent hESCs were dispersed to single cells at d0, allowed to form size controlled EBs and kept in this form until d3. EBs were then collected and plated out onto 0.1% gelatin, where they were cultured until d7, shown in the schematic (A). Specific combinations of cytokines were used at various time points, and this is described in detail in section 2.3.1. Bright field images of cells during at d0 (left), d3 (centre) and d7 (right) of hESC-EC differentiation are shown in B. Images are representative of each time point, and were taken at 10x magnification and scale bars represent 250  $\mu\text{m}$ .

### 3.3.2 Characterisation of hESC-ECs generated via a direct hESC-EC differentiation protocol

Originally, the H9 hESC cell line was differentiated using the 96-well direct hESC-EC differentiation protocol. Cells were harvested at d0, 3, 5 and 7, stained using antibodies against a number of different endothelial and pluripotent cell surface markers, and analysed by flow cytometry. Data presented in Figure 3.3A shows a significant increase in the percentage of total cells positive for two endothelial associated markers, CD31 (Pecam-1) and CD144 (VE-Cadherin), known as CD31<sup>+</sup>CD144<sup>+</sup> hESC-ECs, with approximately 35% of cells expressing this cell surface profile by d7. The CD31<sup>+</sup>CD144<sup>+</sup> cells exist as a distinct population, and this can be seen in the dot plots shown in Figure 3.3C. A concomitant decrease in pluripotency-associated markers was also observed, with on average less than 10% of cells expressing Tra1-60 on d7, significantly lower than on d0, where >90% of cells express this surface marker (Figure 3.4). Quantitative results obtained from FACS analysis were further validated using immunocytochemistry (ICC). Using this technique, it was possible to visualise cells staining positive for both CD144 and CD31 (CD31<sup>+</sup>CD144<sup>+</sup>), with the majority of staining occurring at the surface of positive cells (Figure 3.3E).



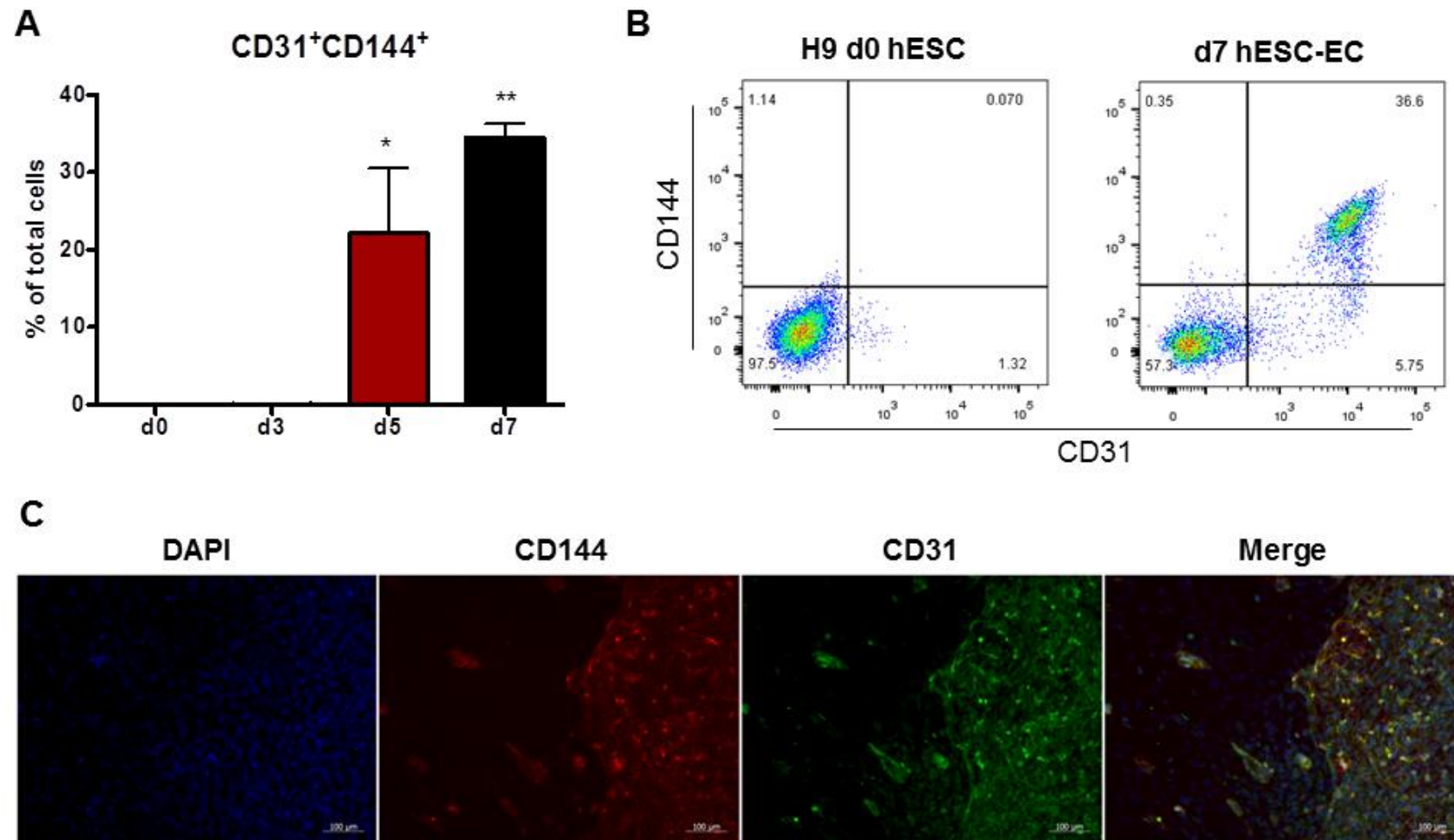


**Figure 3.3 – Analysis of endothelial – associated surface markers during H9 hESC-EC differentiation.**

H9 hESCs were subjected to direct hESC-EC differentiation, and cell surface markers analysed at d0, 3, 5 and 7. Flow cytometry was used to analyse expression of the endothelial markers CD144 (PE-conjugated) and CD31 (APC-conjugated) (A-B). Dot plots shown are representative. Histogram shows average percentage of total cells at each time point from n=3 experiments,  $\pm$  SEM. Repeated measures ANOVA, \* =  $p < 0.05$ , \*\* =  $p < 0.01$ , \*\*\* =  $p < 0.001$  when compared to d0 pluripotent control. d7 hESC-ECs were also subjected to analysis by immunocytochemistry (C). VE-cadherin/CD144 is shown in red, Pecam-1/CD31 in green and DAPI in blue.

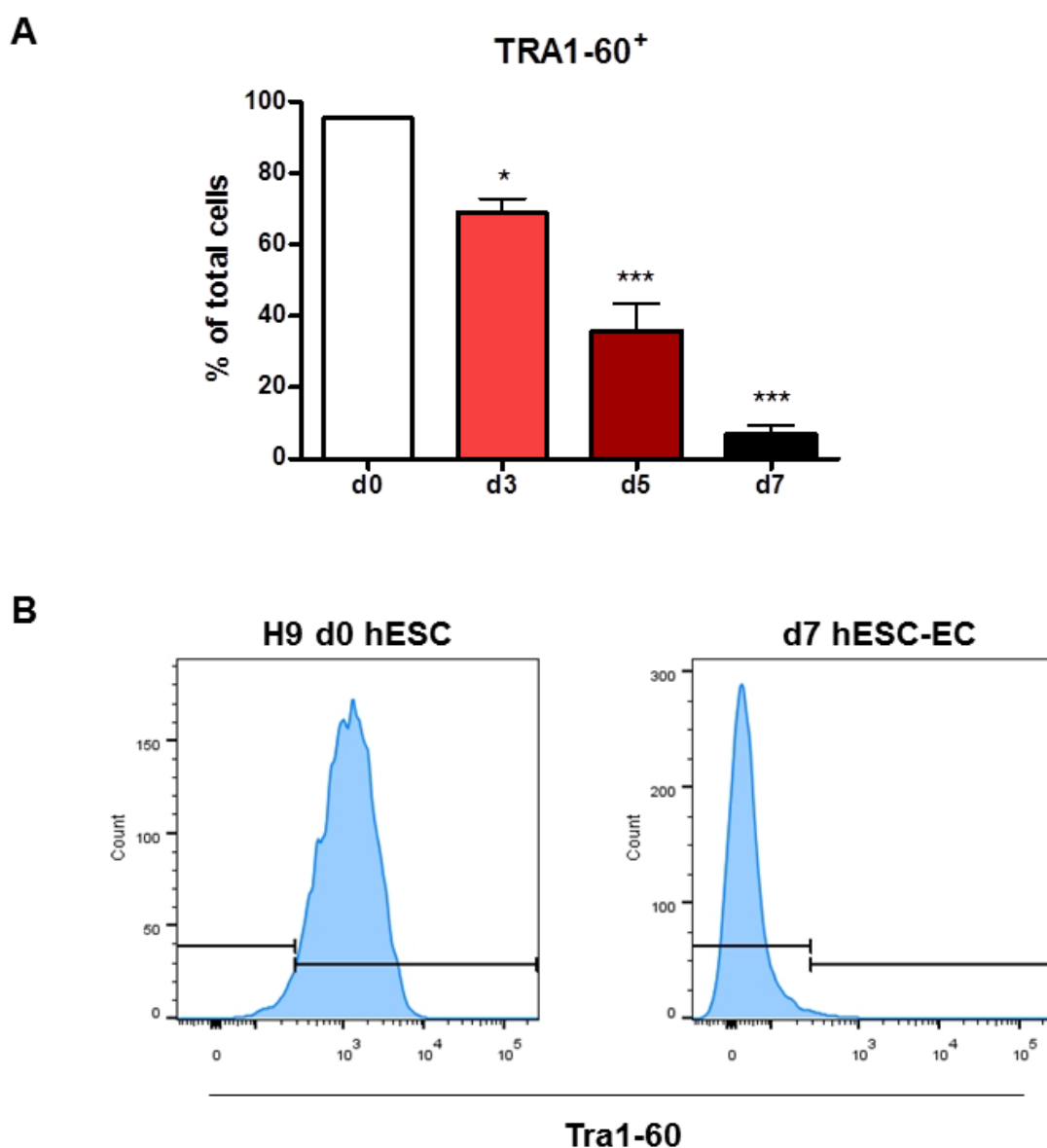


**Figure 3.4 – Analysis Tra1-60 expression during H9 hESC-EC differentiation.**

Cells were also stained for the pluripotency-associated marker Tra1-60 (PE-conjugated). Graph (A) shows average percentage of total cells at each time point from n=3 experiments,  $\pm$  SEM. Repeated measures ANOVA, \* =  $p < 0.05$ , \*\* =  $p < 0.01$ , \*\*\* =  $p < 0.001$  when compared to d0 pluripotent control. Flow cytometry histograms (B) shown are representative of all samples from that specific time point.

Total RNA samples were also collected from d0 hESCs, d1, 2 and 3 EBs and d5 and 7 heterogeneous hESC-EC populations. Samples were then subject to qRT-PCR gene expression analysis, interrogating the mRNA expression profiles of cells throughout hESC-EC differentiation. The expression levels of pluripotency-associated genes, such as *Nanog*, *Oct4* and *Sox2*, stayed constant during the first 3 days of hESC-EC differentiation, before a significant decrease was observed at d5 and 7, following the replating of EBs onto gelatin coated plates in endothelial supportive media. The lowest levels of pluripotency-associated gene expression were observed at d7, with cells continuing to lose their pluripotent phenotype

throughout the duration of hESC-EC differentiation (Figure 3.5A). A concomitant upregulation of *CD31* and *CD144*, both endothelial-associated genes, was also observed throughout hESC-EC differentiation. These genes were shown to be significantly upregulated by d5 and 7, with the greatest upregulation observed on d7, where genes went from almost absent (cT value ~35) to much more highly expressed (cT value ~25) (Figure 3.5B). These changes in expression from almost absent result in large RQ values (~1,500 and ~7,000 for *CD31* and *CD144* respectively), which are not true reflections of the actual fold changes (Figure 3.5).

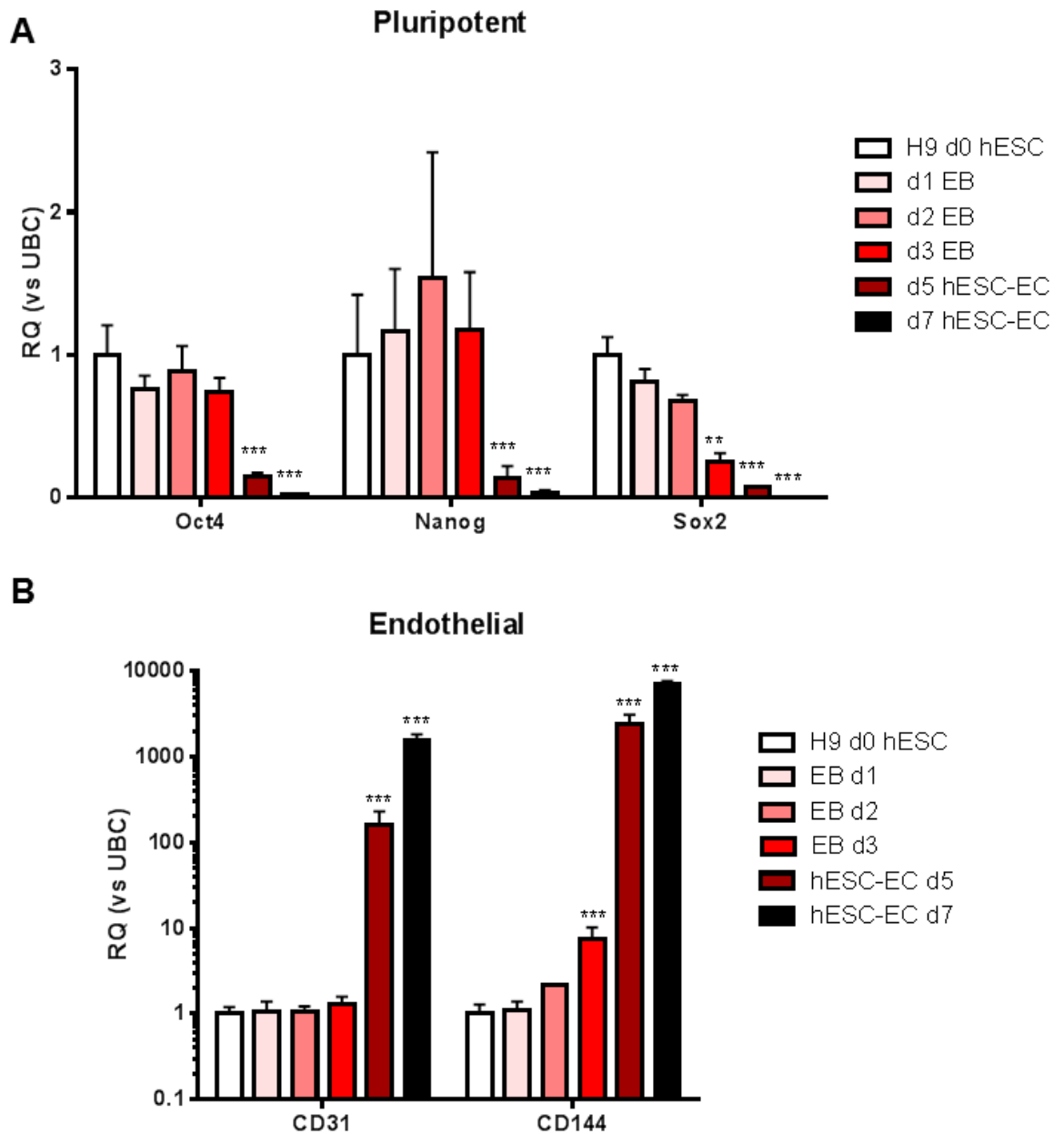


**Figure 3.5 – Gene expression analysis of direct hESC-EC differentiation.**

Pluripotency- (A) and endothelial-associated (B) gene expression was profiled throughout H9 hESC-EC differentiation using qRT-PCR. Cells were harvested from d0 hESCs, d1, 2 and 3 EBs, and d5 and 7 hESC-ECs and RNA extracted for analysis. Repeated measures ANOVA with Tukey post hoc t-test, \* =  $p < 0.05$ , \*\* =  $p < 0.01$ , \*\*\* =  $p < 0.001$  when compared to d0 pluripotent control. Data shown is  $RQ \pm RQ \text{ max}$ , relative to UBC reference gene. RQs calculated from  $n=3$  biological replicates. Y-axis on endothelial gene expression graph is expressed as a Log scale.

To ensure reproducibility of the newly developed differentiation protocol, experiments were also performed using the H1 hESC cell line, another of the original hESC lines derived by Thomson et al. in 1998 (Thomson et al., 1998). Although hESC-EC differentiations performed with this second cell line were less efficient, experiments produced approximately 20-30% CD31<sup>+</sup>CD144<sup>+</sup> hESC-ECs by d7 (Figure 3.6A). Similar to the results observed when using the H9 hESC line, the percentage of total cells expressing both endothelial-associated cell surface markers was increased from d5 of differentiation, with the highest levels observed on d7, and was accompanied by a decrease in the number of cells expressed Tra1-60, when analysed by flow cytometry (Figure 3.6B). The CD31<sup>+</sup>CD144<sup>+</sup> cells again existed as a distinct population, with most cells staining positive for CD144 co-expressing CD31, although the opposite was not always true, with 10% of cells expressing only CD31 (Figure 3.6C). Analysis of gene expression profiles by qRT-PCR also validated results previously shown in H9 hESCs, with results demonstrating a decrease in the levels of pluripotency-associated genes, including *Nanog*, *Oct4* and *Sox2*, throughout differentiation, again with the greatest downregulation occurring on d7 (Figure 3.6D). Significant upregulation of endothelial-associated *CD31* and *CD144* was also shown in d5 and d7 hESC-ECs (Figure 3.6E), with a large induction of *CD144* and *CD31* expression by d7. These data demonstrate the ability to efficiently and reproducibly generate CD31<sup>+</sup>CD144<sup>+</sup> hESC-ECs from different cell lines using this direct hESC-EC differentiation protocol.

Both the gene expression and flow cytometric data show the emergence of CD31<sup>+</sup>CD144<sup>+</sup> immature vascular ECs from d5 of direct hESC-EC differentiation, when experiments were performed using the H1 or H9 hESC line. The percentage of cells expressing endothelial markers continues to increase until d7, with a concomitant increase in the expression of these same two markers (*CD31* and *CD144*) at the RNA level. Therefore, for all subsequent experiments, d7 was chosen as the 'end point' of our direct hESC-EC differentiation, and the term hESC-EC will herein refer to this population.

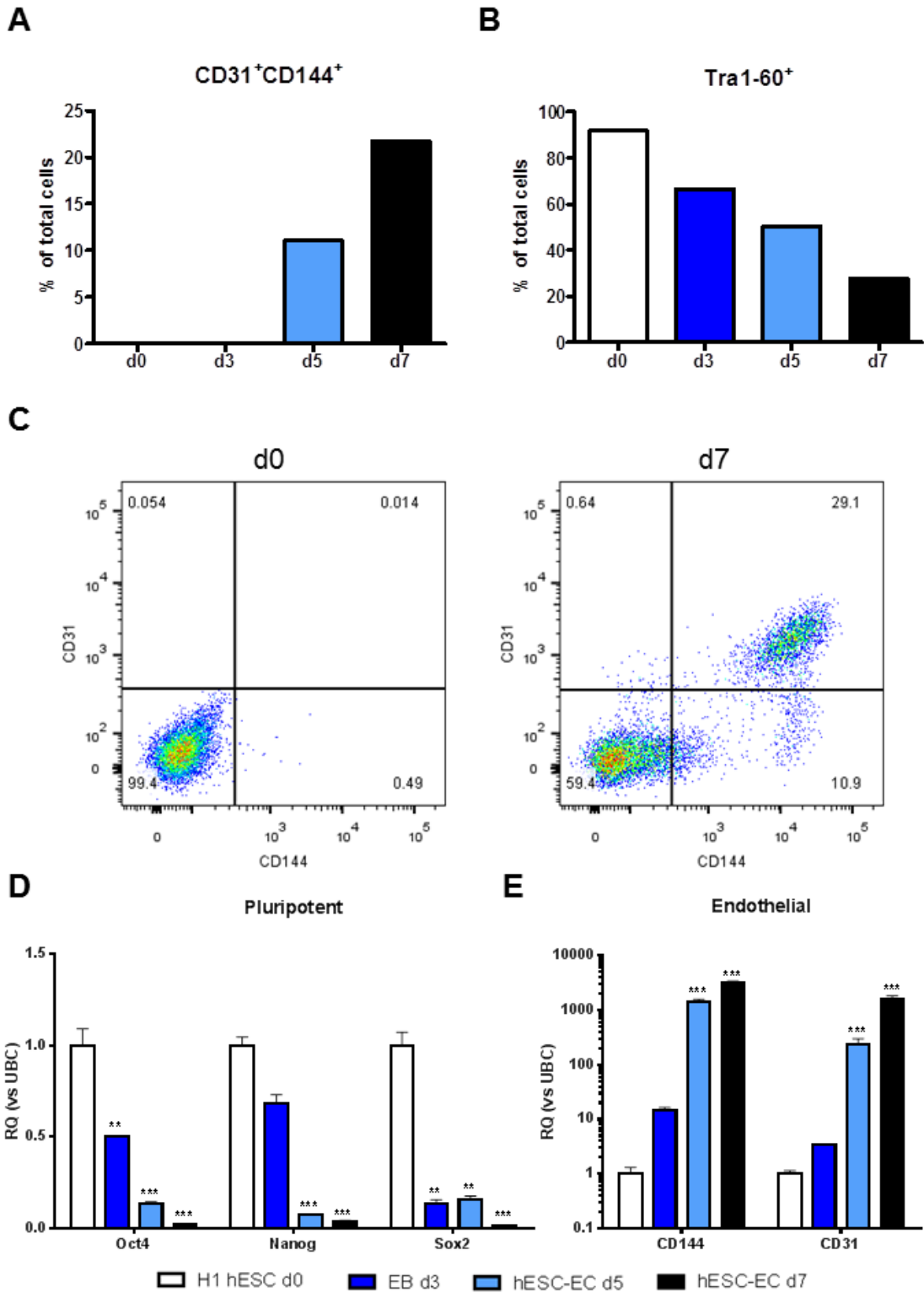


**Figure 3.6 – hESC-EC differentiation in H1.**

Cells were subjected to endothelial differentiation, and d0 H1 hESCs, d3 EBs and d5 and 7 hESC-ECs samples collected and analysed. Cells were stained using PE-conjugated anti-CD144 and APC-conjugated CD31 to assess differentiation efficiency. Average percentages of cells expressing CD31 and CD144 (A) and Tra1-60 (B) are shown in histograms. C shows representative dot plots for CD31 and CD144 at d0 and 7. n=2 experiments. Gene expression analysis for pluripotent (Oct4, Nanog, Sox2; D) and endothelial (CD144 and CD31; E) associated genes was also performed using RNA from the same time points. Graphs show RQ ± RQ max, n=3 experiments. Y-axis of endothelial gene graph is shown in Log scale. Repeated measures ANOVA with Tukey's post hoc comparisons, \* = p<0.05, \*\* = p<0.01, \*\*\* = p<0.001 when compared to d0 pluripotent control.

### 3.3.3 Purification and expansion of CD144<sup>+</sup> hESC-ECs

For further analysis of immature vascular ECs, magnetic activated cell sorting (MACS) was used to isolate and purify CD144<sup>+</sup> cells, as described in section 2.3.2. It was previously observed, using flow cytometry, that almost 100% of cells expressing CD144 were also positive for CD31 (Figure 3.4C and Figure 3.6C). A number of d7 cells, however, stained positive for CD31, but not CD144. Therefore, sorting of immature vascular ECs from the d7 heterogeneous hESC-EC population was performed using a single CD144 MACS selection protocol, described in detail in section 2.3.2. Briefly, cells were harvested and incubated in the presence of anti-CD144 antibodies conjugated to the surface of small magnetic beads. During the incubation, beads would bind CD144<sup>+</sup> hESC-ECs, whereas cells negative for CD144 would remain free in solution. CD144<sup>+</sup> cells were then selected for by passing the entire cell suspension through a column within a magnetic field; CD144<sup>+</sup> cells bound to magnetic beads would be trapped inside the column, whereas unbound cells would pass straight through. The column could then be removed from the magnetic field, and a pure population of CD144<sup>+</sup> hESC-ECs collected.

D7 hESC-ECs were harvested, MACSorted and the resultant positive and negative fractions analysed using flow cytometry. Cells were stained for CD144 and CD31, to ensure high levels of purity and confirm the efficiency of a single CD144 selection to isolate CD31<sup>+</sup>CD144<sup>+</sup> hESC-ECs. Analysis showed high levels of purity in the CD144<sup>+</sup> fraction (approximately 99%) (Figure 3.7B), whereas <10% of cells were CD31<sup>+</sup>CD144<sup>+</sup> in the CD144<sup>-</sup> fraction. Once purified, CD144<sup>+</sup> and CD144<sup>-</sup> cells were replated into 6-well plates, pre-coated with 0.1% gelatin, at a density of  $1 \times 10^5$  cells per well. Cells were cultured for a further 7 days, taking them to d14, in endothelial-supportive Lonza EGM-2 media, containing the FBS component and supplemented with 50ng/mL VEGF. At d14, there were clear morphological differences between the cells cultured from the d7 CD144<sup>+</sup> fraction, and those from the CD144<sup>-</sup> fraction (Figure 3.7C). CD144<sup>-</sup> cells appeared to be much smaller and densely packed, and appeared to grow at a much faster rate. Conversely, the cells cultured from the CD144<sup>+</sup> fraction formed a homogenous monolayer of cells, which begin to adopt a 'cobblestone-like' morphology. Analysis of the cells using flow cytometry revealed that only very low percentages of d14 cells, cultured from the CD144<sup>-</sup> fraction, were

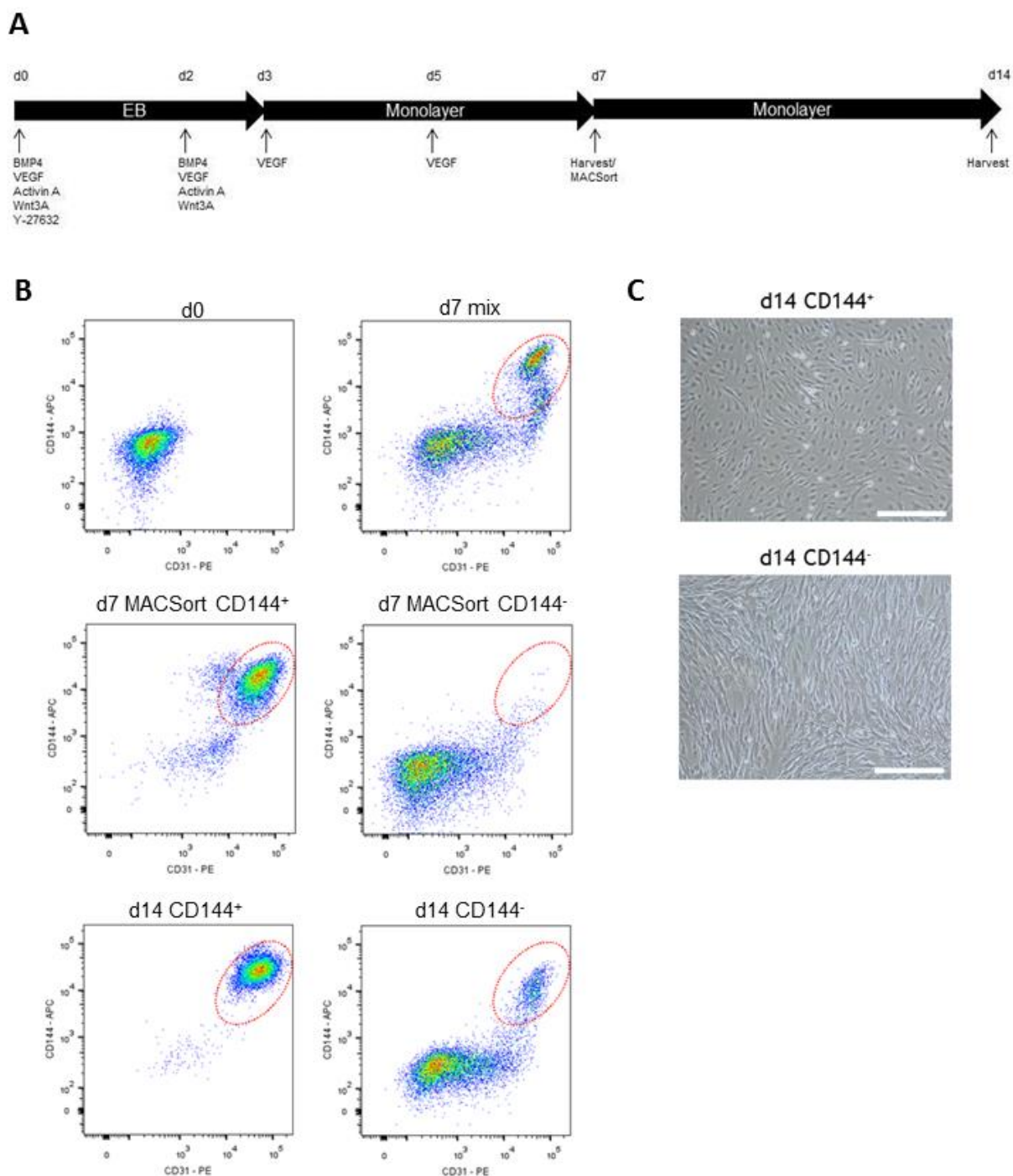


### Figure 3.7 – Sorting and further culture of CD144<sup>+</sup> hESC-ECs

H9 hESCs were subjected to direct hESC-EC differentiation. MACSorting of CD144<sup>+</sup> cells was performed on d7, and cells were analysed, replated and cultured for a further 7 days (A). Flow cytometric analysis was performed to assess the purity of cells at each step (B). Dot plots shown are representative of each time point. Both CD144<sup>+</sup> and CD144<sup>-</sup> fractions were plated out onto gelatin at a density of  $1 \times 10^5$  cells per well. Cells were cultured for a further 7 days in LONZA EGM-2 containing the FBS component and supplemented with 50ng/mL VEGF. Morphological analysis of cells was performed on d14 (C).  $n=4$ , representative images are shown. Scale bars represent 100 $\mu$ m.



CD31<sup>+</sup>CD144<sup>+</sup>, whereas almost 100% of cells cultured from the CD144<sup>+</sup> fraction were positive for both endothelial markers (Figure 3.7B). Data presented here, demonstrated the potential scalability of this protocol, with expansion of pure CD31<sup>+</sup>CD144<sup>+</sup> populations possible.

### 3.3.4 Tubule formation capacity of d14 CD144<sup>+</sup> IVECs

In order to assess the function capacity of cells produced using our direct hESC-EC differentiation, Matrigel tubule formation assays were performed. Previous, unsuccessful attempts were made to assess EC function using heterogeneous d7 hESC-ECs and MACSorted d7 CD144<sup>+</sup> hESC-EC. Tubule formation assays were, therefore, performed using purified d14 CD144<sup>+</sup> immature vascular ECs (IVECs). Cells were plated out onto matrigel at a density of  $2 \times 10^4$  cell per well in a 96-well plate, in Lonza EGM-2 media supplemented with 50 ng/mL VEGF and tubule formation was assessed after 24 h (described in more detail in section 2.4.1).

After 24 h, the d14 CD144<sup>+</sup> IVECs were able to form tubules, in a similar way to the human umbilical vein endothelial cells (HUVEC), which were used as a positive control. Pluripotent H9 hESCs were used as a negative control, and were unable to stick down and form tubules on the Matrigel matrix. This data demonstrated the angiogenic and tubule forming capacities of the cells generated using this newly developed, direct hESC-EC differentiation protocol.

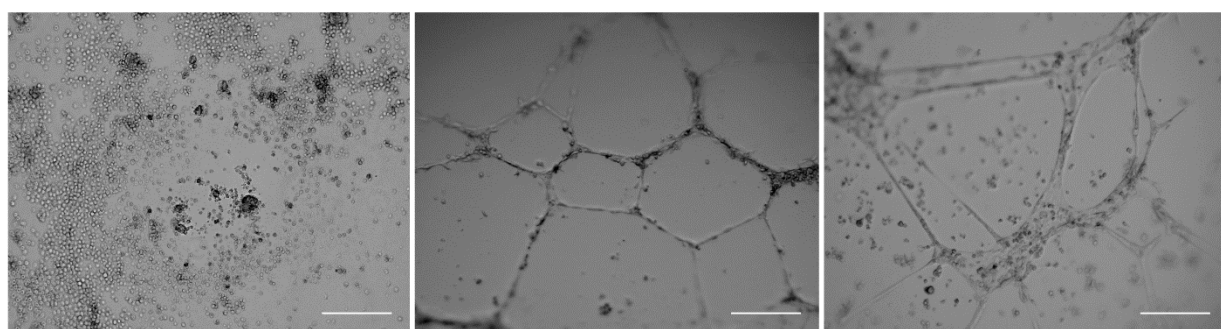


**Figure 3.8 – Tubule formation capacity of d14 CD144<sup>+</sup> IVECs.**

CD144<sup>+</sup> d7 hESC-ECs were MACSorted, replated and cultured for a further 7 days to obtain d14 CD144<sup>+</sup> IVECs. Cells were then harvested and plated onto matrigel to assess their tubule formation capacity (right panel). HUVEC (centre) and pluripotent H9 hESCs (left) were used as positive and negative controls, respectively. n=3 experiments. Scale bars represent 250  $\mu\text{m}$ .

### 3.3.5 Identification and characterisation of a CD326<sup>low</sup>CD56<sup>+</sup> progenitor population

To study mechanisms involved in early commitment of hESCs to mesoderm, as well as their subsequent commitment to the vascular endothelium, analysis was performed to identify an early stage mesoderm progenitor population (MP) existing within direct hESC-EC differentiation. As described previously, Evseenko et al. identified a population with the cell surface marker profile CD326<sup>-</sup>CD56<sup>+</sup> (Evseenko et al., 2010). The study demonstrated that this population was transient, appearing on d3.5 of a general mesodermal differentiation, and was also multipotent, capable of differentiating into a number of different mesodermal cell types, including haematopoietic cells, cardiomyocytes and smooth muscle.

To assess the existence of this CD326<sup>-</sup>CD56<sup>+</sup> MP population within the direct hESC-EC differentiation system, time course experiments were performed, using both H1 and H9 hESC lines. It was hypothesised that these cells would appear at a comparable time point in our hESC-EC system, as a similar cytokine mixture and timing was used to induce mesodermal differentiation, and this would be before the emergence of more mature EC markers at d5 and d7. Therefore, d0 hESCs, d3 EBs, and d5 and 7 hESC-ECs were harvested, stained using PE-conjugated mouse anti-human CD56 and FITC-conjugated mouse anti-human CD326, and subjected to analysis by flow cytometry.

Analysis of the cells by flow cytometry showed that the percentage of pluripotent hESCs expressing CD326 was at a level similar to previous studies, where it has been suggested to play a role in the maintenance of pluripotency (Lu et al., 2010). CD56 was, however, not expressed on the surface of any d0 hESCs (Figure 3.9A and B). Throughout differentiation, it was observed that cells underwent a transition, whereby the CD326, present on the surface of the cell, was gradually lost. Coupled with this, cells began to acquire expression of CD56. The emergence of a CD326<sup>low</sup>CD56<sup>+</sup> population was observed on d3 of hESC-EC differentiation when experiments were performed using either H1 or H9 hESCs (Figure 3.9A-D), before the appearance of the more mature EC markers CD31 and CD144 (Figure 3.4 and Figure 3.6). The CD326<sup>low</sup>CD56<sup>+</sup> MP population accounted for approximately 30-50% of cells on d3 during H9 hESC-EC

differentiation (Figure 3.9A and C) and 10% of cells during H1 hESC-EC differentiation (Figure 3.9B and D), demonstrating its reproducibility across distinct hESC cell lines. The percentage of MP cells, present at d3, was largely representative of the overall differentiation efficiency; experiments with higher percentages of CD326<sup>low</sup>CD56<sup>+</sup> cells on d3 often also had higher percentages of CD31<sup>+</sup>CD144<sup>+</sup> hESC-ECs on d7. Flow cytometric analysis of d5 and 7 showed that these CD326<sup>low</sup>CD56<sup>+</sup> MP cells are present on these days, in the heterogeneous hESC-EC populations, although a distinct population of cells are present which have lost both CD326 and CD56 (Figure 3.9A and B).

As well as analysis of cell surface markers, profiling of mesoderm-associated genes was performed using mRNA qRT-PCR. Total RNA was collected from d0 pluripotent hESCs, d3 EBs, and d5 and 7 heterogeneous hESC-ECs (cells from d1 and 2 EBs were also harvested in experiments performed with H9 hESCs), and the expression of 3 mesoderm-associated genes, *Brachyury (T)*, *Mesp1*, and *Mixl1*, was investigated (Figure 3.10A and B). Expression of these genes was low in d0 pluripotent hESCs, and in the d7 hESC-EC samples. All three of these mesoderm-associated genes were significantly upregulated in samples from d3 EBs; *Brachyury* 1426-fold in H9 and 384-fold in H1, *Mesp1* 164-fold in H9 and 252-fold in H1 and *Mixl1* 348-fold in H9 and 272-fold in H1. In H9s, it was observed that this increase was gradual, as expression was also significantly upregulated in both d1 and d2 EB samples, although fold changes were much lower (Figure 3.10A). This peak of expression coincided with the emergence of the CD326<sup>low</sup>CD56<sup>+</sup> MP population, supporting the hypothesis that these cells represent the initiation of mesodermal lineage commitment, occurring within this hESC-EC *in vitro* differentiation system.

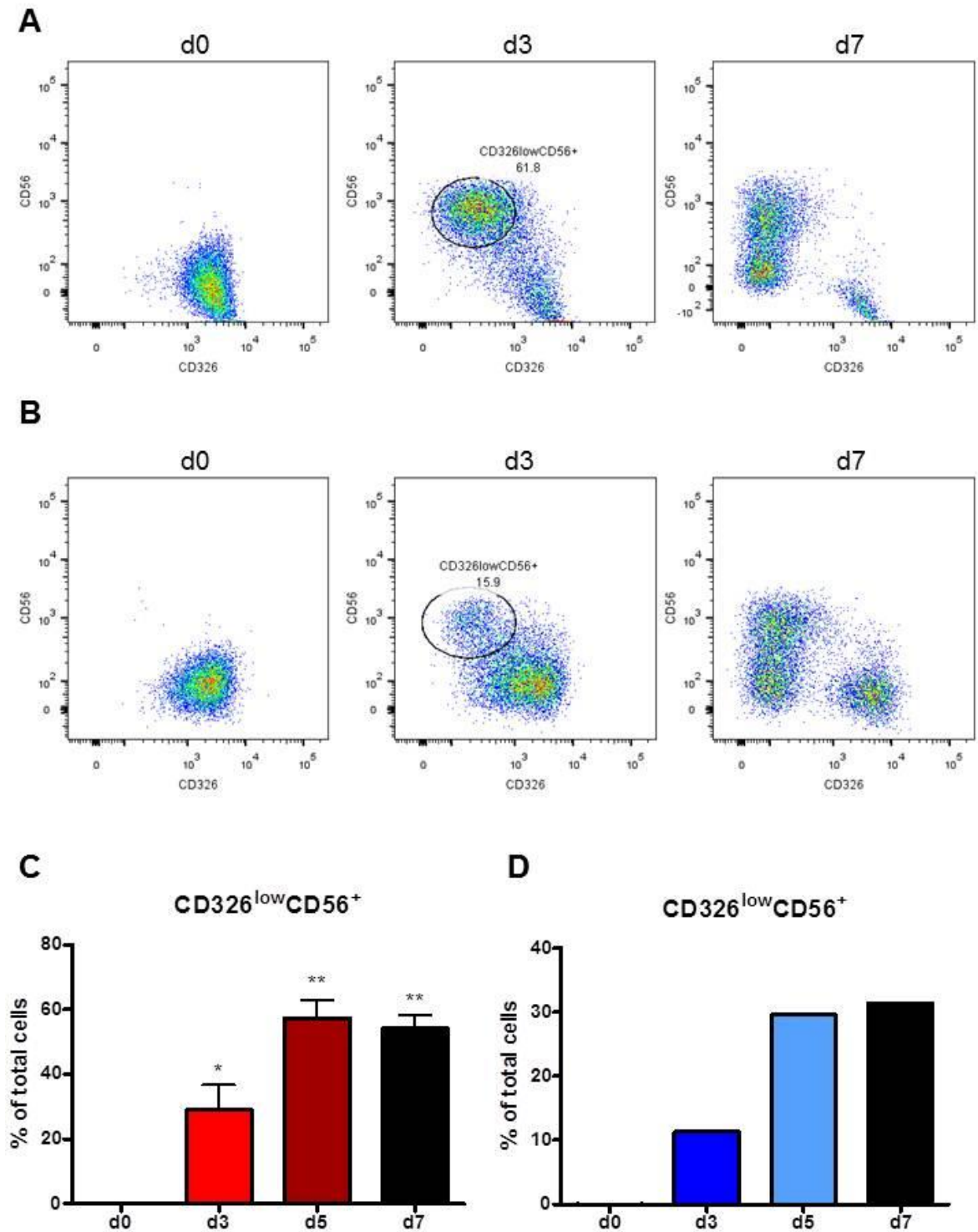


**Figure 3.9 – Identification of a previously published CD326<sup>low</sup>CD56<sup>+</sup> mesoderm progenitor population in direct hESC-EC differentiation.**

Flow cytometry was used to profile the expression of a previously published CD326<sup>low</sup>CD56<sup>+</sup> mesoderm progenitor cell population, existing within hESC-EC differentiation. Cells were harvested at d0, 3, 5 and 7 and stained using PE-conjugated anti-CD56 and FITC-conjugated anti-CD326 antibodies. This population was found to exist in both differentiating H9 (A and C) and H1 (B and D) hESC cell lines. Dot plots show representative samples from d0, 3 and 7 and graphs show mean percentage of total cells with error bars (C only) showing SEM. Repeated measures ANOVA with Tukey's post hoc comparisons, \* =  $p < 0.05$ , \*\* =  $p < 0.01$ , \*\*\* =  $p < 0.001$  when compared to d0 pluripotent control. H9,  $n=3$ . H1,  $n=2$ .

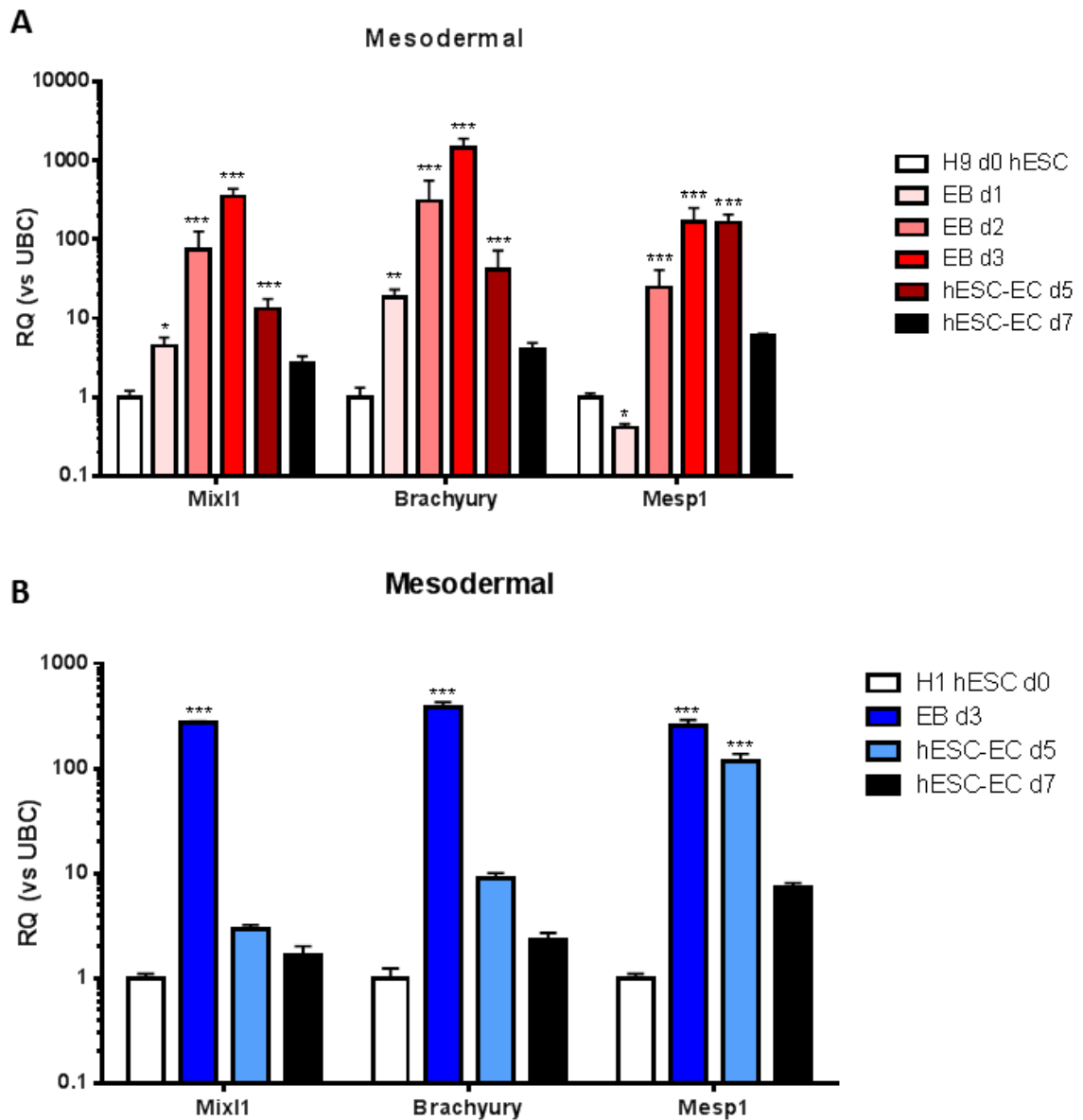


**Figure 3.10 – Analysis of mesoderm-associated genes during H9 and H1 hESC-EC differentiation.**

Expression profiles of mesoderm-associated genes (*Mixl1*, *Brachyury* and *Mesp1*) during direct hESC-EC differentiation were assessed using qRT-PCR. H9 (A) and H1 (B) hESCs were differentiated and samples collected for RNA analysis. Repeated measures ANOVA with Tukey's post hoc comparisons, \* =  $p < 0.05$ , \*\* =  $p < 0.01$ , \*\*\* =  $p < 0.001$  when compared to d0 pluripotent control. Data shown is  $RQ \pm RQ \text{ max}$ , relative to UBC reference gene. Y-axis shown as Log scale.  $n=3$ .

As the  $CD326^{\text{low}}CD56^{\text{+}}$  MP population was still present in d5 and 7 hESC-EC samples, 3-colour staining was performed in order to assess co-expression of CD326, CD56 and CD144 (Figure 3.11 and Figure 3.12). Samples were collected from d0 hESCs, d3 EBs and d5 and 7 hESC-ECs from direct endothelial differentiation using H1 hESCs. Interestingly, it was observed that all  $CD144^{\text{+}}$  cells, both at d5 and d7, were negative for CD326, with negligible levels of cells

staining for both markers (Figure 3.11). As CD326 has been suggested to play a role in the maintenance of pluripotency, this finding supports previous data, showing a loss of pluripotency-associated markers, at both mRNA and protein levels, occurring throughout hESC-EC differentiation. Distinct CD326<sup>low/-</sup> populations were then assessed for CD144 expression (Figure 3.12). As shown previously (Figure 3.4 and Figure 3.6), no CD144<sup>+</sup> cells were detected in any of the d3 samples, when approximately 20% of cells present were CD326<sup>low</sup>CD56<sup>+</sup>, but as differentiation progressed there was an increasing percentage of cells displaying CD144 at d5 ( $\approx$ 18%) and d7 ( $\approx$ 31%). On d5, 42% of CD326<sup>low</sup>CD56<sup>+</sup> cells expressed CD144, with all CD144 cells present at this time point also staining for CD56 (Figure 3.11). By d7, however, the majority of CD326<sup>low</sup>CD56<sup>+</sup> cells were negative for CD144, also apparent from analysis of CD56 and CD144 co-expression (Figure 3.11). In contrast, >90% of CD326<sup>-</sup>CD56<sup>-</sup> cells, a population only observed at this time point, stained positive for CD144 (Figure 3.12).

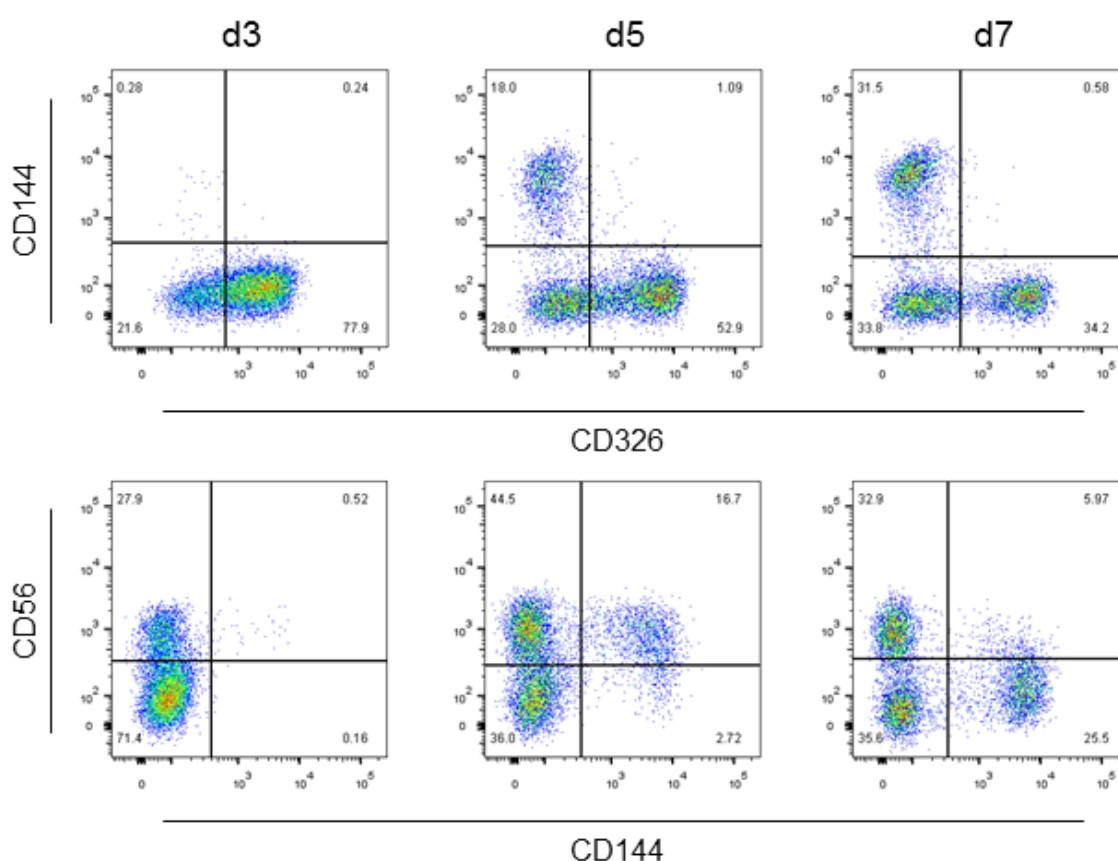


**Figure 3.11 – Co-expression of CD144 and CD326 or CD56 on d3, 5 and 7.**

Cells were harvested at d3, 5 and 7 during H1 hESC-EC differentiation, stained using 3 different antibodies; PE conjugated anti-CD56, APC conjugated anti-CD144 and FITC conjugated anti-CD326 and analysed using flow cytometry. Co-expression of CD144 with CD326 (top panel) and CD56 (bottom panel) is shown in dot plots. Gates were determined using matched isotype and unstained controls and compensation calculated using singly stained samples. n=1.

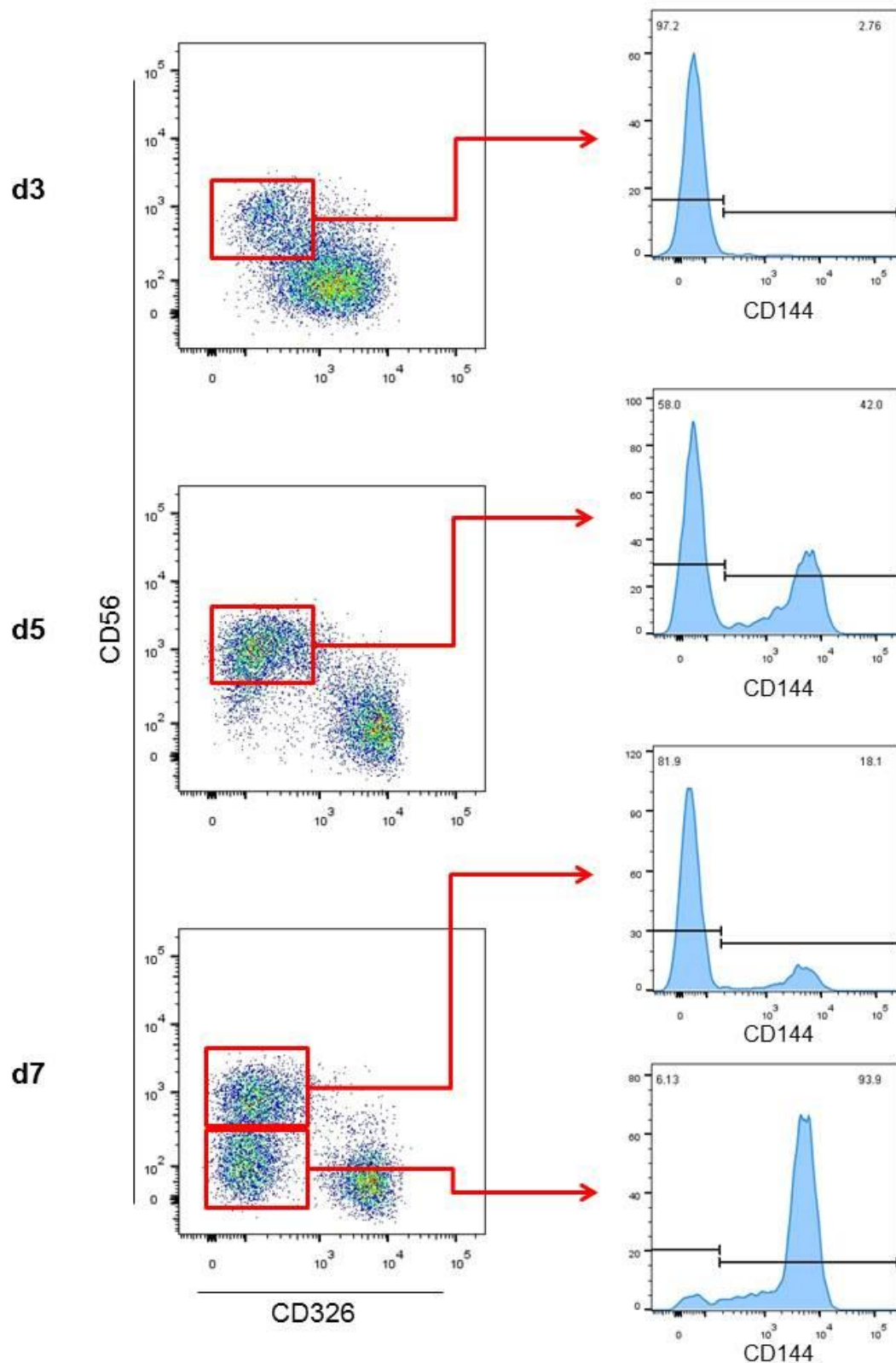


**Figure 3.12 – CD144 staining of d3, 5 and 7 CD326<sup>low</sup>CD56<sup>+</sup>.**

d3, 5 and 7 H1 hESC-ECs were stained using PE conjugated anti-CD56, APC conjugated anti-CD144 and FITC conjugated anti-CD326 and analysed using flow cytometry. CD326<sup>low</sup>CD56<sup>+</sup> populations were gated at each time point (red lines) and cells analysed for CD144 expression. Compensation was performed using singly stained controls. Numbers on histograms represent percentage of cells in specified gate. n=1.

Taken together, this data demonstrates the presence of a  $CD326^{low}CD56^{+}$  MP population, existing transiently during hESC-EC differentiation. This population also occurs alongside the peak of mesoderm associated genes, substantiating the claims that this population is a multipotent MP cell population. Further characterisation of this population using 3-colour flow cytometry also suggests that  $CD31^{+}CD144^{+}$  ECs may emerge from these MPs, as all  $CD144^{+}$  cells on d5 of hESC-EC were also positive for CD56, before the cells lose this marker on d7, although experimental n numbers would need to be increased to confirm this.

### 3.3.6 Isolation and further characterisation of the $CD326^{low}CD56^{+}$ population

In order to further investigate the phenotype of these cells, fluorescence activated cell sorting (FACS) was used to isolate the  $CD326^{low}CD56^{+}$  MP population. Pure samples were then collect, cells were lysed and total RNA was extracted, before analysis was performed using TaqMan® mRNA qRT-PCR. Heterogeneous d3 samples (approximately 35-60%  $CD326^{low}CD56^{+}$ ), were collected from direct hESC-EC differentiation performed using H9 hESCs, and subjected to FACS to isolate the  $CD326^{low}CD56^{+}$  MP cells, as well as the  $CD326^{high}CD56^{-}$  cells, hereafter known as the negative cell fraction (NCF). Purity of cells after FACS was high, with >97%  $CD326^{low}CD56^{+}$  cells in the MP fraction and <3%  $CD326^{low}CD56^{+}$  in the NCF sample. Example data collect from these FACS experiments are shown as dot plots in Figure 3.13.

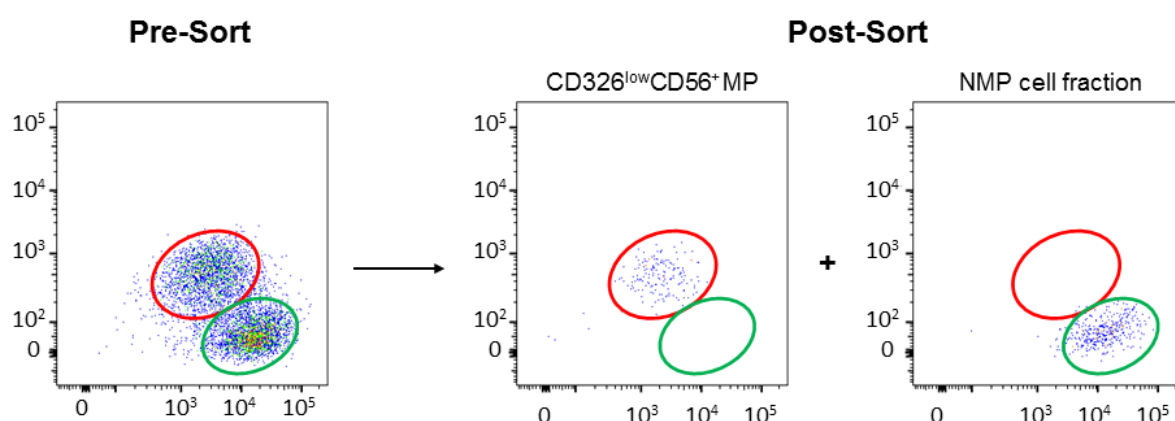


**Figure 3.13 – FACS sorting of  $CD326^{low}CD56^{+}$  progenitor populations.**

Representative example of dot plots obtained before and after FACS sorting of  $CD326^{low}CD56^{+}$ . H9 hESCs were harvested at d3, and stained with PE-conjugated anti-CD56 and APC-conjugated anti-CD326 before they were subjected to sorting using a BD Aria I or III. Dot plots shown above show the heterogeneous d3 population before FACS sorting, and the 2 post-sort populations;  $CD326^{low}CD56^{+}$  and the 'negative' cells. n=4.



Gene expression analysis was then performed, using TaqMan® qRT-PCR, for a number of pluripotent- (*Nanog*, *Sox2*, *Oct4*) (Figure 3.14A), mesodermal- (*Brachyury* (*T*), *Mesp1*, *Mixl1*) (Figure 3.14B), and endothelial- (*CD31*, *CD144*) (Figure 3.14C) associated genes. As previously observed (Figure 3.4 and Figure 3.6), the expression level of pluripotency-associated genes was significantly decreased as hESC-EC differentiation progressed, when compared to levels seen in d0 pluripotent hESCs. Surprisingly, levels of *Nanog* and *Oct4* were found to be significantly lower in the d3 MP samples than in the NCF. This suggests a rapid loss of pluripotency in MP cells (<3 days), compared to cells in the NCF, supporting claims that this population of cells are already committed, either just to the mesoderm or to a more defined cell type, e.g. ECs.

It was originally hypothesised that mesoderm-associated genes would be expressed at significantly higher levels in the CD326<sup>low</sup>CD56<sup>+</sup> MP population than in the NCF population. Evseenko et al. used microarray analysis to demonstrate a significant upregulation of mesoderm-associated genes, such as *Brachyury*, *Mixl1*, *KDR*, *MESP1*, *MESP2* and *SNAI2*, in CD326<sup>low</sup>CD56<sup>+</sup> cells compared to d0 hESCs (Evseenko et al., 2010). Using qRT-PCR, analysis showed a significant upregulation of *Brachyury*, *Mesp1* and *Mixl1* in the d3 CD326<sup>low</sup>CD56<sup>+</sup> MP cells, when compared to d0 pluripotent control (Figure 3.14B). However, although observed expression levels of these genes significantly higher in MP cells, they were also seen to be significantly upregulated in the NCF. Furthermore, mesoderm-associated gene expression was either significantly lower (*Brachyury*, or unchanged (*Mixl1* and *Mesp1*) in d3 CD326<sup>low</sup>CD56<sup>+</sup> MPs when compared to levels seen in the d3 NCF cells. One explanation for this is that the cells have already passed the peak of mesodermal gene expression, as they begin to express CD56 on their surface, whilst losing the expression of CD56. There may possibly exist an earlier MP population within our d3 heterogeneous EBs, which is as yet undefined, and this may contribute to the high levels of *Brachyury*, *Mesp1* and *Mixl1* in this population.

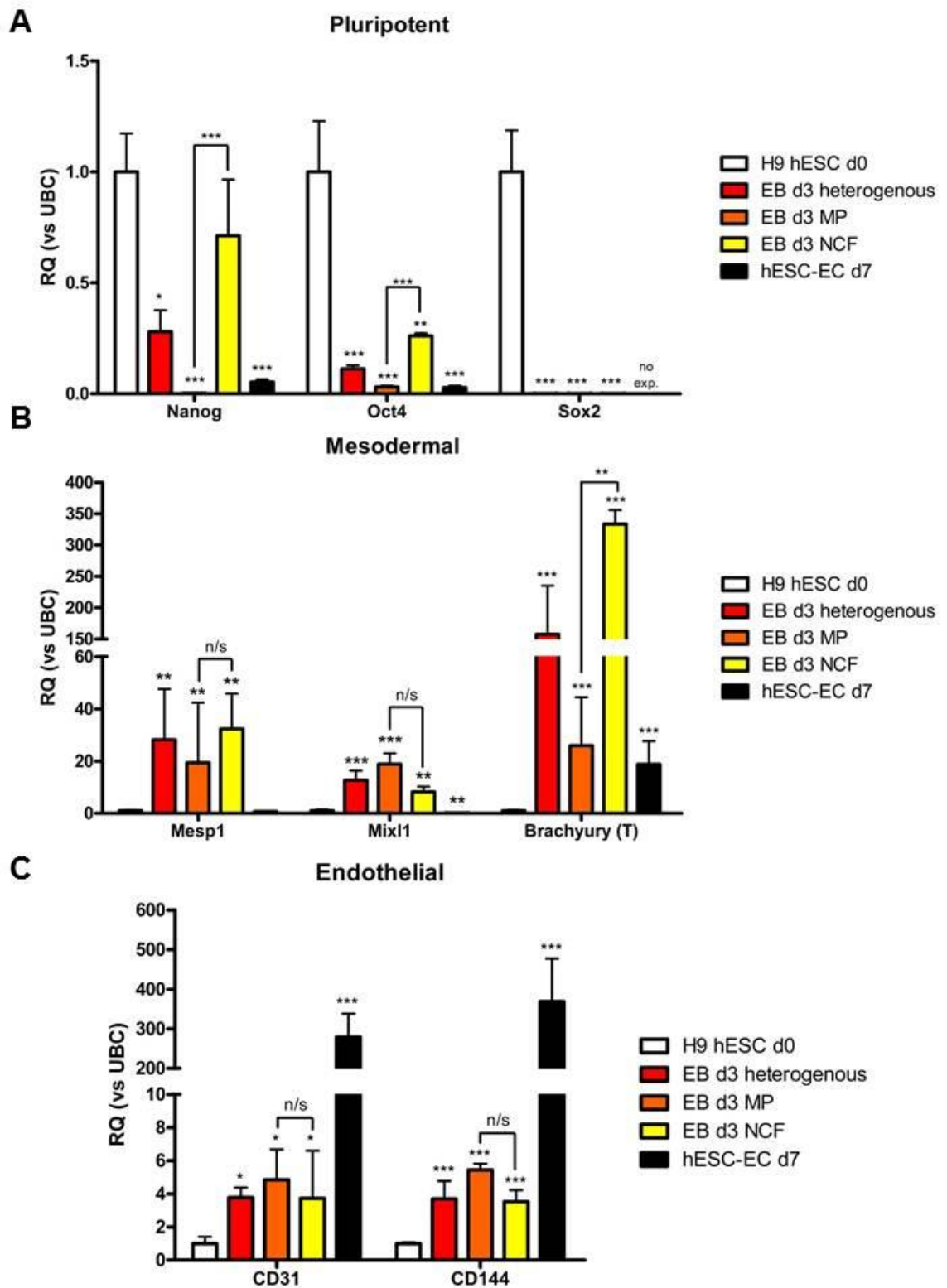


**Figure 3.14 – Expression of pluripotency-, mesodermal- and endothelial-associated genes in FACSsorted CD326<sup>low</sup>CD56<sup>+</sup> cells.**

mRNA expression of pluripotency- (A), mesodermal- (B) and endothelial- (C) associated genes in samples from H9 hESCs during direct hESC-EC differentiation, including d0 pluripotent hESCs, heterogeneous d3 EB, FACSsorted d3 CD326<sup>low</sup>CD56<sup>+</sup> MP and NCF, and d7 hESC-EC samples. Repeated measures ANOVA with Tukey's post hoc comparisons, \* =  $p < 0.05$ , \*\* =  $p < 0.01$ , \*\*\* =  $p < 0.001$ , when compared to d0 pluripotent control unless indicated. Data shown is RQ  $\pm$  RQ max, calculated relative to UBC reference gene.  $n=4$ . MP – mesoderm progenitor, NCF – negative cell fraction.

Expression of endothelial-associated genes (*CD31*, *CD144*), was shown to increase as cells progressed through hESC-EC differentiation, consistent with previous results (Figure 3.14C). The fold change in expression of these genes was higher in d3 MPs (*CD31* 5-fold, *CD144* 5-fold) than in the d3 NCF (*CD31* 4-fold, *CD144* 4-fold) when compared to d0 pluripotent hESCs, although this difference was non-significant. The increase in endothelial-associated genes, coupled with the rapid decrease in pluripotency genes and lower expression of mesoderm-associated genes than expected, may suggest that the  $CD326^{\text{low}}CD56^+$  MP cells are more committed than previously thought, and that there may exist a subset of these cells, or of the NCF cells, which represent an even more primitive multipotent MP population.

To ascertain a more in depth gene expression profile of these cells, TaqMan® Low Density Array (TLDA) cards were used to analyse the expression of a larger number of genes. TLDA cards allow for higher throughput screening of up to 48 genes in 8 different samples and, in this study, were designed to profile mesoderm- and endoderm-associated genes, as well as a number of pluripotent and ectoderm-associated genes.

Cards contained a number of previously profiled genes, including *Nanog*, *Oct4* (*POU5F1*), *Sox2*, *CD31* (*Pecam-1*), *Mesp1*, *Mixl1* and *Brachyury* (*T*). Expression of these genes was similar to that seen when analysed using qRT-PCR (Figure 3.14). Pluripotency-associated genes (*Nanog*, *Oct4*, *Sox2*) were shown to significantly decrease during differentiation, and also to be expressed at significantly lower levels in the  $CD326^{\text{low}}CD56^+$  MPs than in NCF cells (Table 3.1). *Mesp1* and *Mixl1* were shown to be significantly upregulated in both MPs and NCF, although there was no significant difference in expression between the two groups on d3 (Figure 3.14B; Table 3.1). Mesoderm-associated *Brachyury*, however, was shown to be expressed at significantly higher levels in the NCF than in the  $CD326^{\text{low}}CD56^+$  MPs (Figure 3.14B; Table 3.1). Like during previous profiling qRT-PCR profiling, the endothelial-associated *CD31* was significantly upregulated during hESC-EC differentiation. However, unlike during previous analysis, *CD31* was observed to be expressed at significantly higher levels in  $CD326^{\text{low}}CD56^+$  cells, than in d3 NCFs (Figure 3.14C; Table 3.1). Taken together, this data supports claims that these cells have already lost their pluripotency and committed to the mesoderm, or possibly further to specific cell lineages. In this system, these cells may not

be as immature as had been suggested by Evseenko et al. and may, in fact, already be beginning to acquire a more committed phenotype.

	Gene name	d3 MP		d3 NCF		Significant difference between MP and NCF?	
		RQ	P-value	RQ	P-value	Y/N	P-value
Pluripotent	POU5F1	0.011	***	0.124	***	Y	***
	FZD5	0.032	***	0.109	***	Y	**
	NANOG	0.003	***	0.379	n/s	Y	***
	SOX2	0.003	***	0.027	***	Y	**
Mesoderm	GATA2	90.05	***	10.6	***	Y	***
	ACTC1	12.39	***	0.678	n/s	Y	***
	HAND1 <sup>+</sup>	1	N/A	0.146	***		
	KDR	15.18	***	4.5	***	Y	***
	MESP1	303.91	***	575.25	***	N	n/s
	MIXL1	331.79	***	477.67	***	N	n/s
	NKX2.5	170.89	***	51.57	***	Y	**
	PECAM1	18.83	**	1.1	n/s	Y	**
	SNAI1	6.68	***	10.61	***	N	n/s
	SOX7	53.64	***	1.71	n/s	Y	***
	T	388.48	***	2295.39	***	Y	***
Endoderm/Mesendoderm	DKK1	338.5	***	151.89	***	N	n/s
	CER1	97.46	***	17.91	**	N	n/s
	CXCR4	3.16	*	2.01	n/s	N	n/s
	FOXA2	2.95	n/s	12.79	*	N	n/s
	GATA4	366.14	***	172.06	***	N	n/s
	GATA6	570.15	***	447.14	***	N	n/s
	GSC	49.14	**	56.67	**	N	n/s
	SOX17	91.36	***	106.2	***	N	n/s
Ectoderm	NES	1.15	n/s	0.559	*	Y	**
	NKX2.2	No expression		No expression			
	PAX6	No expression		No expression			

**Table 3.1 – TLDA card analysis of d3 MP and NCFs during hESC-EC differentiation.**

mRNA expression of a larger number of genes in FACSsorted d3 CD326<sup>low</sup>CD56<sup>+</sup> MP and NCF samples from H9 hESC-EC differentiation. Repeated measures ANOVA with Tukey's post hoc comparisons, \* = p<0.05, \*\* = p<0.01, \*\*\* = p<0.001, when compared to d0 pluripotent control unless indicated. + = no expression in d0 hESCs, direct comparison made between d3 CD326<sup>low</sup>CD56<sup>+</sup> MPs and NCFs. Data shown is RQ, calculated relative to GAPDH reference gene. n=3. MP – mesoderm progenitor, NCF – negative cell fraction, n/s – non significant.

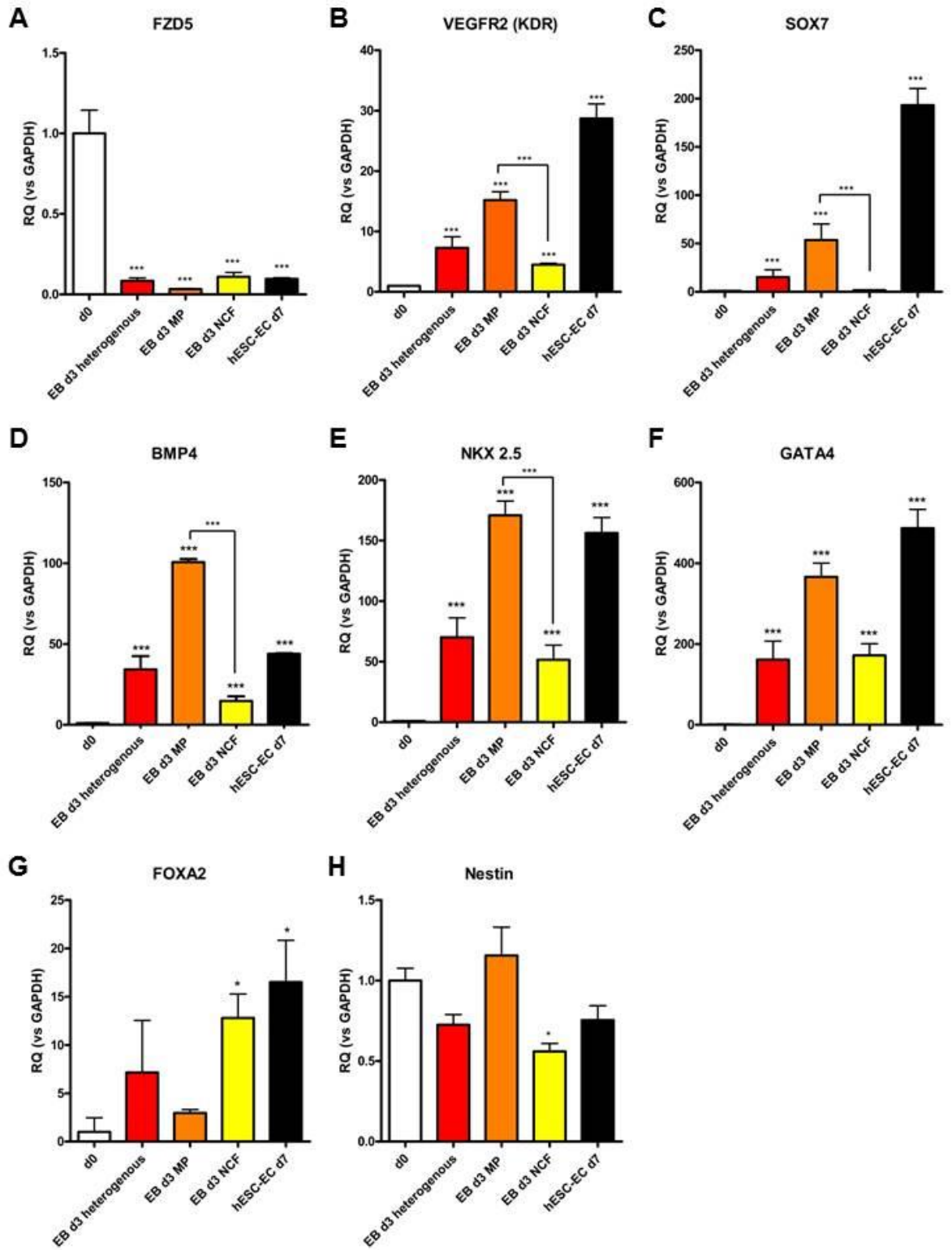


**Figure 3.15 – Histograms of selected gene expression from TLDA card analysis.**

Histograms showing mRNA expression in d0 pluripotent hESCs, FACSsorted d3 CD326<sup>low</sup>CD56<sup>+</sup> MP and NCF samples and d7 hESC-ECs from H9 differentiation for selected genes from TLDA card analysis. Repeated measures ANOVA with Tukey's post hoc comparisons, \* = p<0.05, \*\* = p<0.01, \*\*\* = p<0.001, when compared to d0 pluripotent control unless indicated. Data shown is RQ ± RQ max, calculated relative to GAPDH reference gene. n=3. MP – mesoderm progenitor, NCF – negative cell fraction.

Frizzled class receptor 5 (*FZD5*), thought to be the receptor for Wnt5A and previously seen to be downregulated during differentiation of embryonal carcinoma cell lines (Walsh et al., 2003), was shown to be significantly downregulated during hESC-EC differentiation (Figure 3.15A; Table 3.1), in a similar way to other pluripotency-associated genes.

*VEGFR2* (*KDR*; *CD309*; *Flk1*), a mesoderm-associated gene also commonly used to identify early endothelial progenitors, was significantly upregulated during hESC-EC differentiation (Figure 3.15B). Interestingly, this gene was expressed at higher levels in the  $CD326^{\text{low}}CD56^+$  MP cells (15-fold increase) than in the NCF (5-fold increase), when compared to d0 pluripotent control. Another gene shown to be upregulated to significantly higher levels in the MP cells (54-fold) than in the NCF (2-fold), is *Sox7* (Figure 3.15C; Table 3.1). A member of the Sry-related HMG box gene family, *Sox7* is involved in cardiovascular development, and has been shown to control transcription in hemogenic endothelium, where it has been shown to bind and activate the expression of CD144 maintaining the endothelial phenotype of these cells (Costa et al., 2012). Recently, it has even been shown that *Sox7* is directly regulated by *ETV2*, activating transcriptional networks, and therefore playing a role in EC development and angiogenesis (Behrens et al., 2014). A member of the same family as *Sox7*, *Sox17* was also shown to be upregulated in MPs (91-fold) and, together with *Sox18*, has been shown to work alongside *Sox7* in the development of the cardiovascular system. Coupled with the increase in other more mature endothelial-associated markers (*CD31*; Figure 3.14C), the expression of these genes in  $CD326^{\text{low}}CD56^+$  MP cells supports the hypothesis that these cells have committed towards a mesodermal lineage, and are possibly already starting to become specified towards an EC phenotype.

Other mesoderm-associated genes, such as *BMP4*, *NKX2.5* and *GATA4* were also found to be expressed at higher levels in the isolated  $CD326^{\text{low}}CD56^+$  population than in the NCF cells (Figure 3.15D-F; Table 3.1). *BMP4* has previously been shown to be involved in specification to the mesodermal lineage (Winnier et al., 1995, Zhang et al., 2008), although upregulation in this case may be in response to treatment with high concentrations of this protein during d0-3 of hESC-EC differentiation (Figure 3.2A). *HAND1*, also shown to be involved in mesodermal lineage specification (Barnes et al., 2010, Maska et al., 2010) and whose

expression was not detected in d0 pluripotent hESCs, was expressed at significantly higher levels in d3 MP cells than in the NCF (Table 3.1).

The d3 NCF samples were shown to express *Sox17* (106-fold increase), *FoxA2* (13-fold increase) and *GSC* (*Goosecoid*) (57-fold increase) at higher levels than the CD326<sup>low</sup>CD56<sup>+</sup> MP cells, which did not show a significant upregulation of *FoxA2* (3-fold increase) (Table 3.1; Figure 3.15G). All three of these genes have been shown to be involved in formation of endoderm and mesendoderm, a bipotent progenitor with both mesodermal and endodermal potential (Tada et al., 2005, Wang et al., 2011). This may suggest the presence of a population of mesendodermal or endodermal progenitor cells, present in the NCF on d3. These cells also have lower levels of *HAND1* and *BMP4*, both of which are associated with a more definitive mesodermal phenotype (Table 3.1; Figure 3.15D).

As expected, expression of ectoderm-associated genes was largely undetected in all tested samples (Table 3.1). Though the mRNA *Nestin*, an ectoderm-associated gene, was detected in all samples, its expression was low and was found to be largely unchanged throughout differentiation, although a significant downregulation was observed in the NCF cells when compared to d0 pluripotent hESCs (Table 3.1; Figure 3.15H).

Collectively, the gene expression profile of these cells suggests a definitive mesoderm progenitor either existing as a CD326<sup>low</sup>CD56<sup>+</sup> population or existing as a smaller population within this specific cell fraction, on d3 of direct hESC-EC differentiation.

### 3.4 Discussion

In summary these experiments shown the development of a differentiation protocol for the generation of IVECs from hESCs, known as hESC-ECs. Through optimisation of an original 6-well format assay, an efficient 96-well EB-based method was developed, producing sufficient numbers of CD31<sup>+</sup>CD144<sup>+</sup> cells by d7 of differentiation. Isolation, culture and expansion of these cells was also possible, resulting in a pure population of CD31<sup>+</sup>CD144<sup>+</sup> IVECs by d14, which were functional, as demonstrated by their ability to form tubules when plated on a Matrigel cell matrix.

Numerous studies have been previously published, describing various methods for the derivation of ECs from hESC and hiPSCs. While some protocols have attempted to be clinically relevant (Kaupisch et al., 2012, Orlova et al., 2014a), many others still involve the use of undefined ECM or serum-containing medium, or require co-culture of cells with stromal cell lines (Rufaihah et al., 2011, Choi et al., 2012). In a recent publication, describing a highly efficient hPSC-EC differentiation protocol, despite using fully defined medium, Patsch and colleagues used the undefined cell matrix Matrigel for both the culture and differentiation of cells (Patsch et al., 2015). The undefined nature of these conditions raises concerns about transfer of non-human pathogens and contaminants, and therefore differentiation protocols involving the use of serum or stromal cell lines cannot be easily adapted for clinical use as a cell therapy. Additionally, these undefined reagents can introduce unknown factors, which cannot be monitored and may contribute to differentiation via a variety of signalling pathways. Furthermore, due to the nature of their production, there can be inherent batch to batch variability in these reagents, reducing the reproducibility of differentiation experiments. Here, a newly developed, fully defined, efficient, serum- and feeder-free protocol for hESC-EC differentiation has been presented. Although reagents used within these studies are not compliant with good manufacturing practice (GMP), the practices and regulations required to conform to guidelines recommended by specific agencies for the production and licensing of various products, all have the potential to be made GMP-compliant.



Initially, hESC-EC differentiation experiments had been performed using a 6-well methodology, but this lacked reliability and consistency between experiments and cell lines. One explanation for this may have been intra- and inter-experimental differences observed in the formation of EBs. Classically, the formation of stem cell aggregates, or EBs, has been used to induce the simultaneous formation of mesoderm, endoderm and ectoderm from ESCs and iPSCs, thus demonstrating their pluripotency (Itskovitz-Eldor et al., 2000). In recent years, EB culture has been adapted in many studies to incorporate cytokines and growth factors which specifically drive cells towards different lineages from this early stage. Use of factors such as BMP4, Activin A, Wnt3A and VEGF, as demonstrated in the presented study, have been shown to direct differentiation toward a mesodermal and endothelial cell fate. Recently, studies have also demonstrated the use of glycogen synthase kinase 3 (GSK3) inhibitors in this context (Bao et al., 2015, Patsch et al., 2015). GSK3 is inhibited by Wnt signalling and, therefore, the use of GSK3 inhibitors mimics this to drive mesodermal development. Despite development of this direct approach, however, many of these differentiation protocols include crude methods of EB formation, whereby size and density are not controlled, such as partial digestion or, as in this hESC-EC protocol, mechanical cutting of pluripotent cell monolayers, yielding colonies and aggregates of an assortment of sizes. A number of studies have shown that EB size can influence both lineage differentiation of cells, and the reproducibility of cell differentiation experiments *in vitro* (Ng et al., 2005, Bauwens et al., 2008). Therefore, a number of methods have been developed to produce EBs of controlled size and density (Ng et al., 2005, Burrige et al., 2007). Ungrin and colleagues were able to develop a robust method for the development of size controlled EBs from hESCs, using Pluronic F-127 coated 96- or 384-well round bottomed cell culture vessels, and a centrifugation step (Ungrin et al., 2008). The 96-well spin EB-based technique was then adapted to increase reliability and efficiency of direct hESC-EC differentiation. Although the formation of the EBs using a 96-well spin EB-based method, adopted for direct hESC-EC differentiation in the presented studies, is more time consuming and technically demanding than the original 6 well protocol, the use of this method increased reproducibility and robustness of our direct hESC-EC experiments. Percentages of CD31<sup>+</sup>CD144<sup>+</sup> hESC-ECs produced by d7 were not only consistent between experiments, but also between different

cell lines. Further analysis could be performed to confirm that EBs formed using the 96-well spin EB-based methodology were consistent in size and density.

Although efficient, EB-based differentiation methods, particularly those using centrifugation to form spin-EBs, have often been criticised for the difficulties associated with adaptation for scaling up EC production. 2D monolayer protocols are easily scalable, and have been shown to easily generate large numbers of hESC-ECs (Kane et al., 2010, Orlova et al., 2014a, Patsch et al., 2015). Here, it has been demonstrated that d7 CD144<sup>+</sup> hESC-ECs can be isolated, replated and expanded, with ~100% of cells CD31<sup>+</sup>CD144<sup>+</sup> after 7 days of further culture. Further optimisation of this would allow for generation of even larger numbers of cells, as protocols could be scaled up to larger culture vessels, such as T25, T75 or even T150 culture flasks.

Extensive characterisation of hESC-EC differentiation, profiling marker expression at the protein and mRNA levels using flow cytometry and qRT-PCR, revealed a significant increase in the percentage of CD31<sup>+</sup>CD144<sup>+</sup> cells at d7. This was coupled with significant decreases in the numbers of cells expressing the pluripotency marker Tra1-60 and the levels of pluripotency-associated TFs, such as *Nanog* and *Oct4*. Despite this, the specific phenotype of the resultant hESC-ECs generated was not investigated. For more in depth characterisation of these cells, markers of arterial, venous and lymphatic vessels could be profiled. Mature endothelium is heterogeneous, both in structure and function, with a variety of cell markers present amongst a diversity of different EC types (Aird, 2007). Arterial cells have been shown to express markers such as ephrinB2, Hey2 and neuropilin-1, whereas EphB4, a receptor for ephrinB2, and COUP-TFII have been described as venous cell markers (Wang et al., 1998, Herzog et al., 2001, Fischer et al., 2004, You et al., 2005, Kortgen et al., 2013). Recently, Orlova and colleagues demonstrated the presence of arterial and venous markers on the surface of hPSC derived ECs, as well as the presence of lymphatic endothelial markers, such as vascular endothelial growth factor receptor 3 (VEGFR3) and lymphatic vessel hyaluronan receptor 1 (LYVE1) (Orlova et al., 2014a, Orlova et al., 2014b). From this, it was concluded that these cells have an embryonic phenotype, with the potential to further differentiate into various EC types, although this was not experimentally validated. Further characterisation of hESC-ECs, produced using the direct hESC-EC differentiation, would determine

whether these cells also possess this embryonic phenotype, or whether they have already begun to acquire a more specialised EC characteristics. This would introduce the possibility of driving EC differentiation and maturation towards specific EC types, thus allowing for generation of an optimum cell type for specialised angiogenic cell therapies.

CD31<sup>+</sup>CD144<sup>+</sup> cells, obtained on d14 of hESC-EC differentiation, after hESC-ECs had been isolated and expanded, were able to perform functionally *in vitro*. It was demonstrated that cells were able to form tubules when plated onto Matrigel cell matrix, similarly to mature HUVECs. Recently published guidelines from the American Heart Association have, however, suggested that the Matrigel tubule assay is not a suitable *in vitro* representation of angiogenesis, due to the observation that other cell types, for example, VSMCs and fibroblasts, also form similar structures when plated on this matrix (Simons et al., 2015). Therefore, an alternative model of *in vitro* angiogenesis, for example a 3D vascular tubule formation or sprouting assay (Koh et al., 2008), should be performed using these cells. A number of additional *in vitro* assays, such as measurement of endothelial nitric oxide production and acetylated LDL (Ac-LDL) uptake, and *in vivo* experiments, such as angiogenic potential of cells in a murine model of hind limb ischemia, could have also been performed (Kane et al., 2010). Orlova et al. described two novel assays to determine the functional capacity of ECs generated from hPSCs, including 2D co-culture with hESC-derived pericytes to model endothelia-pericyte interactions *in vitro* and measurement of vascular competence in a zebrafish xenograft *in vivo* model (Orlova et al., 2014a). A recent study by Patsch and colleagues demonstrated the barrier function of generated hPSC-ECs by measuring cellular impedance, a measurement of cell growth behaviour. Using this assay, hPSC-ECs were shown to form tight monolayers, and the impedance was decreased with the addition of the vasoactive agent Thrombin (Patsch et al., 2015). Additionally, Patsch also performed assays to measure barrier-tightness using trans-endothelial electrical resistance (TEER), and hPSC-EC:leukocyte binding after stimulation with inflammatory cytokines. Time constraints prevented further investigation into the functional capabilities of the cells generated from the presented hESC-EC differentiation protocol; however, there are numerous experiments which may be performed going forward.

By day 7 of hESC-EC differentiation, only 20-50% of cells are CD31<sup>+</sup>CD144<sup>+</sup>, leaving questions over the identity of the remaining 50-80% of cells. These cells are no longer pluripotent, as is demonstrated by the low numbers of cells staining positive for Tra1-60, and the low expression of *Nanog*, *Oct4* and *Sox2* at the transcript level. Recently, a protocol for the simultaneous generation of ECs and pericytes from hPSCs has been published, with the pericytes existing in the CD31<sup>-</sup> fraction of differentiating cells (Orlova et al., 2014c), and one possibility is that cells similar to these are being generated. Another option is that the remaining cells are supportive of differentiation, and without them cells would not receive the correct environmental stimulus to encourage endothelial specification, although this has not been validated and further *in vitro* characterisation would be needed to verify either of these explanations.

These studies also demonstrated the presence of a previously published CD326<sup>low</sup>CD56<sup>+</sup> mesoderm progenitor population, existing at d3 of direct hESC-EC differentiation. Gene expression profiling revealed that, even at this early time point, these cells have rapidly lost their pluripotency, demonstrated by the loss of *Nanog*, *Oct4* and *Sox2* at the mRNA level, something which is not observed to the same extent in the NCF cell samples. High percentages of cells still express Tra1-60 on their surface at d3, however, and experiments to identify which fraction - the CD326<sup>low</sup>CD56<sup>+</sup> MPs or NCF - still express this marker, could be performed to further validate these findings. Additionally, levels of pluripotency associated mRNAs will be modulated more quickly than protein levels and, therefore, it is not wholly unexpected that Tra1-60 is still expressed on the surface of these cells after downregulation of *Oct4*, *Nanog* and *Sox2*. Similarly to previously published results, we observed an upregulation of mesoderm-associated genes in CD326<sup>low</sup>CD56<sup>+</sup> MP cells, when compared to d0 pluripotent hESCs (Evseenko et al., 2010). Unlike this study, however, Evseenko and colleagues did not report the differences in gene expression between isolated MPs and NCFs. From this data, it is possible to speculate the existence of another, potentially less committed, mesodermal or mesendodermal progenitor within the NCF, due to the significant upregulation of mesoderm-associated genes within these samples. Moreover, genes associated with the endothelial lineage, for example *CD31*, were shown to be upregulated in the d3 CD326<sup>low</sup>CD56<sup>+</sup> MPs, demonstrating that these cells may already be starting to

commit towards the EC lineage, or that cells are being primed for differentiation in this direction. The cardiac-associated gene *NKX2.5* was also found to be expressed at significantly higher levels in the  $CD326^{low}CD56^{+}$  cells than the NCF. Although shown to be involved in mesodermal specification, primarily *NKX2.5* has been associated with heart development. Furthermore, *CER1* was also highly upregulated in the d3 MPs, although there was no significant difference in expression when compared to the NCF. Similar to *NKX2.5*, *CER1* has previously been shown to be involved in cardiac mesoderm formation in differentiating ESCs (Liu et al., 2014) and in the antagonism of both Nodal and BMP to drive cardiomyocyte commitment of cardiovascular progenitors (Cai et al., 2013). It may, therefore, be hypothesised that the large increase in the expression of these genes in  $CD326^{low}CD56^{+}$  progenitors indicates that these cells are primed for further mesodermal differentiation, possibly towards cardiovascular lineages.

Evseenko et al. also demonstrated the multipotent potential of their isolated  $CD326^{low}CD56^{+}$  progenitors, showing their ability to differentiate to hematopoietic, endothelial, mesenchymal, smooth muscle and cardiac cells (Evseenko et al., 2010). Due to time constraints, experimental validation of this multipotency in  $CD326^{low}CD56^{+}$  cells from direct hESC-EC differentiation has not yet been performed. This would be needed in order to confirm the phenotype of these cells. Additionally, experiments to further elucidate the surface marker profile of these cells may be performed. The profile of these cells is still highly debatable, and a number of other studies have isolated similar cell populations using alternative cell surface antigens. One study, performed using co-culture with OP9 stromal cell lines, identified two distinct populations of mesoderm progenitors (Choi et al., 2012). The first, defined as  $APLNR^{+}PDGFR\alpha^{+}$ , was shown to be a more primitive mesoderm progenitor. The second, a more committed mesoderm progenitor, was described as  $KDR^{bright}APLNR^{+}PDGFR\alpha^{low/-}$  or hematovascular mesodermal precursors (HVMP). These cells were shown to be distinct from the  $APLNR^{+}PDGFR\alpha^{+}$  cells, and were possibly equivalent to embryonic angioblasts, with the potential to form both ECs and hematopoietic cells. In addition to this, Drukker et al. used a flow cytometry-based large scale screen to identify novel cell surface markers, to define specific populations of cells representative of primitive endodermal, mesodermal, vascular endothelial and trophoblast progenitors from hPSCs (Drukker et al., 2012). In this study,

cells positively expressing Receptor Tyrosine Kinase-Like Orphan Receptor 2 (ROR2<sup>+</sup>) were shown to express mesoderm-associated mRNAs, such as *Brachyury* and *Mesp1*, and could generate differentiated mesoderm tissues. Similarly to the CD326<sup>low</sup>CD56<sup>+</sup> identified in direct hESC-EC differentiation, ROR2<sup>+</sup> cells were shown to express pluripotency genes at lower levels (~50-fold reduction) when compared to undifferentiated pluripotent control cells. That study also identified a CD87<sup>+</sup> vascular endothelial progenitor cell fraction, expressing a gene profile similar to that of human microvascular ECs, and able to form tubules on matrigel. It may, therefore, be of interest to further investigate the specific surface marker profile of the CD326<sup>low</sup>CD56<sup>+</sup> MPs.

Identification of the CD326<sup>low</sup>CD56<sup>+</sup> MP will allow in depth characterisation of the first stages of commitment and differentiation. Specifically, use of the MP population will allow for miRNA profiling, via the use of microarray technology, to monitor differential expression of these non-coding RNAs within this system. As previously stated, miRNAs have been shown to play important roles in the differentiation of hPSC to ECs (Kane et al., 2012, Luo et al., 2013), and it is, therefore, hypothesised that they will also play central roles in emergence of mesodermal and endothelial populations within this hESC-EC differentiation system.

## **Chapter 4    Development and characterisation of an indirect hESC-EC differentiation protocol**

## 4.1 Introduction

First demonstrated almost 100 years ago (Jordan, 1916), it is now commonly accepted that the development of the vascular and hematopoietic systems are closely linked during *in vivo* embryogenesis. Definitive hematopoietic stem cells (HSCs) originate in the aorta-gonad-mesonephros (AGM) region of the developing embryo (Medvinsky et al., 1996). Clusters of hematopoietic cells have been identified attached to the ventral endothelial lining in the aorta of developing vertebrates (Tavian et al., 1996, Taoudi et al., 2007), suggesting this is the site of HSC emergence, a hypothesis supported by extensive work performed showing a clear relationship between ECs and HSCs in the AGM (Zovein et al., 2008).

Studies have focused on the presence of small populations of specialised bipotent precursor cells, with characteristic endothelial phenotype and the ability to generate hematopoietic cells (HCs) and HSCs (Zovein et al., 2008). This process, whereby ECs undergo a phenotypic switch to HCs, is known as the endothelial-to-hematopoietic transition (EHT). The term hemogenic endothelium (HE) has been coined to describe these specialised ECs, responsible for the generation of HC via EHT.

Jaffredo and colleagues were amongst the first to demonstrate this phenomenon *in vivo*, whereby CD45<sup>-</sup> ECs in the developing chick embryo were tagged using Dil-conjugated Ac-LDL, a molecule specifically endocytosed by ECs. Just 1 day later, populations of LDL<sup>+</sup>CD45<sup>+</sup> cells were present as both clusters and single cells, suggesting a phenotypic switch from endothelial to HC (Jaffredo et al., 1998, Jaffredo et al., 2000). The same process has been subsequently documented in a number of other *in vivo* systems of vertebrate development (Bertrand et al., 2010, Boisset et al., 2010). Data obtained from lineage tracing of endothelium, via the utilisation of an inducible VE-cadherin Cre line, was also used to support this model (Zovein et al., 2008).

*In vitro* generation and differentiation of HE has also been studied. In 1998, Nishikawa et al. identified this population during the differentiation of mESCs to HCs (Nishikawa et al., 1998). Within this differentiation system, they identified the diverging point of endothelial and hematopoietic lineages, and showed that a Flk1<sup>+</sup>CD144<sup>+</sup>CD45<sup>-</sup> progenitor cell population exhibited hemoangiogenic



potential. The hemogenic capacity of specialised HE cells, generated from differentiating mESCs, has also been observed using continuous single-cell imaging (Eilken et al., 2009). Using this technology, Eilken et al. demonstrated that mESC-derived mesodermal cells, differentiated via coculture with OP9 stromal cells, give rise to HE colonies. These HE cells were observed to first adopt an EC identity, with cells negative for the HC marker CD45, while expressing CD144, forming tight junctions with adjacent cells, assuming an EC-like morphology and with the ability to uptake Ac-LDL. During EHT, these cells lose their endothelial phenotype, migrate from their EC colonies, gain CD45 expression, morphologically transform to blood cells and begin to proliferate as suspension cells. HE cells were unable to generate SMCs or cardiomyocytes, confirming that they are not early multipotent mesoderm progenitor cells, and their lack of CD45 expression contradicts suggestions that these cells may be bipotent blood and endothelial precursors expressing molecules from both lineages.

Studies have also been performed to identify HE populations within hPSC differentiation systems, as described in detail in section 1.6.2.1 (Choi et al., 2012, Ditadi et al., 2015). Using an OP9 co-culture system, Choi et al. were able to identify a  $CD144^+CD73^-CD235a/CD43^-CD117^{intermediate}$  cell population, with primary EC characteristics and the ability to further generate HCs and mature ECs (Choi et al., 2012). A more defined system was employed by Ditadi and colleagues, who identified a  $CD34^+CD43^-CD31^+CD144^+KDR^+CD117^{low}$  population, able to undergo EHT to form  $CD45^+$  HCs, which could then undergo further definitive hematopoiesis (Ditadi et al., 2015). These cells were also shown to form both venous and arterial ECs, both of which were able to form functional vessels during an *in vivo* Matrigel plug assay.

The development of multiple differentiation protocols, providing distinct routes for the generation of hESC derived ECs, will allow for more in depth study of mechanisms involved in the commitment of cells to specific lineages. Pathways and molecules, identified as playing key roles in endothelial commitment during more direct hESC-EC differentiation assays, can be verified in an independent system for the generation of the same ECs. This will, therefore, result in the elucidation of mechanisms involved specifically in hESC-EC differentiation and

commitment, and identification of processes more generally involved in differentiation or specification of cells to the mesodermal lineage. Many previous publications documenting the existence of HE *in vitro* have focused on the development of HCs and HSCs from these progenitors. In the present study, experiments were designed to optimise generation of CD31<sup>+</sup>CD144<sup>+</sup> hESC-ECs, switching cells from a bipotent HE to a more mature EC phenotype via the manipulation of culture conditions. Derivation of an equivalent population of CD144<sup>+</sup>CD31<sup>+</sup> ECs using a distinct differentiation protocol would allow for validation of any miRNAs, identified as having potential roles in endothelial differentiation and commitment, in an independent system, specifically one routed through the formation of HE progenitors. This indirect hESC-EC differentiation system will also allow for the determination of miRNA specificity; it is highly likely miRNAs differentially expressed in hESC-ECs but not hESC-HC and hESC-HSCs from the same culture are EC-specific.

## 4.2 Aims

The aims of this chapter were as follows:

- Characterise hypothesised hemogenic endothelial progenitor cells, existing within a defined hematopoietic differentiation protocol.
- Develop and optimise a protocol for production of hESC-ECs from these hemogenic endothelial progenitors.
- Determine the existence of CD326<sup>low</sup>CD56<sup>+</sup> progenitor cells within this indirect hESC-EC differentiation.

## 4.3 Results

### 4.3.1 Preliminary characterisation of adherent cells in a defined hematopoietic differentiation system

Previously, a 30-day, defined hematopoietic differentiation protocol had been developed in the lab of Dr J. Mountford, and it described in detail in section 2.3.3. In the presented studies, experiments used the first 10 days of this differentiation system. Briefly, cells were mechanically cut into clumps at d0, using the StemPro® EZ Passage tool, before being placed into 6-well ultra-low attachment plates, where they were allowed to form EBs. After 3 days EBs were collected and dispersed, before they were plated out into 6-well culture plates or T25 culture flasks at specific densities, where they were maintained until d10. Cells were cultured in Stemline II hematopoietic expansion medium of specific mesodermal- and hematopoietic-cytokines (Figure 4.1A).

After EB dispersal on d3, cells become adherent, undergo a low level of expansion and, between d7-10, begin to ‘bud’, producing suspension cells. This phenomenon was observed in experiments using both H1 and H9 hESCs (Figure 4.1B). Adherent cells can form colonies, and appear morphologically similar to ECs, whereas the suspension cells have a HC morphology, appearing round and shiny when viewed using a phase contrast brightfield microscope (Figure 4.2). It was, therefore, hypothesised that these adherent cells, giving rise to budding hematopoietic progenitor (HP) suspension cells from d7, were a population of specialised bipotent HE cells, existing during hPSC-hematopoietic differentiation.

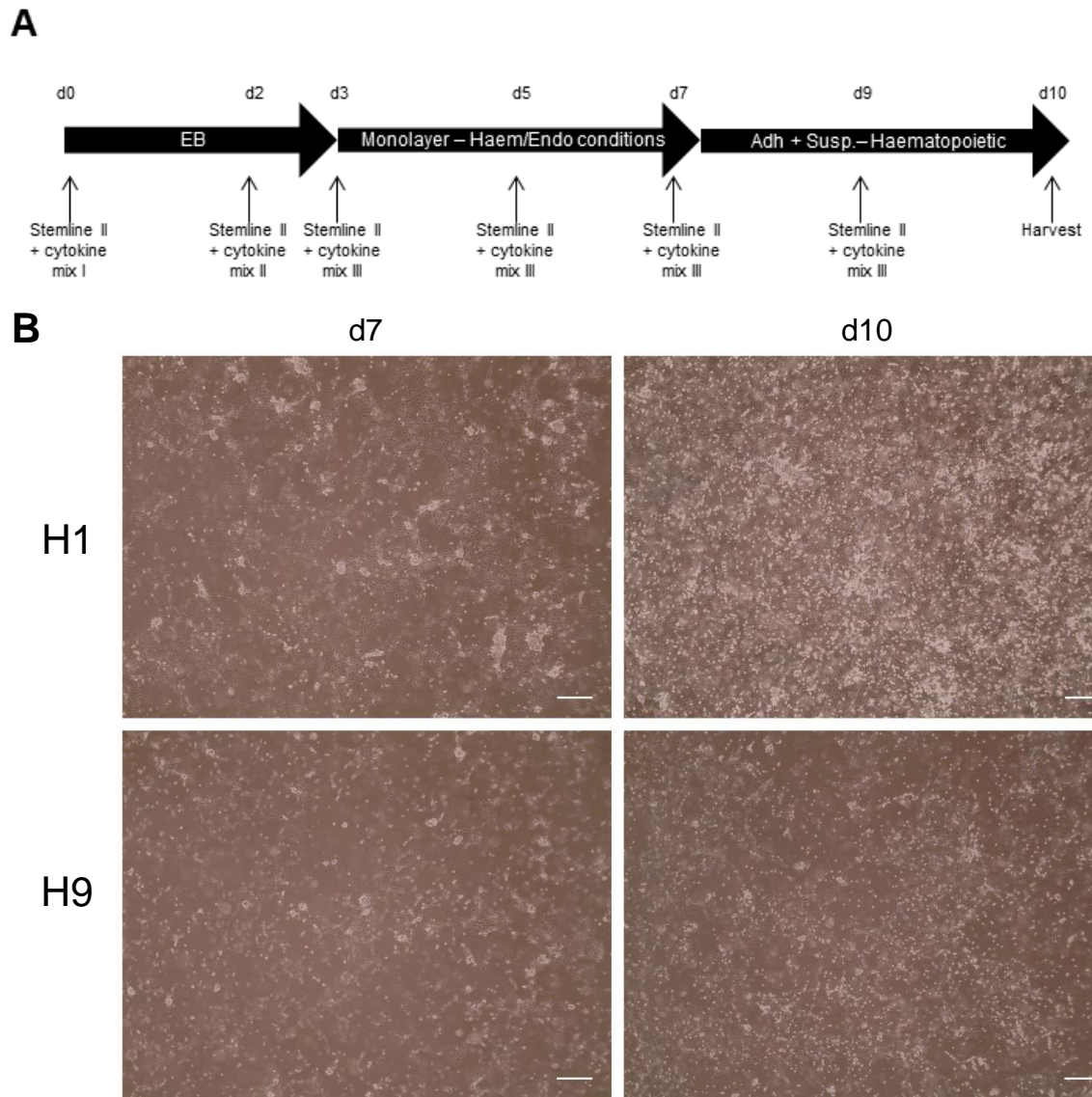


**Figure 4.1 – Schematic and morphological analysis of d7 and d10 of a defined hematopoietic differentiation protocol.**

Pluripotent hESCs were mechanically passaged at d0, transferred to ultra-low attachment culture dishes, and allowed to form EBs. EBs were collected and dispersed on d3, where they were cultured until d10, as shown in the schematic (A). Cytokine mix I = BMP4, VEGF, Activin A, Wnt3A and Inhibitor VIII. Cytokine mix II = Cytokine mix I + FGF $\alpha$ , SCF and  $\beta$ -Estradiol. Cytokine mix III = BMP4, VEGF, FGF $\alpha$ , SCF,  $\beta$ -Estradiol, IGF2, TPO, Heparin and IMBX. Specific concentrations of cytokines are described in detail in section 2.3.3. Morphological analysis (B) of H1 (top panels) and H9 (bottom panels) hESCs was performed on d7 (left panels) and d10 (right panels) of hematopoietic differentiation. Images were taken at 10x magnification and scale bars represent 100  $\mu$ m.

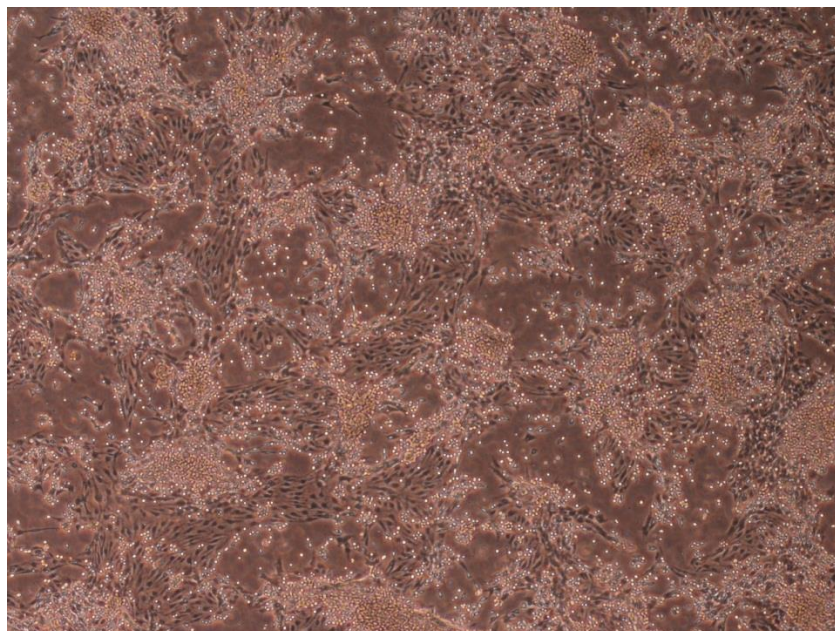


**Figure 4.2 – d7 adherent and budding cells during hematopoietic differentiation.**

Phase contrast image clearly demonstrating the presence of adherent and budding cells on day of hematopoietic differentiation. Differentiation shown performed using RC9b hESC line. Representative image, 10x magnification.

Taking the first 10 days of this protocol as a window for the emergence of a HE population, a panel of endothelial- and hematopoietic-associated makers for was devised for analysis using flow cytometry. In these initial studies, performed using H1 hESCs, 2-colour flow cytometry was employed to gain insight into the cell surface marker profile of both suspension and adherent cells, from days 7 and 10 of hematopoietic differentiation. This would allow for preliminary identification and characterisation of any possible HE progenitor populations, existing within this culture system. Primarily, five different antibody combinations were used, each containing one PE-conjugated and one APC-conjugated antibody (Table 4.1).

Combination (Figure 4.3)	APC-conjugated	PE-conjugated
A	CD34	CD45
B	CD235a	CD71
C	CD43	CD31
D	CD144	CD31
E	CD235a	CD144

**Table 4.1 – 2-colour flow cytometry antibody combinations.**

Antibody combinations used for initial flow cytometry studies. More information on antibodies is provided in Section 2.7, Table 2.7.

First, cells were analysed for a number of hematopoietic cell surface markers; CD34 and CD45, CD235a (Glycophorin A) and CD71, and CD43 and CD31 (Figure 4.3A-C). The combination of CD34 and CD45 is associated with HP cells, with the presence of CD45 on CD34<sup>+</sup>CD45<sup>+</sup> cells discriminating from CD34<sup>+</sup>CD45<sup>-</sup> endothelial progenitor populations (Case et al., 2006). As would be expected, the d10 suspension samples contained the highest percentage of CD34<sup>+</sup>CD45<sup>+</sup> cells (~26%), suggesting these cells are moving toward a HP phenotype (Figure 4.3A). Approximately 47% of d7 suspension cells stained positive for CD34, however, there was no expression (<0.5%) of CD45 in any cells from this sample (Figure 4.3A). Publications have previously suggested that CD34<sup>+</sup>CD45<sup>-</sup> cells may represent an early or emerging population of HP cells (Venditti et al., 1999), although it could also be suggested that CD34<sup>+</sup>CD45<sup>-</sup> cells may express CD235a, and therefore have progressed beyond the HSC phenotype, and become a more defined HC. This would, therefore, explain the presence of a large CD34<sup>+</sup>CD45<sup>-</sup> population in the d10 suspension samples (approximately 28%).

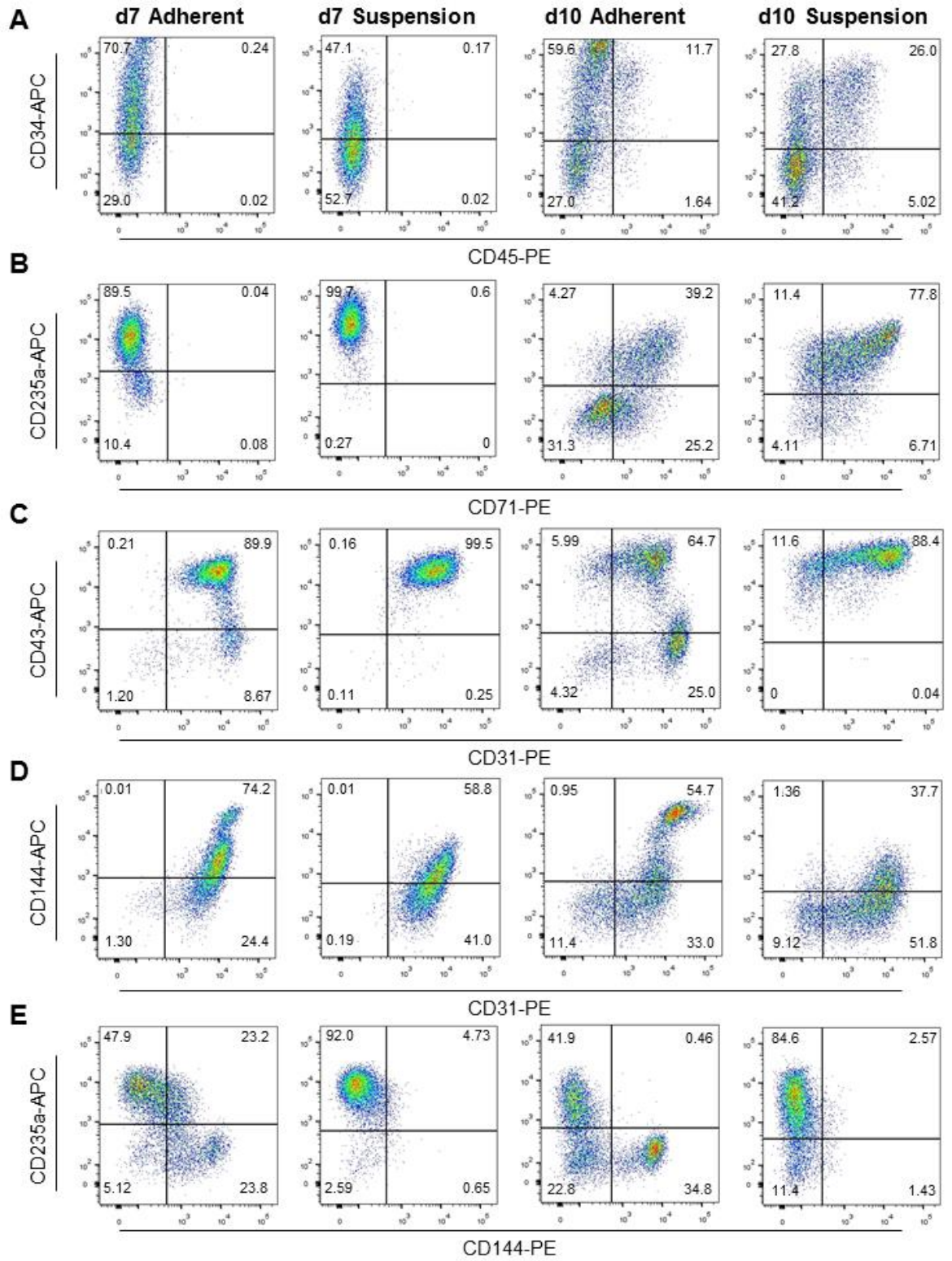


**Figure 4.3 – 2-colour flow cytometric analysis of HE markers in a defined hematopoietic differentiation system.**

Suspension and adherent cells were harvested at d7 and d10 of hematopoietic differentiation using H1 hESCs, and stained using a variety of endothelial and hematopoietic antibodies. Plots above are representative of that sample group. Gates were determined using matched isotype controls for each sample group. n=3.

Both populations of adherent cells (d7 and d10) showed higher levels of expression of CD34 than the suspension cells, both in terms of total percentage of cells expressing this markers and fluorescence intensity. Although CD34 is commonly used to identify early HP cells, it is also expressed on the surface of vascular ECs and circulating endothelial progenitor cells (Civin et al., 1984, Fina et al., 1990, Urbich et al., 2004), giving a possible explanation for the high levels of expression in these cells. There was no expression of CD45 (<0.5%) in d7 adherent cells, supporting claims these cells may be early HP cells or have a more EC phenotype. In the d10 adherent cell population, however, ~11% of cells stained positive for CD45. This may be due to the presence of contaminating suspension cells, not removed during washing, or CD34<sup>+</sup>CD45<sup>+</sup> cells in this sample group may represent those cells currently in the process of ‘budding’ and, therefore, still attached to the adherent cells on the culture surface.

The combination of CD235a, a cell surface antigen whose expression is restricted to erythroid precursors and circulating red blood cells, and CD71 (also known as Transferrin receptor) antibodies, allowed for identification of potential erythroid precursors (Chasis et al., 1992, Marsee et al., 2010). On d7, high levels of adherent and suspension cells expressed CD235a (89.5% and 99.7% respectively), although the intensity was brighter in suspension cells and there was the existence of a small (10.4%) CD235a<sup>-</sup> population in the adherent cell sample (Figure 4.3B). At d10, however, high percentages of the suspension cells (77.8%) were CD235a<sup>+</sup>CD71<sup>+</sup> suggesting a large proportion of hematopoietic commitment in these cells. Approximately 40% of d10 adherent cells had the CD235a<sup>+</sup>CD71<sup>+</sup> marker profile, although, again, this could be due to contaminating or ‘budding’ suspension cells present in the sample (Figure 4.3B). A substantial percentage of d10 adherent cells were negative for both CD235a (56.5%), with 31.3% expressing neither CD235a nor CD71. Lastly, CD43, a marker of hematopoietic commitment (Vodyanik et al., 2006), was used in combination with CD31, expressed on the surface of leukocytes and HSCs (Baumann et al., 2004). In the d7 suspension sample, almost all cells (>99%) were CD43<sup>+</sup>CD31<sup>+</sup>. By d10, a high percentage of suspension cells were still highly double positive for these two markers (~88%), but some cells had lost or were losing expression of CD31 (11.6% CD43<sup>+</sup>CD31<sup>-</sup>) (Figure 4.3C). In adherent cells, although the majority of cells were still CD43<sup>+</sup>CD31<sup>+</sup> (89.9% and 64.7% at d7 and 10 respectively), there was a distinct



population of CD43<sup>-</sup>CD31<sup>+</sup> cells, which increased in size between d7 and d10 (from 8.7% to 25%) (Figure 4.3C). Although present on the surface of HSCs and leukocytes, CD31 has classically been associated with ECs, involved in EC adhesion and present at cell-cell junctions (Muller et al., 1989, Albelda et al., 1990). This suggests that the populations of CD43<sup>-</sup>CD31<sup>+</sup>, present in the adherent cell samples, may represent an emerging population of ECs or, more likely, HE progenitors.

The EC surface marker combination of CD31 and CD144, a marker classically used in the identification of vascular ECs (Breier et al., 1996) (Figure 4.3D), was then employed to investigate this further. This marker combination had been previously used to measure the numbers of hESC-ECs generated during direct hESC-EC differentiation as described previously (Chapter 3). Although the highest percentage of CD31<sup>+</sup>CD144<sup>+</sup> cell overall was observed in the d7 adherent sample, a smaller CD31<sup>+</sup>CD144<sup>high</sup> population was also present, which increased in size by d10 in the adherent, and was not present in either suspension cell sample. In fact, only a small percentage of cells expressed CD144 at all in the d10 suspension sample, as it appears all cells were losing or had lost expression of this marker. These results suggested a more EC or HE phenotype in both adherent cell samples, and a more HP or HSC phenotype in the suspension cells.

To verify this, cells were finally stained for a combination of CD144 and CD235a (Figure 4.3E). This combination of an endothelial (CD144) and a hematopoietic (CD235a) surface marker, is the basis of the HE marker profile described by Choi et al. (Choi et al., 2012), and would allow for more definitive identification of HE. Choi et al. suggest that HE cells are CD144<sup>+</sup>CD235a<sup>-</sup>, and populations matching this profile were observed in both d7 and d10 adherent samples (23.8% and 34.8% respectively). By d10, adherent cells expressing either CD235a or CD144 were mutually exclusive, with no cells expressing both of these markers. In both sets of suspension cells, almost all cells were CD144<sup>-</sup>CD235a<sup>+</sup> (92% and 84.6% on d7 and d10 respectively), suggesting the absence of EC or HE populations within these non-adherent cellular fractions. This was in contrast to the previous combination (Figure 4.3D), where >50% of cells were positive for CD144 in both d7 samples (compared to 47% and 5.38% in adherent and suspension in the CD235a/CD144 combination), and almost 40% in d10 suspension cells (compared to 4% in the CD235a/CD144 combination). This may be due to

antibody variability, antibodies used were from different companies (Table 2.7), and different fluorophores were used; APC-conjugated anti-CD144 with CD31 and PE-conjugated anti-CD144 with CD235a. One explanation may be that suspension cells express low levels of CD144; the bright APC fluorophore may show this as positively staining for CD144, whereas the PE antibody may show this as CD144 negative. This explains the presence of the CD31<sup>+</sup>CD144<sup>high</sup> population in the CD31/CD144 combination, which correlates to the CD144<sup>+</sup> cells in the d7 and 10 adherent samples when stained with CD144 and CD235a (Figure 4.3D-E).

Taken together, these data suggest a possible HE progenitor population, existing within the adherent cells, both at d7 and d10 of hematopoietic differentiation.

### 4.3.2 Multi-colour flow cytometry to identify HE populations within a defined hematopoietic differentiation system

To gain a more in depth surface marker profile of these possible HE progenitors, a larger, 6-colour flow cytometry panel was devised (Table 4.2), based on the definition of HE progenitors previously published by Choi and colleagues (Choi et al., 2012). Utilising a combination of hematopoietic and endothelial cell surface markers, Choi et al. defined these cells as CD144<sup>+</sup>CD73<sup>-</sup>CD235a/CD43<sup>-</sup>CD117<sup>intermediate</sup> and this was the profile investigated in this study, with the addition of CD31. The panel of antibodies used, and their conjugated fluorophores are shown in Table 4.2.

Antibody	Fluorophore	Excitation (nm)	Emission (nm)@
CD144	PE	488	578
CD31	FITC	488	520
CD43	PE-Cy7	488	785
CD117	PerCP-Cy5.5	488	695
CD73	APC	640	660
CD235a	BV421	405	421

**Table 4.2 – 6-colour flow cytometry antibody panel.**

Table shows antibodies used in 6-colour flow cytometry panel and their conjugated fluorophores. Excitation and maximum emission wavelengths for each fluorophore are also shown. BV421 = Brilliant Violet 421 (BD Biosciences).

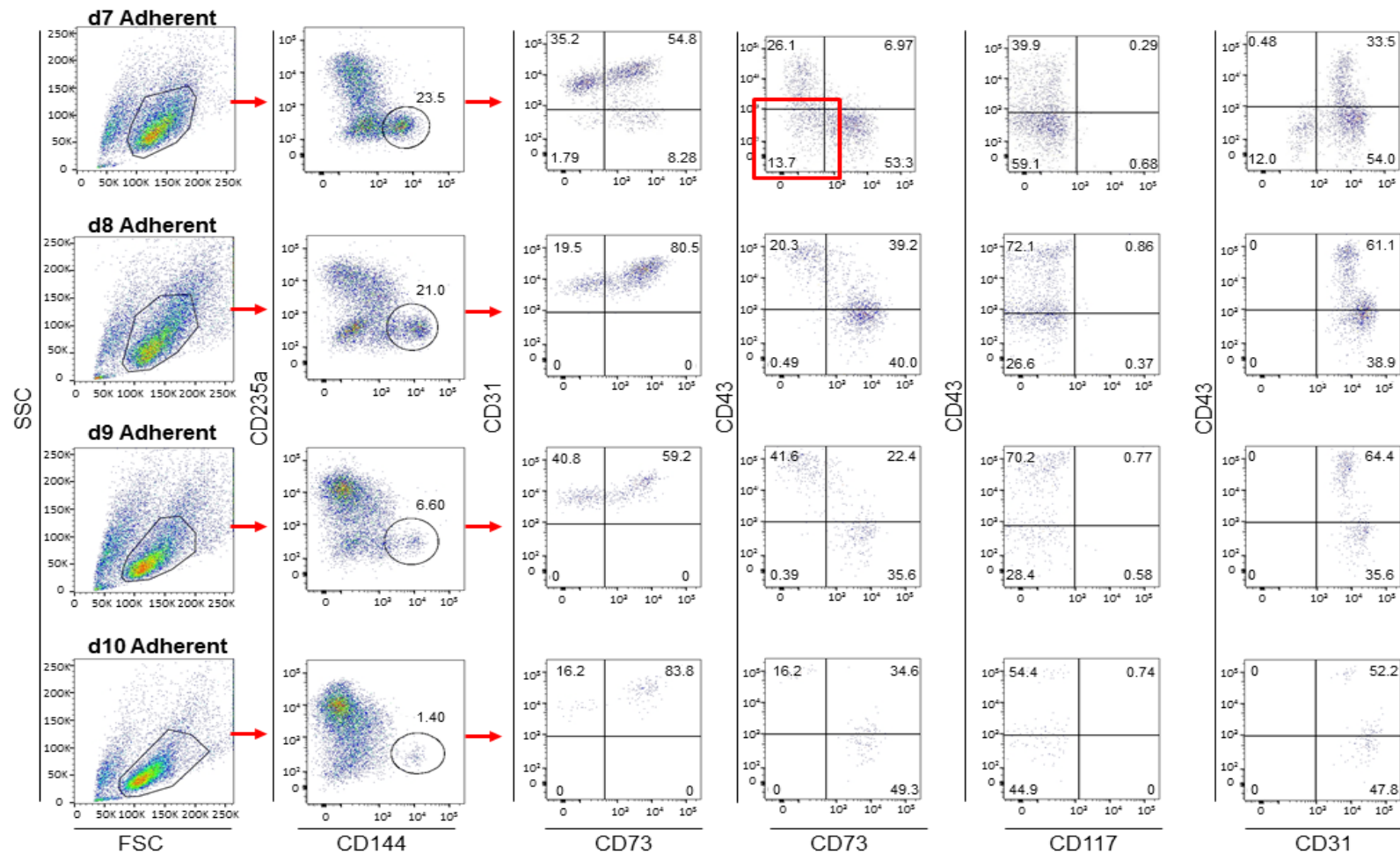


Figure 4.4 – 6-colour flow cytometric analysis of d7-10 adherent cells. Adherent cells were harvested d7, 8, 9 and 10 of hematopoietic differentiation using H1 hESCs, stained and analysed using flow cytometry. Plots above are representative of that sample group. Gates were determined using matched isotype controls for each sample group, compensation was performed using singly stained controls and FMO controls were performed at each time point. n=3.

Suspension and adherent cells were harvested at d7, 8, 9 and 10, and stained using the antibodies shown in Table 4.2. Using the same basis as Choi and colleagues, cells were first gated for CD144<sup>+</sup>CD235a<sup>-</sup> populations (Figure 4.4). Using this population, events were then analysed for expression of CD43, representing cells committed to the hematopoietic lineage, CD31, an endothelial marker, CD73, also an established EC marker (Thomson et al., 1990) and CD117 (c-Kit), a marker of early stage angiohematopoietic progenitors (Choi et al., 2012). The numbers of adherent cells in the CD144<sup>+</sup>CD235a<sup>-</sup> population decreased throughout differentiation, with the lowest numbers of cells present on d10, and the highest on d7, where approximately 24% of cells fit this description. Within the CD144<sup>+</sup>CD235a<sup>-</sup> population, at all time points (d7-d10), almost all events were also CD31 positive, implying that these cells are CD31<sup>+</sup>CD144<sup>+</sup>CD235a<sup>-</sup> (Figure 4.4). The co-staining of all cells for two EC markers, suggests a predominantly EC phenotype in the CD144<sup>+</sup>CD235a<sup>-</sup> cells, similar previously published definitions of HE (Nishikawa et al., 1998, Zovein et al., 2008, Choi et al., 2012, Ditadi et al., 2015), and in concurrence with data collected by Choi et al. Unlike previously published data, however, CD117 staining was not observed on any cells throughout this experiment (Figure 4.4), including in the non-CD144<sup>+</sup>CD235a<sup>-</sup> cell fraction (data not shown).

The expression of CD73, however, was variable. CD31<sup>+</sup>CD144<sup>+</sup>CD235a<sup>-</sup> Adherent cells from d7 were mixed in terms of CD73, with those expressing the highest levels of CD31 also expressing CD73 (CD31<sup>+</sup>CD73<sup>+</sup>), possibly indicative of a more mature EC phenotype (Figure 4.4). 35% of cells at this time point, however, were CD31<sup>+</sup>CD73<sup>-</sup>. As differentiation progressed, larger percentages of cells were seen to co-express CD31 and CD73, and the CD31<sup>+</sup>CD73<sup>-</sup> population was reduced in size (16.2% by d10). This may indicate a loss of HE cells from d7-10, as medium becomes more supportive of HP suspension cells. CD43 staining, signifying cells committed to a hematopoietic fate, was also variable in the CD31<sup>+</sup>CD144<sup>+</sup>CD235a<sup>-</sup> cells (Figure 4.4). At d7, the majority of CD31<sup>+</sup>CD144<sup>+</sup>CD235a<sup>-</sup> cells were also CD43<sup>-</sup> (approximately 60%), with a decrease in the size of this population as differentiation progressed (approximately 35-45% on d8-10). Choi et al. hypothesised that HE cells were negative for both CD43 and CD73. To therefore investigate this hypothesis, cells were analysed for co-expression of CD43 and CD73. A population of CD31<sup>+</sup>CD144<sup>+</sup>CD235a<sup>-</sup>CD43<sup>-</sup>CD73<sup>-</sup>

cells was present only in d7 adherent cell samples (Figure 4.4; red gate), before being lost by d8-10 time points. Taken together, alongside previously published data, these results suggest that the  $CD31^+CD144^+CD235a^-CD43^-CD73^-$  population may be a HE population, equivalent to the  $CD144^+CD73^-CD235a/CD43^-CD117^{\text{intermediate}}$  cells identified by Choi.

As well as the adherent cells, suspension cells were also harvested at the same time points (d7, 8, 9 and 10) and analysed using the same panel of cell surface markers (Table 4.2). In suspension samples, however,  $CD144^+CD235a^-$  cells were not present at any time point (Figure 4.5). Profiles were similar between all four samples, with the majority of cells (>75%) possessing the surface marker profile  $CD144^-CD235a^+$ . All of the cells were also positive for both CD43 and CD31, whilst staining negative for CD73, giving the profile  $CD31^+CD144^-CD235a^+CD43^+CD73^-$ . This, therefore, confirmed suggestions that these cells are a population of emerging HPs, and do not contain the HE population.

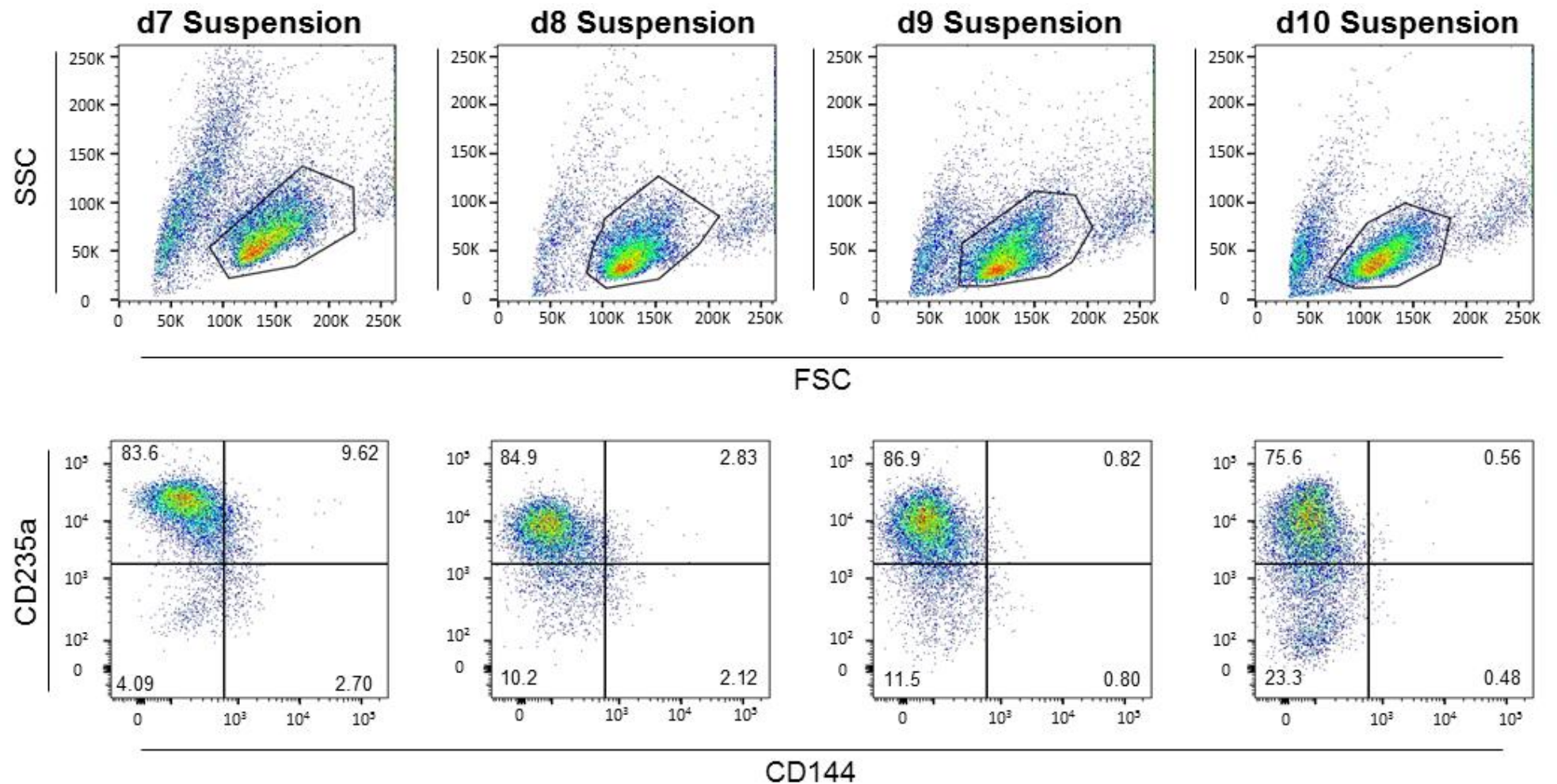


**Figure 4.5 – CD235a/CD144 staining of d7-10 suspension cells.**

Suspension cells were harvested d7, 8, 9 and 10 of hematopoietic differentiation using H1 hESCs, stained and analysed using flow cytometry. Plots above are representative of that sample group. Gates were determined using matched isotype controls for each sample group. n=3.

To further characterise these cells, total RNA samples were also collected from d0 hESCs, d7,8 9 and 10 adherent cells and d7 and d10 suspension cells. Samples were then subjected to gene expression profiling using Taqman® qRT-PCR, examining the levels of endothelial, hematopoietic and pluripotent genes (Figure 4.6). *CD144*, *CD31* and *CD34*, all endothelial-associated genes, are significantly upregulated in all time points after d0, including at the d3 EB stage (Figure 4.6). Specifically, *CD144* is highly upregulated to similar levels in all of the adherent cell samples, and in the d7 suspension cells. In the d10 suspension cells, however, the levels of *CD144* mRNA expression were significantly lower than in all adherent cell samples and the d7 suspension cells. This suggests that suspension cells lose the expression of *CD144* between d7 and d10, as cells become more committed to a hematopoietic cell fate. The expression pattern of *CD31* was similar, with a significant upregulation in levels of this gene in all samples when compared with d0 pluripotent hESCs (Figure 4.6A). In contrast to *CD144*, however, *CD31* was also upregulated to the same levels in d10 suspension cells, as in the rest of the samples. As stated previously, *CD31* is also expressed on the surface of leukocytes, and erythroid progenitors (Baumann et al., 2004), and, therefore, high expression in the d10 suspension cells, combined with low *CD144* expression indicates that these cells are of a more hematopoietic fate. This is further confirmed by the expression profiles of *CD34*, also associated with both endothelial and hematopoietic cell types, and *CD43* (Figure 4.6B). *CD34* was, again, significantly upregulated in all time points after d0. The highest levels of expression were observed in d8-10 adherent cells, although there was no significant difference in levels in all suspension and adherent time points, possibly due to the expression of this gene in both HPs, and vascular ECs and circulating EPCs. In terms of hematopoietic gene expression, the highest levels of *CD43* were observed in the d10 suspension cells (Figure 4.6B), with significantly lower expression in the adherent cell samples. Higher levels of expression in the d7 and d10 suspension cells, coupled with *CD144*, *CD31* and *CD34* expression, shows that these cells are beginning to move toward the hematopoietic lineage by d7, with the levels of commitment increased further by d10, supporting flow cytometry data (Figure 4.3, Figure 4.4). In contrast, adherent cells show a predominantly EC phenotype, with lower levels of hematopoietic-associated genes, although *CD43* is still upregulated in these cells when compared to d0 hESCs and d3 EBs.

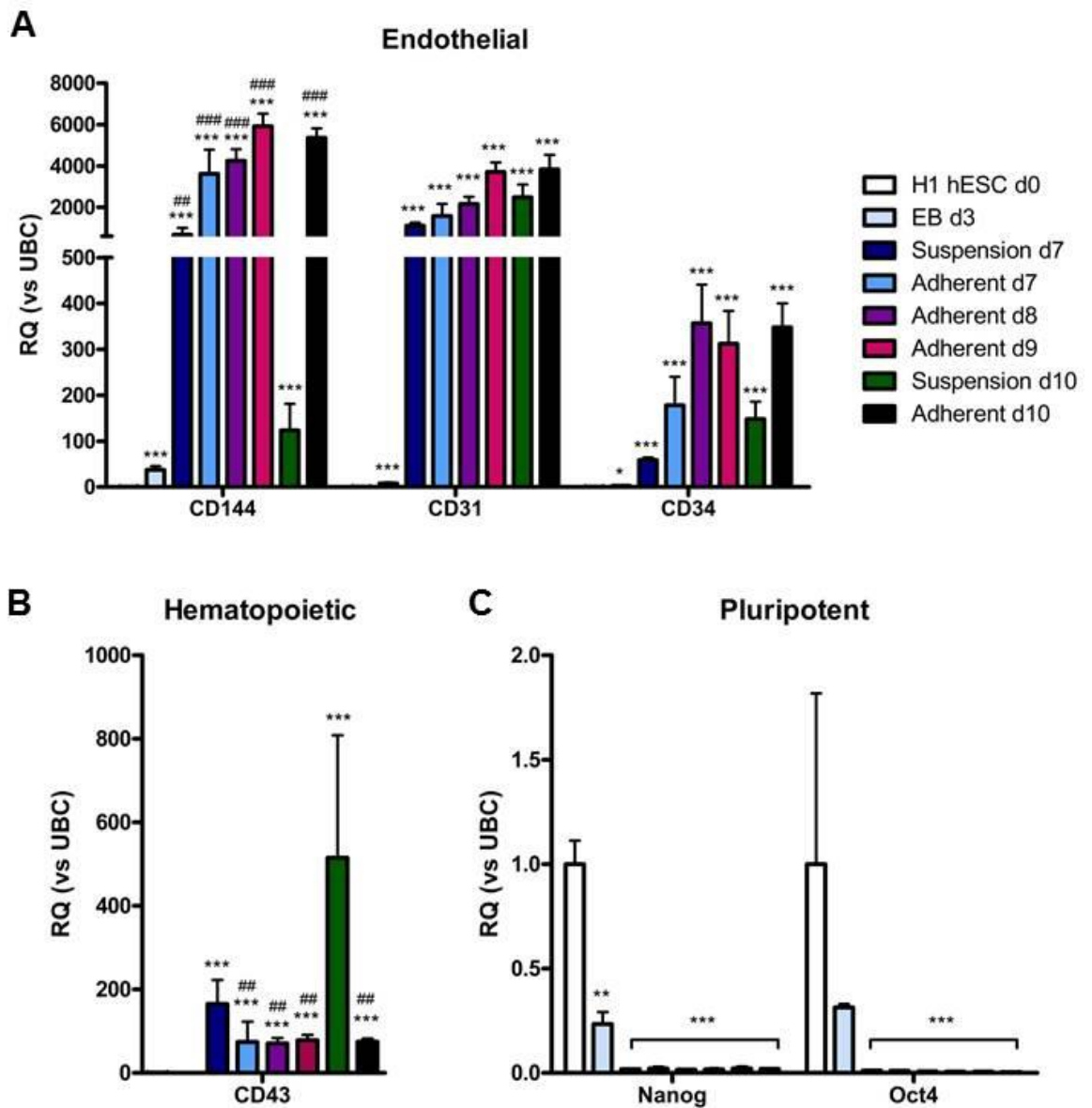


**Figure 4.6 – Gene expression analysis of suspension and adherent cells in a defined hematopoietic differentiation system.**

Expression profiles of endothelial- (*CD144*, *CD31* and *CD34*) (A), pluripotent- (*Nanog* and *Sox2*) (B) and hematopoietic- (*CD43*) (C) associated genes in adherent cells from d7-10 and suspension cell from d7 and d10 during hematopoietic differentiation of H1 hESCs, determined using qRT-PCR. Repeated measures ANOVA with Tukey post hoc t-test, \* =  $p < 0.05$ , \*\*\* =  $p < 0.001$  vs. H1 d0 hESCs, ## =  $p < 0.01$ , ### =  $p < 0.001$  vs. d10 suspension cells. Data shown is RQ  $\pm$  RQ max, relative to UBC. n=3.



Levels of pluripotent genes were also assessed in these samples. Both *Nanog* and *Oct4*, pluripotency-associated TFs, were found to be significantly downregulated during differentiation (Figure 4.6C). *Nanog* was significantly downregulated by d3, and both genes were expressed at near-undetectable levels by d7, demonstrating, as would be expected, a loss in pluripotency as hESCs differentiate, becoming committed toward specific lineages.

The results collected from the qRT-PCR analysis of the cell samples are consistent with the flow cytometry data and, taken together, these data suggest that the d7 adherent cells possess the most EC or HE phenotype.

### **4.3.3 Optimisation of an indirect hESC-EC differentiation protocol**

Following the identification and characterisation of a possible CD31<sup>+</sup>CD144<sup>-</sup>CD235a<sup>+</sup>CD43<sup>+</sup>CD73<sup>-</sup> HE progenitor population, it was hypothesised that the phenotype of these cells may be controlled by cell culture conditions. Currently, during hematopoietic differentiation, adherent cells from d7 are kept in culture conditions supportive of hematopoietic expansion. Therefore, if placed into endothelial supportive conditions cells would be driven toward an EC fate and, thus, this protocol may be used as an additional, indirect, method of hESC-EC generation.

To examine this hypothesis, and to optimise the day on which cells are transferred to endothelial-supportive conditions, suspension cells were removed from the culture system. Remaining adherent cells were washed to limit suspension cell carry over, and medium was replaced with the EC-supportive Lonza EGM-2, containing the FBS component and supplemented with 50 ng/mL VEGF. Cells were placed into endothelial conditions on d7, 8 or 9 and cultured for 3, 2 or 1 day until d10 (d7+3, d8+2 and d9+1, respectively). D10 was chosen as an end point, as this is the time at which, during hematopoietic differentiation, suspension cells at d10 are removed and their culture continues without the adherent cells. After 10 days, the resultant cells were photographed for morphological analysis, harvested for analysis by flow cytometry and total RNA samples taken for gene expression profiling. A schematic detailing the experimental design is shown in Figure 4.7.

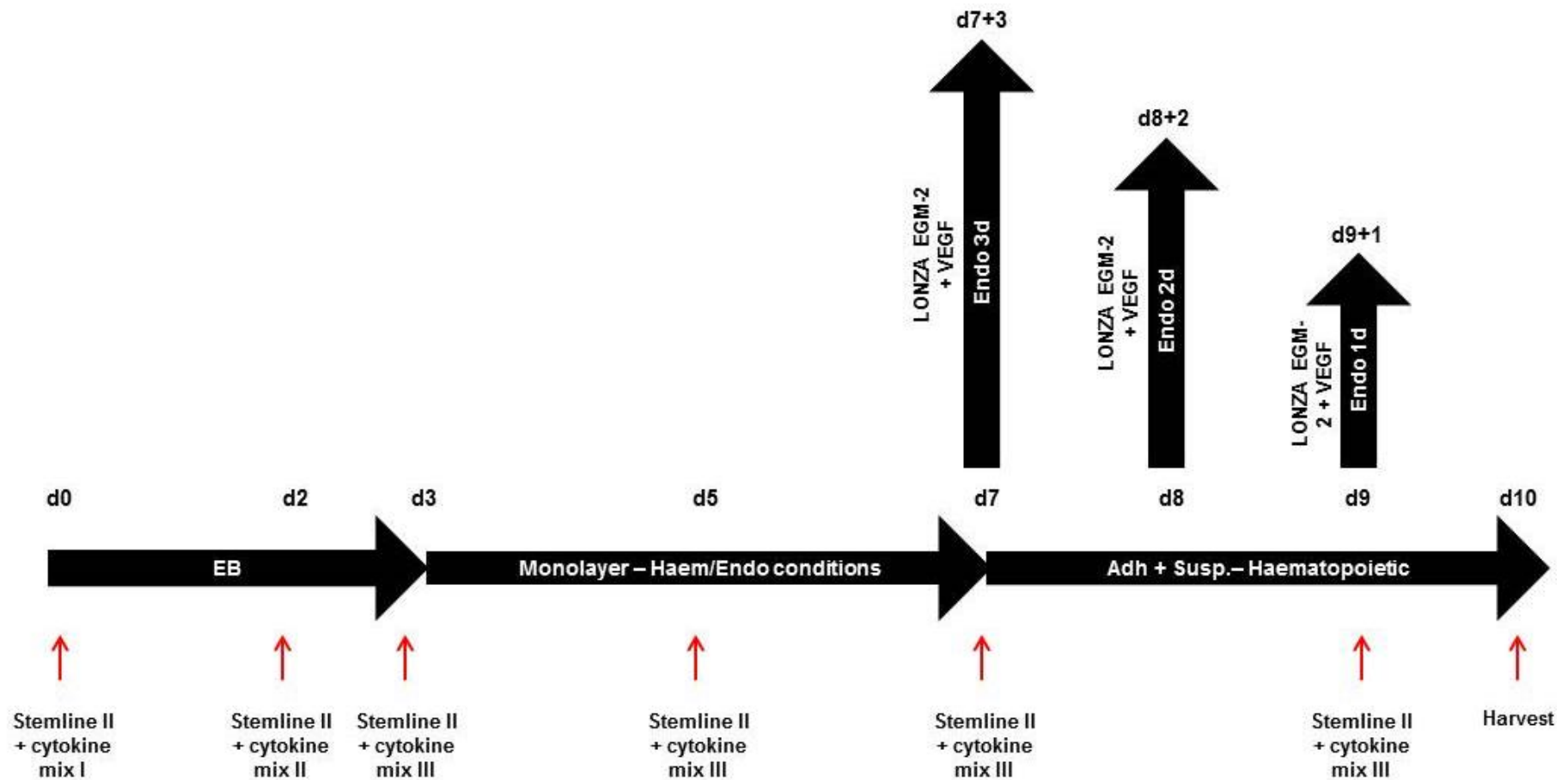


**Figure 4.7 – Schematic of indirect hESC-EC differentiation system.**

Cytokine mix I = BMP4, VEGF, Activin A, Wnt3A and Inhibitor VIII. Cytokine mix II = Cytokine mix I + FGF $\alpha$ , SCF and  $\beta$ -Estradiol. Cytokine mix III = BMP4, VEGF, FGF $\alpha$ , SCF,  $\beta$ -Estradiol, IGF2, TPO, Heparin and IMBX. Specific concentrations of cytokines are described in detail in section 2.3.3.

By d10, cultures which had been in endothelial-supportive conditions for 3 days (d7+3) contained fewer suspension cells than those in medium for 1 or 2 day; (d9+1 and d8+2, respectively (Figure 4.8A). Adherent cells cultured in endothelial-supportive conditions for 1, 2 and 3 days (d9+1, d8+2 and d7+3), had expanded to a confluent, homogenous monolayer by d10, with a morphology similar to that of mature ECs. In contrast to this, however, d10 adherent cells, cultured in only medium and cytokines supporting hematopoietic differentiation, did not form a confluent monolayer, clumped together, and displayed high levels of budding, producing larger amounts of suspension cells.

In order to characterise the cells produced, d7+3, d8+2 and d9+1 samples were subjected to the 6-colour flow cytometry antibody panel detailed in section 4.3.2 (Table 4.2). This would determine whether hESC-ECs had been generated and, if so, whether they were still HE, or whether they had gained a more definitive EC marker profile. In this experiment, d10 adherent cells, continually cultured in hematopoietic conditions until they were harvested, were used as a comparison. Firstly, samples were assessed for the percentage of CD31<sup>+</sup>CD144<sup>+</sup> cells, the criteria used to determine levels of hESC-ECs generated during direct differentiation (Chapter 3). There was a significant increase in the proportion of cells expressing these two markers in d7+3 samples (up to 80%), when compared with d0 pluripotent controls (Figure 4.8A, Figure 4.9). On average, percentages of CD31<sup>+</sup>CD144<sup>+</sup> cells were also increased in d8+2 (approximately 50%) and d9+1 samples (approximately 40%), although not significantly (Figure 4.9), however, this may be due to variability between experimental replicates. The percentage CD31<sup>+</sup>CD144<sup>+</sup> decreased when cells had spent less time in the endothelial-supportive conditions, with the highest levels at d7+3 and the lowest at d9+1. In d10 adherent cells, numbers of CD31<sup>+</sup>CD144<sup>+</sup> were very low (Figure 4.8B, Figure 4.9), although this varied with the success of the hematopoietic differentiation to d7. Differentiations producing high numbers of budding cells and, subsequently, suspension cells, resulted in lower levels of CD31<sup>+</sup>CD144<sup>+</sup> d10 adherent cells. High numbers of suspension cells may result in culture conditions favouring further generation of suspension cells, no longer supporting adherent cells, therefore causing a reduction in the numbers of CD31<sup>+</sup>CD144<sup>+</sup> HE cells. This initial data suggest that transfer of cells to endothelial-supportive conditions at d7 is optimum for the generation of hESC-ECs.

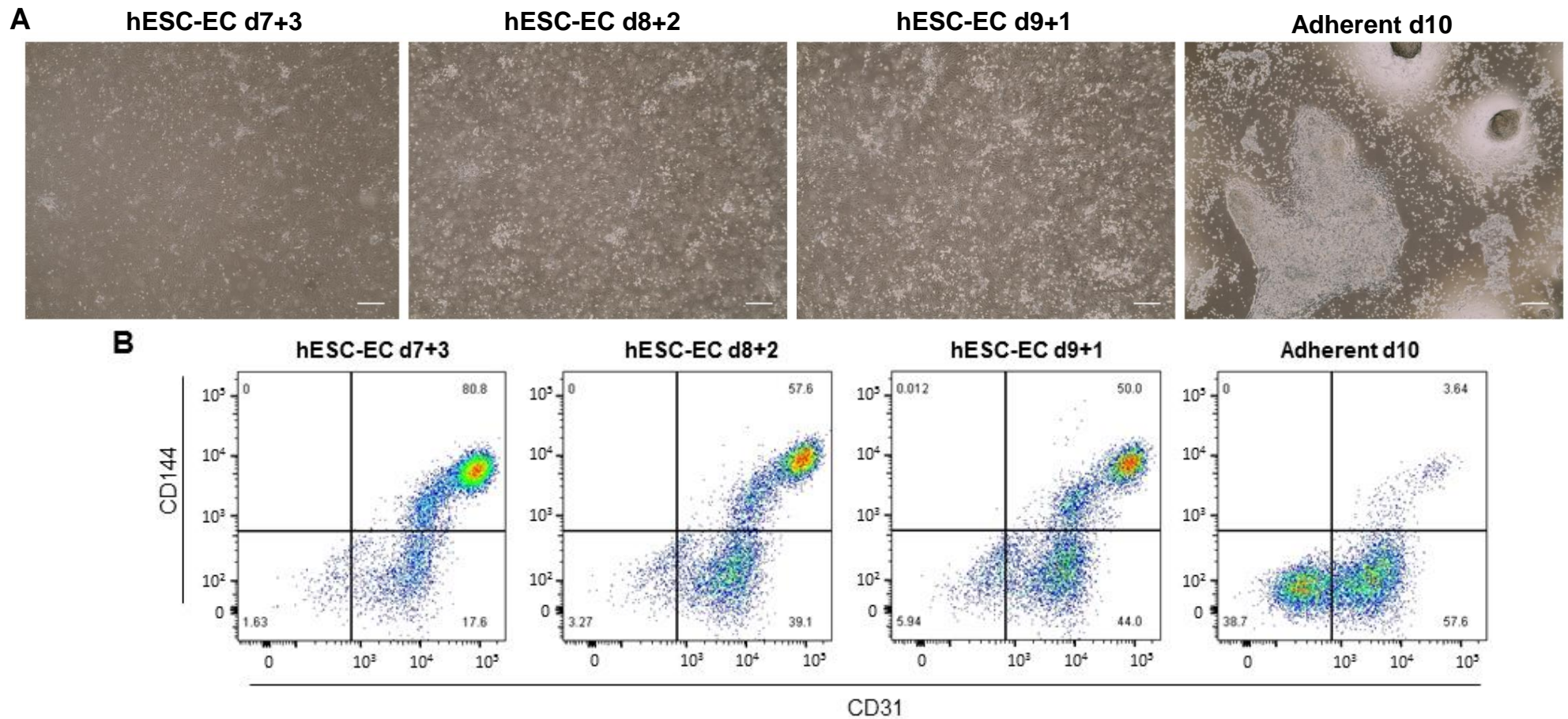


**Figure 4.8 – Optimisation of a newly developed indirect hESC-EC differentiation system.**

Adherent cells were put into endothelial medium on d7, d8 or d9 of hematopoietic differentiation and cultured until d10 (d7+3, d8+2 and d9+1, respectively). Morphological analysis of cells was performed (B). Adherent d10 cells shown have had suspension cells removed for clearer analysis. Brightfield images were taken at 10x magnification, scale bars represent 100  $\mu$ m.  $n=3$ . On d10, cells were also harvested, stained using PE-conjugated anti-CD144 and FITC-conjugated anti-CD31 (as part of a larger 6-colour panel), and analysed using flow cytometry (A). Compensation was performed using single-stained controls and FMO controls performed to ensure correct compensation.

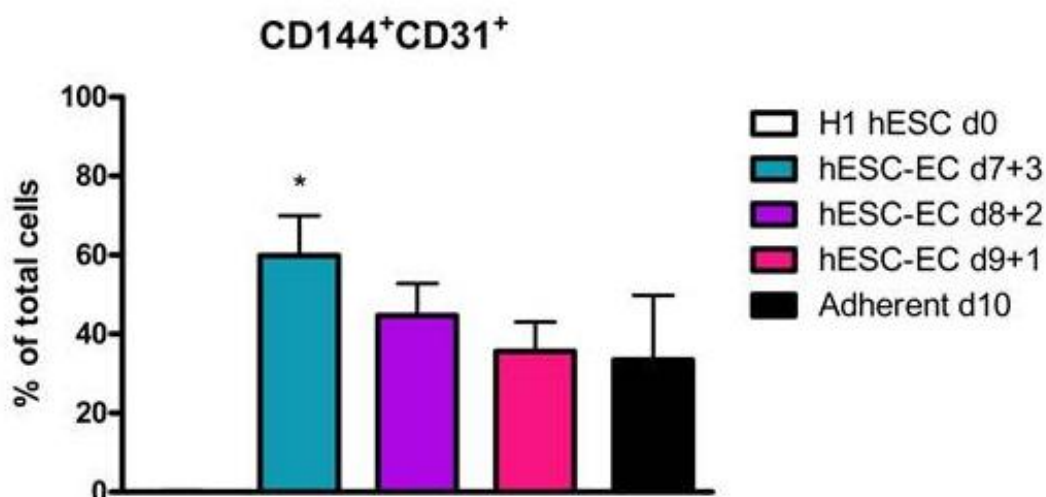


**Figure 4.9 – Average percentage of CD31<sup>+</sup>CD144<sup>+</sup> hESC-ECs**

Histogram of CD31/CD144 flow cytometry data, combined from n=3 different indirect hESC-EC differentiation optimisation experiments (A). Average percentages of double positive cells are plotted with SEM. Repeated measures ANOVA with Tukey's post hoc comparisons, \* = p<0.05.

To further investigate the surface marker profile of the generated d7+3 hESC-ECs, CD31<sup>+</sup>CD144<sup>+</sup> were gated and analysed for the expression of further endothelial (CD73) and hematopoietic (CD235a, CD43) markers. Shown in Figure 4.10, CD31<sup>+</sup>CD144<sup>+</sup> cells were mainly negative for both hematopoietic markers CD43 and CD235a, similarly to the CD31<sup>+</sup>CD144<sup>+</sup>CD235a<sup>-</sup>CD43<sup>-</sup>CD73<sup>-</sup> HE progenitor population, suggesting a largely EC phenotype in these cells. Additionally, and unlike the HE progenitor population identified on d7, 100% of these cells are also positive for CD73, an EC surface marker, indicating that these cells possess a more committed EC phenotype than the bipotent HE progenitor cells, verifying that these cells are hESC-ECs and not HE cells.

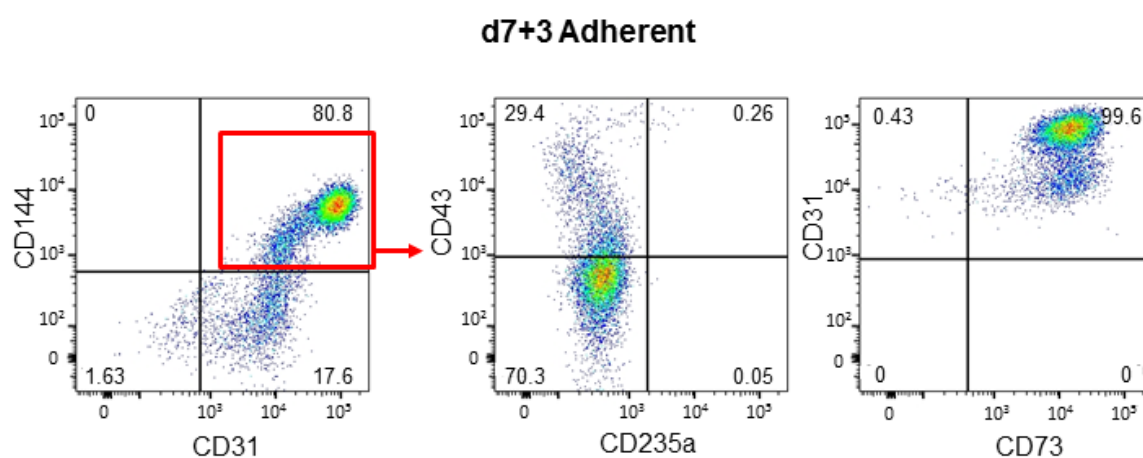


**Figure 4.10 – Further analysis of surface marker expression in CD31<sup>+</sup>CD144<sup>+</sup> d7+3 cells.**

After initial analysis, d7+3 CD31<sup>+</sup>CD144<sup>+</sup> were further gated and analysed for their expression of further EC (CD73) and HC (CD235a, CD43) markers. Red gate indicates cells included in further analysis. Dot plots shown are representative of multiple experiments, gates drawn based on negative isotype and unstained control samples. Compensation performed using singly stained controls. n=3.

To allow for further characterisation of the phenotypic profile of these cells, total RNA was also collected from d7+3, d8+2 and d9+1 samples, as well as pluripotent d0 hESCs and suspension and adherent cells from d10 of hematopoietic differentiation. Pluripotent (*Nanog*, *Oct4*), hematopoietic (*CD43*) and endothelial (*CD144*, *C31* and *CD34*) genes were all profiled using Taqman® qRT-PCR (Figure 4.11). As observed previously, *Nanog* and *Oct4* were significantly down regulated during differentiation, as hESCs lose their pluripotency and become committed to specific lineages and cell types (Figure 4.11A). *CD43* was significantly upregulated in all samples compared to d0 pluripotency cells (Figure 4.11B). Additionally, significantly higher levels of *CD43* were detected in the HP-containing d10 suspension samples, than in d7+3, 8+2, 9+1 or d10 adherent cells. Levels were also significantly higher in d9+1 and d10 adherent samples than in d7+3 cells. Profiling of endothelial-associated genes showed that, although significantly upregulated in all samples when compared to d0 pluripotent controls, the highest levels of expression were in d7+3 and d8+2 (Figure 4.11C). Specifically, levels of *CD144*, *CD31* and *CD34* were all significantly higher in the d7+3 cells than in the d10 suspension cells. Combined with data from flow cytometric analysis, these findings suggest that the addition of endothelial-supportive conditions to adherent cells on d7 generates high percentages of committed hESC-ECs. The resultant hESC-ECs, express high levels of EC markers and low levels of hematopoietic and pluripotent markers when assessed using qRT-PCR and flow cytometry. Cells appeared similar to mature ECs, demonstrating a ‘cobblestone-like’ morphology, and were no longer ‘budding’, therefore ceasing generation of HP suspension cells. Furthermore, it was observed that, in contrast to the d7  $CD31^+CD144^+CD235a^-CD43^-CD73^-$  HE cells, d7+3 cells expressed the endothelial marker *CD73*, suggesting they were more committed to an EC fate than the bipotent HE progenitors. Thus, d7+3 conditions were chosen as optimum for the indirect generation of hESC-ECs, and were henceforth used as an endpoint in this differentiation system.

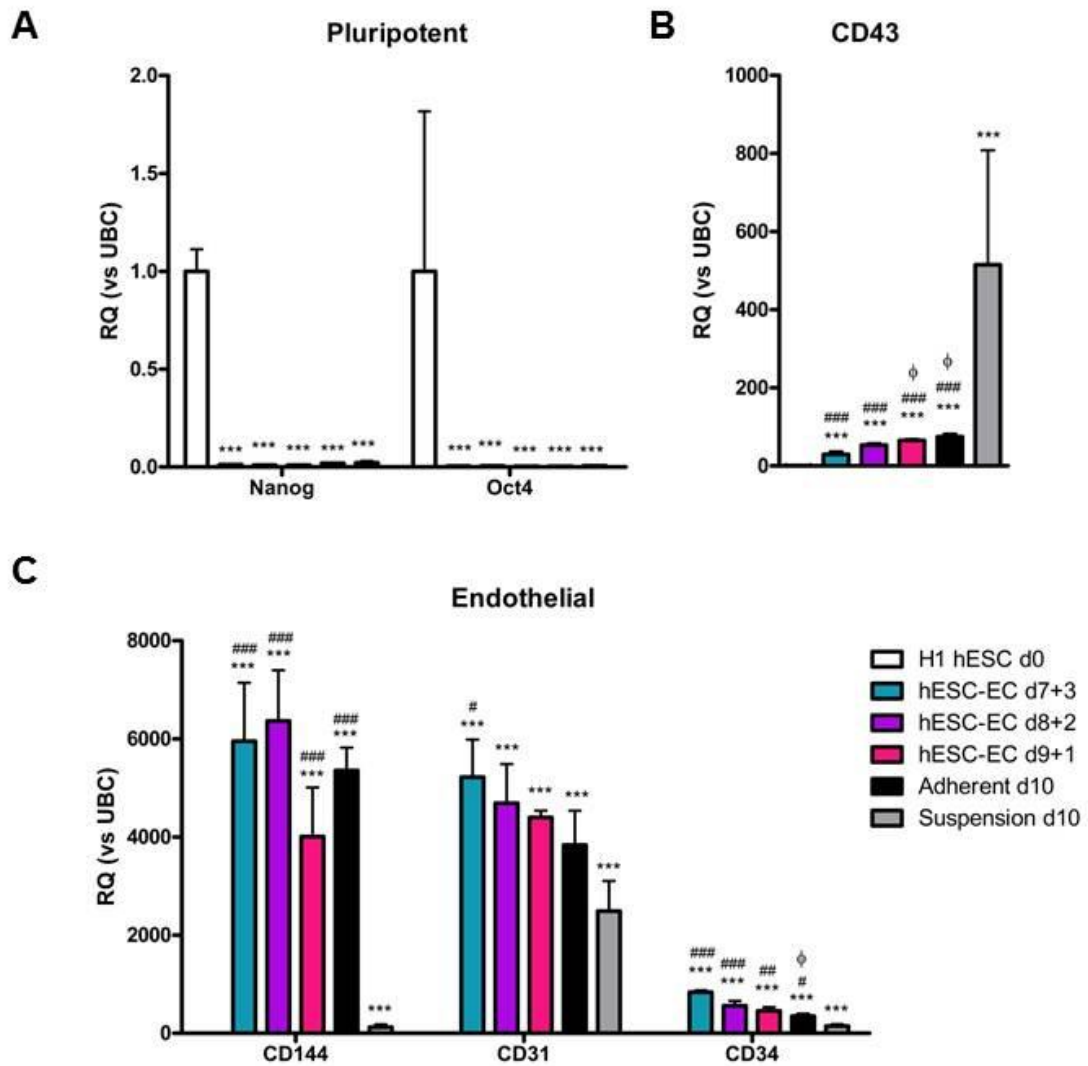


**Figure 4.11 – Gene expression profiling of generated hESC-ECs.**

Pluripotent- (A), hematopoietic- (B) and endothelial- (C) associated gene were analysed in samples from H1 hESCs during direct hESC-EC differentiation, including d0 pluripotent hESCs, d7+3, d8+2 and d9+1 hESC-EC and d10 adherent and suspension samples. Data shown is RQ  $\pm$  RQ max, calculated relative to UBC. Repeated measures ANOVA with Tukey's post hoc comparisons, \*\*\* =  $p < 0.001$ , vs. H1 d0 hESCs, # =  $p < 0.05$ , ## =  $p < 0.01$ , ### =  $p < 0.001$  vs. d10 suspension cells,  $\phi$  =  $p < 0.05$  vs. d7+3 hESC-ECs.  $n=3$ .

After assessing hESC-EC generation, levels of pluripotency associated cell surface markers were also assessed in the newly generated hESC-EC differentiation protocol. This would ensure that there are no pluripotent cells contaminating d7+3 samples. In order to fully assess this, levels of two pluripotency-associated cell surface markers were measured using flow cytometry; Tra1-60 and SSEA3 (Figure 4.12). Approximately 80% of cells were Tra1-60+SSEA3+ in the d0 H1 control (Figure 4.12A-B), indicative of high levels of pluripotency, as would be expected. By d7, however, levels were significantly reduced, with <1% of cells positive for either Tra1-60 or SSEA3, and levels were similar in d7+3 and d10 adherent (cultured in hematopoietic conditions) cell samples. This, together with the presented gene expression data, confirms a loss of pluripotency during differentiation, with no pluripotent cells detected after d7.

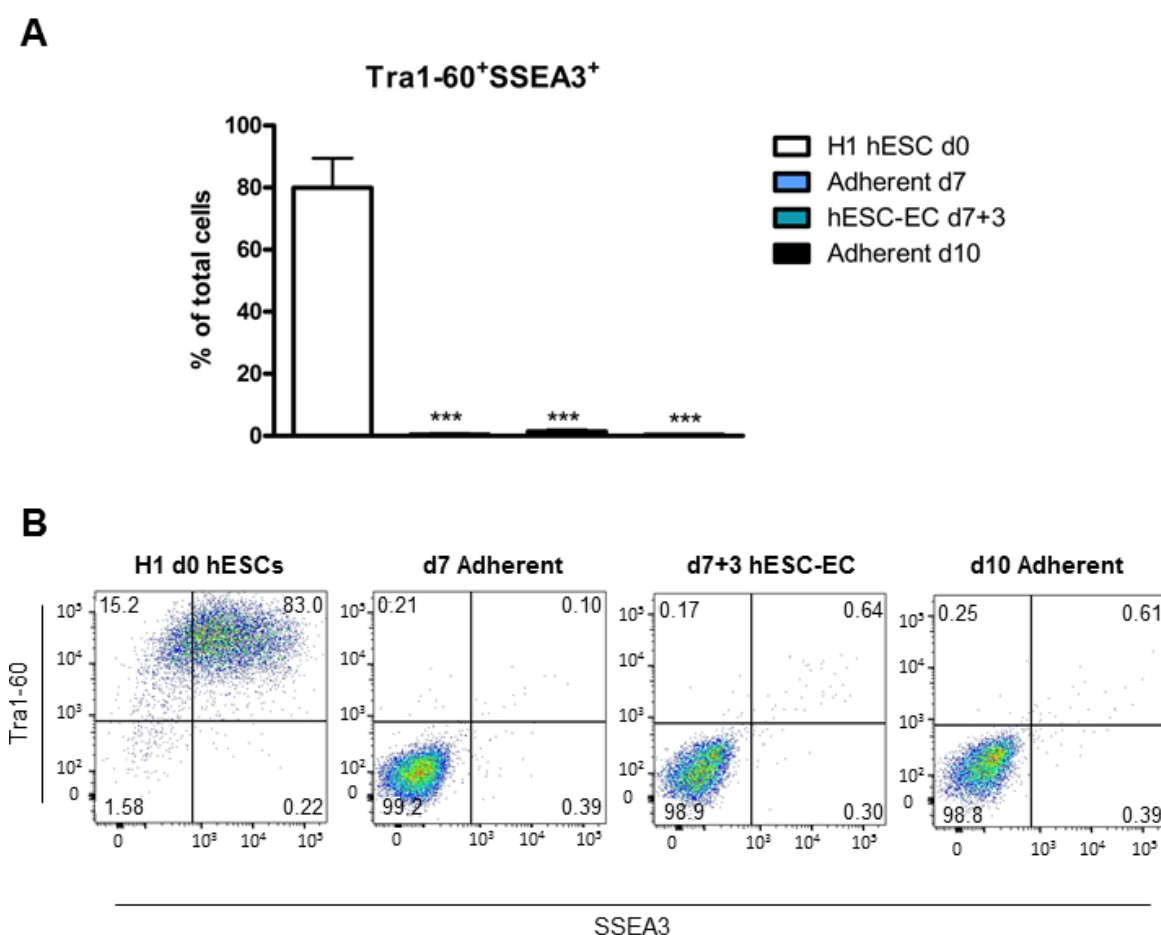


**Figure 4.12 – Analysis of pluripotency associated cell surface markers in H1 indirect hESC-EC differentiation.**

Cells at various time points during indirect hESC-EC differentiation were assed for expression of Tra1-60 and SSEA3, two pluripotency-associated markers, using flow cytometry. Histogram (A) shows average percentages of cells expressing both of these markers at the indicated time points, error bars represent SEM.



Dot plots (B) give representative examples of staining in each sample group.  $n=3$ . Repeated measures ANOVA with Tukey's post hoc comparisons, \*\* =  $p<0.01$  vs H1 d0 hESCs. To ensure reproducibility and robustness of the newly developed indirect hESC-EC differentiation protocol, experiments were repeated using the H9 hESC line (Figure 4.13, Figure 4.14). D7+3 hESC-ECs and d10 suspension and adherent cells (from hematopoietic differentiation) were assessed by flow cytometry for the expression of CD31 and CD144. Similarly to differentiations performed with H1s, there was a significant increase in the proportion of CD31<sup>+</sup>CD144<sup>+</sup> cells in d7+3 samples, with on average 66% of cells expressing both of these EC-associated markers. Lower numbers of cells expressed these markers in the d10 adherent cells, whereas in the suspension sample no cells stained positive for CD144. Morphological analysis of d7+3 cells (Figure 4.13C) showed that cells expanded to form a homogenous monolayer when cultured in these endothelial-supportive conditions.

Moreover, cells were also analysed for the expression of the pluripotency associated markers SSEA3 and Tra1-60 (Figure 4.14). Again, similarly to samples from H1 indirect hESC-EC differentiations, these markers were expressed at high levels in d0 H9 hESCs (72.1%), before being downregulated. In d7+3 and d10 adherent samples, <1% of cells were Tra1-60<sup>+</sup>SSEA3<sup>+</sup>, suggesting that, similarly to differentiations performed with H1 hESCs, there are no pluripotent cells remaining at this time point.

Together, these data suggest that the newly developed indirect hESC-EC differentiation protocol is efficient, generating high levels of CD31<sup>+</sup>CD144<sup>+</sup> cells after 10 days (d7+3) and low levels of Tra1-60<sup>+</sup>SSEA3<sup>+</sup> cells. The protocol is also reproducible and robust, having been tested in multiple hESC cell lines.

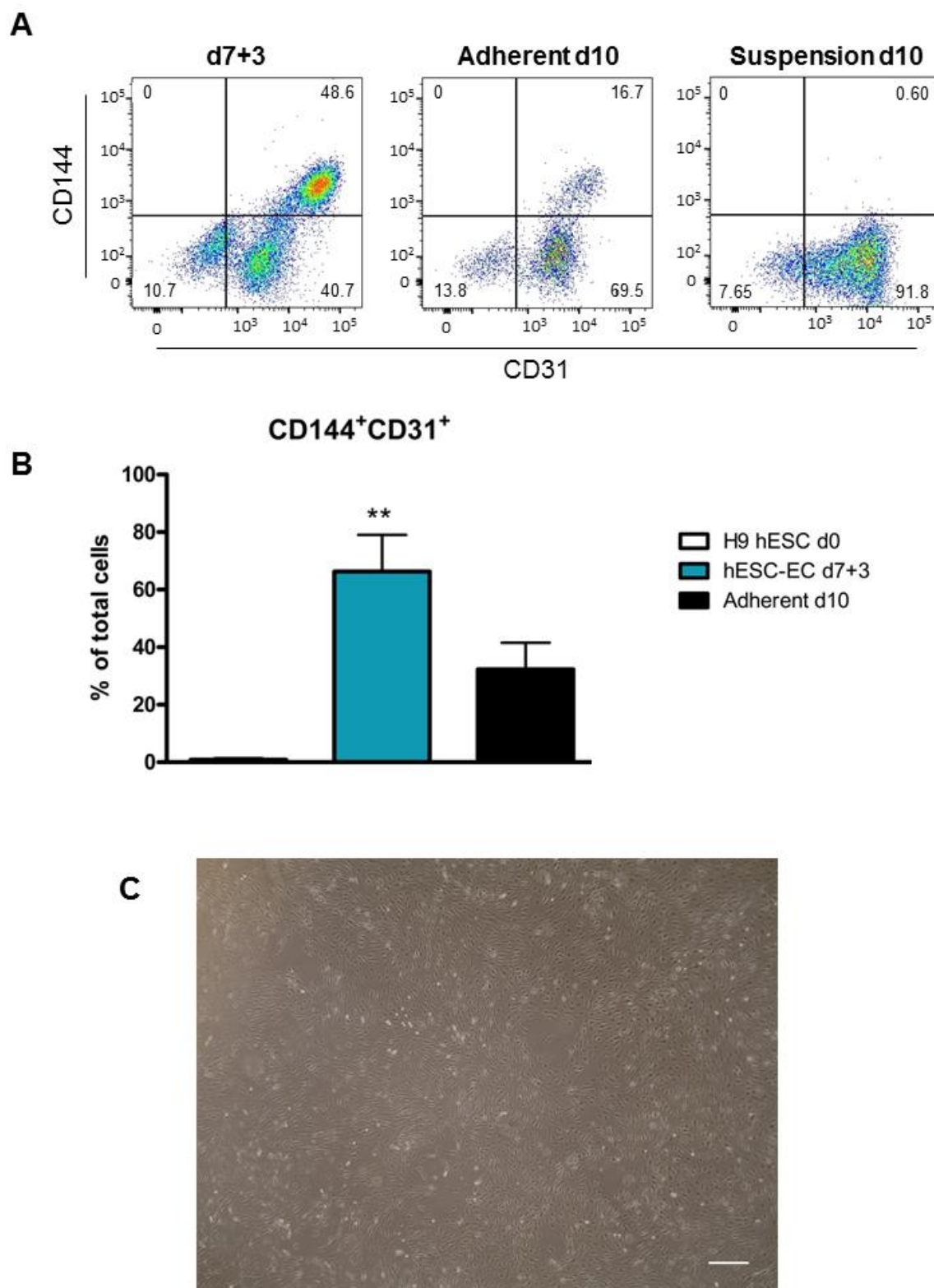


**Figure 4.13 – Indirect hESC-EC differentiation in H9 hESCs.**

After optimisation, indirect hESC-EC differentiation was performed using H9 hESCs. d7+3 hESC-ECs were harvested, stained for CD31 and CD144 and analysed using flow cytometry. Hematopoietic differentiation was also continued from d7 and adherent and suspension cells from d10 were stained for comparison. Average percentages of CD144<sup>+</sup>CD31<sup>+</sup> are presented in the histogram, error bars are SEM (B). Brightfield imaging of d7+3 cells show a similar morphology to H1 d7+3 hESC-ECs (C). Image shown taken at 10x magnification, scale bar represents 100  $\mu$ m. All dot plots shown are representative for sample group. n=3. Statistical comparisons (B), repeated measures ANOVA with Tukey's post hoc comparisons, \*\* = p<0.01 vs H9 d0 hESCs.

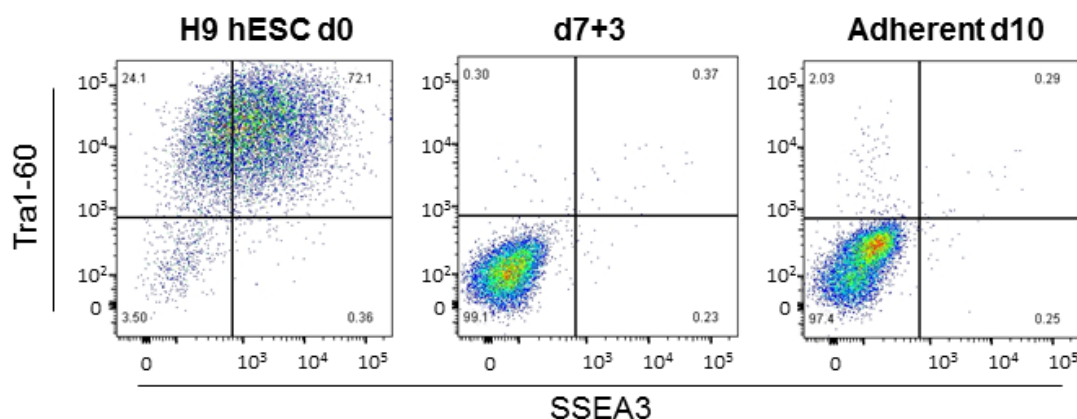


**Figure 4.14 – Assessment of pluripotency markers in H9 indirect hESC-EC differentiation.** d0 hESCs, d7+3 hESC-EC and d10 adherent cells were also stained for pluripotent markers using PE-conjugated anti-Tra1-60 and APC-conjugated anti-SSEA3 (D). All dot plots shown are representative for sample group.

#### 4.3.4 Identification of a $CD326^{low}CD56^{+}$ MP population during indirect hESC-EC differentiation

The first 3 days of the hematopoietic differentiation protocol, and subsequently indirect hESC-EC differentiation, is similar to the first 3 days of direct generation of hESC-ECs. It was believed that mesodermal commitment occurs between d0-3 of hematopoietic differentiation, when cells are cultured as EBs (Figure 4.1A). A transiently existing  $CD326^{low}CD56^{+}$  MP population was previously identified on d3 of direct hESC-EC differentiation, as described in section 3.3.5 (Evseenko et al., 2010). The  $CD326^{low}CD56^{+}$  expression profile is based on cells undergoing EMT during generation of the mesodermal germ layer (Lehembre et al., 2008, Evseenko et al., 2010, Lu et al., 2010). Therefore, experiments were performed to determine whether this population also existed at the equivalent time point within the newly developed indirect hESC-EC differentiation.

Cells were harvested at a variety of time points, including d3 EBs, and the expression of CD326 and CD56 was assessed using flow cytometry (Figure 4.15A-B). As observed previously, H1 pluripotent hESCs highly express CD326 (<96%) but not CD56 (Figure 4.15A). By the d3 EB stage of differentiation, however, a number of cells have begun to lose expression of CD326, and this is coupled with a gain of the CD56 cell surface marker. This resultant population is the previously identified  $CD326^{low}CD56^{+}$  MP population, and represents, on average, approximately 40% of cells at d3 (Figure 4.15B), a significant increase when compared to d0 pluripotent controls.

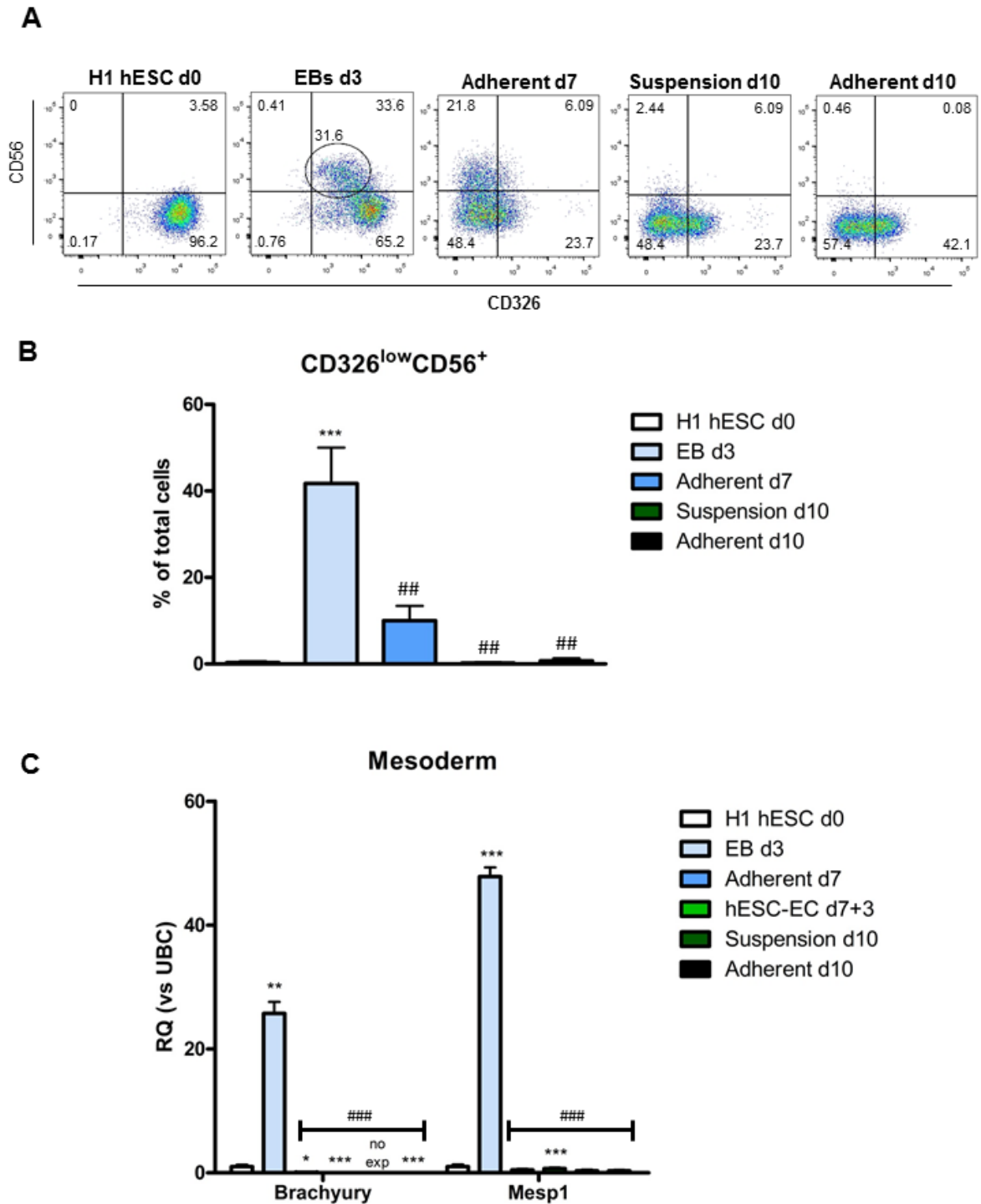


**Figure 4.15 – Identification of CD326<sup>low</sup>CD56<sup>+</sup> MPs during hematopoietic and indirect hESC-EC differentiation.**

Indirect hESC-EC differentiation was probed to assess the existence of the previously identified CD326<sup>low</sup>CD56<sup>+</sup> mesoderm progenitor population. Cells were stained for CD326 and CD56 and analysed using flow cytometry on d0, in adherent d7 cells and in suspension and adherent cells at d10 (A). Average percentage of CD326<sup>low</sup>CD56<sup>+</sup> cells in each sample group is shown in the histogram (B). RNA was collected at the same time points, as well as d7+3 hESC-ECs, and analysed for the expression of mesoderm-associated *Brachyury* and *Mesp1* (C). Data shown is RQ  $\pm$  RQ max, calculated relative to UBC. Repeated measures ANOVA with Tukey's post hoc comparisons, \* =  $p < 0.05$ , \*\* =  $p < 0.01$ , \*\*\* =  $p < 0.001$ , vs. H1 d0 hESCs, ## =  $p < 0.01$ , ### =  $p < 0.001$ , vs. d3 EBs. No exp = undetectable expression when analysed by Taqman qRT-PCR. n=3.

After d3, however, the percentage of CD326<sup>low</sup>CD56<sup>+</sup> cells decreases, and by d10 the majority of cells (<50%) were negative for either of these markers. The presence of the CD326<sup>low</sup>CD56<sup>+</sup> MP population at d3 also coincides with the peak mesoderm-associated gene expression. Levels of *Brachyury* and *Mesp1* were measured using Taqman® qRT-PCR, and were found to be significantly upregulated in d3 EB samples (Figure 4.15C). These genes were then significantly downregulated at later time points, as cells become committed toward HE, EC and HP phenotypes. These data verify the existence of a CD326<sup>low</sup>CD56<sup>+</sup> MP population within the newly developed indirect hESC-EC differentiation. This also supports claims that these cells are multipotent, as they can produce both EC and HCs within this culture system.

## 4.4 Discussion

Previously published work, centred on the formation of a common hematopoietic and endothelial progenitor, has focused on the generation of HSCs and HPs (Choi et al., 2012, Ditadi et al., 2015). This study focuses on the derivation of hESC-ECs from a common HE progenitor population. Data presented here describes the development of an indirect hESC-EC differentiation protocol, efficiently generating large numbers of CD31<sup>+</sup>CD144<sup>+</sup> hESC-ECs by d10. Through the characterisation of a pre-existing CD31<sup>+</sup>CD144<sup>+</sup>CD235a<sup>-</sup>CD43<sup>-</sup>CD73<sup>-</sup> HE population, present during a defined hPSC-hematopoietic differentiation, an efficient protocol for hESC-EC generation was optimised. By d10, including 7 days in hematopoietic-supportive condition followed by 3 days in EC growth medium, production of suspension cells had ceased and cells had expanded to form a confluent homogenous adherent monolayer. These cells expressed the endothelial markers CD144, CD31 and CD73, and were negative for both hematopoietic (CD235a and CD43) and pluripotent-associated (Tra1-60 and SSEA3) markers, when analysed using flow cytometry. This was additionally verified when the gene expression profile of these cells were assessed.

Unlike the previously shown direct hESC-EC differentiation, this indirect protocol does not employ a 96-well spin-based technique for EB formation. Instead, cells are mechanically cut into clumps and transferred to ultra-low attachment 6-well plates, where they spontaneously form EBs and, in contrast to direct hESC-EC differentiation, this does not appear to affect experimental reproducibility in this system. Formation of EBs using the previously described 96-well spin-based method is time consuming and difficult to adapt for scaling up EB production, the 6-well EB-formation method, however, does not have this problem, and is much more scalable. Additionally, using the newly developed indirect hESC-EC differentiation system, high percentages of CD31<sup>+</sup>CD144<sup>+</sup> were generated. On average, these percentages were higher than those generated using the direct hESC-EC differentiation protocol. Previously, generation of hESC-ECs via the formation of HE has been relatively inefficient, although studies have focused on mechanisms and generation of HSCs and HP cells (Choi et al., 2012, Ditadi et al., 2015), with Choi et al. showing only ~6% of cells expressing CD144 by d5. Percentages of CD31<sup>+</sup>CD144<sup>+</sup> hESC-ECs generated by d10 in the present study are comparable to the numbers produced by Patsch and colleagues, who recently

described a direct differentiation protocol, generating both ECs and VSMCs from hPSCs (both iPSCs and ESCs), which generated high percentages (up to 80%) of CD144<sup>+</sup> cells (Patsch et al., 2015), although this high percentage was only obtained after sorting and further culture of generated ECs. In other recently published studies, performed by Orlova et al., only 10-30% of cells were CD31<sup>+</sup>CD34<sup>+</sup> ECs by d10, substantially less than the numbers generated using the indirect hESC-EC differentiation (Orlova et al., 2014a, Orlova et al., 2014c).

The indirect hESC-EC differentiation protocol also has scope for production of large numbers of pure CD31<sup>+</sup>CD144<sup>+</sup> hESC-ECs. Numerous studies, including those presented in Chapter 3, have previously shown that low percentages of hESC-ECs can be isolated from heterogeneous mixes of cells, usually generated at the end of differentiation protocols, replated and cultured. Via isolation, using either MACS or FACS, and further expansion of cells, near pure populations (>95%) of hESC-ECs have been generated (Levenberg et al., 2002, White et al., 2013, Orlova et al., 2014a, Orlova et al., 2014c). In contrast, during indirect hESC-EC differentiation, cells were simply plated out at a density of  $5 \times 10^5$  cells in a T25 culture flask on d3, and by d10 a confluent monolayer, of approximately 80% CD31<sup>+</sup>CD144<sup>+</sup> hESC-ECs, had formed. Additional experiments could be performed to assess whether further culture of these cells increases purity, or whether expansion is possible after depletion of non-CD31<sup>+</sup>CD144<sup>+</sup> hESC-ECs. The protocol could also be optimised to scale up the size of the culture vessel used, resulting in the generation of greater hESC-EC numbers. Specific EC phenotypes of generated cells could also be investigated, as Ditadi and colleagues demonstrated distinct populations of arterial and venous ECs, present in their differentiation, routed through the formation of a common HE precursor (Ditadi et al., 2015). As described previously (Section 3.4), further characterisation of both surface markers and transcription factors, present in the CD31<sup>+</sup>CD144<sup>+</sup> d7+3 hESCs could be performed to determine the exact phenotype of these cells on d10.

Although CD31<sup>+</sup>CD144<sup>+</sup> hESC-ECs, generated using the indirect differentiation protocol, were extensively characterised using flow cytometry and gene expression profiling, no functional studies were performed. To fully validate the EC phenotype of these cells, a number of *in vitro* or *in vivo* functional assays must be performed, as described in detail in Section 3.4. Recently published

studies have suggested that classical EC functional assays are perhaps no longer appropriate, and have therefore used alternatives, such as co-culture with hPSC-derived pericytes, zebrafish xenograft, analysis of trans-endothelial electrical resistance and barrier formation via the measurement of cellular impedance (White et al., 2013, Orlova et al., 2014a, Orlova et al., 2014c). Time constraints, however, prevented thorough functional characterisation of CD31<sup>+</sup>CD144<sup>+</sup> hESC-ECs, generated using the indirect protocol.

This study also demonstrated that the HE profile, previously identified by Choi and colleagues in their undefined, OP9 co-culture-based differentiation, also identifies a population of progenitor cells existing within a more defined hematopoietic differentiation system (Choi et al., 2012). As stated previously, undefined conditions, such as the use of serum and stromal cell co-culture, introduce non-human pathogens, contaminants and unknown factors into differentiation systems. Defined systems, therefore, are not only advantageous in terms of downstream clinical relevance, but also allow for precise control of the extracellular environment, and exact knowledge of factors added to the system. The HE population defined by Ditadi and colleagues had a similar surface marker profile to the one described in this study and by Choi et al., with the addition of CD34<sup>+</sup>, CD184<sup>-</sup> and KDR<sup>+</sup>, and without determining the expression of CD235a (Ditadi et al., 2015).

Both previous publications, describing the formation of HE from hPSCs, have identified multiple other progenitor populations existing within their specific differentiation systems. Choi et al., identified seven specialised populations, each of which possessed defining characteristics, such as CD144<sup>+</sup>CD73<sup>+</sup>CD235a/CD43<sup>-</sup>CD117<sup>high</sup> non-HEP cells, which possess a mainly EC phenotype, and CD144<sup>+</sup>CD73<sup>-</sup>CD43<sup>low</sup>CD235a<sup>+</sup>CD41a<sup>-</sup>CD117<sup>-</sup> angiogenic hematopoietic progenitors, primarily a HP cell possessing hematopoietic function, but capable of generating ECs (Choi et al., 2012). Experiments could be performed to further elucidate the exact profile and phenotype of other cell populations, existing as adherent cells on d7 of hematopoietic and indirect hESC-EC differentiation. This may include characterisation by flow cytometry, isolation and further culture, gene expression profiling and performance of functional assays to test for hematopoietic and EC function, such as analysis of the colony forming potential of cells and AcLDL uptake.



Further work could also be performed to demonstrate the direct production of suspension cells from the hypothesised bipotent HE progenitor population. Previous work used live cell imaging and time lapse photography to visualise the formation of CD43<sup>+</sup> and CD45<sup>+</sup> hematopoietic suspension cells from CD144<sup>+</sup> adherent HE cells (Choi et al., 2012, Ditadi et al., 2015), and this technique could be utilised to also demonstrate this in the presented differentiation system.

The expression of Runx1, a transcription factor indispensable for the emergence of HSCs, could also be investigated in the cell population from this differentiation system. Although Ditadi et al. found that Runx1 was not expressed in HE cells, and that expression only occurs post-EHT (Ditadi et al., 2015), other studies have shown its expression in HE and during EHT (Chen et al., 2009a, Ng et al., 2010a). Additionally, in a murine model of HE development, it was demonstrated that an enhancer, located intronically in Runx1, also marks HE and HSCs, suggesting an important role for this axis in HE and HSC differentiation (Ng et al., 2010a). Colleagues in Edinburgh are currently working on Runx1 reporter lines, which could possibly be used to observe the expression of this gene in HE and HSCs in this system. Specifically, these cells, alongside live cell imaging techniques, could be utilised to monitor the emergence of Runx1 positive cells from HE progenitors.

One major difference between the progenitor defined in this study and the one identified by Choi and colleagues, is the presence of CD117, also known as c-kit, a receptor tyrosine kinase which binds and recognises the ligand SCF (Lennartsson et al., 2012), a cytokine added in the hematopoietic and indirect hESC-EC differentiation protocols. CD117 and its ligand have long been known to play important roles in hematopoiesis. CD117 is found expressed on the surface of HSCs and HPs and is responsible for the inhibition of apoptosis in human erythroid progenitor cells through activation of phosphoinositide 3-kinase (PI3K) (Ogawa et al., 1991, Broudy, 1997, Sui et al., 2000). Another study, documenting properties and differences of four hESC lines, additionally demonstrated that CD117 is expressed at varying levels in H1 hESCs maintained in a feeder-free culture system (Carpenter et al., 2004). During this study, however, expression of CD117 was not detected on any of the cells profiled, including suspension, adherent and d0 pluripotent hESCs (Figure 4.4). Both previously published

methods for the derivation of HE from hPSCs, describe HE cells as expressing low or 'intermediate' levels of the CD117 surface marker, with Choi and colleagues suggesting its expression can be used to distinguish between HE and non-HE progenitors (Choi et al., 2012, Kennedy et al., 2012, Ditadi et al., 2015). Although multiple CD117 antibodies were tested, this may suggest an antibody problem in the presented research and a positive control sample should have been used in order to ensure this was working correctly. Alternatively, the lack of CD117 expression may be due to internalisation of the receptor on SCF binding. Historical studies have demonstrated that upon SCF binding, CD117 is activated, internalised and then degraded via the ubiquitin/endosomal pathway, with reappearance on the cell surface requiring protein synthesis (Broudy et al., 1998, Jahn et al., 2002). High concentrations of SCF are added from d3 of hematopoietic and, subsequently, indirect hESC-EC differentiation. Therefore, to further investigate and validate the expression of CD117 within the HE and HP populations, techniques other than flow cytometry, which relies on the staining of cell surface antigens, must be used. Immunocytochemistry would allow for visualisation of internalised receptors in these cell populations. As a result, definitive conclusions involving the expression of CD117 in populations, occurring throughout the described hematopoietic and indirect hESC-EC differentiations, cannot be made.

Here, the presence of the previously characterised CD326<sup>low</sup>CD56<sup>+</sup> MP population, during indirect hESC-EC and hematopoietic differentiation, was also confirmed. This further strengthened the argument that these cells are an early progenitor cell population, occurring just as cells commit to the mesodermal germ layer (Evseenko et al., 2010) or slightly later, when cells have already started to move toward an EC or HE cell fate (Chapter 3). Although the presence of this progenitor was shown in two differentiation systems, both involve the generation of hESC-ECs, and closely related hematopoietic cells. Therefore, it would be beneficial to investigate the presence of these progenitors in other mesodermal differentiation systems, such as during the generation of cardiomyocytes from hPSCs, these cells could also be isolated and their ability to generate cells of different lineages assessed (discussed in more detail in section 3.4). Furthermore, on average the percentages of CD326<sup>low</sup>CD56<sup>+</sup> cells, present on d3 of indirect hESC-EC differentiation, are higher than those observed in the

direct system, making it easier to study these cells, and mechanisms involved in their formation, within this differentiation system.

Optimisation and characterisation of this protocol, along with the identification of the CD326<sup>low</sup>CD56<sup>+</sup> MP, will allow for analysis and elucidation of possible mechanisms, including signalling molecules and non-coding RNAs, with roles in endothelial lineage commitment. Mechanisms identified from in depth analysis of the direct hESC-EC differentiation protocol can be validated in this, distinct, differentiation system. This will allow for distinguishing of mechanisms involved in specific endothelial lineage commitment, mesodermal commitment or those involved generally in loss of pluripotency and differentiation.

## **Chapter 5 miRNA profiling and modulation during hESC-EC differentiation**

## 5.1 Introduction

The discovery of numerous classes of non-coding RNAs has challenged the traditional central dogmas of molecular biology, introducing new levels of cell-type specific gene regulation. As previously stated, a variety of these non-coding RNAs, including miRNAs and lncRNAs, have been implicated in the differentiation and commitment of pluripotent cells to a variety of lineages, as well as in regulation and maintenance of pluripotency. Specifically, a number of publications have identified miRNAs and lncRNAs playing important roles in differentiation and commitment to the endothelial lineage (Hassel et al., 2012, Kane et al., 2012, Klattenhoff et al., 2013, Kurian et al., 2015).

Currently there are 1881 human miRNA stem loop sequences recorded on miRBase, an online database of published miRNA sequences and annotation (Kozomara et al., 2014), with each of these stem loops giving rise to two individual mature miRNAs, the -5p and -3p strands. Although highly sensitive for quantitative profiling of individual mRNA and miRNAs, qRT-PCR methods are low-throughput, and so cannot be used to investigate genome-wide miRNA profiles. Therefore, in order to gain unbiased and global analysis of miRNA expression, studies have employed the use of large scale microarray screens (Liu et al., 2004, Thomson et al., 2004, Liu et al., 2008). This technology involves the use of 40-60-mer oligonucleotide probes, synthesised to target specific mature miRNA sequences. Briefly, miRNAs, contained within the RNA sample, are labelled with fluorescent tag. These miRNAs are then allowed to hybridise to the aforementioned oligonucleotide probes, which are bound to an array surface. Arrays are washed to remove unbound RNA, and fluorescence is then read using specialised microarray scanners. Frequently, the array surface is known as a 'chip' or 'slide', and each one can run multiple samples simultaneously, therefore, allowing for high-throughput screening of large numbers of samples. To date, vast numbers of studies using this technology have been published, with applications ranging from analysing specific miRNA expression signatures in a range of tissue types (Liu et al., 2004), to monitoring changes which occur during the onset and development of various disease states, including cardiovascular disease and cancer (Lu et al., 2005, Chen et al., 2008a, Fichtlscherer et al., 2010).

Indeed, numerous studies have also utilised microarray technology to identify miRNAs with potential roles in the commitment and differentiation of hPSCs to ECs (Yoo et al., 2011b, Kane et al., 2012, Luo et al., 2013, Yoo et al., 2013). Initially, this method of genome-wide profiling was used to demonstrate possible roles for miR-181a, -181b and -99b in a fully-defined monolayer hESC-EC differentiation system (Kane et al., 2012). In this study, Kane and colleagues demonstrated that the expression levels of these three miRNAs were increased in a differentiation-dependent manner. Additionally, it was also shown that lentiviral-mediated overexpression of miR-181a, -181b, -99b or all three miRNAs in combination, increased the efficiency of hESC-EC differentiation. Despite this, however, the authors did not describe any mRNA targets, or mechanisms of action for these miRNAs. Therefore, there is no conclusive evidence to suggest that upregulation of miR-181a, -181b and -99b is due to specific roles for these miRNAs in hESC-EC differentiation, and not just as a consequence of the development of an EC phenotype.

More recently, microarray technology was used to identify two other mature miRNAs with possible roles in commitment of hPSCs to the endothelial lineage; miR-150 and miR-200c (Luo et al., 2013). In this study, samples were taken at days 0, 3, 6 and 9 during hESC-EC differentiation, and subjected to analysis by microarray, whereby it was discovered that miR-150 and -200c were significantly upregulated during hESC-EC differentiation. Modulation of these miRNAs showed that inhibition and overexpression causing significant decreases and increases in EC-associated genes, respectively. Further investigation allowed Luo to demonstrate that these miRNAs exerted their effects through their common target, ZEB1. In addition to identification of novel miRNAs, Luo et al. also used the microarray screen to demonstrate hESC-EC differentiation-dependent increases in previously published angiogenic and endothelial-associated miRNAs, as well as significant decreases in the pluripotency-associated miR-302 family.

These studies demonstrate how miRNA technology can be used effectively to identify potential miRNAs of interest, via the profiling of samples taken from different time points. However, both of the aforementioned studies have focused on miRNA which may drive the production of ECs from hPSCs, and neither focused on early mesodermal differentiation. As published data suggest an integral role for miRNAs during development, it was hypothesised that

miRNAs are heavily involved in the specification of pluripotent cells to specific germ layers. Using the previously defined CD326<sup>low</sup>CD56<sup>+</sup> MP population, appearing on d3 of hESC-EC differentiation, the presented study aimed to identify and characterise miRNAs involved in early mesodermal and endothelial commitment.

## 5.2 Aims

The aims of this chapter were as follows:

- To profile miRNAs differentially regulated during direct hESC-EC differentiation.
- Validation of chosen miRNAs in both direct and indirect hESC-EC differentiation.
- Create and optimise lentiviral vectors for the overexpression of miRNAs.
- To modulate the expression of these miRNA using lentiviral vectors, during hESC-EC differentiation and in pluripotent cells.

## 5.3 miRNA microarray screen

Microarray analysis was performed in conjunction with Sitemic Ltd. (West of Scotland Science Park, Glasgow, UK), using the Agilent SurePrint Human miRNA Microarray platform. SurePrint G3 Human v16 miRNA 8x60K microarray slides were used, with each slide containing 8 individual arrays. These slides contain 60-mer Agilent SurePrint synthesised probes for 1,199 human miRNAs, with sequence data sourced from the miRBase public database (Kozomara et al., 2014). Samples were prepared and analysed on the array as described in section 2.5.4.

### 5.3.1 Normalisation and Data Analysis

Data collected from the array was then normalised using the *AgiMicroRNA* method (Lopez-Romero, 2011). Analysis was performed using R statistical analysis software (<https://www.R-project.org>) and Sitemic Ltd. proprietary algorithms.

Statistical significance was calculated using paired Student's t-tests to compare specific groups. miRNAs were considered to be significantly changed if the calculated fold change was greater than or equal to 1.5, with a False Discovery Rate (FDR) of less than 0.05.

### 5.3.2 Experimental Design

In order to profile miRNAs differentially regulated during hESC-EC differentiation total RNA was taken from cells harvested at d0 H9 hESCs, d3 FACSorted CD326<sup>low</sup>CD56<sup>+</sup> MPs, d3 non-CD326<sup>low</sup>CD56<sup>+</sup> NCF cells and d7 samples containing hESC-ECs (Figure 5.1). The experiment was designed to document significant changes in miRNAs occurring at these specific time points during hESC-EC differentiation, in order to identify miRNAs with roles in commitment of cells to mesodermal (d3) and endothelial (d7) lineages. RNA from these 4 sample groups were collected from 4 separate hESC-EC differentiation experiments, with differentiations performed on cells from consecutive passages of H9 hESCs. All 4 of these experimental replicates were then analysed. To collect d3 samples, cells were FACSorted to collect two different fractions; CD326<sup>low</sup>CD56<sup>+</sup> MPs and the non-CD326<sup>low</sup>CD56<sup>+</sup> NCF. 8 plates of EBs (approximately 768 individual EBs)



were pooled to ensure sufficient material for high quality RNA preparation, with samples containing less than  $1 \times 10^6$  cells after FACS sorting not used in the screen. Additionally, d3 heterogeneous samples, taken before FACS sorting, were taken from the same experiment, although this was not run on the array and only used during Taqman® qRT-PCR of identified miRNAs.

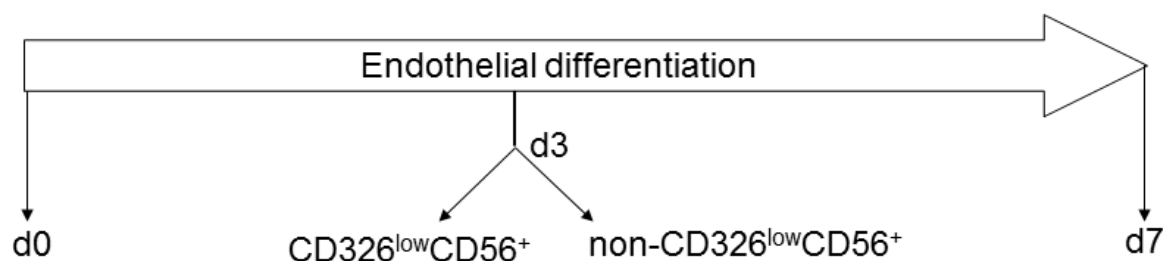


**Figure 5.1 – miRNA microarray experimental design.**

An  $n=4$  samples were collected from 4 different H9 hESC-EC differentiation experiments. Total RNA was collected from pluripotent d0 H9 hESCs, d3 CD326<sup>low</sup>CD56<sup>+</sup> MPs, d3 non-CD326<sup>low</sup>CD56<sup>+</sup> NCF and d7 cells.

Briefly, comparisons of data were made between all groups (d3 MPs, d3 NCFs and d7) and d0 H9 hESCs, in order to identify miRNAs significantly changed throughout the course of hESC-EC differentiation. miRNAs identified to be significantly up- or downregulated during differentiation may play important roles in the regulation of proteins and factors involved in the commitment of cells to an EC phenotype. Moreover, using these comparisons expression of previously published and characterised miRNAs, such as the pluripotency-associated miR-302 family and endothelial-associated miR-126 and miR-10a, may be investigated and validated within the presented direct hESC-EC differentiation system.

Additionally, comparisons were made between the two d3 sample groups, profiling changes in miRNA expression between the CD326<sup>low</sup>CD56<sup>+</sup> MPs, a population committed to the mesoderm and possibly endothelial lineages, and the NCF samples, suggested to contain a number of other populations, including mesendodermal and endodermal progenitors. It was hypothesised that miRNAs with large differences in expression levels between these two groups may play specific roles in mesodermal and endothelial lineage commitment.

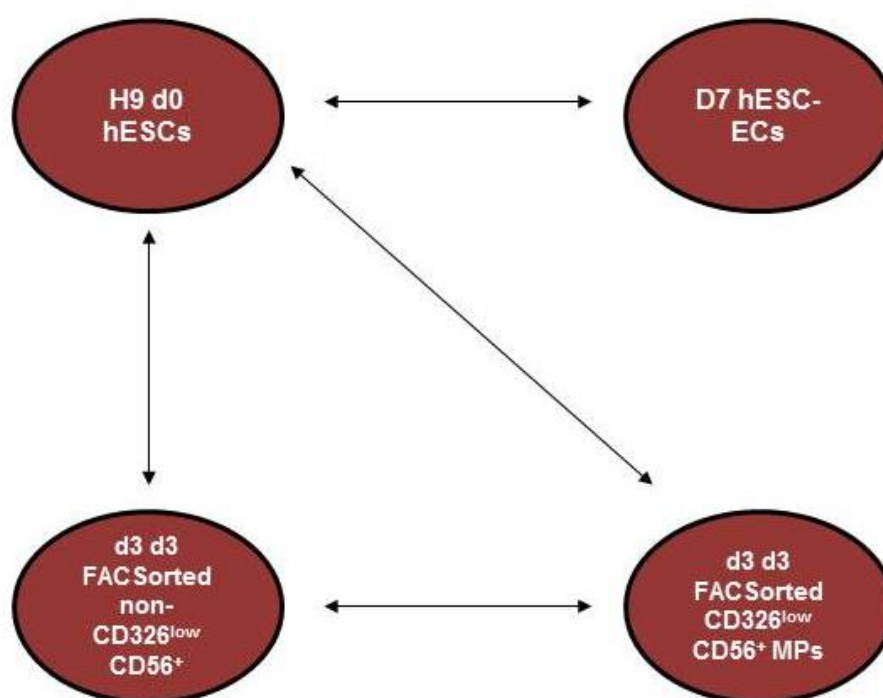


**Figure 5.2 – Schematic of comparisons performed**

Comparisons between groups are represented by arrows in the above schematic.

### 5.3.3 Quality control

#### 5.3.3.1 RNA Quality control

For the collection of high quality results from the microarray screen, RNA quality was tested to ensure it was of sufficiently high quality. As stated previously, only samples with an RNA integrity number or RIN >7 were used for further analysis. RIN values range between 1 and 10, with a RIN of 10 signifying high quality RNA. This was assessed by running samples on the Agilent 2200 TapeStation as described in section 2.5.4. Agilent analysis also produced electrophoresis plots or a ‘virtual gel’ (Figure 5.3, Table 5.1) and electropherograms (Figure 5.4) for each sample. Electropherograms for each sample show distinct peaks representing 18S and 28S ribosomal RNA (rRNA), indicative of high quality RNA, these two bands are also visible in Figure 5.3. All RNA samples used in this study achieved a RIN value of >9, with 6 samples obtaining RINs of 10 (Figure 5.3, Table 5.1).

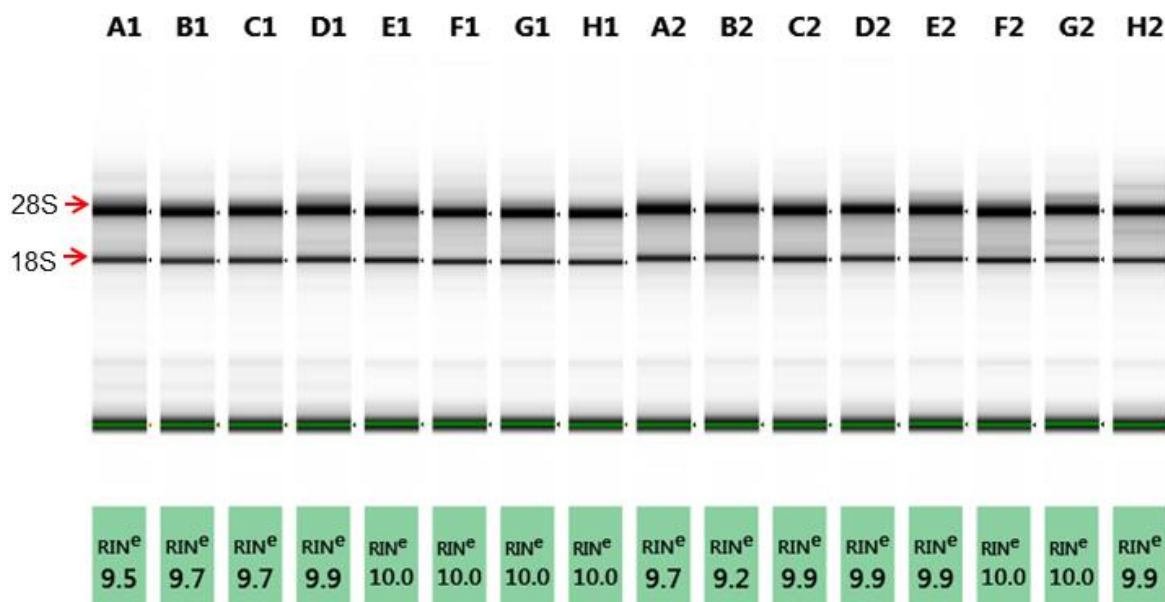


**Figure 5.3 – Agilent TapeStation analysis of RNA quality.**

Electrophoresis plots for all 16 samples with corresponding RIN values shown below. Arrows indicate 18S and 28S rRNA bands. Sample labels are shown across the top, with corresponding sample names shown in Table 5.1.

Sample Name	Gel Label
d0 n=1	A1
d0 n=2	B1
d0 n=3	C1
d0 n=4	D1
d3 CD326 <sup>low</sup> CD56 <sup>+</sup> MP n=1	E1
d3 CD326 <sup>low</sup> CD56 <sup>+</sup> MP n=2	F1
d3 CD326 <sup>low</sup> CD56 <sup>+</sup> MP n=3	G1
d3 CD326 <sup>low</sup> CD56 <sup>+</sup> MP n=4	H1
d3 non-CD326 <sup>low</sup> CD56 <sup>+</sup> NCF n=1	A2
d3 non-CD326 <sup>low</sup> CD56 <sup>+</sup> NCF n=2	B2
d3 non-CD326 <sup>low</sup> CD56 <sup>+</sup> NCF n=3	C2
d3 non-CD326 <sup>low</sup> CD56 <sup>+</sup> NCF n=4	D2
d7 n=1	E2
d7 n=2	F2
d7 n=3	G2
d7 n=4	H2

**Table 5.1 – Array samples and corresponding TapeStation gel labels.**  
Labels correspond to those shown in Figure 5.3.

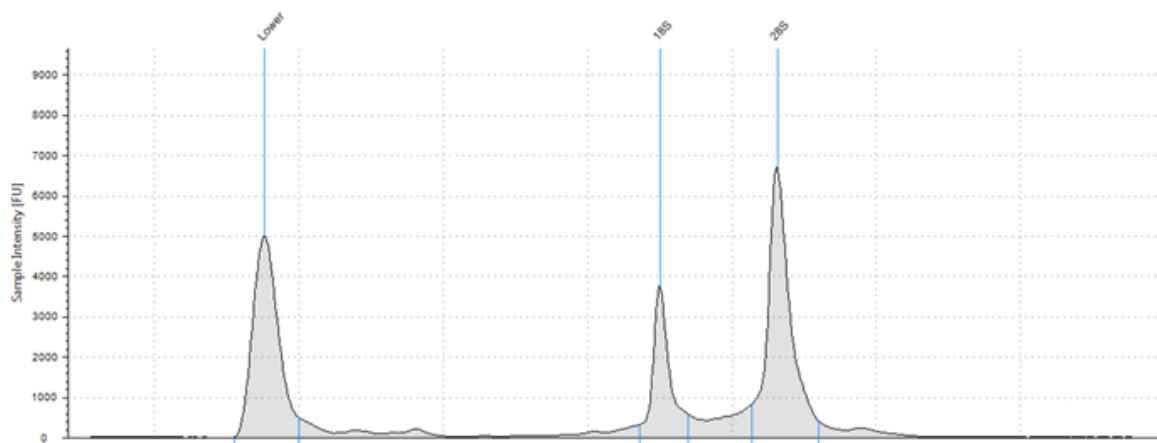


**Figure 5.4 – Typical TapeStation electropherogram.**

A representative electropherogram generated by samples when analysed using the Agilent 2200 TapeStation system. Blue lines indicate (from left to right) the lower marker and the 18S and 28S rRNAs, used for RIN value calculation. Trace shown is for d0 2 sample (B1 in Figure 5.3).

### 5.3.4 Differentiation Quality Control

hESC-EC differentiation samples to be run on the array were also subjected to analysis by flow cytometry to ensure successful differentiations. D0 H9 hESCs, d3 heterogeneous EBs and d7 cells were harvested and stained to look at percentages MP ( $CD326^{\text{low}}CD56^+$ ) endothelial ( $CD31^+CD144^+$ ), and pluripotent ( $Tra1-60^+SSEA3^+$ ) cells at each of these time points (Figure 5.5).

Levels of  $CD326^{\text{low}}CD56^+$  MP cells were found to be low in d0 pluripotent cells, before increasing significantly to approximately 60% in the d3 heterogeneous EB samples (Figure 5.5A). Additionally, by d7 the percentage of cells with this surface marker profile had decreased to <20%. This demonstrates a peak in MP cell numbers at d3 of hESC-EC differentiation, hypothesised to be the point at which cells have committed to mesoderm, in line with previous data (Chapter 3).

To measure differentiation efficiencies, the levels of  $CD31^+CD144^+$  hESC-ECs and  $Tra1-60^+SSEA3^+$  pluripotent cells were measured at these same time points. As demonstrated previously, a significant increase  $CD31^+CD144^+$  expressing cells, coupled with a significant decrease in the numbers of cells expressing  $Tra1-60$  and  $SSEA3$ , was observed throughout direct hESC-EC differentiation (Figure 5.5B-C). The lowest levels of  $Tra1-60^+SSEA3^+$  cells were observed in d7 samples, where on average <5% of cells stained for these two markers, similar to previous

results (Chapter 3). D7 samples also contained the highest percentages of CD31<sup>+</sup>CD144<sup>+</sup> hESC-ECs (Figure 5.5B). The percentages of CD31<sup>+</sup>CD144<sup>+</sup> hESC-ECs obtained during these 4 differentiations (approximately 15%) was lower than had been previously observed (Chapter 3) and ideally differentiations would have been repeated to obtain samples with a higher CD31<sup>+</sup>CD144<sup>+</sup> hESC-EC content. Due to time and financial constraints, specifically involved in the FACSorting of d3 cells, however, miRNA microarray analysis proceeded using these samples.

Taken together, this data demonstrates that hESC-EC differentiations, from which samples were collected for miRNA microarray analysis, were successful. Changes in cell surface marker expression were similar to those seen during characterisation of the protocol (Chapter 3). Corresponding RNA samples were subsequently processed for use during the microarray screen as described in section 2.5.1.

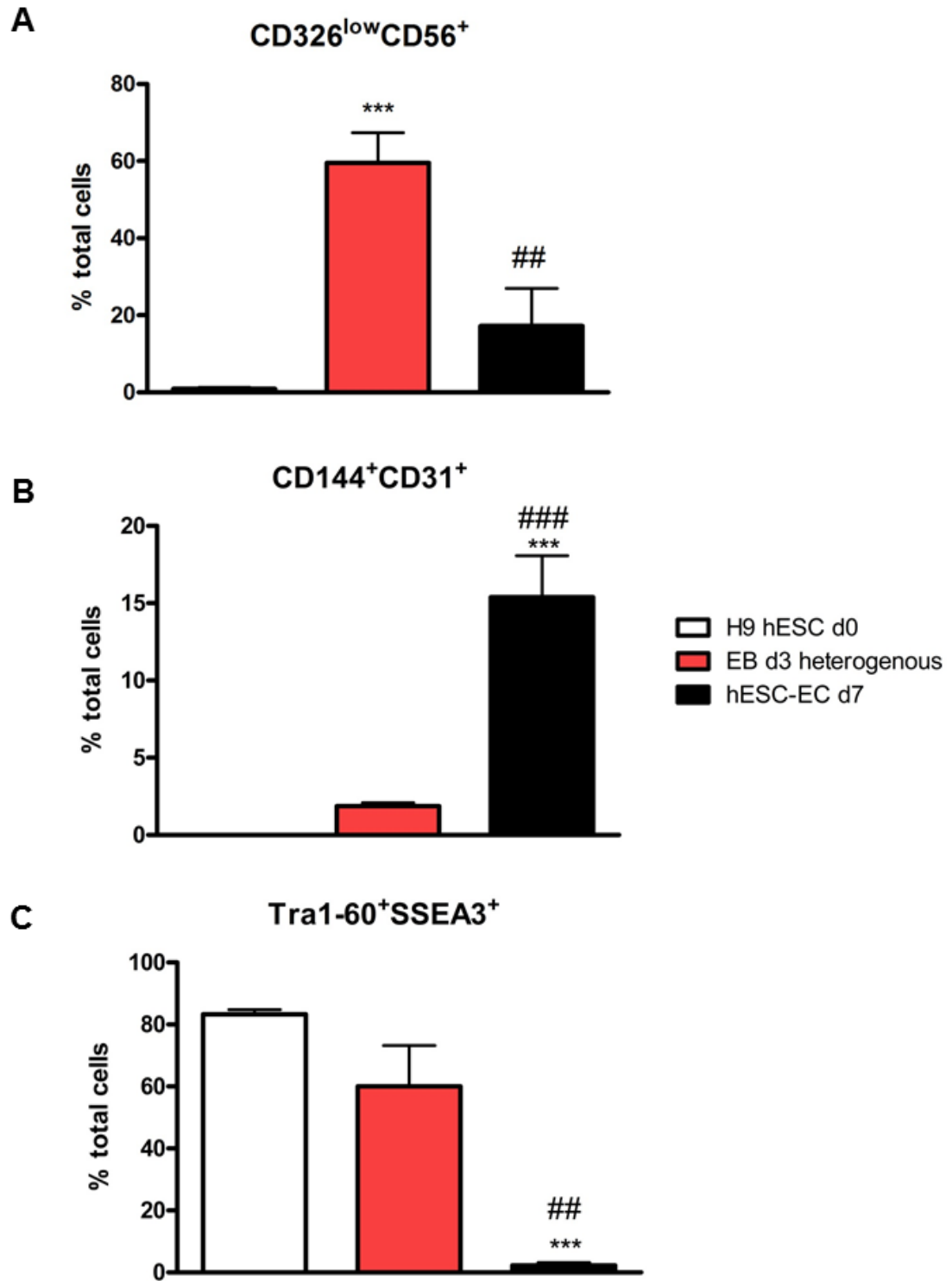


**Figure 5.5 – Flow cytometric analysis of hESC-EC differentiation samples used in microarray screen.**

D0 pluripotent H9 hESCs, heterogeneous d3 (taken before FACSsorting) and d7 cells were also harvested and subject to analysis by flow cytometry to examine Tra1-60<sup>+</sup>SSEA3<sup>+</sup>, CD326<sup>low</sup>CD56<sup>+</sup> and CD31<sup>+</sup>CD144<sup>+</sup> populations. N=4 experiments. Statistical significance was calculated using a repeated measures ANOVA, with Tukey's post hoc comparisons. \*\*\* = p<0.001 vs d0 H9 hESCs, and ## = p<0.01, ### = p<0.001 when compared to d3 heterogeneous samples.

### 5.3.4.1 FACSsorting

Fluorescence activated cell sorting (FACS) was performed using samples collected on d3 of direct hESC-EC differentiation. CD326<sup>low</sup>CD56<sup>+</sup> MPs were isolated from heterogeneous samples and the remaining cells, hereby known as NCF, were also collected. After sorting, small samples of collected cells were run back through the machine, ensuring purification of cells was successful (Figure 5.6). The purity of cells after sorting was high, with >95% CD326<sup>low</sup>CD56<sup>+</sup> in sorted samples, compared to approximately 65% in d3 heterogeneous samples (Figure 5.6 left and centre panels). Additionally, <1% of cells in the NCF samples were CD326<sup>low</sup>CD56<sup>+</sup>, with the majority of cells in this fraction having retained the CD326<sup>high</sup>CD56<sup>-</sup> profile, previously demonstrated to be associated with hESCs (Evseenko et al., 2010). Dot plots obtained from samples are shown in Figure 5.6.

Once obtained samples were lysed using QIAzol lysis reagent and processed for analysis as described in sections 2.5.1 and 5.3.3.1.

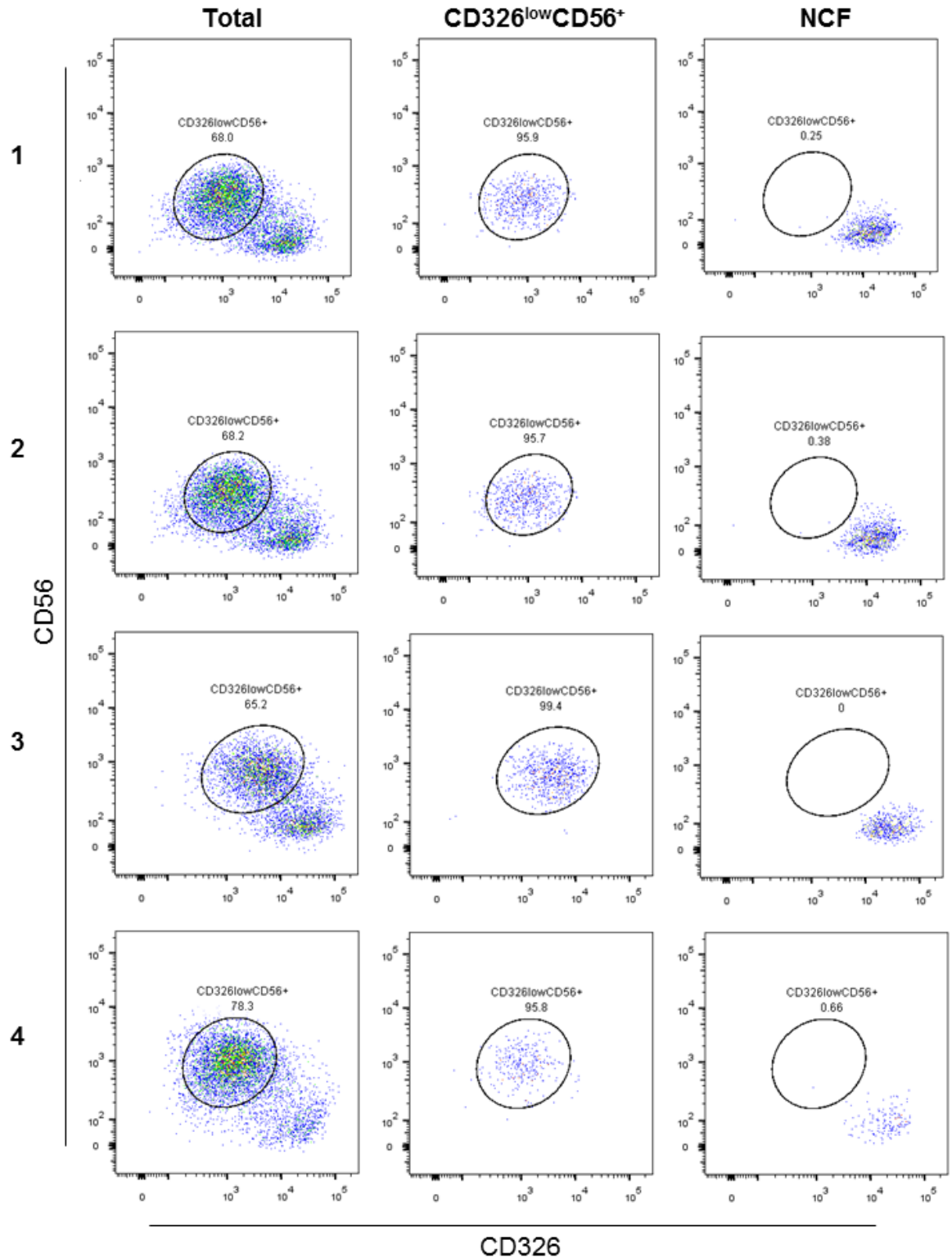


**Figure 5.6 – FACS sorting of d3 CD326<sup>low</sup>CD56<sup>+</sup> MP cells for miRNA microarray.**

Dot plots showing staining of CD326 and CD56 in d3 samples before and after FACS sorting. Left panel shows staining in heterogeneous samples, centre panel shows staining in cells collected in the CD326<sup>low</sup>CD56<sup>+</sup> fraction during FACS, and the far right panel shows staining in the NCF after FACS. Circular gate labelled 'CD326<sup>low</sup>CD56<sup>+</sup>' indicates CD326<sup>low</sup>CD56<sup>+</sup> MP population in that specific sample group, with the associated number showing percentage of total cells located within the gate. Numbers on left hand side indicate experimental n number.



## 5.4 Results

### 5.4.1 miRNA profiling – array

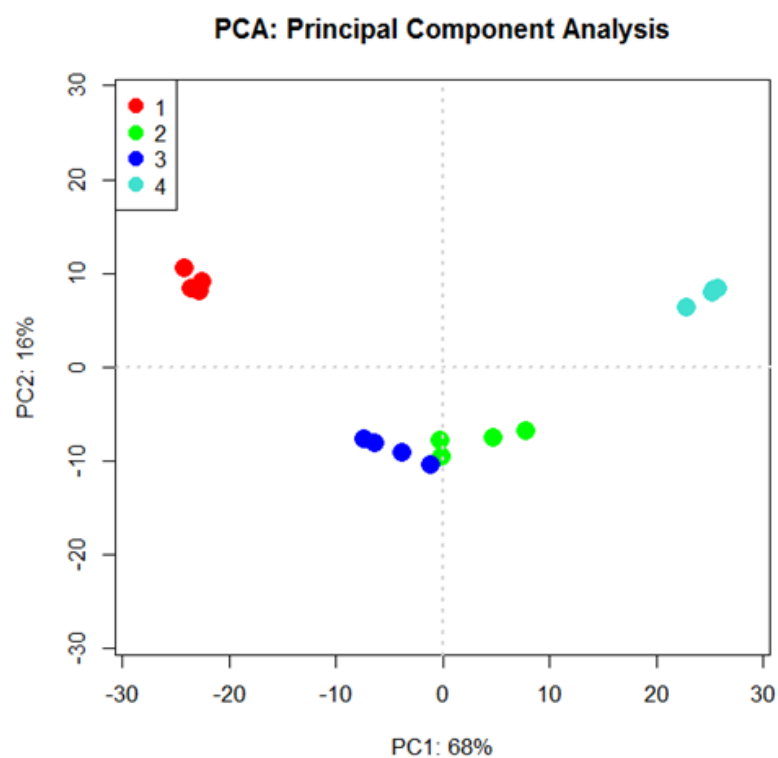
#### 5.4.1.1 Principle component analysis

Principle component analysis (PCA) is a mathematical model which performs linear transformations on variables within a data set to produce variables known as principle components (PC). Performing this analysis allows for identification of patterns within a data set, highlighting global similarities and differences between specific samples and sample groups. This, in turn, allows for the plotting of multidimensional PCA maps, an analytical tool used for visualisation of these identified similarities and differences. PCA maps for data sets are shown in Figure 5.7.

Here, it was demonstrated that the 4 samples from each of the 4 individual groups (d0 H9 hESCs, d3 CD326<sup>low</sup>CD56<sup>+</sup> MPs, d3 NCFs and d7 hESC-ECs) cluster together and separately from the other groups (Figure 5.7A), suggesting differences in overall miRNA expression profiles between all groups. The pluripotent d0 H9 hESCs cluster very tightly together, on the left hand side of the map, away from the other 3 groups (Figure 5.7A, red dots). This further validates previous suggestions, made during differentiation characterisation (Chapter 3), that cells rapidly lose their pluripotent phenotype during hESC-EC differentiation. D7 samples, containing the CD31<sup>+</sup>CD144<sup>+</sup> hESC-ECs, also clustered quite tightly together, away from all other samples (Figure 5.7A, light blue data points). Again, this suggested that these cells have a distinct miRNA profile, with large differences when compared to the other sample groups. In particular, these cells have lost all pluripotency and committed specifically to the endothelial lineage, apparent on the PCA map due to the clustering of the d7 samples furthest away from the d0 pluripotent cells.

Both d3 samples (CD326<sup>low</sup>CD56<sup>+</sup> MPs and NCF), however, clustered relatively close together when viewed on the PCA map, although individual samples from the groups clustered together (Figure 5.7A, royal blue and green data points). This indicated that, while distinct from d0 and d7 samples, these samples may share a number of similarities in their miRNA expression profile. An additional PCA was also performed just using the two d3 CD326<sup>low</sup>CD56<sup>+</sup> MP and NCF

A



B

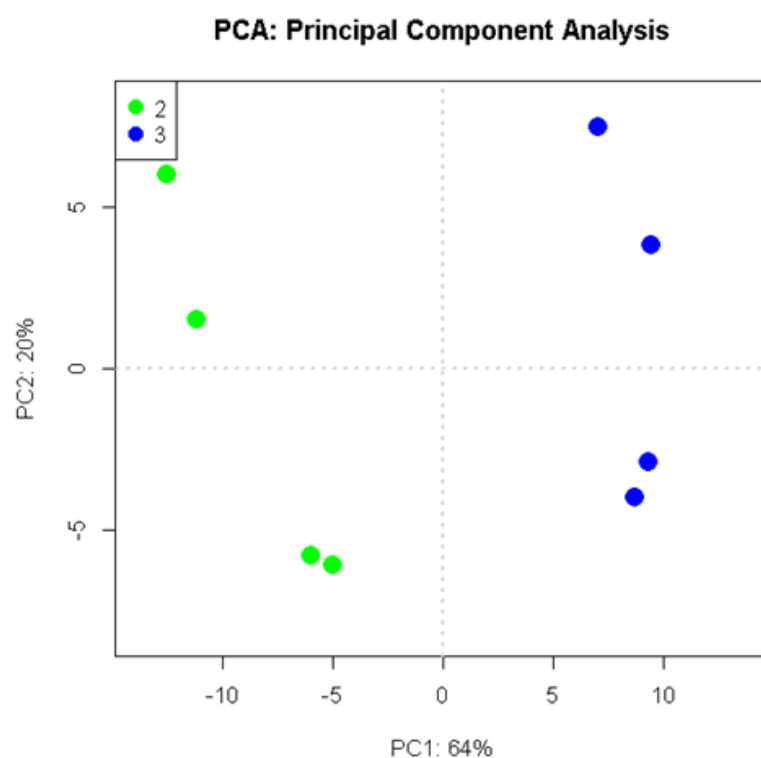


**Figure 5.7 – Principle component analysis.**

Data collected from the Agilent SurePrint miRNA microarray were subjected to PCA. Each dot represents one sample, with colours showing different groups. Groups are as follows: 1/Red – d0 H9 hESCs, 2/Green – d3 CD326<sup>low</sup>CD56<sup>+</sup> MPs, 3/Royal blue – d3 NCF, 4/Light blue – d7. Top panel (A) shows PCA performed including all 16 samples, bottom panel (B) shows analysis of only d3 CD326<sup>low</sup>CD56<sup>+</sup> MP and d3 NCF samples.

samples (Figure 5.7B). Using this map, the clustering of samples from these groups was clearly separate, although it is still clear that there is some level of similarity between the two. As described previously (Chapter 3), data has suggested that both of these groups contain multipotent progenitor populations, with the CD326<sup>low</sup>CD56<sup>+</sup> fraction containing mesodermal and possible EC progenitors, and the NCF possibly containing a mix of mesodermal, endoderm and mesendodermal progenitors, which may explain the close clustering of these two groups. Furthermore, the close spacing of these groups on the PCA map also suggested that there would only be a small number of differentially expressed miRNAs between these two sample groups. It could be hypothesised, therefore, that any miRNA whose expression is significantly different between these two d3 sample groups may play an important role in lineage specification, specifically to the mesoderm and subsequently to the endothelium.

#### 5.4.1.2 Pluripotency-associated miRNAs

After global analysis and comparisons of sample groups, groups of previously characterised miRNAs were examined to assess their expression within the direct hESC-EC differentiation system. Initially, the expression of pluripotency-associated miRNAs was analysed. Consisting of 10 individual highly homologous mature miRNAs (including -3p and -5p strands from 5 different miRNA stem loops), it has been well documented that miRs from the miR-302 cluster are expressed at high levels in hESCs, with specific roles in the maintenance or pluripotency and control of cell cycle (Houbaviy et al., 2003, Card et al., 2008, Rosa et al., 2011, Zhang et al., 2015), discussed in more detail in section 1.8.1.

The ‘lead’ strands of all 5 miRNAs in this cluster (miR-302a-3p, -302b-3p, -302c-3p, -302d-3p and -367-3p) were detected in all samples run on the miRNA microarray screen (Figure 5.8). All 5 were significantly downregulated in the d7 hESC-EC samples, and expressed at lower levels in d3 CD326<sup>low</sup>CD56<sup>+</sup> MPs than in the NCF samples. These results were subsequently verified using Taqman® qRT-PCR (Figure 5.9). Due to the similar expression profiles of all miR-302 cluster miRNAs in the microarray screen, only miR-302a (Figure 5.9A) and -302b (Figure 5.9B) were validated using this method. Both of these miRNAs were significantly downregulated in heterogeneous and CD326<sup>low</sup>CD56<sup>+</sup> MP d3 samples, but not in

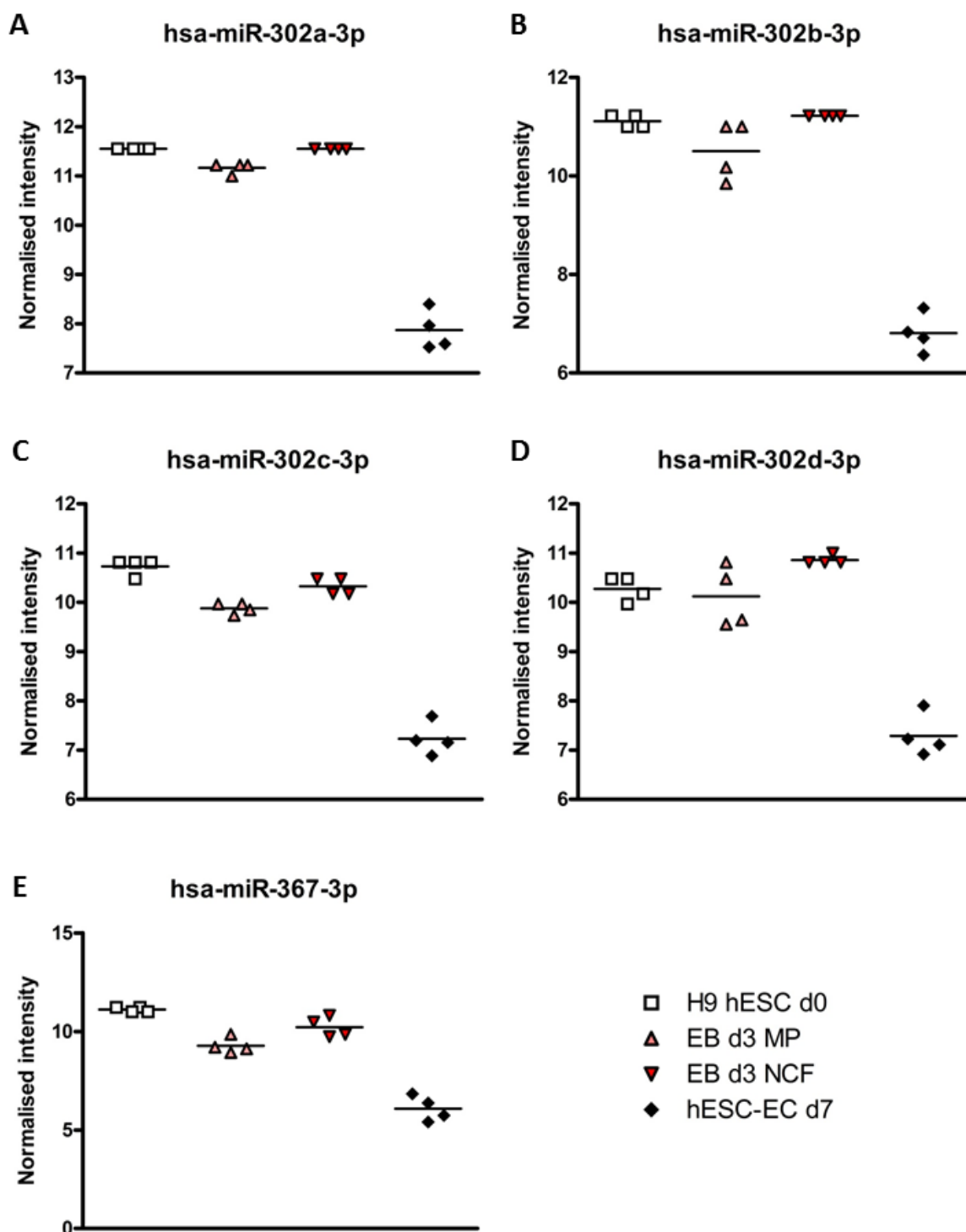


**Figure 5.8 – Microarray analysis of pluripotency-associated miRNAs.**

Previously published pluripotency-associated miRNA profiles were assessed using data from the miRNA microarray. Specifically, miRNAs from the miR-302 family were analysed; miR-302a (A), -302b (B), -302c (C), -302d (D) and miR-367 (E), with the -3p strands of all of these miRNAs previously defined as the 'lead' strand. Each individual data point in the dot plots represent the value obtained from 1 sample on the microarray, with values plotted as normalised intensities, determined as described in section 5.3.1. Bars represent the mean for each sample group. n=4 samples.

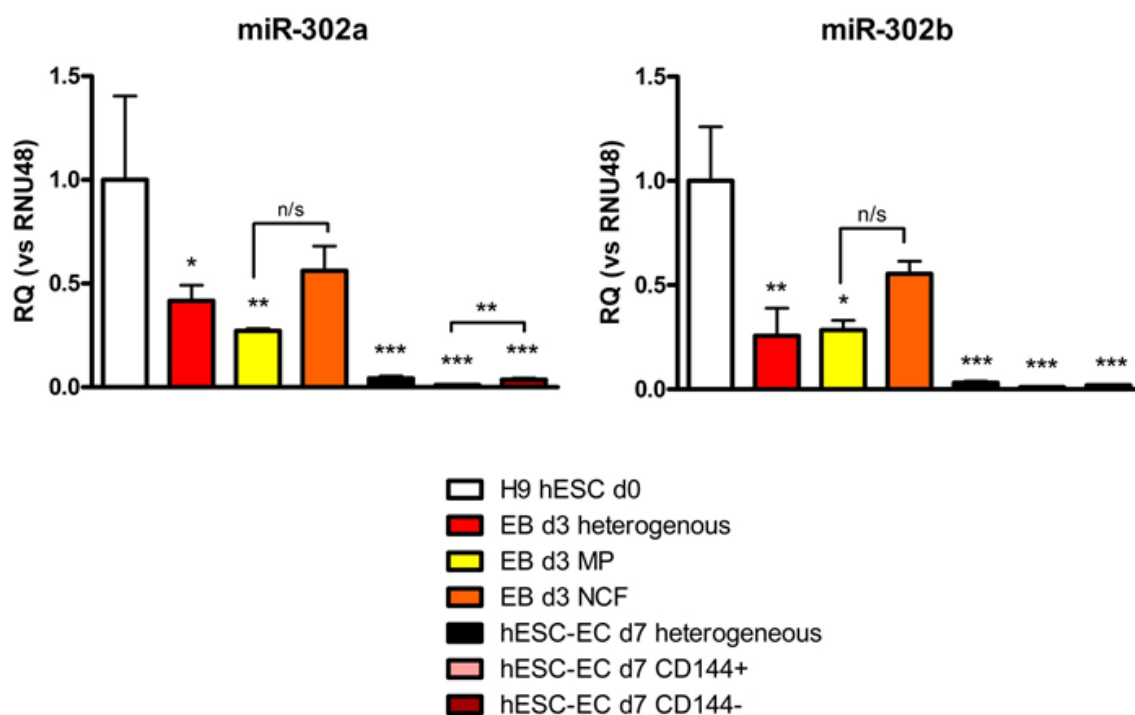


**Figure 5.9 – qRT-PCR validation of pluripotent-associated miRNA.**

After analysis by miRNA microarray, samples were subject to analysis by Taqman® qRT-PCR to validate findings. Total RNA from d0 hESCs, heterogeneous and FACSsorted samples from d3, and heterogeneous and MACSorted samples from d7 was analysed for expression of 2 miRNAs from the miR-302 family; miR-302a and -302b. Histograms show RQ ± RQ Max, calculated against RNU48 reference RNA. Significance calculated using a repeated measures ANOVA with Tukey post hoc comparison; \* =  $p < 0.05$ , \*\* =  $p < 0.01$ , \*\*\* =  $p < 0.001$  vs. d0 pluripotent control. n/s = non-significant, MP = CD326<sup>low</sup>CD56<sup>+</sup> mesoderm progenitor, NCF = negative cell fraction. n=4.

the NCF. This is in line with previous data (Chapter 3), showing pluripotency-associated genes, such as *Nanog* and *Oct4*, are downregulated to significantly lower levels in the CD326<sup>low</sup>CD56<sup>+</sup> MP cells than in the NCF. Taken together, these data support the hypothesis that these MP cells have lost their pluripotency, and have, or are beginning to, commit toward the mesoderm, or possibly an even more mature cell phenotype. Additionally, these miRNAs were even further downregulated by d7 of hESC-EC differentiation (Figure 5.9). Total RNA was also collected from MACSorted CD144<sup>+</sup> and CD144<sup>-</sup> d7 hESC-ECs, and miR-302a was expressed at significantly lower levels in CD144<sup>+</sup> cells than in CD144<sup>-</sup>, although the expression levels in both sample groups was still significantly downregulated when compared to d0 pluripotent hESCs. This may suggest that, although cells in both sample groups have lost pluripotency, the CD144<sup>+</sup> cells have already begun to develop a more mature EC phenotype.

Downregulation of miR-302a (Figure 5.10A) and -302b (Figure 5.10B) was also observed during indirect hESC-EC differentiation, when total RNA samples were analysed using Taqman® qRT-PCR. Although a significant reduction in expression

was observed for both miRNAs in all d7 and d10 samples, including d7+3 hESC-ECs, downregulation occurred more slowly in this differentiation system (Figure 5.10). No significant downregulation was observed by d3 of indirect hESC-EC differentiation, though only heterogeneous d3 samples were analysed. Isolation of CD326<sup>low</sup>CD56<sup>+</sup> MP cells may have revealed a significant downregulation in these two miRNAs, in concurrence with observations in the direct hESC-EC system. Taken alongside previous gene expression data, this confirms the loss of pluripotency in cells during both indirect and direct hESC-EC differentiation.

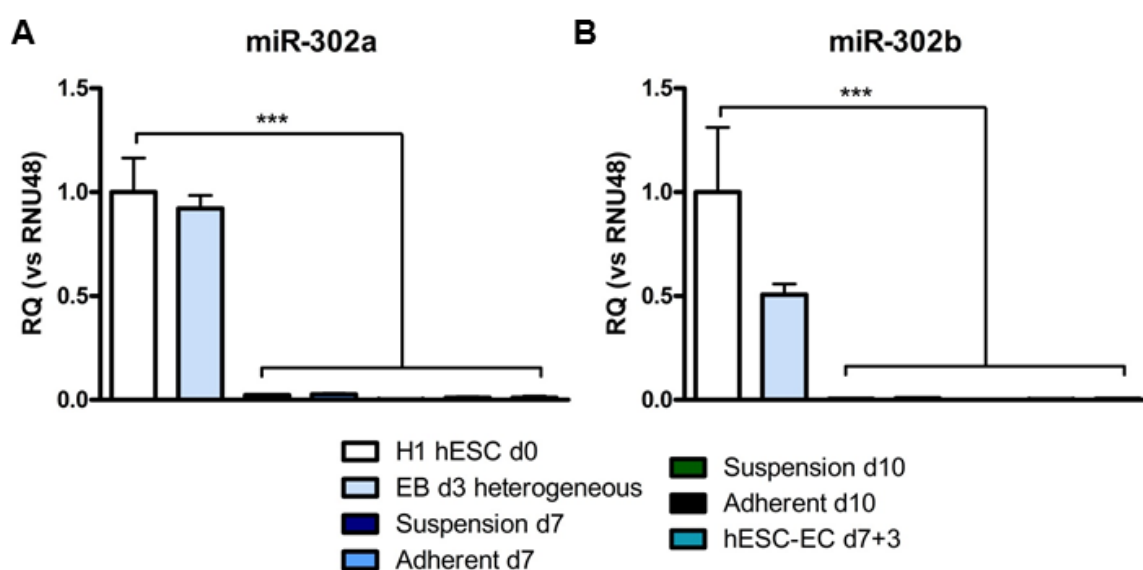


**Figure 5.10 – Expression of miR-302a and -302b during indirect hESC-EC differentiation.**

The expression of miR-302a (A) and -302b (B) were also profiled during indirect hESC-EC differentiation. Total RNA was collected from d0 H1 hESCs, heterogeneous d3 samples, suspension and adherent samples at d7 and 10, and d7+3 hESC-ECs, and analysed using qRT-PCR. Histograms show RQ  $\pm$  RQ Max, relative to RNU48 reference RNA. Repeated measures ANOVA with Tukey post hoc comparisons used to calculate significance, \*\*\* =  $p < 0.001$  vs. d0 hESCs.  $n=4$ .

#### 5.4.1.3 Endothelial-associated miRNAs

In addition to those associated with pluripotent cells, the expression profiles of miRNAs previously identified to have a role in EC function and phenotype were also analysed using data collected from the microarray screen. Lead strands of miR-126 (Figure 5.11A) and miR-10a (Figure 5.11B) were found to be significantly upregulated in the d7 hESC-EC samples. Both of these miRNAs have been shown to play roles in the regulation of angiogenesis and EC function, and are upregulated during differentiation of PSCs to ECs (Kane et al., 2010, Hassel et al., 2012).

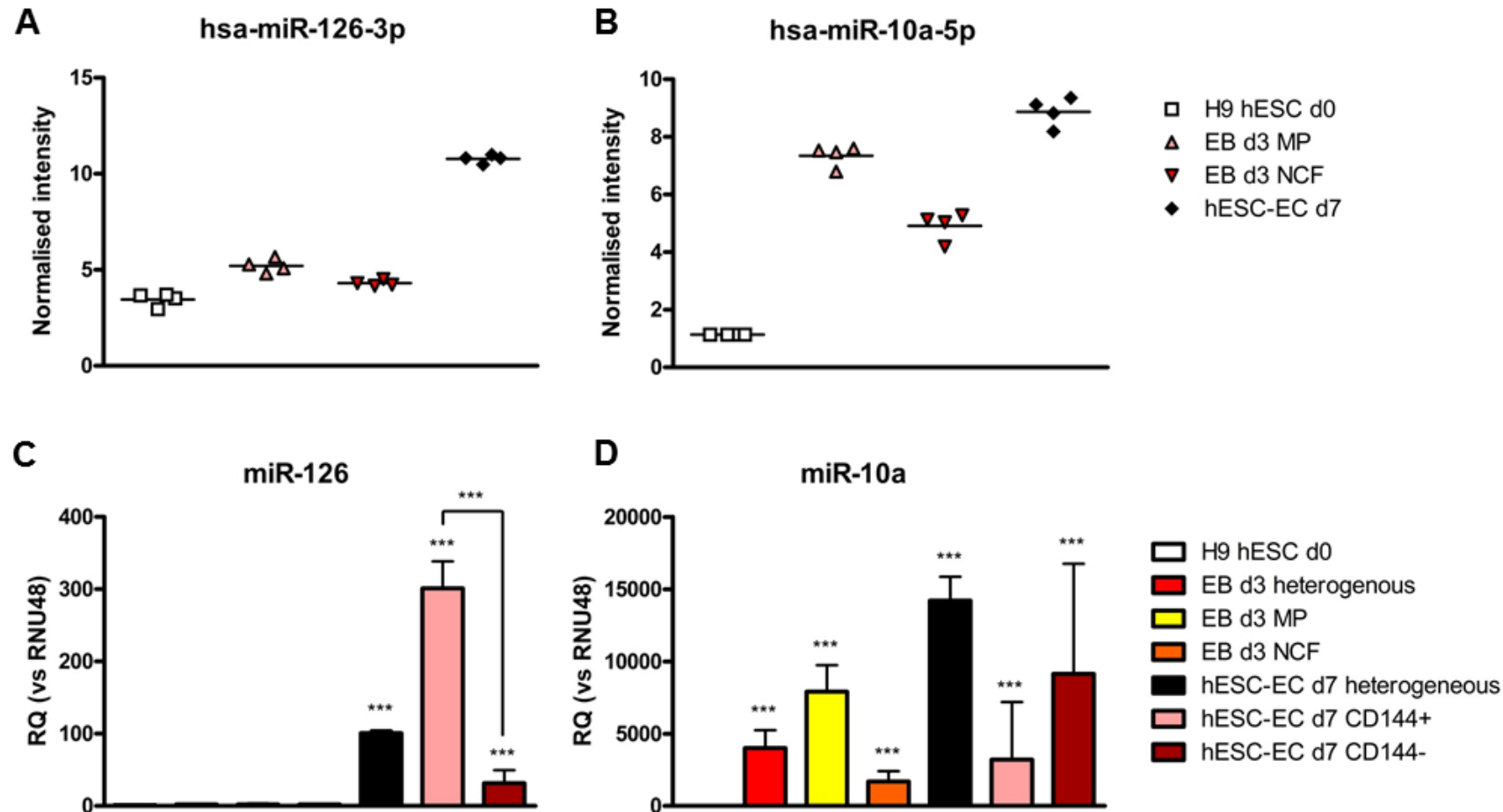


**Figure 5.11 – Profile of endothelial-associated miRNAs during direct hESC-EC differentiation.**

miRNAs previously identified to play a role in EC function and development were analysed using microarray (A-B) and qRT-PCR (C-D) analysis. N=4 H9 direct hESC-EC differentiation samples were analysed to profile the expression of miR-126 (A and C) and miR-10a (B and D). Dot plots (A-B) show normalised intensity values for 4 individual samples run on miRNA microarray screen, with the line representing the mean value. Histograms (C-D) show RQ  $\pm$  RQ Max calculated using RNU 48 reference gene. Repeated measures ANOVA with Tukey post hoc comparisons used to calculate significance; \*\*\* =  $p < 0.001$  vs. d0 pluripotent control. MP = CD326<sup>low</sup>CD56<sup>+</sup> mesoderm progenitor, NCF = negative cell fraction.

Additionally, both of these miRNAs were observed to be expressed at higher levels in the CD326<sup>low</sup>CD56<sup>+</sup> MPs than in the NCF samples, showing a similar expression pattern to EC-associated genes such as *CD31* and *CD144* (Chapter 3). This, therefore, supports the previously stated hypothesis that the MP cells have already started to commit toward an EC phenotype, losing their multipotency and, therefore, their ability to differentiate into any mesodermal cell type, although further experiments would be needed to confirm this.

These data were, once again, verified using qRT-PCR. Using this method of miRNA profiling, miR-126 was only significantly upregulated by d7 of hESC-EC differentiation, when cells begin to acquire a more mature EC phenotype, and not in any of the d3 samples. Like miR-302a and b, the expression of these miRNAs was also examined in total RNA samples obtained from MACSorted CD144<sup>+</sup> and CD144<sup>-</sup> d7 cells from direct hESC-EC differentiation. Interestingly, miR-126 was expressed at significantly higher levels (approximately 300-fold increase compared to pluripotent hESCs) in CD144<sup>+</sup> hESC-ECs when compared to CD144<sup>-</sup> d7 cells (approximately 30-fold increase compared to d0 pluripotent hESCs). This further validates claims that the CD31<sup>+</sup>CD144<sup>+</sup> cells are committed toward an EC fate.

The expression profile of miR-10a was different from that of miR-126. Overall, miR-10a was shown to be upregulated throughout hESC-EC differentiation. Additionally, a significant upregulation was observed in all d3 samples, heterogeneous, CD326<sup>low</sup>CD56<sup>+</sup> MPs and NCF (approximately 5000, 8000 and 1500-fold upregulation in each of these samples, respectively) when compared to d0 hESCs. Although not significantly different from d3 NCF samples, the highest levels of miR-10a upregulation were seen in the MPs, consistent with the hypothesis that, even at this early stage in differentiation, MPs have already started to gain an EC phenotype. At d7, although there was no significant difference between heterogeneous, CD144<sup>+</sup> and CD144<sup>-</sup> hESC-ECs, the highest level of expression was recorded in the heterogeneous samples (Figure 5.11D). Surprisingly, the lowest levels of miR-10a were observed in the d7 CD144<sup>+</sup> cells, in contrast to data shown by Hassel et al., who demonstrated that miR-10a was significantly enriched in CD144<sup>+</sup>CD309<sup>+</sup> cells derived from mESCs (Hassel et al., 2012). This may be due to large amounts of variation in expression between experimental replicates, or it may be a species difference. Alternatively,



however, the pattern of miR-10a expression observed here may suggest a role for this miRNA in endothelial commitment, and the formation of endothelial precursors.

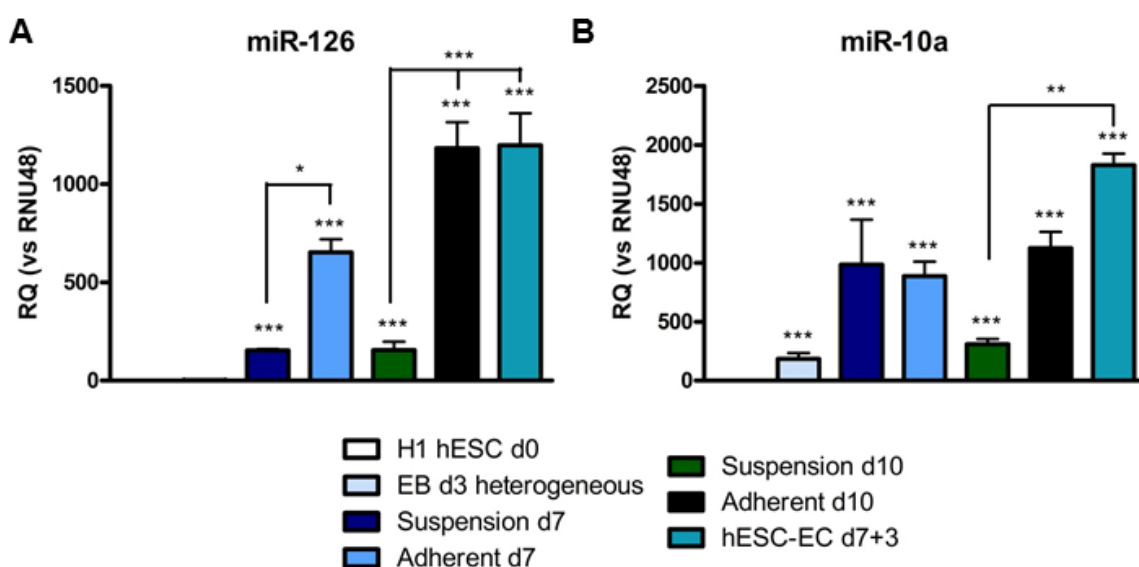


**Figure 5.12 – miR-126 and -10a during indirect hESC-EC differentiation.**

The endothelial-associated miR-126 (A) and miR-10a (B) were profiled in RNA samples from indirect H1 hESC-EC differentiation. Histograms show RQ  $\pm$  RQ Max calculated relative to the RNU48 reference RNA. Repeated measures ANOVA with Tukey's post hoc comparisons was used to calculate significance; \* =  $p < 0.05$ , \*\* =  $p < 0.01$ , \*\*\* =  $p < 0.001$  vs d0 hESCs unless comparisons specified. Samples from  $n=4$  differentiation experiments.

In the indirect hESC-EC differentiation system, both endothelial-associated miRNAs, miR-126 (Figure 5.12A) and miR-10a (Figure 5.12B), were shown to be significantly upregulated throughout differentiation, with the highest levels of expression observed by d10. Similarly to the direct hESC-EC differentiation system, miR-126 was not detected at d3, whereas miR-10a was shown to be significantly upregulated even at this early time point. Taken together with previous data, and that published by Hassel and colleagues (Hassel et al., 2012), it could be suggested that miR-10a plays a role in early EC development, whereas miR-126 is more important in mature EC function.

Both miR-126 and miR-10a were expressed at higher levels in the adherent cells than in suspension cells, with significant differences in miR-126 at d7 and d10 (Figure 5.12A) and in miR-10a in d10 samples (Figure 5.12B). Furthermore, the highest levels of expression for both miRNAs were observed in d7+3 hESC-ECs (Figure 5.12), strengthening data showing that these cells have developed a more mature EC phenotype than the d7 HE cells (Chapter 4).

#### 5.4.1.4 EC differentiation associated miRNAs

As stated previously, a number of miRNAs have also been implicated in hESC-EC differentiation. Data collected from the miRNA microarray screen was then used to examine the expression of these miRNAs within the presented direct hESC-EC differentiation system. Previously, Kane et al. had demonstrated the upregulation of 3 different miRNAs, miR-181a, -181b and -99b, during generation of hESC-ECs using a 21 day monolayer differentiation protocol (Kane et al., 2012). Within the direct hESC-EC differentiation system, these 3 miRNAs were significantly upregulated, with the highest level of expression occurring on d7, alongside the appearance of CD31<sup>+</sup>CD144<sup>+</sup> hESC-ECs (Figure 5.13). The lead strands of miR-181a (Figure 5.13A) and miR-181b (Figure 5.13B) were shown to have the same expression profile, as well as similar levels of expression, during direct hESC-EC differentiation. Both members of the miR-181 family, these miRNAs are highly homologous, and are transcribed as one, poly-cistronic transcript from two different alleles within the genome and, therefore, it is not unexpected that this is the case. High homology between miRNAs suggests shared mRNA targets and, therefore, implicates these miRNAs in similar cellular pathways.

miR-99b, however, is not a member of the miR-181 family, and exhibits a different expression pattern when profiled during direct hESC-EC differentiation. Unlike the other EC-associated miRNAs, miR-99b was undetected in all 4 samples from the d0 pluripotent hESC, d3 CD326<sup>low</sup>CD56<sup>+</sup> MP and d3 NCF groups, before being significantly upregulated at d7 (Figure 5.13C).

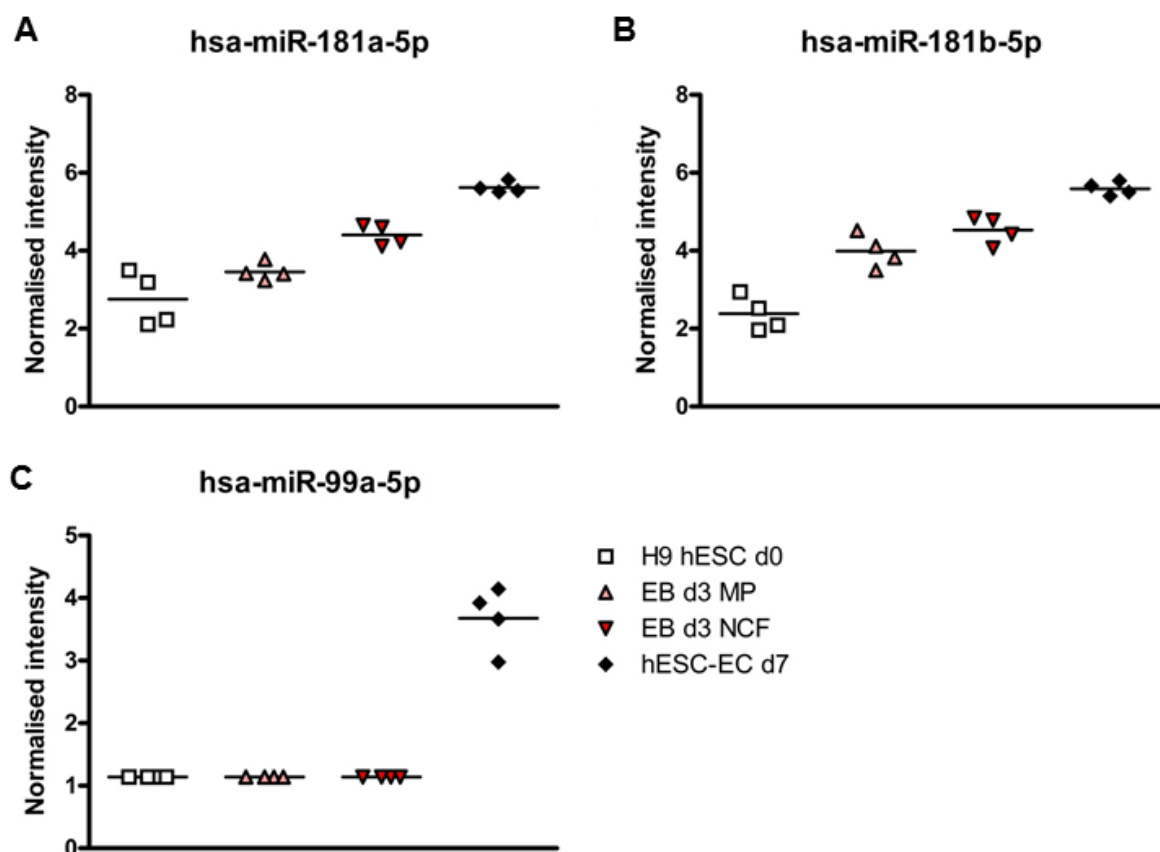


**Figure 5.13 – Expression miR-181a, -181b and 99b**

miR-181a (A), -181b (B) and -99b (C) were previously described to play a role in hESC-EC differentiation by Kane et al. (2012). Expression profiles of these miRNAs were then examined using data obtained from the microarray screen. The -5p strand of all of these miRNAs has been previously defined as the 'lead' strand. Each individual data point in the dot plots represent the value obtained from 1 sample on the microarray, with values plotted as normalised intensities, determined as described in section 5.3.1. n=4 samples.

Unlike miR-126 and miR-10a, none of the miRNAs described by Kane and colleagues were upregulated in d3 CD326<sup>low</sup>CD56<sup>+</sup> MPs, when compared to NCF samples (Figure 5.11 and Figure 5.13). In fact, miR-181a and -181b were expressed at higher levels in the NCF samples and miR-99b, as previously stated, as undetected in all samples until d7. Collectively, this suggests that these three miRNAs may not be essential for EC commitment and differentiation. Instead, upregulation is merely correlates with EC commitment and the appearance of hESC-ECs, with these miRNAs playing roles in mature EC function and angiogenesis. Indeed, a recent publication has demonstrated a role for both miR-181a and -99b in the regulation of mRNAs associated with hypertension in human microvascular ECs (Kriegel et al., 2015), and miR-181b has been previously shown to be involved in the regulation of NF-κB signalling in the vascular endothelium (Sun et al., 2012).

In 2013, Luo and colleagues also used a microarray screen to identify potential miRNA candidates involved in EC differentiation (Luo et al., 2013). Using this technology and a variety of follow-up experiments, Luo demonstrated the involvement of miR-150 and miR-200c in EC differentiation from hESCs, through their shared target ZEB1. When profiled in the presented direct hESC-EC differentiation system, however, the expression pattern of these miRNAs did not match this previously published data. In contrast, neither the lead nor passenger (-5p and -3p, respectively) strand of miR-150 was detected in any of the samples analysed using the microarray screen. Additionally, the lead strand of miR-200c was shown to be expressed at lower levels in all 4 samples from the d3 CD326<sup>low</sup>CD56<sup>+</sup> MP and d7 groups, than in d0 pluripotent hESC and d3 NCF samples (Figure 5.14).

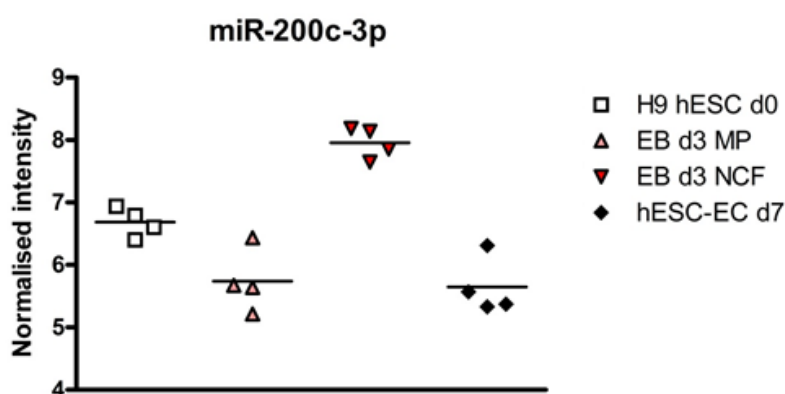


**Figure 5.14 – miR-200c expression during direct hESC-EC differentiation.**

Luo et al. (2013) previously described the involvement of miR-200c in the differentiation of hESCs to ECs. The expression profile of this miRNA was, therefore, analysed in the direct hESC-EC differentiation using data collected from the microarray screen. Each individual data point in the dot plots represent the value obtained from 1 sample on the microarray, with values plotted as normalised intensities, determined as described in section 5.3.1. d7 hESC-EC samples are total RNA collected from all cells present on d7 of direct hESC-EC differentiation. n=4 samples.

#### 5.4.1.5 Other notable mesoderm-associated miRNAs

Due to the unbiased and global nature of microarray technology, data for other, previously characterised, groups of miRNAs was collected. Specifically, the expression levels of miRNAs, identified to play roles in the differentiation and function of other mesodermal cell types such as cardiomyocytes, skeletal muscle and hematopoietic cells, were assessed. Data collected from TLDA cards (shown in Chapter 3) showed higher expression of genes associated with other mesodermal cell types, such as *NKX2.5*, in the d3 MP cells when compared with

NCF samples. It was, therefore, hypothesised that miRNAs associated with other cells of the mesoderm would be expressed in a similar way.

Existing as a cluster within the genome, miR-1 and miR-133 are transcribed together and have been widely shown to be specifically expressed in the skeletal and cardiac muscle (Zhao et al., 2005). miR-1 has specifically been implicated in heart development, playing roles in cardiogenesis and cardiac cell fate decisions, with miR-133 involved in the specification of cells to skeletal muscle (Ivey et al., 2008). Previously (chapter 3), it was shown that genes associated with cardiac development, such as *NKX2.5*, were significantly upregulated in d3 MP cells, when compared to the NCF samples (Table 3.1). Therefore, the expression of these cardiac-associated miRNAs was assessed. Data from the microarray screen recorded no expression of either miR-1 or miR-133 in samples from any time point (d0, d3 MP, d3 NCF or d7 hESC-ECs). Interestingly, this is in contrast to previously published data, showing the miR-1 and miR-133 promote mesoderm formation from human and mouse ESCs, and prevent the induction of endo- and ectodermal lineage specification (Ivey et al., 2008). Coupled with previous gene and miRNA expression data, this supports the hypothesis that d3 CD326<sup>low</sup>CD56<sup>+</sup> MP cells, even at this early stage, may already be committed toward an EC phenotype, possibly due to the specialised culture conditions. This, therefore, explains the absence of miRNAs from other mesodermal lineages, as downregulation and degradation may have already occurred at this early stage in EC commitment. Furthermore, Ivey et al. used an undefined hESC differentiation protocol to induce the formation of mesoderm and cardiac lineages. As stated previously, the use of undefined reagents within hESC differentiation protocols introduces unknown factors into systems. Induction of miR-1 and miR-133 may be more specific to later cardiac and skeletal muscle specification, with early expression induced in this undefined system due to stimulation by one of these unknown factors and, therefore, explaining why these miRNAs are undetectable in samples from the presented defined hESC-EC differentiation.

Additionally, miR-451a, a miRNA associated with erythropoiesis *in vivo* (Dore et al., 2008, Patrick et al., 2010), was only detected in one d7 sample, out of all of those run on the array. Dore and colleagues demonstrated an upregulation of miR-451 during induction of erythroid maturation of human CD34<sup>+</sup> cells and

murine erythroleukemia cells, as well as being expressed in mouse blood (Dore et al., 2008). The miR-451 transcript is bi-cistronic, and also codes for miR-144, additionally shown by Dore to be upregulated during erythroid maturation. Similarly, miR-144 was not detected in any of the 16 samples analysed in the microarray screen. As these miRNAs are associated with erythropoiesis, a process occurring later in lineage and cell type specification, it would not be expected to detect either miR-144 or miR-451 in these samples. Instead, these results demonstrate that the developed direct hESC-EC differentiation pathway is completely independent from the indirect pathway, with no upregulation of common hematopoietic-associated miRNAs.

#### 5.4.1.6 Pairwise comparisons to identify novel miRNAs

In order to identify novel miRNAs, which may play a role in early mesodermal and endothelial commitment and specification of hESCs during hESC-EC differentiation, analysis focused on miRNAs differentially expressed between d3 CD326<sup>low</sup>CD56<sup>+</sup> MPs and d3 NCF samples. As described previously (section 5.3.1), a paired T-test was performed to make a direct comparison between these groups. Only miRNAs with a fold change (FC) >1.5 and a false discovery rate (FDR) <0.05 were deemed to be differentially expressed, with fold changes generated for d3 CD326<sup>low</sup>CD56<sup>+</sup> MPs, relative to d3 NCF samples.

Direction of expression change (vs d3 NCF)	Number of differentially expressed miRNAs
Upregulated	21
Downregulated	30

**Table 5.2 – miRNAs differentially expressed between d3 CD326<sup>low</sup>CD56<sup>+</sup> and NCF samples.** Differentially expressed miRNAs are defined as having a FDR<0.05 and FC>1.5.

Although over 1,000 miRNAs were profiled using the Agilent® microarray screen, only a small subset of 51 were found to be differentially expressed between d3 MP and NCF samples (Table 5.2,

Upregulated			Downregulated		
miRNA	Fold change	FDR	miRNA	Fold change	FDR
hsa-miR-483-3p	28.17	0.025	hsa-miR-105-5p	-17.72	0.025

hsa-miR-145-5p	12.81	0.032	hsa-miR-429	-8.67	0.015
hsa-miR-10b-5p	5.54	0.022	hsa-miR-200a-3p	-7.26	0.021
hsa-miR-132-3p	5.54	0.034	hsa-miR-203a	-6.86	0.013
hsa-miR-10a-5p	5.41	0.039	hsa-miR-139-5p	-6.18	0.036
hsa-miR-372-3p	4.67	0.036	hsa-miR-767-5p	-6.15	0.048
hsa-miR-455-5p	4.52	0.047	hsa-miR-200c-3p	-4.65	0.042
hsa-miR-373-3p	4.43	0.025	hsa-miR-525-3p	-4.46	0.007
hsa-miR-371a-3p	3.94	0.026	hsa-miR-141-3p	-4.39	0.014
hsa-miR-145-3p	3.64	0.032	hsa-miR-515-3p	-4.27	0.007
hsa-miR-155-5p	3.05	0.023	hsa-miR-181d-5p	-4.12	0.023
hsa-miR-378a-3p	2.84	0.027	hsa-miR-519b-3p	-4.06	0.009
hsa-miR-455-3p	2.77	0.023	hsa-miR-516b-5p	-3.98	0.005
hsa-miR-193a-5p	2.70	0.032	hsa-miR-522-3p	-3.92	0.020
hsa-miR-23b-3p	2.39	0.025	hsa-miR-135b-5p	-3.52	0.011
hsa-miR-629-5p	2.30	0.015	hsa-miR-183-5p	-3.31	0.023
hsa-miR-373-5p	2.28	0.048	hsa-miR-96-5p	-3.13	0.023
hsa-miR-3651	1.94	0.014	hsa-miR-551b-3p	-3.12	0.019
hsa-miR-126-3p	1.87	0.036	hsa-miR-210-3p	-3.01	0.048
hsa-miR-20a-5p	1.58	0.025	hsa-miR-518b	-2.88	0.013
hsa-miR-365a-3p	1.55	0.025	hsa-miR-519c-3p	-2.87	0.027
			hsa-miR-526-5p	-2.59	0.014
			hsa-miR-520g-3p	-2.59	0.048
			hsa-miR-520b	-2.44	0.045
			hsa-miR-182-5p	-2.29	0.023
			hsa-miR-181a-5p	-1.92	0.025
			hsa-miR-1247-5p	-1.91	0.049
			hsa-miR-517a-3p	-1.75	0.048
			hsa-miR-205-5p	-1.66	0.033
			hsa-miR-517b-3p	-1.58	0.007

Table 5.3). Of these 51 miRNAs, 21 were found to be upregulated and 30 downregulated. Within the upregulated miRNAs were miR-126-3p, which was shown to be expressed  $\approx 1.9$ -fold higher in the MPs, and miR-10a-5p, expressed  $\approx 5.4$ -fold higher in MPs than in NCF samples (

Upregulated			Downregulated		
miRNA	Fold	FDR	miRNA	Fold	FDR

	<u>change</u>			<u>change</u>	
hsa-miR-483-3p	28.17	0.025	hsa-miR-105-5p	-17.72	0.025
hsa-miR-145-5p	12.81	0.032	hsa-miR-429	-8.67	0.015
hsa-miR-10b-5p	5.54	0.022	hsa-miR-200a-3p	-7.26	0.021
hsa-miR-132-3p	5.54	0.034	hsa-miR-203a	-6.86	0.013
hsa-miR-10a-5p	5.41	0.039	hsa-miR-139-5p	-6.18	0.036
hsa-miR-372-3p	4.67	0.036	hsa-miR-767-5p	-6.15	0.048
hsa-miR-455-5p	4.52	0.047	hsa-miR-200c-3p	-4.65	0.042
hsa-miR-373-3p	4.43	0.025	hsa-miR-525-3p	-4.46	0.007
hsa-miR-371a-3p	3.94	0.026	hsa-miR-141-3p	-4.39	0.014
hsa-miR-145-3p	3.64	0.032	hsa-miR-515-3p	-4.27	0.007
hsa-miR-155-5p	3.05	0.023	hsa-miR-181d-5p	-4.12	0.023
hsa-miR-378a-3p	2.84	0.027	hsa-miR-519b-3p	-4.06	0.009
hsa-miR-455-3p	2.77	0.023	hsa-miR-516b-5p	-3.98	0.005
hsa-miR-193a-5p	2.70	0.032	hsa-miR-522-3p	-3.92	0.020
hsa-miR-23b-3p	2.39	0.025	hsa-miR-135b-5p	-3.52	0.011
hsa-miR-629-5p	2.30	0.015	hsa-miR-183-5p	-3.31	0.023
hsa-miR-373-5p	2.28	0.048	hsa-miR-96-5p	-3.13	0.023
hsa-miR-3651	1.94	0.014	hsa-miR-551b-3p	-3.12	0.019
hsa-miR-126-3p	1.87	0.036	hsa-miR-210-3p	-3.01	0.048
hsa-miR-20a-5p	1.58	0.025	hsa-miR-518b	-2.88	0.013
hsa-miR-365a-3p	1.55	0.025	hsa-miR-519c-3p	-2.87	0.027
			hsa-miR-526-5p	-2.59	0.014
			hsa-miR-520g-3p	-2.59	0.048
			hsa-miR-520b	-2.44	0.045
			hsa-miR-182-5p	-2.29	0.023
			hsa-miR-181a-5p	-1.92	0.025
			hsa-miR-1247-5p	-1.91	0.049
			hsa-miR-517a-3p	-1.75	0.048
			hsa-miR-205-5p	-1.66	0.033
			hsa-miR-517b-3p	-1.58	0.007

Table 5.3), as stated previously (section 5.4.1.3).

<b>Upregulated</b>			<b>Downregulated</b>		
<u>miRNA</u>	<u>Fold change</u>	<u>FDR</u>	<u>miRNA</u>	<u>Fold change</u>	<u>FDR</u>



hsa-miR-483-3p	28.17	0.025	hsa-miR-105-5p	-17.72	0.025
hsa-miR-145-5p	12.81	0.032	hsa-miR-429	-8.67	0.015
hsa-miR-10b-5p	5.54	0.022	hsa-miR-200a-3p	-7.26	0.021
hsa-miR-132-3p	5.54	0.034	hsa-miR-203a	-6.86	0.013
hsa-miR-10a-5p	5.41	0.039	hsa-miR-139-5p	-6.18	0.036
hsa-miR-372-3p	4.67	0.036	hsa-miR-767-5p	-6.15	0.048
hsa-miR-455-5p	4.52	0.047	hsa-miR-200c-3p	-4.65	0.042
hsa-miR-373-3p	4.43	0.025	hsa-miR-525-3p	-4.46	0.007
hsa-miR-371a-3p	3.94	0.026	hsa-miR-141-3p	-4.39	0.014
hsa-miR-145-3p	3.64	0.032	hsa-miR-515-3p	-4.27	0.007
hsa-miR-155-5p	3.05	0.023	hsa-miR-181d-5p	-4.12	0.023
hsa-miR-378a-3p	2.84	0.027	hsa-miR-519b-3p	-4.06	0.009
hsa-miR-455-3p	2.77	0.023	hsa-miR-516b-5p	-3.98	0.005
hsa-miR-193a-5p	2.70	0.032	hsa-miR-522-3p	-3.92	0.020
hsa-miR-23b-3p	2.39	0.025	hsa-miR-135b-5p	-3.52	0.011
hsa-miR-629-5p	2.30	0.015	hsa-miR-183-5p	-3.31	0.023
hsa-miR-373-5p	2.28	0.048	hsa-miR-96-5p	-3.13	0.023
hsa-miR-3651	1.94	0.014	hsa-miR-551b-3p	-3.12	0.019
hsa-miR-126-3p	1.87	0.036	hsa-miR-210-3p	-3.01	0.048
hsa-miR-20a-5p	1.58	0.025	hsa-miR-518b	-2.88	0.013
hsa-miR-365a-3p	1.55	0.025	hsa-miR-519c-3p	-2.87	0.027
			hsa-miR-526-5p	-2.59	0.014
			hsa-miR-520g-3p	-2.59	0.048
			hsa-miR-520b	-2.44	0.045
			hsa-miR-182-5p	-2.29	0.023
			hsa-miR-181a-5p	-1.92	0.025
			hsa-miR-1247-5p	-1.91	0.049
			hsa-miR-517a-3p	-1.75	0.048
			hsa-miR-205-5p	-1.66	0.033
			hsa-miR-517b-3p	-1.58	0.007

**Table 5.3 – Differentially expressed miRNAs and their changes in expression between d3 CD326<sup>low</sup>CD56<sup>+</sup> and NCF samples.**

Where differential expression is defined as a fold change > 1.5, and a FDR < 0.05. FDR = false discovery rate.

Interestingly, three different miRNA stem loops were shown to have both -3p and -5p strands upregulated in CD326<sup>low</sup>CD56<sup>+</sup> MPs, when compared to NCF samples (

Upregulated			Downregulated		
<u>miRNA</u>	<u>Fold change</u>	<u>FDR</u>	<u>miRNA</u>	<u>Fold change</u>	<u>FDR</u>
hsa-miR-483-3p	28.17	0.025	hsa-miR-105-5p	-17.72	0.025
hsa-miR-145-5p	12.81	0.032	hsa-miR-429	-8.67	0.015
hsa-miR-10b-5p	5.54	0.022	hsa-miR-200a-3p	-7.26	0.021
hsa-miR-132-3p	5.54	0.034	hsa-miR-203a	-6.86	0.013
hsa-miR-10a-5p	5.41	0.039	hsa-miR-139-5p	-6.18	0.036
hsa-miR-372-3p	4.67	0.036	hsa-miR-767-5p	-6.15	0.048
hsa-miR-455-5p	4.52	0.047	hsa-miR-200c-3p	-4.65	0.042
hsa-miR-373-3p	4.43	0.025	hsa-miR-525-3p	-4.46	0.007
hsa-miR-371a-3p	3.94	0.026	hsa-miR-141-3p	-4.39	0.014
hsa-miR-145-3p	3.64	0.032	hsa-miR-515-3p	-4.27	0.007
hsa-miR-155-5p	3.05	0.023	hsa-miR-181d-5p	-4.12	0.023
hsa-miR-378a-3p	2.84	0.027	hsa-miR-519b-3p	-4.06	0.009
hsa-miR-455-3p	2.77	0.023	hsa-miR-516b-5p	-3.98	0.005
hsa-miR-193a-5p	2.70	0.032	hsa-miR-522-3p	-3.92	0.020
hsa-miR-23b-3p	2.39	0.025	hsa-miR-135b-5p	-3.52	0.011
hsa-miR-629-5p	2.30	0.015	hsa-miR-183-5p	-3.31	0.023
hsa-miR-373-5p	2.28	0.048	hsa-miR-96-5p	-3.13	0.023
hsa-miR-3651	1.94	0.014	hsa-miR-551b-3p	-3.12	0.019
hsa-miR-126-3p	1.87	0.036	hsa-miR-210-3p	-3.01	0.048
hsa-miR-20a-5p	1.58	0.025	hsa-miR-518b	-2.88	0.013
hsa-miR-365a-3p	1.55	0.025	hsa-miR-519c-3p	-2.87	0.027
			hsa-miR-526-5p	-2.59	0.014
			hsa-miR-520g-3p	-2.59	0.048
			hsa-miR-520b	-2.44	0.045
			hsa-miR-182-5p	-2.29	0.023
			hsa-miR-181a-5p	-1.92	0.025
			hsa-miR-1247-5p	-1.91	0.049
			hsa-miR-517a-3p	-1.75	0.048
			hsa-miR-205-5p	-1.66	0.033

hsa-miR-517b-3p	-1.58	0.007
-----------------	-------	-------

Table 5.3); miR-145, miR-455 and miR-483, although miR-483-5p FDR was  $>0.05$  ( $\approx 0.09$ ). Recently, an increasing number of studies have demonstrated a role for classical ‘passenger’ or ‘star’ strand miRNAs (Yang et al., 2011). Furthermore, publications have shown that both the -5p and -3p strand of a single miRNA stem loop can exhibit the same expression pattern (Mitra et al., 2015), and possibly play similar regulatory roles (Shan et al., 2013, Yang et al., 2013). It was, therefore, hypothesised that these three identified miRNA stem loops play important regulatory roles during hESC-EC differentiation and commitment. Further work was then performed to validate the findings from the miRNA microarray and investigate this resultant hypothesis.

#### 5.4.1.7 miR-143/145 cluster

As miR-145 is transcribed as a cluster alongside miR-143, in a cluster known as miR-143/145. The miR-143/145 cluster is a poly-cistronic transcript, processed to produce 4 distinct mature miRNAs (Figure 5.15A); miR-143-3p, miR-143-5p (\*), miR-145-5p and miR-145-3p (\*) and, therefore, expression of all 4 miRNAs contained within this cluster were investigated. Similarly to miR-145-5p and -3p, miR-143-3p, the classically known ‘lead’ strand of the miRNA, was demonstrated to be expressed at higher levels ( $\approx 2$ -fold) in d3 CD326<sup>low</sup>CD56<sup>+</sup> MPs when compared with NCF samples, although the FDR was  $>0.05$ . miR-143-5p, however, was not detected in any of the samples run on the microarray screen. Assessment of miRNA profiles throughout the duration of direct hESC-EC differentiation demonstrated an additional increase in the expression of miR-145-5p (Figure 5.15A), -145-3p (Figure 5.15B) and -143-3p (Figure 5.15C) by d7 (Figure 5.15). The increase in expression in d3 CD326<sup>low</sup>CD56<sup>+</sup> MPs, coupled with the increase at d7, suggested a possible role for these miRNAs in early mesodermal and endothelial commitment.

Taqman® qRT-PCR was then used to confirm the expression pattern of these miRNAs. Initially, pri-miR-143 and pri-miR-145 levels were assessed. As described previously, pri-miRNAs are the stem loop structures containing both the -3p and -5p miRNA strands (Figure 5.15A), before processing by Drosha and Dicer. As would be expected from miRNAs transcribed together, both pri-miRNAs were demonstrated to exhibit a similar expression pattern, with both being

significantly upregulated during hESC-EC differentiation (Figure 5.16). Pri-miR-145 was upregulated to slightly higher levels (approximately 150-fold) than pri-miR-143 (approximately 100-fold) at d7 when compared with d0 pluripotent hESCs. As both miRNAs are transcribed together, the difference in the levels of expression may suggest a more prominent role for the mature miR-145 miRNAs within this system, as pri-miR-143 may be targeted for degradation. Additionally, both pri-miRNAs were shown to be expressed at significantly higher levels in d3 MPs than the NCF samples (Figure 5.16A and B).

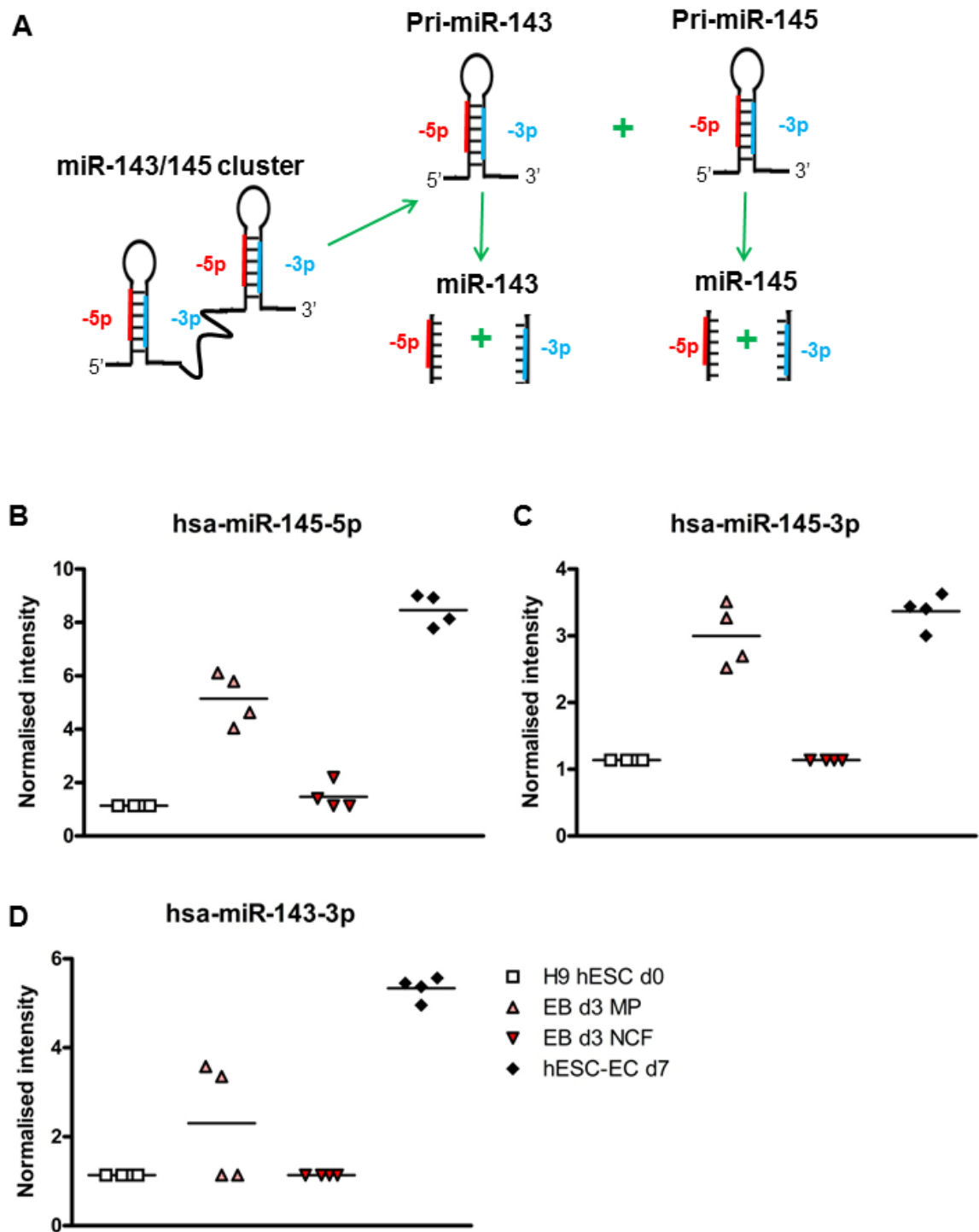


**Figure 5.15 – Microarray profiling of miR-143/145 cluster during hESC-EC differentiation.** miR-143 and -145 are transcribed together in a cluster, which is processed to produce 4 mature miRNAs (A). 3 of the miRNAs in this cluster were detected in the microarray screen, miR-145-5p (B), miR-145-3p (C) and miR-143-3p (D). Dot plots show normalised expression data for n=4 samples in each group, with lines representing the mean value.

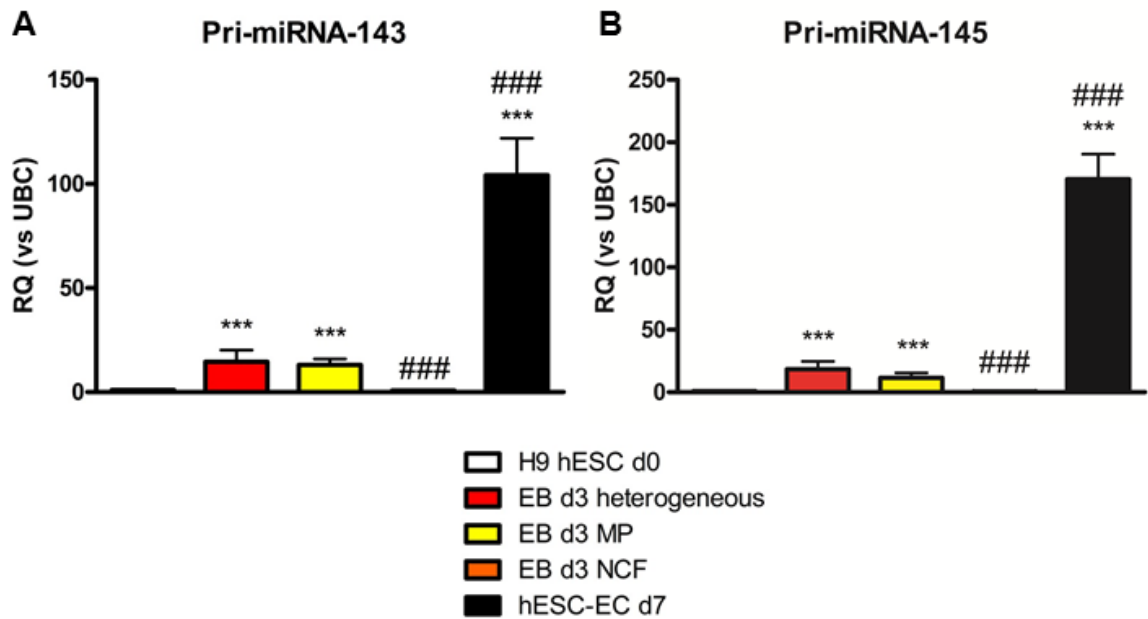


**Figure 5.16 – qRT-PCR for pri-miR-143 and -145 during direct hESC-EC differentiation.**

Total RNA collected from d0 H9 hESCs, d3 heterogeneous, d3 CD326<sup>low</sup>CD56<sup>+</sup> MP, d3 NCF and d7 samples were analysed for expression of pri-miR-143 (A) and -145 (B), the stem loop structures existing before processing (Figure 5.15A). Histograms show RQ  $\pm$  RQ Max calculated relative to the UBC reference gene. Repeated measures ANOVA with Tukey's post hoc comparisons was used to calculate significance; \* =  $p < 0.05$ , \*\* =  $p < 0.01$ , \*\*\* =  $p < 0.001$  vs d0 hESCs, # =  $p < 0.05$ , ### =  $p < 0.001$  vs d3 MP. Samples from  $n=4$  differentiation experiments.

Once expression profiles obtained from the microarray screen were validated for the two pri-miRNAs, expression levels of mature miRNAs from the miR-143/145 cluster were also analysed using qRT-PCR. Although only three of the four miRNAs were detected in data from the microarray screen (miR-143-3p, -145-5p, -145-3p), all four mature miRNAs from the cluster were validated experimentally. As all other miRNAs from the miR-143/145 cluster had the same expression pattern, it was hypothesised that miR-143-5p, classically known as the 'passenger' strand of miR-143, would be regulated in the same way. Analysis by Taqman® qRT-PCR is more sensitive than the microarray screen, and will therefore detect expression of miRNAs which may have been previously missed, such as miR-143-5p. Indeed, when profiled it was demonstrated that all 4 mature miRNAs exhibited the same expression pattern, with all significantly upregulated in d7 samples when compared to d0 pluripotent controls (Figure 5.17A-D). The previously defined 'lead' strands (mi-145-5p and miR-143-3p), were shown to have the highest levels of upregulation (Figure 5.17A and C), although the passenger strands were also shown to be highly upregulated (approximately 100 and 30-fold for miR-145-3p (Figure 5.17B) and miR-143-5p (Figure 5.17D), respectively). Moreover, all four miRNAs were upregulated in the d3 MP samples, when compared to d0 hESCs, and their expression was

significantly higher in these samples than in those from the NCF. Overall, these data allude to a possible role for the miR-143/145 cluster in regulation of hESC differentiation and commitment to mesodermal and early endothelial lineages.

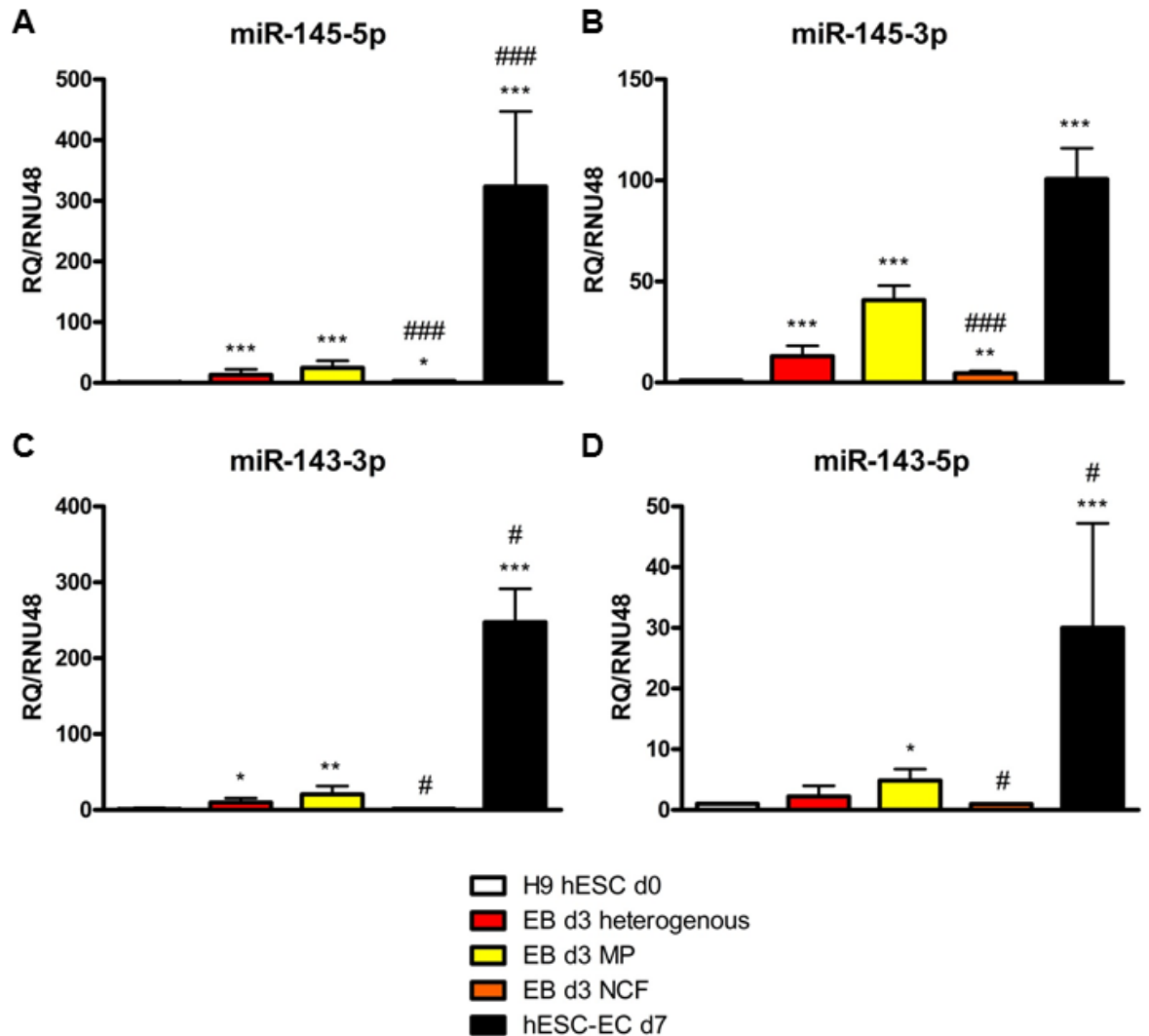


**Figure 5.17 – qRT-PCR validation of miR-143/145 cluster expression.**

Expression profiles of miR-145-5p (A), -145-3p (B) and -143-3p (C) were analysed in total RNA samples used for the microarray screen, plus a heterogeneous d3 samples, using Taqman® qRT-PCR. Additionally, the expression of the remaining miRNA in the cluster, miR-143-5p (D), was also examined. Histograms show RQ  $\pm$  RQ Max calculated relative to the RNU48 reference RNA. Repeated measures ANOVA with Tukey's post hoc comparisons was used to calculate significance; \* =  $p < 0.05$ , \*\* =  $p < 0.01$ , \*\*\* =  $p < 0.001$  vs d0 hESCs, # =  $p < 0.05$ , ### =  $p < 0.001$  vs d3 MP. Samples from  $n=4$  differentiation experiments. MP = mesoderm progenitor, NCF = negative cell fraction.

After validation in direct hESC-EC differentiation, expression levels were examined in total RNA samples from indirect hESC-EC differentiation. Analysis of these miRNAs in a linked, but independent, system allowed for initial investigations into their specificity; whether they are involved in general mesodermal, hemogenic endothelial or specifically EC specification of hESCs. Similarly to direct differentiation, all four of the mature miRNAs from the cluster share the same expression pattern, and are significantly upregulated throughout differentiation and, therefore, during commitment of cells to an EC phenotype (Figure 5.18A-D).

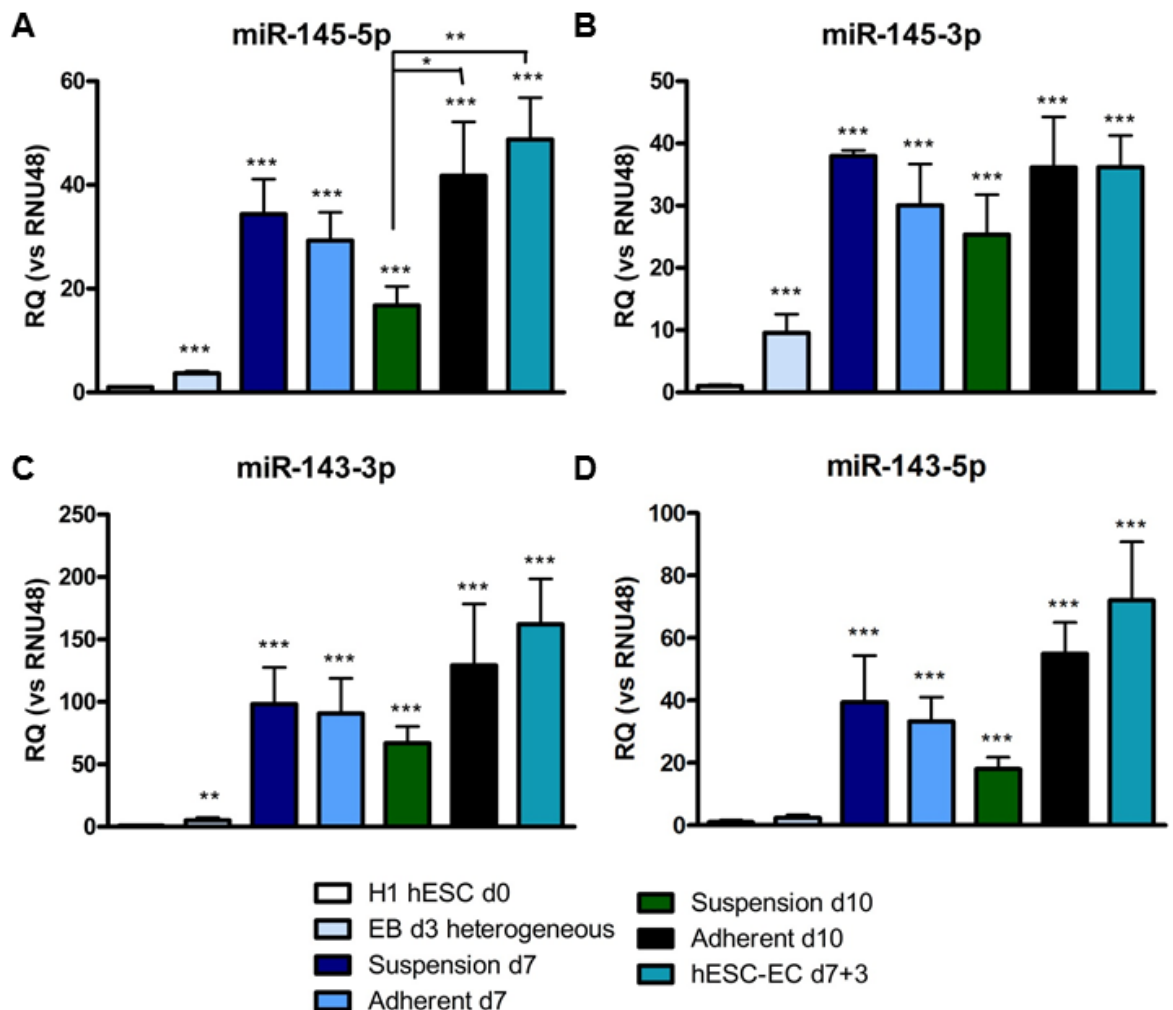


**Figure 5.18 – qRT-PCR analysis of miR-143/145 expression during indirect hESC-EC differentiation.**

Total RNA samples collected during indirect hESC-EC differentiation were assessed for the expression of miR-145-5p (A), -145-3p (B), -143-3p (C) and -143-5p (D). Histograms show RQ  $\pm$  RQ Max calculated relative to the RNU48 reference RNA. Repeated measures ANOVA with Tukey's post hoc comparisons was used to calculate significance; \* =  $p < 0.05$  \*\* =  $p < 0.01$ , \*\*\* =  $p < 0.001$  vs d0 hESCs, unless indicated.



The highest levels of expression for all four of the miRNAs appeared to be in d10 adherent or d7+3 hESC-EC samples, with a significant increase in expression in these groups when compared to d0 pluripotent hESCs (Figure 5.18). Additionally, although still higher than levels seen in d0 pluripotent controls, expression of the miR-143/145 cluster was lower in d10 suspension cells than adherent or d7+3 samples, and this difference was significant for miR-145-5p (Figure 5.18A). This may suggest that the miR-143/145 cluster has a role in differentiation to both hematopoietic and endothelial lineages, or in general mesodermal differentiation. High levels of upregulation at all time points after d3, but at slightly lower levels in d10 suspension cells, may suggest that these miRNAs are involved in endothelial specification, and their presence in d7 and d10 adherent cells is due to the presence of HE progenitors and ECs (as detailed in chapter 4).

All miRNAs, with the exception of miR-143-5p (Figure 5.18D), were shown to be significantly upregulated by d3, although all samples were heterogeneous d3 samples (Figure 5.18A-C), containing all cells present in EBs at this time point during indirect hESC-EC differentiation. Previous data (Chapter 4) showed that, although a high percentage of cells ( $\approx 40\%$ ) were CD326<sup>low</sup>CD56<sup>+</sup> MPs, there were a large number of non-CD326<sup>low</sup>CD56<sup>+</sup> MPs present at d3. Therefore, isolation and collection of total RNA from a purified CD326<sup>low</sup>CD56<sup>+</sup> MP cell population, in a similar way to that shown during direct hESC-EC differentiation, would be necessary to fully determine differences in expression between d0 pluripotent cells and d3 MPs, as well as between MP and NCF samples at d3. Although no significant difference is present between d0 and d3 for miR-143-5p in these samples, the heterogeneity may mask changes and, if d3 MP and NCF samples were isolated, large differences may become apparent.

Taken together, these data show that all four miRNAs from the miR-143/145 cluster have similar expression levels, and may all be regulated by the same mechanisms during hESC-EC differentiation. This, therefore, led to the hypothesis that this cluster plays an important role in mesodermal, hematoendothelial or endothelial specification of hESCs.

### 5.4.1.8 miR-483

Array data also suggested a potential role for the miR-483 stem loop in hESC-EC differentiation and mesodermal specification. A significant difference in expression of miR-483-3p was observed between d3 CD326<sup>low</sup>CD56<sup>+</sup> MP and NCF samples. The miR-483-5p strand, although not deemed to be significantly changed, had one of the largest fold changes, expressed  $\approx 9$ -fold higher in MPs than in NCF samples. Large variations in miR-483-5p expression in NCF samples may explain the high FDR value (0.087). When normalised intensities from the microarray screen (calculated as described in section 5.3.1) were plotted for all samples at all time points, it was observed that expression of this miRNA was increased throughout the duration of hESC-EC differentiation (Figure 5.19A-B). Moreover, both miR-483-3p (Figure 5.19A) and -5p (Figure 5.19B) exhibit a similar pattern of expression, with the exception of in d0 pluripotent hESCs, where miR-483-3p is undetected.

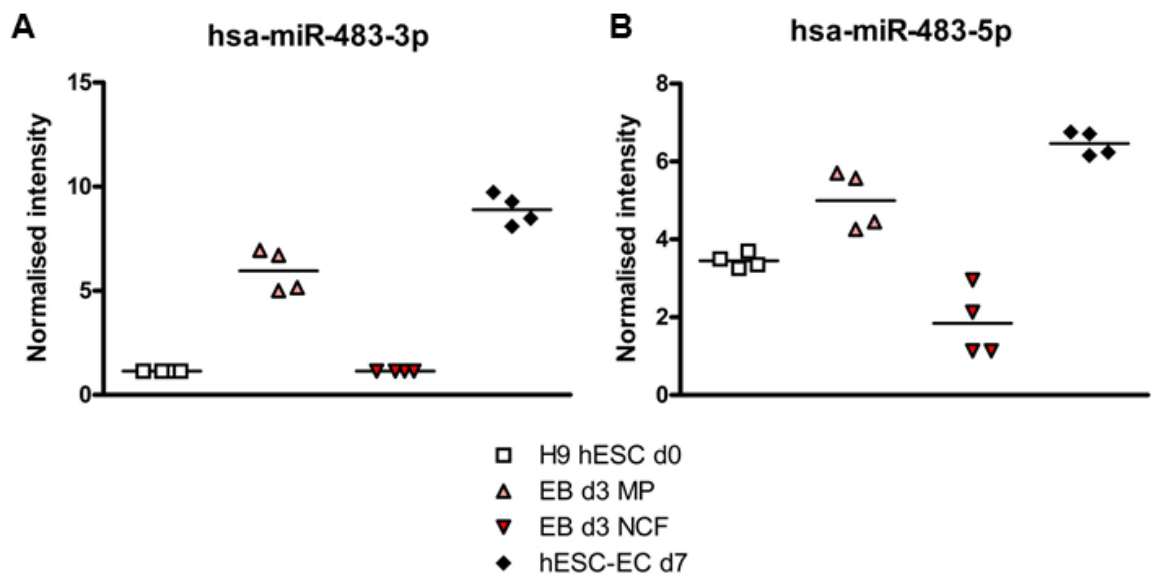


**Figure 5.19 – miR-483 stem loop expression.**

miR-483-3p (A) and miR-483-5p (B) were expressed at significantly higher levels in d3 CD326<sup>low</sup>CD56<sup>+</sup> MP cells than in d3 NCF samples when assessed using microarray technology. Dot plots show expression of these two miRNAs during d0-7 of direct hESC-EC differentiation. Individual points on the graphs represent values for each of the 4 samples in each group, with the line representing the mean value.

These findings were subsequently validated using qRT-PCR, in samples from both direct and indirect hESC-EC differentiation experiments. Both miR-483-3p and -5p were shown to be significantly upregulated in hESC-EC samples generated using the direct (Figure 5.20A-B) and indirect (Figure 5.20C-D) differentiation protocols, although the levels of upregulation were higher in samples taken from the direct system. Differences between the d3 MP and NCF fractions were also consistent with data collected from the microarray, when expression was validated using qRT-PCR. Levels of both miRNAs were shown to be significantly upregulated in d3 MPs (approximately 30 and 5-fold for miR-483-5p and -3p, respectively), when compared to d0 pluripotent hESCs, and also expressed a significantly higher level than in cells contained in the NCF samples (Figure 5.20A-B).

Similar differences in both -5p and -3p strand expression, combined with significantly higher levels of both miRNAs in MP cells, when compared to d3 NCF samples, led to the hypothesis that both strands of this miRNA stem loop are involved in the commitment and differentiation of hESCs the mesodermal and endothelial lineages. Data collected from the indirect differentiation system, showing significantly higher expression of both mature miRNAs in d7+3 hESC-ECs, than in d10 suspension HC cells, suggests that miR-483 specifically plays a role in endothelial specification, and not in hematopoietic specification. This is further supported by the observation that the levels of both miRNAs appear to decrease from d7 to d10 in suspension cells, as they become more committed to a hematopoietic phenotype (as described in chapter 4), although this difference is not significant (Figure 5.20C-D).

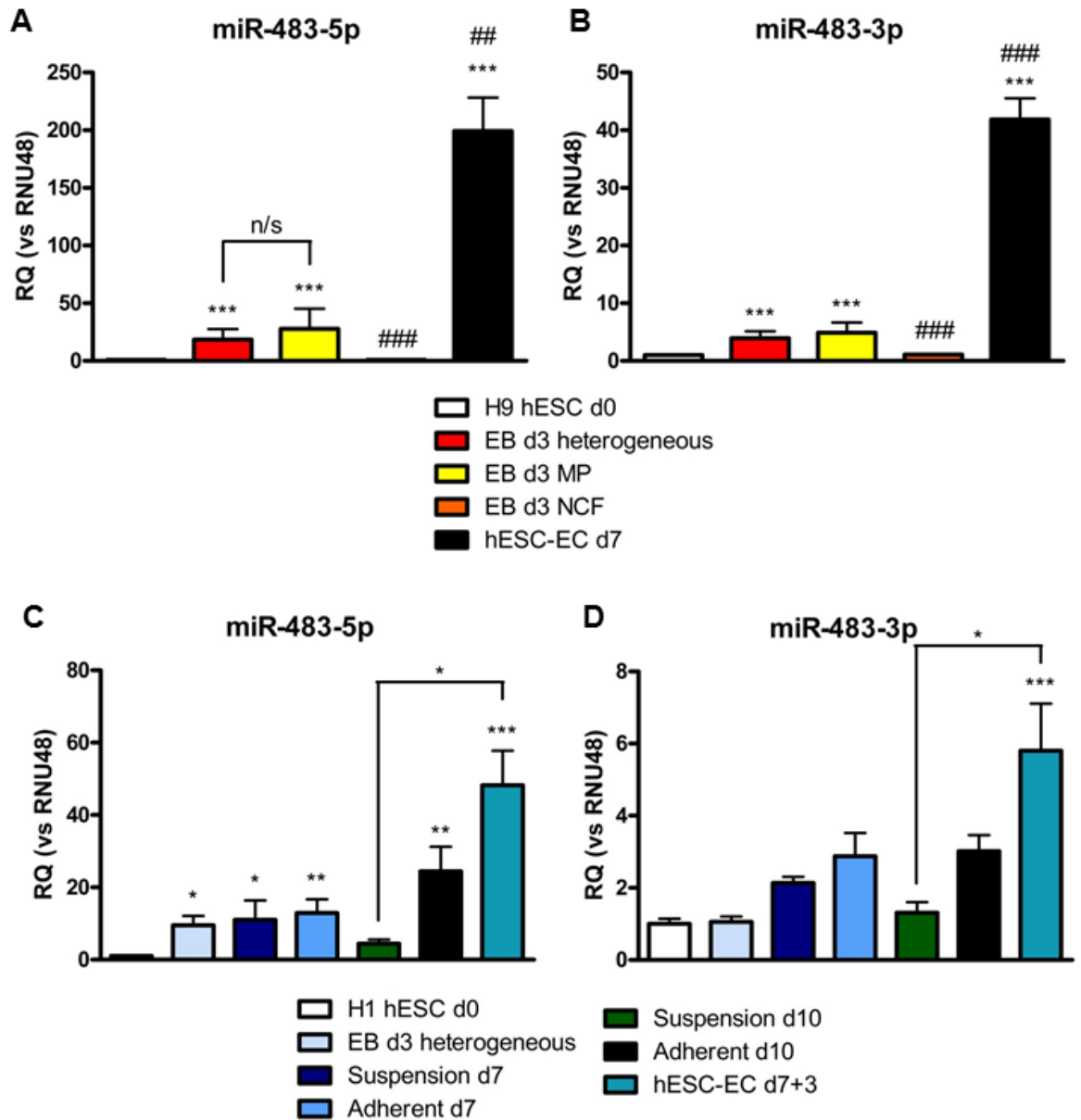


**Figure 5.20 – qRT-PCR validation of miR-483 expression during hESC-EC differentiation.**

Both strands of the miR-483 stem loop, -5p (A, C) and -3p (B, D), were assessed for expression in RNA samples taken from direct (A-B) and indirect (C-D) hESC-EC differentiation. Direct differentiation samples included FACSsorted CD326<sup>low</sup>CD56<sup>+</sup> MP and NCF samples, whereas FACSsorting was not performed during indirect differentiation. Histograms show RQ  $\pm$  RQ Max calculated relative to RNU48 reference RNA. Repeated measures ANOVA with Tukey's post hoc comparisons was used to calculate significance; \* =  $p < 0.05$  \*\* =  $p < 0.01$ , \*\*\* =  $p < 0.001$  vs d0 hESCs, unless indicated, for A-B ## =  $p < 0.01$ , ### =  $p < 0.001$  vs d3 MP. Samples from  $n=4$  differentiation experiments. MP = mesoderm progenitor, NCF = negative cell fraction, n/s = non-significant.

#### 5.4.1.9 miR-455

Finally, the microarray screen also demonstrated significant differences in the expression of both -5p and -3p strands of miR-455, when direct comparisons of d3 CD326<sup>low</sup>CD56<sup>+</sup> MP and NCF samples were performed. Again, when normalised intensities, obtained from the microarray screen, were plotted for each sample, an overall increase in expression was observed during hESC-EC differentiation (Figure 5.21A-B). Levels in the d3 MP samples were significantly higher than those in cells included in the d3 NCF in data from the microarray screen, although this could only be validated using qRT-PCR for miR-455-3p (Figure 5.21C-D). Both miR-455-3p and -5p were significantly upregulated in d3 MP and d7 hESC-EC samples, when compared to d0 pluripotent hESCs, although the upregulation was much smaller than that observed for both miR-483 and the miR-143/145 cluster. Because of this, coupled with the fact that there was no significant difference in miR-455-5p expression between d3 MP and NCF samples, it was hypothesised that this miRNA stem loop may not play an important role in EC differentiation. Therefore, it was decided that no further work would be performed involving miR-455.

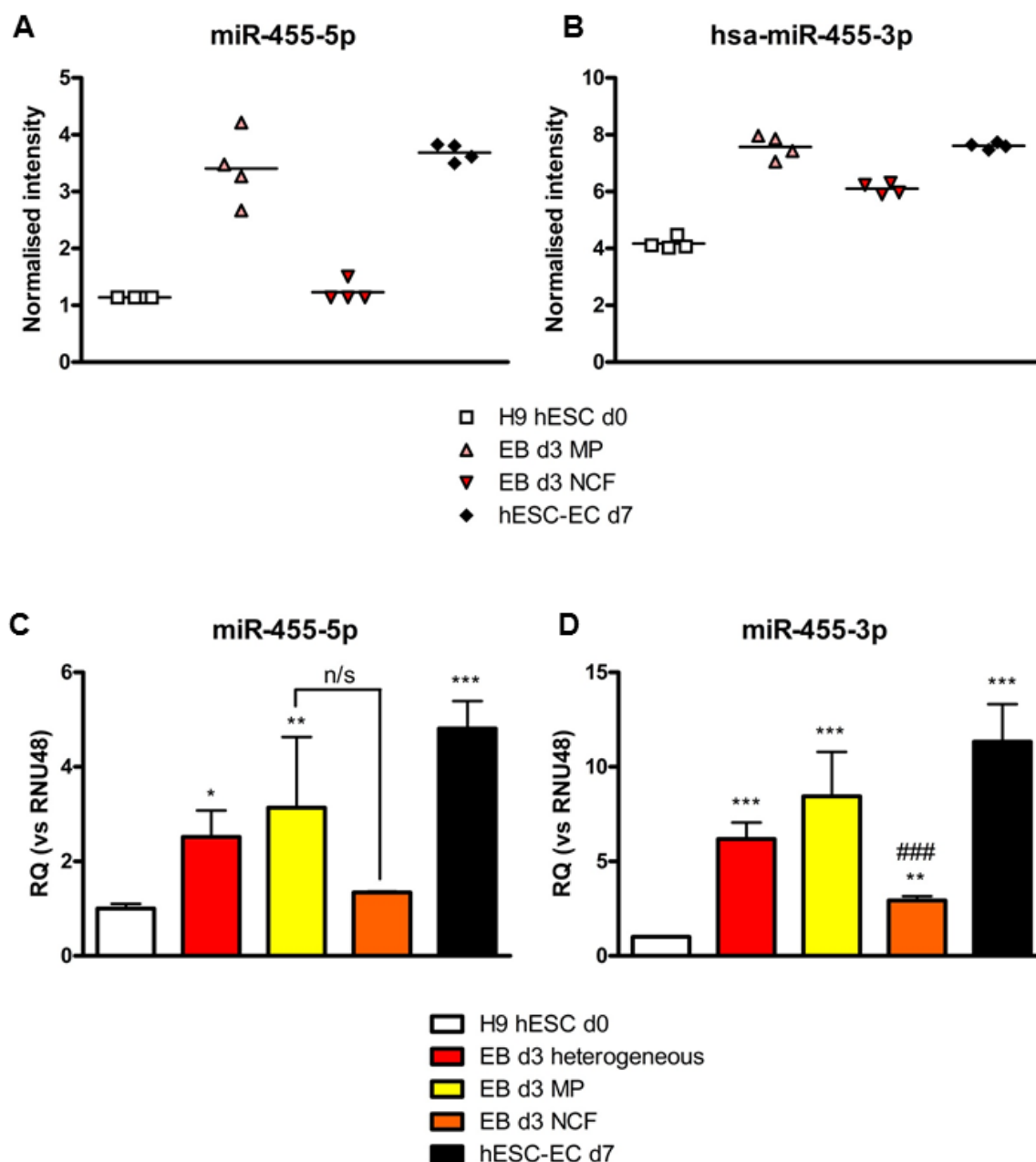


**Figure 5.21 – miR-455 during direct hESC-EC differentiation.**

Microarray analysis revealed that miR-455-5p (A) and miR-455-3p (B) were significantly changes between d3 MP and d3 NCF samples. Normalised intensities, obtained from miRNA microarray, for each sample are plotted above (A and B), with lines signifying the mean value for specified group. Taqman® qRT-PCR was employed for validation of these expression profiles in total RNA samples from direct hESC-EC differentiation (C and D). n=4 samples, statistical significance calculated using a repeated measures ANOVA with Tukey post hoc comparisons, \* =  $p < 0.05$ , \*\* =  $p < 0.01$ , \*\*\* =  $p < 0.001$  vs. d0 hESCs, ### =  $p < 0.001$  vs. d3 MP. MP =  $CD326^{low}CD56^{+}$  mesoderm progenitor, NCF = negative cell fraction, n/s = non-significant.

## 5.4.2 Modulation of miRNA during hESC-EC differentiation

Combined data from the microarray screen and qRT-PCR validation in both differentiation systems led to the hypothesis that the miR-483 stem loop plays an important role in hESC-EC specification, and that the miR-143/145 cluster may play an important role in mesodermal, endothelial or hematopoietic lineage specification.

To further investigate these hypotheses, experiments were performed to modulate the expression of miR-483 and the miR-143/145 cluster during hESC-EC differentiation. Initially, attempts were made to overexpress the miRNAs using lentiviral vectors. Known for their ability to integrate into the host genome, and therefore provide long term expression of a transgene, lentiviruses are a specific genus of retroviruses, and include human immunodeficiency virus 1 (HIV-1) (Naldini et al., 1996a, Naldini et al., 1996b, Buchsacher et al., 2000). Additionally, lentiviruses have the ability to infect both dividing and non-dividing cells, making them a powerful tool for transgene delivery both *in vitro* and *in vivo*. Although there have been significant improvements in methodology, hPSCs remain notoriously difficult to transfect (Villa-Diaz et al., 2010) and overexpression of miRNAs using pre-miRNAs can be challenging. Lentiviral-mediated miRNA delivery provides an efficient and long term method of overexpression in this system and was, therefore, chosen for use in this study.

Four different lentiviral vectors were generated; lenti-miR-143/145, for the overexpression of all four miRNAs from the 143/145 cluster, lenti-miR-143 and lenti-miR-145, for the overexpression of -3p and -5p strands of miR-143 and miR-145 individually, and lenti-miR-483, for the delivery and overexpression of the miR-483 stem loop.

### 5.4.2.1 Making lentiviral vectors

Initially, lenti-miR-143/145, lenti-miR-143 and lenti-miR-145 were generated. Briefly, miRNA transgenes were obtained using PCR amplification from the genome of H9 hESCs. This reaction was performed using the primers described in section 2.8.2 (Table 2.8). DNA gel electrophoresis was performed to ensure the correct genomic fragments had been amplified. Once confirmed, fragments were

subsequently ligated into the pcDNA<sup>TM</sup>3.3 plasmid, as described in section 2.8. After ligation into pcDNA<sup>TM</sup>3.3, plasmids were transfected into 293T cells to assess the expression of individual mature miRNAs (Figure 5.22).

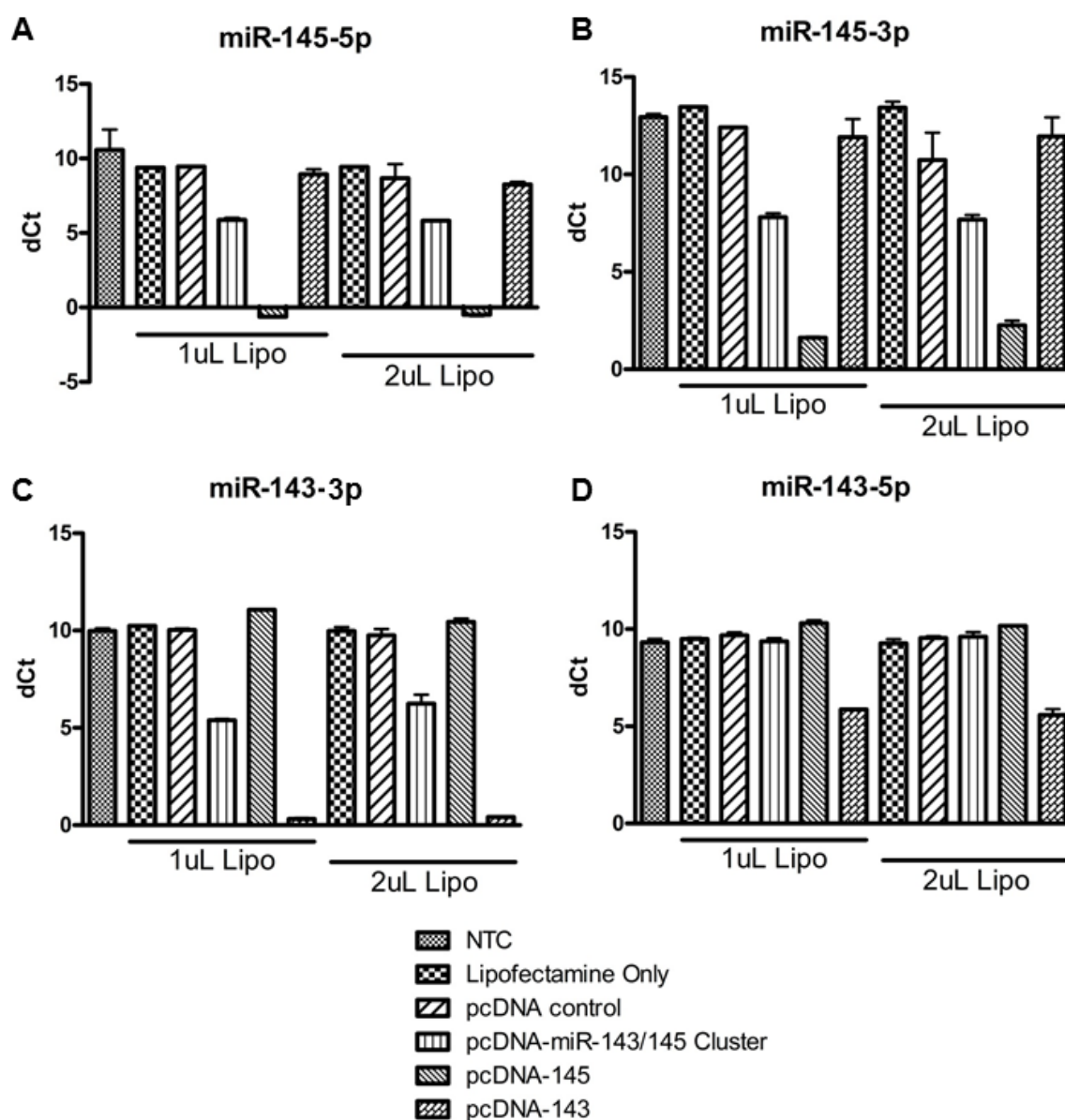


**Figure 5.22 – Transfection of pcDNA<sup>TM</sup>3.3(+)-miR-143/145 constructs in 293s.**

HEK 293s were seeded at a density of  $8 \times 10^4$  in a 12-well tissue culture plate. Transfections were performed using 1 or 2  $\mu$ L Lipofectamine<sup>®</sup> 2000 (indicated below graphs) and 1  $\mu$ g of plasmid DNA. Experiments were performed using pcDNA<sup>TM</sup>3.3-miR-143/145, pcDNA<sup>TM</sup>3.3-miR-143, pcDNA<sup>TM</sup>3.3-miR-145 and an empty pcDNA<sup>TM</sup>3.1(+) plasmid was used as a negative control. Lipofectamine only and NTC (non-transfected control) groups were also used as negative controls. Samples were assessed for expression of miR-145-5p (A), -145-3p (B), -143-3p (C) and -143-5p (D). n=2, data above is shown as dCt relative to RNU48 reference RNA (Ct miRNA of interest – Ct reference RNA). Low dCt values represent higher levels of expression.



Transfection with the pcDNA™3.3-miR-143/145 plasmid caused cells to overexpress miR-145-5p, -145-3p and -143-3p, as demonstrated by the lower dCt values (Figure 5.22A-C). The expression of miR-143-5p, however, did not appear to change after transfection (Figure 5.22D), although this may be due to the cell type used, and did not conclusively show that this miRNA is not expressed using this plasmid. Expression of both lead and passenger strands of miR-145 (Figure 5.22A-B) or -143 (Figure 5.22C-D) were modulated when cells were transfected with pcDNA™3.3-miR-145 or pcDNA™3.3-miR-143 respectively. No change in the expression of miR-143 (Figure 5.22C-D) was detected when cells transfected with pcDNA™3.3-miR-145, with the opposite true for pcDNA™3.3-miR-143 transfection (Figure 5.22A-B).

Although no overexpression of miR-143-5p was detected when cells transfected with the plasmid containing the miR-143/145 cluster, it was concluded that these fragments would be excised and ligated into the pSFFV plasmid. These reactions were performed as described in section 2.8, with digests performed using *MluI* and *XhoI* restriction endonucleases. Once generated, the pSFFV-miR-143/145, pSFFV-miR-145 and pSFFV-miR-143 constructs were used to generate lentiviral vectors, as described in section 2.9.

The pcDNA™3.1(+) plasmid containing the miR-483 transgene, coding for the entire miR-483 stem loop (including -3p and -5p strands), was purchased from Genearth (Life Technologies). From this construct, miR-483 was excised and ligated into the pSFFV plasmid, as described for miR-143/145.

#### **5.4.2.2 Initial optimisation of lentiviral doses**

In order to optimise the lentiviral dose needed for transduction of pluripotent hESCs, Lenti-GFP was used to infect cells at a range of MOI values, with the use of a vector containing a fluorescent label allowing for quantitative analysis of transduction via flow cytometry. The lenti-GFP vector contained the GFP gene under the control of the SFFV promoter, the same promoter used in the miR-143/145 and miR-483 constructs. H9 hESCs were seeded at a density of  $1 \times 10^5$  cells per well in a 12-well tissue culture dish. Lenti-GFP was added at an MOI of 5, 10 or 50, with virus containing medium removed after 24 h. As stated previously, MOI, or multiplicity of infection, relates to the number of viral

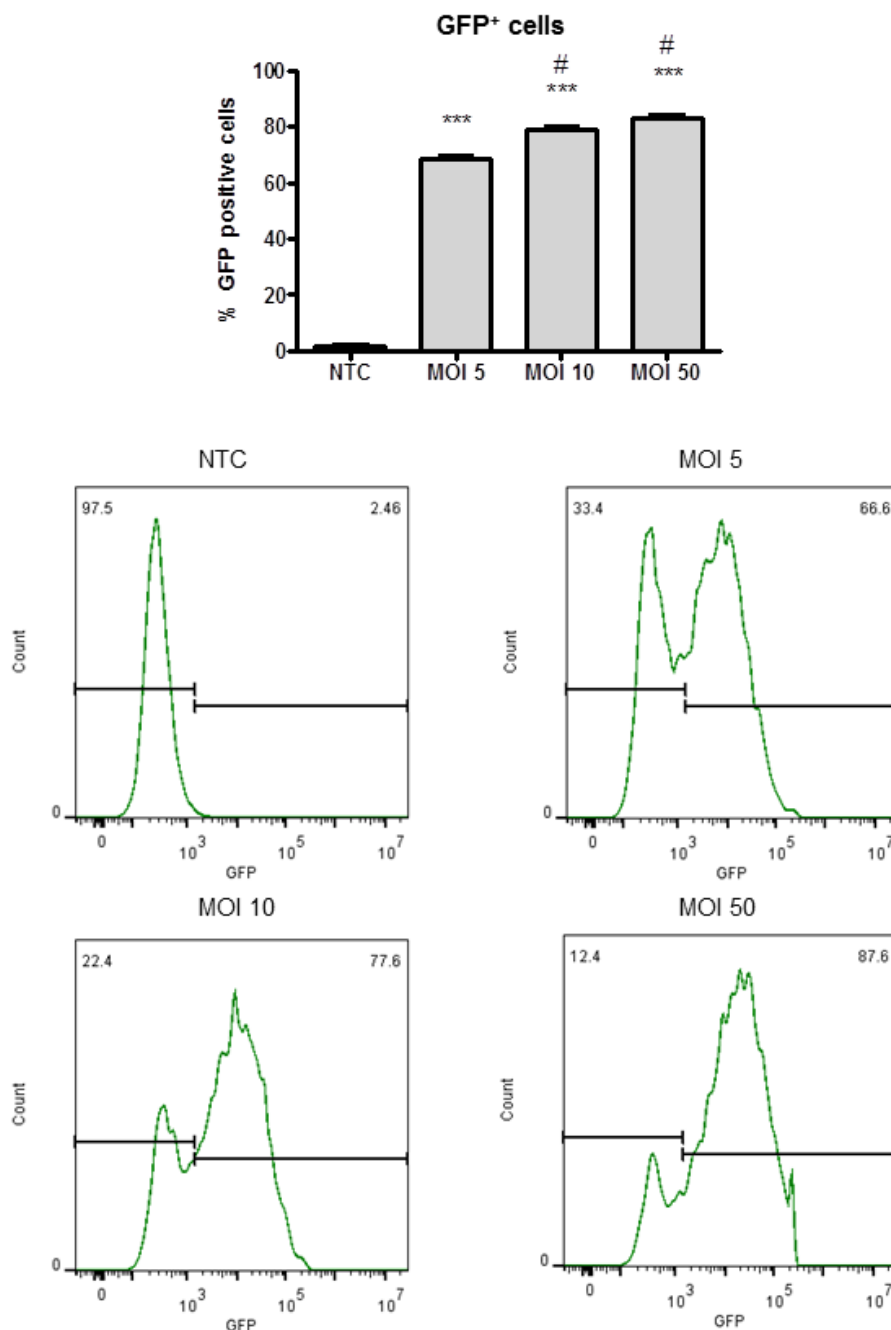


**Figure 5.23 – GFP transduction of hESCs.**

Pluripotent H9 hESCs were plated at a density of  $1 \times 10^5$  cells per well in a 12-well tissue culture dish. Cells were then transduced with Lenti-GFP at MOIs of 5, 10 and 50, with virus removed from media after 24 hours. Transduction efficiency was measured after 72 hours using flow cytometry. Average percentage of cells transduced from  $n=3$  experiments (A), and example flow cytometry histograms for each MOI (B) shown above. NTC = non-transduced control (no virus).

particles added per cell. Cells were harvested and percentage transduction was measured after 72 h, when the peak of lentivirus expression had been reached (Figure 5.23). The level of transduction was high at all MOIs, with significant increases in percentage of GFP<sup>+</sup> cells for all viral concentrations when compared to non-transduced controls (NTC). Additionally, the percentage of GFP<sup>+</sup> cells present at 72 h were significantly higher when cells were transduced with an MOI of 10 or 50, compared to cells treated with an MOI 5. Despite resulting in the

highest percentage of GFP<sup>+</sup> cells, infection using MOI 50 resulted in wide spread cell death. Therefore, from these data, it was decided that an MOI 10 would be used in subsequent experiments as a compromise between high transduction efficiency and low levels of cell death.

### **5.4.3 Modulation of miRNAs in hESCs and hESC-EC differentiation**

#### **5.4.3.1 miR-143/145 cluster**

Before use during hESC-EC differentiation, the lentiviral vectors for overexpression of miR-143/145, miR-143 and miR-145 was tested in HeLa cells, in order to ensure overexpression of miRNAs. Monolayer transduction of HeLa cell was performed using each virus at an MOI of 10 and 20, and cells analysed for miRNA expression after 72 h (Figure 5.24). In the interest of time and to conserve reagents, only the lead strand of each miRNA (miR-145-5p and miR-143-3p) was analysed. Both miR-145-5p (Figure 5.24A) and miR-143-3p (Figure 5.24B) were overexpressed when cells were transduced with lenti-miR-143/145 at both MOIs. Additionally, the expression of miR-143-3p was increased by similar levels ( $\approx$ 5-fold) when HeLa cells were infected using the lenti-miR-143 virus (Figure 5.24B). The lenti-miR-145 virus, however, only induced very small increases in miR-145-5p expression ( $\approx$ 2-fold for MOI 10 and  $\approx$ 2-fold for MOI 20; Figure 5.24A), despite the same transgene inducing marked overexpression of both miR-145-5p and -3p when transfected in the pcDNA 3.3 plasmid in 293T cells (Figure 5.22A). This may, however, be due to differences in expression between cell types and it was, therefore, decided to continue experiments using these viral vectors at an MOI of 10.

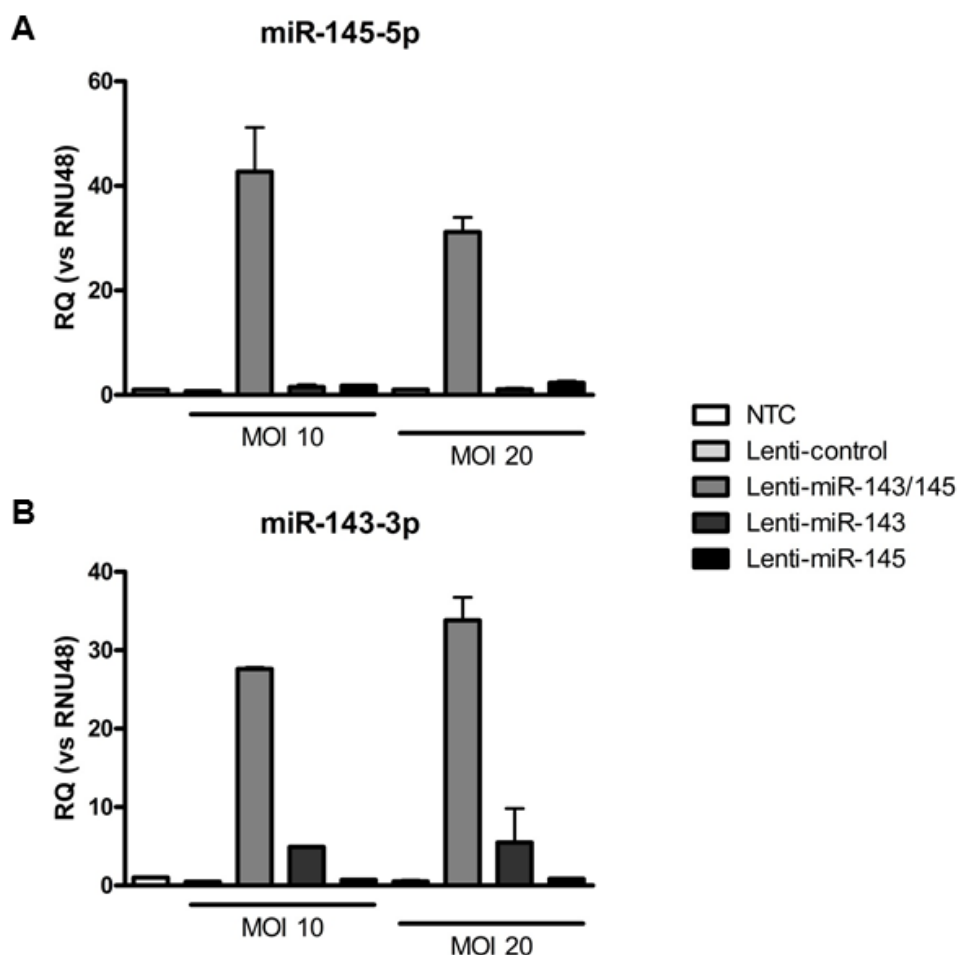


**Figure 5.24 – miR-143/145 overexpression in HeLa cells.**

Monolayer transduction of HeLa cells was performed to check overexpression of miR-143 and miR-145 by lenti-miR-143/145, lenti-miR-143 and lenti-miR-145. Viruses were used at 2 different doses; MOI 10 and MOI 20, indicated below x-axis. Analysis was performed on the two lead strands, miR-145-5p (A) and miR-143-3p (B) using qRT-PCR. n=2, data plotted is RQ  $\pm$  RQ Max.

After optimisation, experiments were performed using the generated lentiviral vectors during hESC-EC differentiation. Based on previous data, it was hypothesised that overexpression of the miR-143/145 cluster would cause an increase in differentiation efficiency, as cells are driven toward a mesodermal or EC phenotype.

As high levels of expression of the lentiviral construct had been observed 72 h post-transduction (Figure 5.22, Figure 5.23, Figure 5.24), cells were treated with viral vectors on d0, in order to overexpress miRNAs during hESC-EC differentiation. As shown previously, the initial step of direct hESC-EC differentiation involved the formation of size controlled EBs and, therefore, unlike in previous optimisation experiments, monolayer transduction of cells could not be performed. Instead, a protocol was developed to infect cells with lentiviral particles in suspension, immediately prior to EB formation. Initially, a

small pilot experiment was performed to ensure efficient transduction of cells during hESC-EC differentiation using this suspension-based protocol. Briefly, transduction was performed at d0, as described in section 2.10.2, using lenti-GFP or lenti-miR-143/145 at a concentration of MOI 10, alongside a non-transduced control (NTC) group. Differentiation was then allowed to progress to d3, where cells were harvested and analysed using flow cytometry and qRT-PCR. Using fluorescence imaging (Figure 5.25A) and flow cytometry (Figure 5.25B), high levels of GFP<sup>+</sup> cells (approximately 85%) were observed by d3 of hESC-EC differentiation, in samples infected with the lenti-GFP virus, when compared to the NTC sample group, as well as the lenti-miR-143/145 transduced group, as this virus did not contain a fluorescent label.

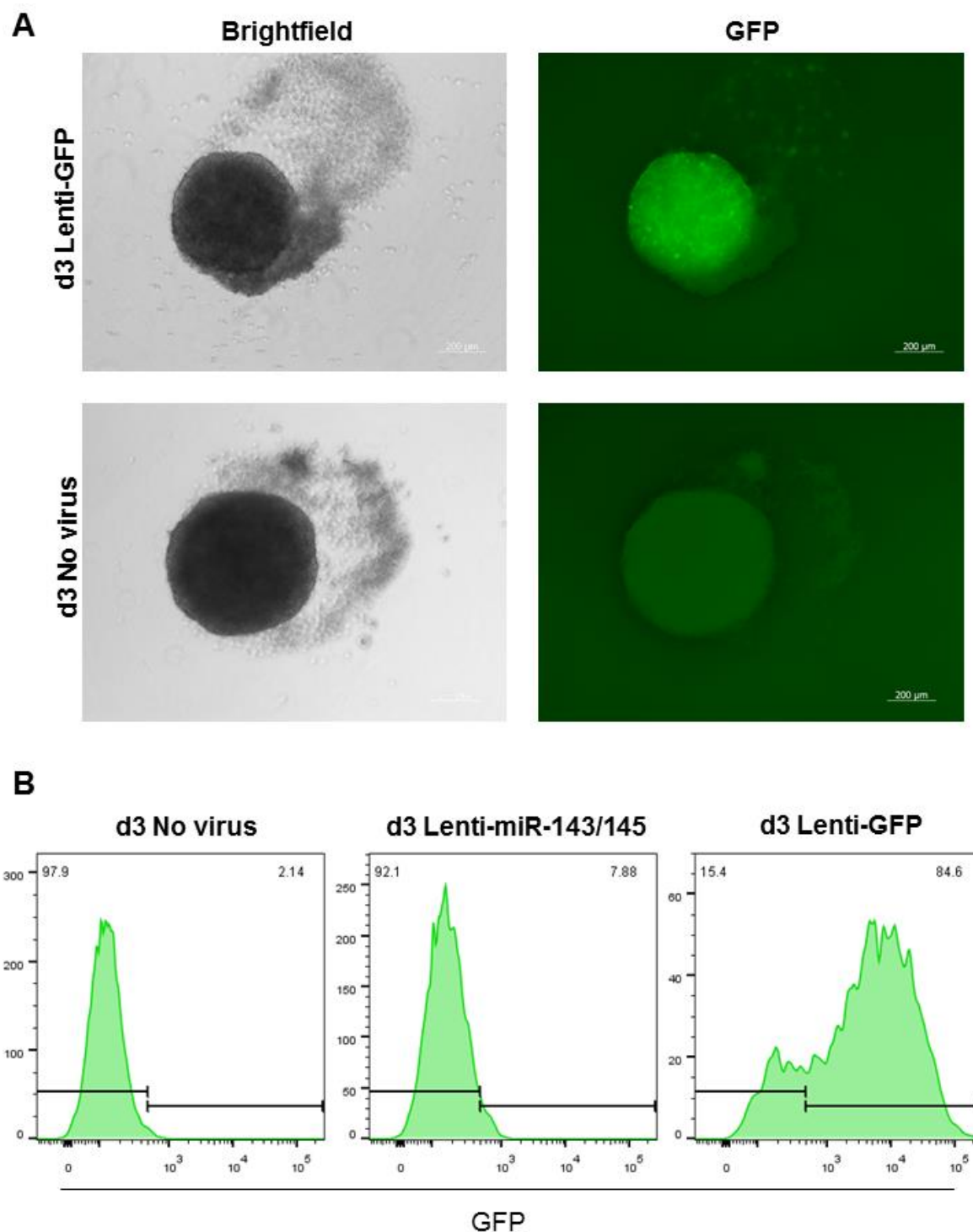


**Figure 5.25 – Preliminary testing of Lentiviral transduction – GFP expression on d3 of hESC-EC differentiation.**

D0 pluripotent H9 hESCs were infected with lenti-GFP, at an MOI of 10, to analyse transduction efficiency. Cells were imaged 72 h post-transduction when cells were still in the EB phase of direct hESC-EC differentiation (A). Scale bars represent 200  $\mu\text{m}$ . Cells were also harvested and analysed using flow cytometry (B). Gates show positive cells, with numbers representing numbers of cells in that gate. n=1.

Additionally, total RNA samples were taken at d0 and from all samples at d3, and the expression of miR-145-5p, -145-3p, -143-5p and -143-3p analysed, using Taqman® qRT-PCR (Figure 5.26A-D). As this was a preliminary study, only a single experimental replicate was performed and, therefore, RQ values could not be calculated. Instead, histograms were plotted using 'dCt' values, which describes the change in expression compared to the housekeeper or reference RNA, with lower Ct values signalling higher levels of expression. From the preliminary data, it was observed that all four miRNAs from the miR-143/145 cluster were overexpressed when cells were infected with the previously generated lenti-miR-143/145 vector, when an MOI of 10 was used. Although all four miRNAs were overexpressed to some extent, miR-145-5p (classically known as the miR-145 'lead' strand) was shown to have the highest level of expression (Figure 5.26A). These preliminary results demonstrated that the generated lentiviral vector, containing the miR-143/145 cluster, successfully overexpressed all four miRNAs to varying extents. Moreover, these results showed that infection of cells by lentivirus using the developed suspension-based protocol was successful, and this method could be used to modulate miRNA expression during a full-scale hESC-EC differentiation time course experiment. As only one experimental replicate was performed, however, no further conclusions could be made from these results.

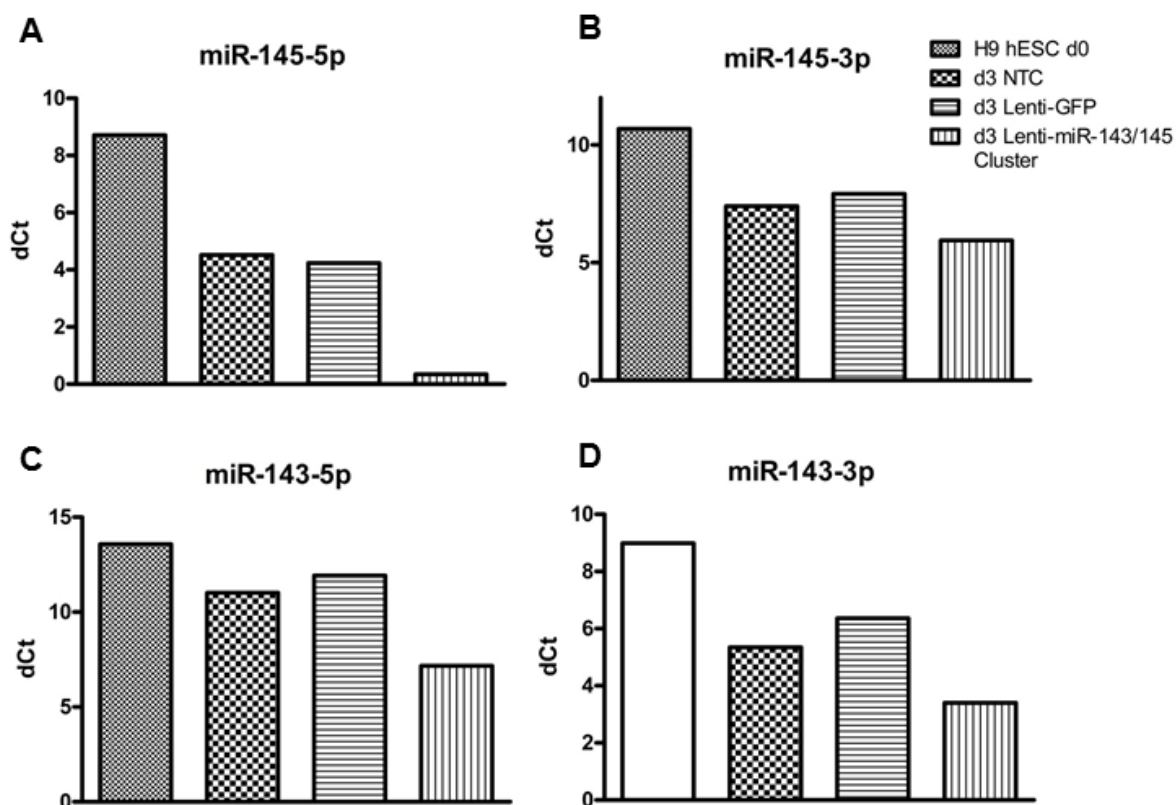


**Figure 5.26 – Initial analysis of miR-143/145 overexpression.**

Total RNA samples were collected from d0 pluripotent H9 hESCs, and all sample groups at d3, including NTC and lenti-GFP and lenti-miR-143/145 infected sample groups. Samples were analysed for expression of miR-145-5p (A), -145-3p (B), -143-5p (C) and -143-3p (D) to determine the success of lentiviral mediated overexpression. Data plotted is dCt, or the change in cycle threshold relative to the RNU48 reference RNA (RNU48 Ct – miRNA of interest Ct). n=1. NTC = non-transduced control/no virus.

Once it had been established that overexpression could be achieved using the generated lentiviral vectors at an MOI of 10, a larger scale experiment was designed to investigate the effect of miR-143/145 overexpression during direct hESC-EC differentiation. Pluripotent hESCs were infected at d0 as previously described (section 2.10.2) and differentiation was performed. Cells were harvested at d3 and d7, and the percentages of CD326<sup>low</sup>CD56<sup>+</sup> MPs and CD31<sup>+</sup>CD144<sup>+</sup> hESC-ECs assessed. Although significantly upregulated when compared to d0 pluripotent controls (data not shown), there was no significant difference in the percentages of cells positive for both CD31 and CD144 between control groups and those infected with the miRNA-overexpressing lentiviral vectors, when analysed using flow cytometry (Figure 5.27A). Cells were also analysed for the expression of these cell surface markers at d3 (data not shown), to determine if the appearance of CD31<sup>+</sup>CD144<sup>+</sup> hESC-ECs was earlier after overexpression of the miR-143/145 cluster, however, there was, similarly, no significant difference between all sample groups. When the percentage of CD326<sup>low</sup>CD56<sup>+</sup> MP cells was examined at d3, it was also observed that there was



no significant difference in the levels of cells displaying this cell surface marker profile between all sample groups (Figure 5.27B).

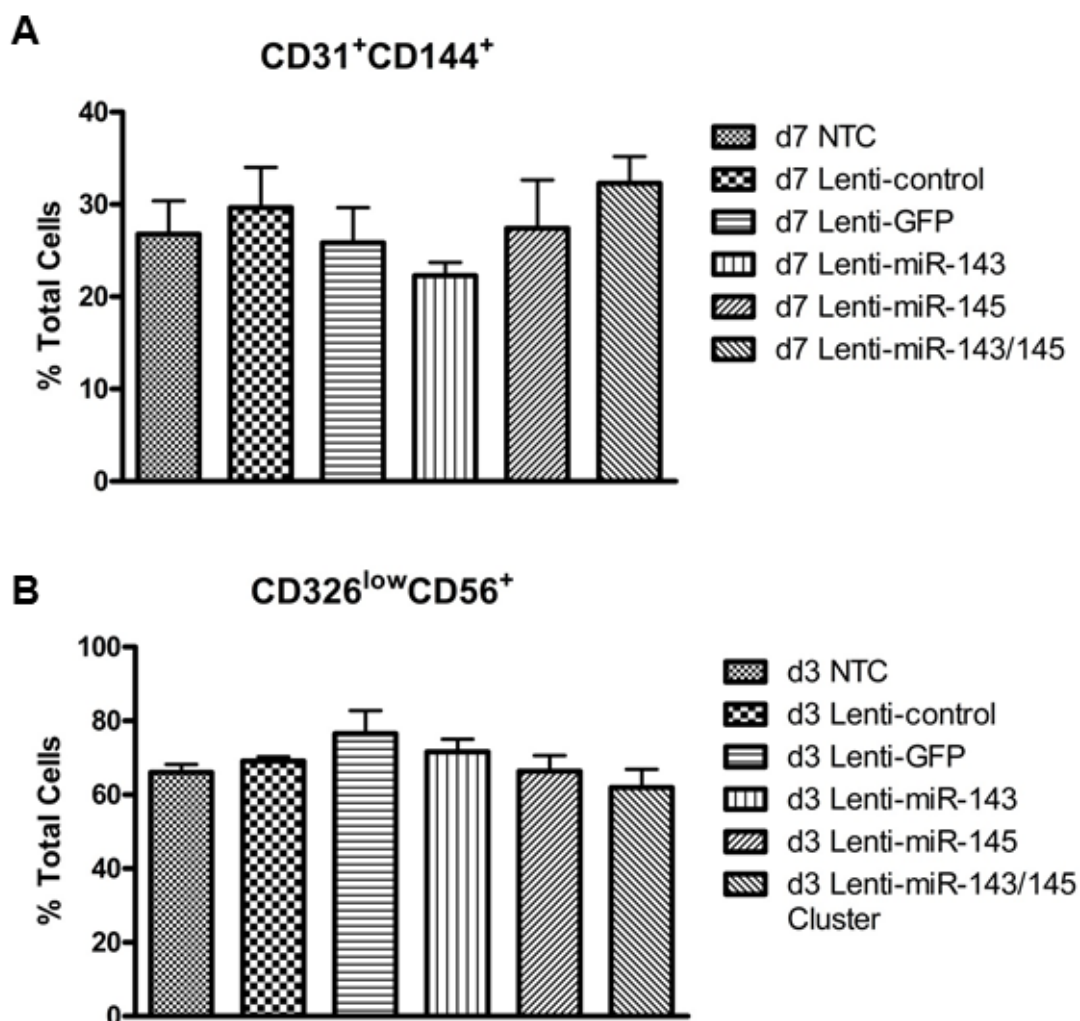


**Figure 5.27 – d7 CD31<sup>+</sup>CD144<sup>+</sup> and d3 CD326<sup>low</sup>CD56<sup>+</sup> populations after miR-143/145 overexpression.**

Infected cells were harvested at d7 (A), to assess the percentage of CD31<sup>+</sup>CD144<sup>+</sup> hESC-ECs, and at d3 (B), to examine the levels of CD326<sup>low</sup>CD56<sup>+</sup> MP cells, stained using specific antibodies and analysed using flow cytometry. Histograms above show average percentages of these populations over 3 experimental replicates. Lenti-miR-143/145 contained the entire cluster, with lenti-miR-143 and lenti-miR-145 containing only miR-143 and miR-145 respectively. Three different negative control groups were included in the analysis, NTC, lenti-GFP and lenti-control. NTC = non-transduced control/no virus. Statistical tests were performed using a repeated measures ANOVA with Tukey's post-hoc comparisons.

As there appeared to be no affect when miR-143 and/or miR-145 were expressed during direct hESC-EC differentiation, qRT-PCR was used to examine the expression of all four miRNAs in this cluster (miR-145-5p, -145-3p, -143-5p, -143-3p), in all sample groups at d0, 3 and 7 (Figure 5.27). In concurrence with previous data, all four miRNAs were shown to be significantly upregulated during hESC-EC differentiation when compared to d0 pluripotent hESC, with the highest levels of expression in samples taken on d7 of hESC-EC differentiation.

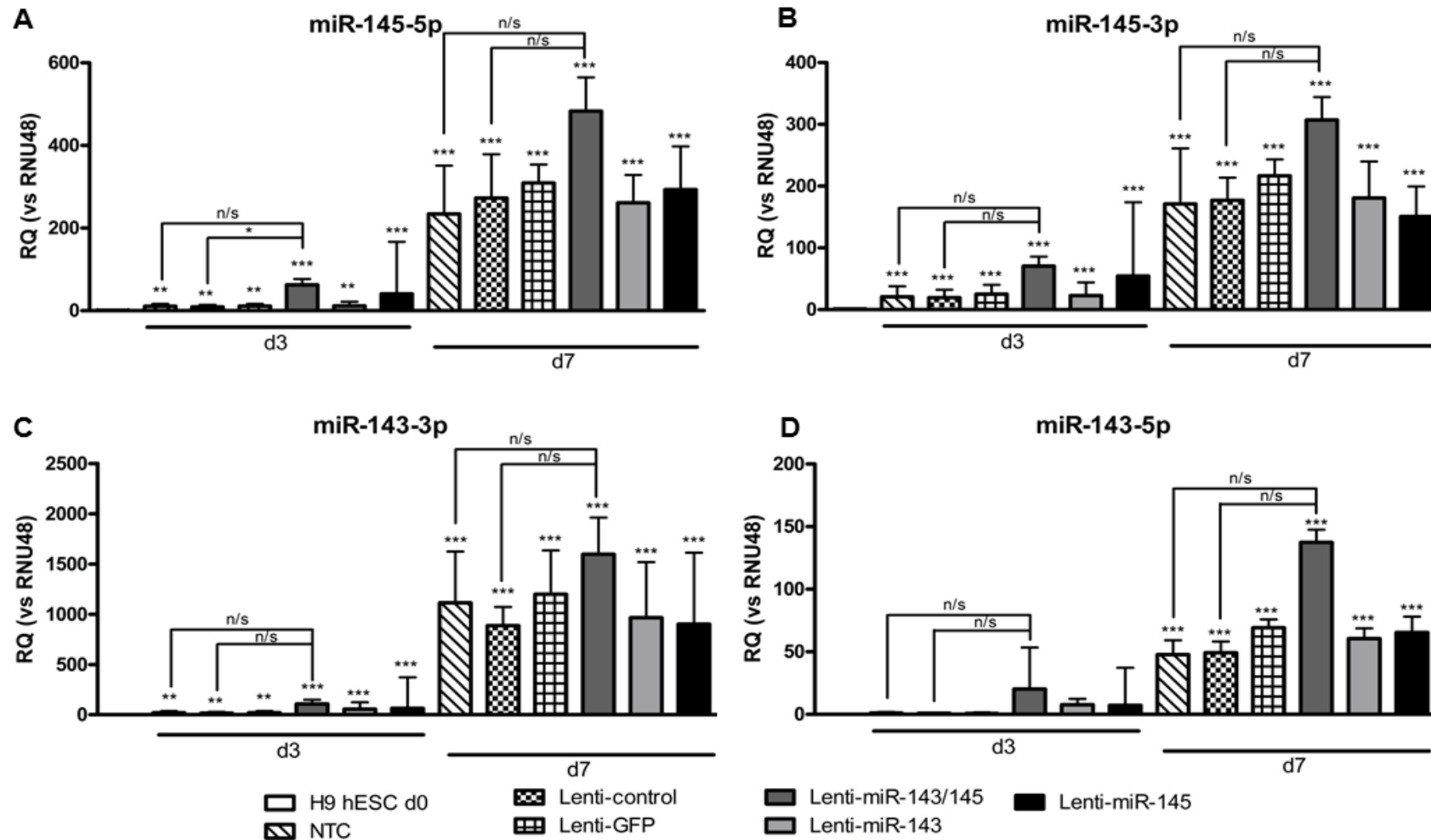


**Figure 5.28 – qRT-PCR analysis of miR-143/145 expression after viral transduction.**

Total RNA samples were taken from d0 pluripotent hESCs, and all sample groups at d3 and d7, including three control groups at each time point and samples transduced with lenti-miR-143/145, lenti-miR-145 and lenti-miR-143. Expression of miR-145-5p (A), -145-3p (B), -143-5p (C) and -143-3p (D) were assessed in all samples using qRT-PCR. Significance calculated using repeated measures ANOVA with Tukey's post hoc comparisons. \* =  $p < 0.05$ , \*\* =  $p < 0.01$ , \*\*\* =  $p < 0.001$  vs d0 pluripotent control, unless indicated. NTC = non-transduced control. Lenti-control = lenti containing an 'empty' pSFFV.

In terms of miRNA overexpression using the lentiviral vectors, the data was less positive. Expression of all four miRNAs appeared to be higher in RNA samples taken from cells infected with the lenti-miR-143/145, expressing the entire miR-143/145 cluster, however, the only significant difference was seen in miR-145-5p expression between d3 lenti-miR-143/145 infected samples and d3 lenti-control (Figure 5.28A).

This may, therefore, explain why there were no significant changes in the percentages of CD31<sup>+</sup>CD144<sup>+</sup> hESC-ECs and CD326<sup>low</sup>CD56<sup>+</sup> MPs during direct hESC-EC differentiation, in cells transduced with lenti-miR-143/145, lenti-miR-143 or lenti-miR-145.

#### 5.4.3.2 miR-483

Lentiviral vectors were also generated to allow for overexpression of miR-483 during hESC-EC differentiation. As for the miR-143/145 overexpressing lentiviral vectors, the overexpression of miR-483-3p and -5p after lenti-miR-483 infection was initially assessed using HeLa cells (Figure 5.29). The virus was used at two MOIs, 10 and 20, to ensure sufficient levels of overexpression were achieved.

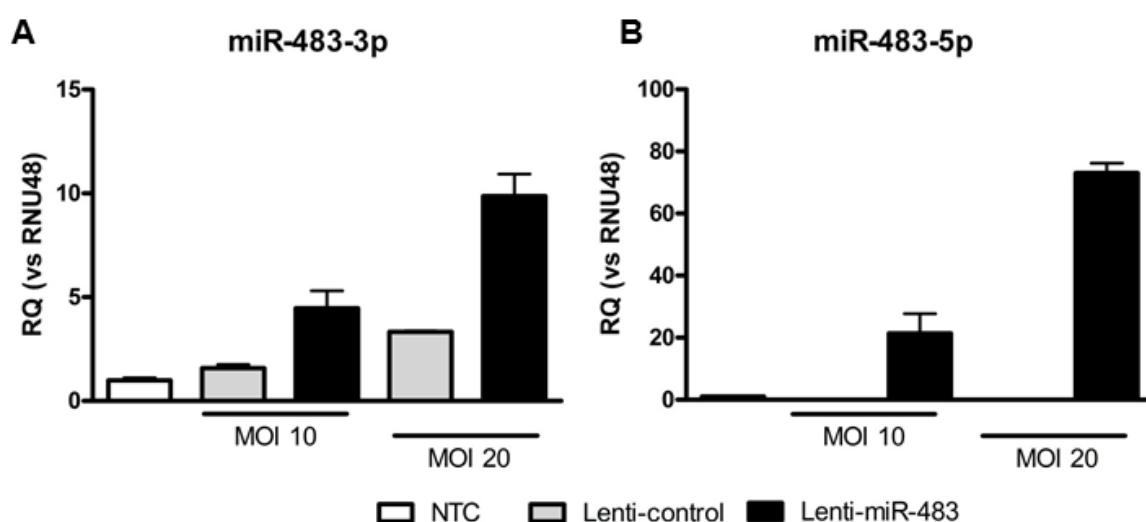


**Figure 5.29 – Lenti-miR-483 transduction of HeLa cells.**

Monolayer transduction of HeLa cells with lenti-miR-483 was performed, and RNA samples analysed to ensure sufficient overexpression of both -3p (A) and -5p (B) miR-483 strands. Virus was used at MOIs of 10 and 20, as indicated below graphs, and a lenti-control virus was used for comparison. n=2, data plotted is RQ ± RQ max.

Both -3p (Figure 5.29A) and -5p (Figure 5.29B) were overexpressed when cells were transduced using the generated lenti-miR-483 virus. Although overexpression was apparent when either concentration was used, cells transduced using an MOI of 20 demonstrated the highest level of expression for both mature miR-483 strands ( $\approx 10$ -fold and  $\approx 75$ -fold for miR-438-3p and -5p respectively). Cells transduced with an MOI of 10 also showed a marked increase in expression for both miRNAs, however, and, therefore, both concentrations were used during hESC-EC differentiation ( $\approx 5$ -fold and  $\approx 20$ -fold for -3p and -5p strands, respectively). Using both concentrations would allow for the observation of any dose-dependent response, as it may be hypothesised that increasing levels of miR-483 may drive the hESC-EC differentiation more efficiently, resulting in higher percentages of CD31<sup>+</sup>CD144<sup>+</sup> hESC-ECs by d7.

To test this hypothesis, d0 pluripotent H9 hESCs were infected with lenti-GFP, lenti-control or lenti-miR-483 at an MOI of 10 or 20, before they were differentiated using the direct hESC-EC system. Transduction was performed in suspension before the formation of size controlled EBs, as described in section 2.10.2, and cells were harvested and analysed at d3 and d7 for the presence of CD326<sup>low</sup>CD56<sup>+</sup> MPs (Figure 5.30A) and CD31<sup>+</sup>CD144<sup>+</sup> hESC-ECs (Figure 5.30B). Similarly to the results obtained with miR-143/145 overexpression, no significant difference in the percentage of d3 CD326<sup>low</sup>CD56<sup>+</sup> MP cells was observed between any of the sample groups (Figure 5.30A). Additionally, although the presence of CD31<sup>+</sup>CD144<sup>+</sup> hESC-ECs was demonstrated in all d7 samples, there were, again, no significant differences recorded between treatment groups (Figure 5.30B).

Taken together, these data show that overexpression of miR-483 does not increase hESC-EC differentiation efficiency, as demonstrated by the percentage of CD31<sup>+</sup>CD144<sup>+</sup> cells by d7 of direct differentiation.

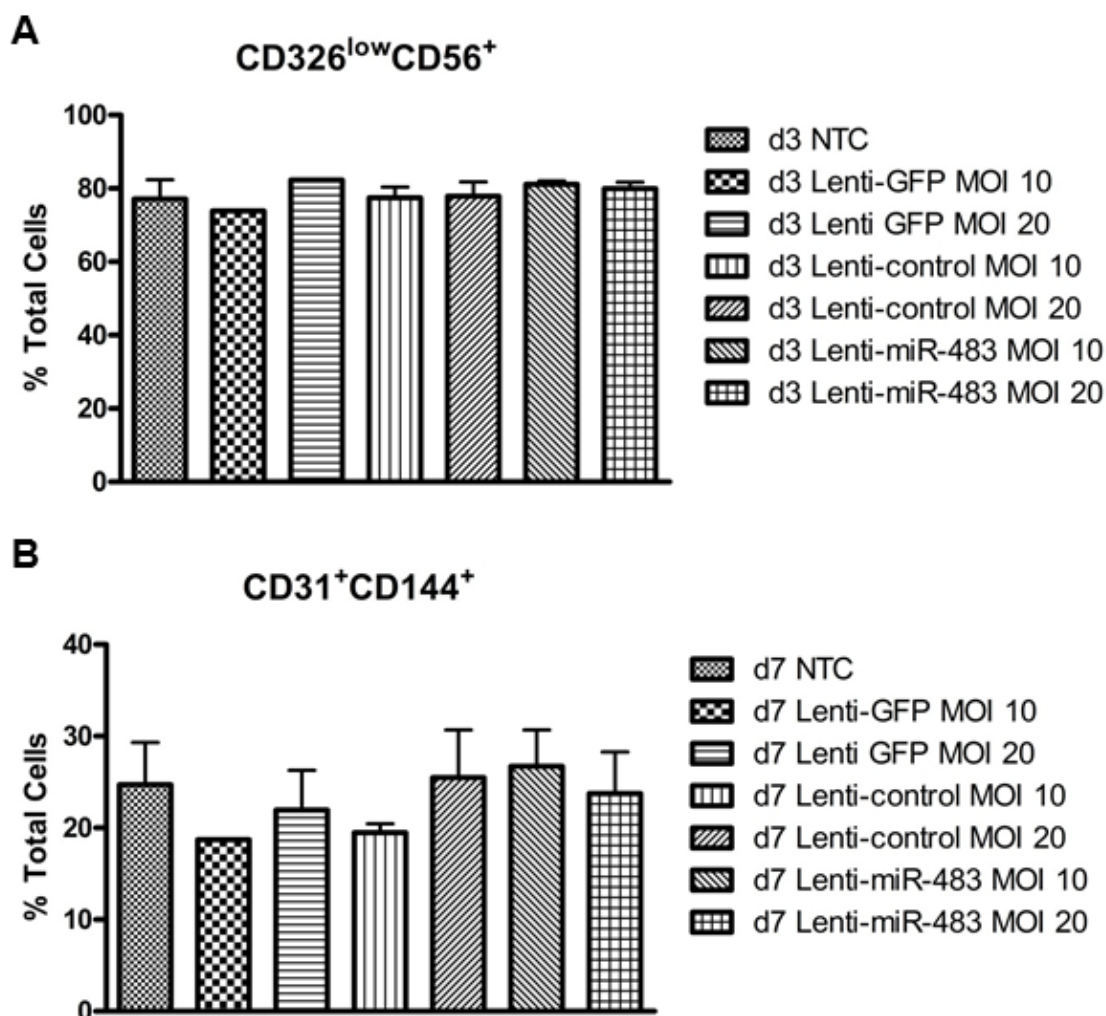


**Figure 5.30 - d7 CD31<sup>+</sup>CD144<sup>+</sup> and d3 CD326<sup>low</sup>CD56<sup>+</sup> populations after miR-483 overexpression.**

Infected cells were harvested at d3 (A), to assess the percentage of CD326<sup>low</sup>CD56<sup>+</sup> hESC-ECs, and at d7 (B), to examine the levels of CD31<sup>+</sup>CD144<sup>+</sup> MP cells, stained using specific antibodies and analysed using flow cytometry. Histograms above show average percentages of these populations over 3 experimental replicates, with the exception of d7 Lenti-GFP MOI 10, which was an experimental n=1. Three different negative control conditions included in the analysis, NTC, lenti-GFP and lenti-control. NTC = non-transduced control/no virus. Statistical tests were performed using a repeated measures ANOVA with Tukey's post-hoc comparisons.

## 5.5 Discussion

Governing of pluripotency and differentiation in hPSCs involves complex networks of genes, TFs, signalling networks and non-coding RNAs, which work together to tightly regulate these processes. Here, the presented studies focus on the identification and characterisation of novel miRNAs, with potential roles in commitment and lineage specification during hESC-EC differentiation, using microarray technology. Through comparisons performed between a purified CD326<sup>low</sup>CD56<sup>+</sup> MP and NCF samples, previously characterised in Chapter 3, it was demonstrated that -3p and -5p strands of three miRNA stem loops exhibited similar expression profiles; miR-145, miR-483 and miR-455. These stem loops were expressed at higher levels in MPs than in NCF samples, and were further upregulated by d7 of direct hESC-EC differentiation. Validation using qRT-PCR confirmed these expression patterns for miR-483 and miR-145, during both direct and indirect hESC-EC differentiation, and additionally identified miR-143, co-transcribed alongside miR-145 as part of the miR-143/145 cluster. Further modulation studies, aiming to understand the roles these miRNAs play during hESC-EC differentiation, however, were inconclusive, as overexpression of the identified miRNAs, using lentiviral vectors, did not show any significant differences in the percentages of either CD326<sup>low</sup>CD56<sup>+</sup> MPs at d3, or CD31<sup>+</sup>CD144<sup>+</sup> hESC-ECs at d7 of direct hESC-EC differentiation.

Using a global analysis, comparing all samples to d0 pluripotent controls, data collected from the microarray screen, and validation of results using Taqman® qRT-PCR, was also used to further characterise both the direct and indirect hESC-EC differentiation systems. The pluripotency-associated miR-302 family were shown to be downregulated as both differentiations progressed, demonstrating a loss in pluripotency. Furthermore, expression profiles of miR-302a and -302b mimicked those of pluripotency genes, such as *Nanog* and *Oct4*, as their expression was lower in CD326<sup>low</sup>CD56<sup>+</sup> MP cells, than in NCF samples on d3, strengthening conclusions made in Chapter 3, that these cells are rapidly losing their pluripotent phenotype. Endothelial-associated miRNAs, miR-126 and -10a, were shown to significantly increase as cells differentiated toward an EC phenotype, with the highest levels in d7 (direct) and d7+3 (indirect) hESC-ECs. Again, these findings are in concordance with gene expression data, further

strengthening the conclusion that d7 cells have become committed to an endothelial phenotype.

Additionally, these EC-associated miRNAs were shown to be expressed at higher levels in CD326<sup>low</sup>CD56<sup>+</sup> MPs than in NCF samples on d3, although the differences in expression did not reach significance. This complements data collected in Chapter 3, showing this same expression pattern in EC-associated genes *CD31* and *CD144*, and supports the hypothesis that these cells are already starting to develop an EC phenotype, although additional experiments would need to be performed to verify this. Furthermore, expression profiles of miR-302a and -302b mimicked those of pluripotency genes, such as *Nanog* and *Oct4*, as their expression was lower in CD326<sup>low</sup>CD56<sup>+</sup> MP cells, than in NCF samples on d3, strengthening conclusions made in Chapter 3, that these cells are rapidly losing their pluripotent phenotype.

Although expression of the majority of previously published miRNAs was similar when profiled within the presented differentiation systems, miR-200c and -150, shown by Luo and colleagues to be involved in the generation of EC from hESCs (Luo et al., 2013), exhibited very different patterns of expression from those previously demonstrated, with miR-150 undetected and miR-200c downregulated during hESC-EC differentiation. One explanation for these disparities are the inherent differences existing between distinct hESC lines. Luo et al. used the Shef hESC lines, obtained from the UK Stem Cell Bank, whereas H9 hESCs were used in this microarray. Previously, publications have demonstrated distinct differences between hESC lines in terms of gene expression, surface marker expression and differentiation bias, possibly due to variations in factors such as genetics and cell culture systems (Allegrucci et al., 2007, Wu et al., 2007). It may be the case that miRNA expression also varies between cell lines, therefore offering an explanation as to why miR-200c and miR-150 are not upregulated in this system. Additionally, differences between hESC-EC differentiation protocols may also explain why these miRNAs observed different expression profiles in the presented direct hESC-EC system. As stated previously, there has been an increasing emphasis on the development of fully defined differentiation and culture systems, in order to reduce the number of unknown factors present in the cellular environment. The system developed by Luo and colleagues involved the use of Matrigel, an undefined cell culture matrix (Luo et al., 2013), which

may have had an influence in signalling, gene and miRNA expression in this system. Furthermore, upregulation of EC-associated genes, although significant, was much lower in studies performed by Luo et al. ( $\approx$ 3-4-fold) than in the direct hESC-EC differentiation studies presented in Chapter 3 ( $>$ 1000-fold). Large variations existing between these two distinct differentiation systems may be, therefore, be responsible for the differences observed in the expression of miR-200c and -150 in these two systems. These findings highlight the need for standardised hESC culture and differentiation protocols, in order to elucidate key mechanisms involved in *in vitro* and *in vivo* lineage specification, an issue which has been previously studied (Denning et al., 2006).

During this study, miRNA overexpression was performed using lentiviral vectors coding for specific miRNA stem loop sequences. Using these vectors, miR-483 and the miR-143/145 cluster were overexpressed, as well as miR-143 and miR-145 individually, during hESC-EC differentiation. Although no significant differences were observed in the percentages of d3 CD326<sup>low</sup>CD56<sup>+</sup> MPs and d7 CD31<sup>+</sup>CD144<sup>+</sup> hESC-ECs between sample groups, this may not necessarily show that these miRNAs do not play a role during mesodermal and endothelial lineage specification. Previously, miR-145-5p has been shown to repress pluripotency through the targeting of Oct4, Sox2 and Klf4, TFs known to be involved in the regulation of the pluripotent phenotype (Xu et al., 2009). Xu and colleagues also demonstrated that overexpression of miR-145-5p in hESCs, through the use of a lentiviral vector, induced differentiation to both meso- and ectodermal lineages. Furthermore, a recent RNA Sequencing (RNA-Seq) experiment, performed in the lab of Professor Baker (data not shown), showed similar expression patterns for a number of lncRNAs whose genomic locations are in close proximity to the miR-143/145 cluster. Indeed, a number of these lncRNAs were shown to include the sequence of pri-miR-143 or -145. Taken together, these data suggest an important role for the miR-143/145 axis in this system, and therefore further investigation and optimisation will be necessary to elucidate this.

Firstly, the time point, at which lentiviral infection was performed may not be optimal and could be optimised. As cells were infected at d0 of hESC-EC differentiation, the peak of lentiviral-associated gene expression, which is thought to occur 72 h post-transduction, would coincide with the appearance of the d3 CD326<sup>low</sup>CD56<sup>+</sup> MP cell population. miRNA overexpression may, therefore,



not occur until cell fate has already been decided, sometime during d1-3 of hESC-EC differentiation. If overexpression of miR-143/145 or miR-483 does influence mesodermal commitment, the window for intervention may have already passed before expression is high enough to have a significant effect. To investigate this, experiments could be performed whereby hESCs are pre-treated with the miRNA-overexpressing lentivirus, before undergoing hESC-EC differentiation. This would allow for miRNA expression to reach a peak before any cell fate decisions were made, allowing definitive conclusions to be made as to whether these miRNAs are involved in mesodermal lineage commitment.

Analysis of miR-143/145 overexpression using qRT-PCR showed that although all miRNAs appear to be upregulated when hESCs transduced with relevant viral vectors, only miR-145-5p on d3, after lenti-miR-143/145 infection, was significantly changed when compared to the lenti-control sample group. Although this may suggest that a higher concentration of virus is needed in order to fully overexpress these miRNAs, it could also be due to a saturation of the system. As these miRNAs become upregulated during hESC-EC differentiation, it may be that overexpression cannot drive the system any further as it has already reached its limit. Instead, knock down experiments could be performed in order to reduce the expression of miR-143/145 or miR-483 to fully investigate their role in hESC-EC commitment. If these miRNAs do play an important role in EC specification and commitment, it would be hypothesised that a decrease in the expression of these miRNAs would result in a reduction in hESC-EC differentiation efficiency. One method of miRNA knockdown is the use of chemically modified, synthetically designed molecules which directly target the miRNA of interest, known as anti-miRNAs or antago-miRNAs. These molecules contain sequences complementary to a specific miRNA, allowing binding of the anti-miRNA, therefore inhibiting the interaction between the miRNA to its target mRNA. These molecules, however, are delivered to the cells via transfection. As stated previously, transfection efficiencies in hPSCs are notoriously low, and therefore knockdown of miRNA expression using anti-miRs or antago-miRs may not be the most practical method. Instead, genetic ablation using the Cas9 nuclease and clustered, regularly interspaced, short palindromic repeats (CRISPRs) system, a newly developed method for genetic modification, could be employed. The Cas9-CRISPR technology, first described in bacterial and archaeal

immunity (Bhaya et al., 2011, Wiedenheft et al., 2012), has been developed to produce a robust highly successful method for genomic editing (Mali et al., 2013, Ran et al., 2013, Shen et al., 2014). Having already been used for genetic modification of hPSCs (Rong et al., 2014), Cas9/CRISPR involves the use of an RNA-guided Cas9 nuclease to create targeted double stranded (DS) breaks in DNA. Depending on the mechanism of DS-break repair, either non-homologous end joining or homologous recombination, genes can be silenced, modified or inserted into the genome. This technology is currently being used within the laboratory to generate miR-143/145 mutant hESC lines, whereby the expression of one or both of the miRNAs in this cluster has been knocked out, which will be subsequently used to further investigate the roles of this cluster in hESC-EC lineage commitment and differentiation.

As shown, the mechanism of miRNA modulation presented here employs the use of lentiviral vectors. Although these vectors are highly efficient and the levels of hESC transduction high, the transgene is randomly integrated into the host genome and this can have serious detrimental effects, for example through activation of adjacent genes (Howe et al., 2008). Activation of genes adjacent to the insertion site and other problems associated with random integration may affect hESC-EC differentiation and may, therefore, mask significant effects caused through miRNA overexpression. To circumvent this problem, targeted insertion of miRNAs into the genome could have been used. Recently, Tay and colleagues demonstrated targeted transgene insertion into the *AAVS1* locus in hiPSCs (Tay et al., 2013). The *AAVS1* locus has been designated as a 'safe harbour' locus, as disruption of the genome in this region does not lead to any phenotypic effects in human cells (Smith et al., 2008, DeKelver et al., 2010). Furthermore, the aforementioned Cas9-CRISPR technology could be employed to efficiently insert specific miRNAs into the hESC genome for overexpression.

Although miR-143/145 and miR-483 expression was validated in samples from both direct and indirect hESC-EC differentiation, as well as in the control hematopoietic differentiation samples taken when using the indirect system, further studies could be performed to assess their expression during differentiation of cells to other lineages. For example, analysis of miR-143/145 and miR-483 expression levels during differentiation to other mesodermal lineages, such as cardiac, could be used alongside data already shown from

hematopoietic differentiation, to definitively assess whether changes in these miRNAs are restricted to hESC-EC differentiation, or whether they are more generally associated with mesodermal lineage commitment. Furthermore, profiling of these miRNAs in ectodermal and endodermal differentiation systems would distinguish between general differentiation-associated miRNAs, which may play roles in the inhibition of pluripotency, and those which are specifically driving cells toward a mesodermal cell fate.

First developed for high-throughput global analysis of changes in mRNA levels, microarray technology has been widely employed for global analysis of changes in miRNA expression during differentiation of hPSCs, and in the identification of novel miRNAs with predicted roles in these processes (Tzur et al., 2008, Wilson et al., 2010, Kane et al., 2012, Luo et al., 2013). As presented here, these screens produce large amounts of data, and analysis can be time consuming. Because of this, only a few of the differentially expressed miRNAs, identified using the miRNA screen, were chosen for validation and further investigation. As shown in Table 5.2, 50 miRNAs were differentially expressed between d3 MP and NCF samples, meaning a great deal of other miRNAs whose role could be investigated. Furthermore, there were large numbers of previously uncharacterised miRNAs whose expression was changed throughout direct hESC-EC differentiation (data not shown), whose roles in the system could also be examined further.

The use of microarray technology has a number of advantages, including the ability to profile expression of all identified miRNAs in large numbers of samples in parallel. Recently, however, there has been a move toward the use of RNA Sequencing, or RNA-Seq, and Next Generation sequencing (NGS) technologies. Briefly, RNA-Seq involves converting a population of RNA to a library of cDNA fragments and adding adaptors onto one or both ends. Experiments can be performed with or without amplification, and each molecule is sequenced in a high throughput manner, with resulting reads aligned to a reference genome (Wang et al., 2009). One advantage of RNA-Seq, in comparison to microarray, is the ability to identify novel RNAs, as it is not limited to the detection of previously recognised transcripts. Indeed, this technology has already been used to identify number of novel lncRNAs, including during hESC-EC differentiation system (Kurian et al., 2015). Furthermore, it is believed that RNA-Seq

technology has a much greater sensitivity for lowly expressed RNAs and, therefore, if instead of microarray technology in the presented study, may have identified an even greater cohort of miRNAs whose expression is differentially regulated throughout hESC-EC differentiation. Indeed, using this technology, the similarity of the miR-143-5p expression profile to the other miRNAs in the cluster may have been detected. Finally, publications have demonstrated that this technology can be used to profile changes in a variety different RNA types in parallel, including mRNAs, lncRNAs, miRNAs, small nucleolar-derived RNAs (snoRNAs) and piwi-interacting RNAs (piRNAs) (Muller et al., 2015). Collecting expression data for all of these RNAs allows for a better understanding of possible RNA:RNA interactions, such as miRNA:mRNA, thus helping assign potential functions to differentially regulated RNAs.

In conclusion, although miRNA overexpression presented here appears to be negative, there is a vast amount of work which could still be performed to investigate the role of miR-143/145 and miR-483, as well as other novel miRNAs identified using the microarray screen, in the differentiation and commitment of cells to both mesodermal and endothelial lineages.

## **Chapter 6    General Discussion**

## 6.1 Discussion

This thesis contains work concerned with identifying roles of specific miRNAs during the commitment and specification of hESCs to both mesodermal and endothelial lineages. hESC-ECs have translational potential in the treatment for ischemic diseases, such as PAD, whereby administration of cells would allow stimulation of angiogenesis and revascularisation of the ischemic tissue. Although the efficiencies of hESC-EC differentiation protocols are improving (Orlova et al., 2014c, Patsch et al., 2015), many require a sorting step to achieve purity. miRNAs have been demonstrated to play roles in a variety of biological processes and cellular functions. Numerous publications have described how specific miRNAs are differentially expressed during hESC-EC generation (Yoo et al., 2011b, Hassel et al., 2012, Kane et al., 2012, Yoo et al., 2012, Luo et al., 2013), and it was, therefore, hypothesised that identification of miRNAs playing essential roles in hESC-EC lineage commitment would allow for manipulation of the differentiation system, in order to increase efficiency and thus avoiding the need for cumbersome separation procedures.

Initially, two distinct protocols for the derivation of hESC-ECs were developed and characterised. The first was described as a direct hESC-EC differentiation system. In this method, H1 and H9 pluripotent hESCs were taken at d0 and allowed to form size controlled EBs, using a 96-well plate-based spin method, in the presence of a number of mesoderm- and endothelial-specifying cytokines and growth factors. After three days in these conditions, EBs were removed from wells, plated out onto gelatin coated tissue culture plates and cultured in endothelial conditions until d7. By d7, the appearance of CD31<sup>+</sup>CD144<sup>+</sup> hESC-ECs was observed, coupled with the downregulation of pluripotency-associated cell surface markers and TFs. Furthermore, it was demonstrated that positive selection of CD144<sup>+</sup> cells using MACS allowed for isolation of pure CD31<sup>+</sup>CD144<sup>+</sup> hESC-EC populations. The purified CD31<sup>+</sup>CD144<sup>+</sup> cells could then be replated, cultured and expanded, and by d14 cells were ≈100% positive for both CD31 and CD144, similar to previously published protocols (Luo et al., 2013, Orlova et al., 2014a, Patsch et al., 2015), and were able to form tubules when plated onto Matrigel. Recently, however, guidelines have been published suggesting that this method of measuring angiogenic potential and function is not specific, and in fact multiple other cell types, including VSMCs, fibroblasts and tumour cells are

able to form similar structures when seeded onto this matrix (Simons et al., 2015). Other *in vitro* angiogenesis assays could be performed using these d14 CD31<sup>+</sup>CD144<sup>+</sup> hESC-ECs, including 3D collagen or fibrin EC lumen formation and sprouting assays and EC-pericyte co-culture assays, as used by Orlova and colleagues (Orlova et al., 2014a).

During *in vivo* development, it has been demonstrated that the vascular and hematopoietic systems are closely linked (Bertrand et al., 2010, Boisset et al., 2010, Kissa et al., 2010, Azzoni et al., 2013). More recently, studies have demonstrated the presence of a bipotent specialised EC, or HE, within *in vitro* differentiation systems (Choi et al., 2009, Ditadi et al., 2015). With this knowledge, a second, indirect protocol for the production of hESC-ECs was developed. The development of a second, distinct hESC-EC differentiation protocol allowed for an additional system in which findings could be validated; candidate miRNAs function could also be investigated in this second system to specifically define whether their function was in endothelial or mesoderm commitment. Using a previously characterised hematopoietic differentiation system, existing within the laboratory of Dr Joanne Mountford, coupled with the marker profile identified by Choi and colleagues (Choi et al., 2012), a CD31<sup>+</sup>CD144<sup>+</sup>CD235a<sup>-</sup>CD43<sup>-</sup>CD73<sup>-</sup> HE progenitor was identified on d7 of differentiation. Optimisation experiments, shown in Chapter 4, demonstrated that if these d7 HE cells were placed into endothelial-supportive conditions, cells could be driven toward a more mature EC phenotype, with high percentages of CD31<sup>+</sup>CD144<sup>+</sup> hESC-ECs present at time point d7+3. Experiments to demonstrate the emergence of HP suspension cells from bipotent adherent HE cells could now be performed. Choi and colleagues use time-lapse imaging technology to visualise the production of CD43<sup>+</sup> suspension cells, directly from CD144<sup>+</sup> HE cells (Choi et al., 2012), and a similar technology could be used here. Furthermore, functional characterisation of generated d7+3 CD31<sup>+</sup>CD144<sup>+</sup> hESC-ECs must be performed.

To further investigate mechanisms, including the role of miRNAs, involved in hESC commitment to mesoderm and subsequent endothelial lineages, an early stage progenitor population was identified. Evseenko and had previously characterised a CD326<sup>-</sup>CD56<sup>+</sup> multipotent progenitor population, existing on d3.5 in a general mesodermal differentiation system (Evseenko et al., 2010). It was

demonstrated that these  $CD326^+CD56^+$  cells expressed high levels of mesoderm-associated genes and could differentiate to multiple mesodermal cell types, including ECs, hematopoietic cells, mesenchymal cells and cardiomyocytes, but were not able to form cells from the endo- or ectodermal lineages (Evseenko et al., 2010). After performing time course analyses using both the direct and indirect hESC-EC differentiation protocols, it was demonstrated that this population existed at d3 in both systems as a  $CD326^{low}CD56^+$  MP, with its appearance coinciding with the peak of mesoderm-associated genes such as *Brachyury* and *Mesp1*. Gene expression analysis of purified  $CD326^{low}CD56^+$  MP cells revealed high levels of mesoderm-associated genes, as well as significantly higher levels of *VEGFR2*, a gene commonly used to characterise early endothelial progenitor cells, than in the d3 NCF samples. Furthermore, the endothelial-associated genes *CD144* and *CD31* were significantly upregulated in  $CD326^{low}CD56^+$  MPs when compared to d0 pluripotent cells, whereas there was no change in their expression in the NCF samples. Taken together, the gene expression profile of these cells suggested that these  $CD326^{low}CD56^+$  cells were a definitive mesoderm or early stage endothelial progenitor population, or contained a smaller progenitor subpopulation of these progenitor cells, and this cell population was subsequently used to study early changes in miRNA expression. In addition to the work performed by Evseenko and colleagues, other studies have described other cell surface marker profiles for the characterisation of early mesodermal progenitor populations, including  $ROR2^+$  and  $APLNR^+PDGFR\alpha^+$  (Choi et al., 2012, Drukker et al., 2012). Therefore, further characterisation experiments could be performed, using large multicolour flow cytometry panels, as demonstrated in Chapter 4, to generate a more defined surface marker profile or to identify sub-populations of mesodermal or endothelial progenitors existing within this  $CD326^{low}CD56^+$  MP population. Furthermore, in depth gene expression profiling of  $CD326^{low}CD56^+$  MPs isolated during indirect hESC-EC differentiation could also provide insight into the exact phenotype of these cells, and whether they are identical to those observed during direct hESC-EC differentiation. Finally, experiments to differentiate the cells toward a variety of mesodermal lineages, such as cardiomyocytes or mesenchymal cells, must be performed. Testing the differentiation capacity of these cells would provide further evidence as to whether the  $CD326^{low}CD56^+$  MP cells, generated in this study, are biased toward endothelial differentiation, or



whether they still possess the capacity to differentiate to other mesodermal cell types.

After characterisation of the generated protocols, and identification of an early stage progenitor population, as described in Chapter 3 and 4, microarray technology was employed to evaluate global changes in miRNA expression during hESC-EC differentiation, as well as for the identification of novel candidate miRNAs with potential roles during endothelial specification and commitment. Both miR-126 and miR-10a have been shown to be involved in the regulation of EC function and angiogenesis (Fish et al., 2008, Wang et al., 2008c, Hassel et al., 2012), and an upregulation of these miRNAs was observed as hESC-EC differentiation progressed. Additionally, the pluripotency-associated miR-302 family was shown to be significantly downregulated during both direct and indirect differentiation. A study had previously identified a role for miR-145 in the inhibition of pluripotency during meso- and ectodermal differentiation of hESCs, via the targeting of pluripotent TFs *Oct4*, *Sox2* and *Klf4* (Xu et al., 2009). During screening and subsequent validation of miRNAs, both -3p and -5p strands of miR-145 were found to be regulated in a similar manner during hESC-EC differentiation, with higher levels in the d3 CD326<sup>low</sup>CD56<sup>+</sup> MPs than in NCF samples, and with a further increase in expression by d7. This was also coupled with an identical expression pattern for -3p and -5p strands of miR-143. These two miRNA stem loops are transcribed together as a cluster, and their role in VSMCs has been well documented (Robinson et al., 2012). It was also observed that both strands from the miR-483 stem loop, whose molecular function outside the field of cancer is relatively unknown, also exhibited this same expression profile. Classically, it was thought that only one of the mature miRNA strands from the pre-miRNA stem loop, referred to as the 'lead' strand had a biological function, with the other strand, known as the 'passenger' strand, thought to be targeted for degradation (Matranga et al., 2005). Recently, however, a number of publications have identified roles for these traditional 'passenger' miRNA molecules (Mah et al., 2010, Yang et al., 2011). Furthermore, miR-17-3p and -5p have been demonstrated to have complementary roles in prostate cancer and hepatocellular carcinoma (Shan et al., 2013, Yang et al., 2013).

miR-143/145 and miR-483 were, therefore, chosen as potential candidates, and work presented at the end of Chapter 5 demonstrated how modulation of these

miRNAs was performed, using lentiviral vectors, during direct hESC-EC differentiation. Although overall results showed no significant difference in either CD326<sup>low</sup>CD56<sup>+</sup> MP or CD31<sup>+</sup>CD144<sup>+</sup> hESC-EC populations, further optimisation of the time point at which lentiviral transduction is performed may still be beneficial. Moreover, overexpression could instead be performed using a Cas9/CRISPR system, whereby miRNA insertion is targeted to the AAVS1 locus (Smith et al., 2008, Ran et al., 2013, Tay et al., 2013, Rong et al., 2014). Alternatively, knockdown of these miRNAs using the Cas9/CRISPR system is currently being performed, and generation of miR-145, miR-143, miR-143/145 and miR-483 knockout lines would allow definitive evidence to suggest whether these miRNAs play crucial roles in specification and commitment of hPSCs toward mesodermal and endothelial lineages. In studies presented here, modulation was only performed during direct hESC-EC differentiation, and not in cells subject to differentiation using the indirect system. As stated previously, the development of this second system allows for an additional level of interrogation in terms of whether candidate miRNAs are specifically involved in endothelial commitment, mesodermal commitment, general differentiation, or in loss of pluripotency. Therefore, further work would involve the modulation of miR-143/145 and miR-483 during indirect hESC-EC differentiation.

## 6.2 Future perspectives

As stated previously, large amounts of data have been generated using the miRNA microarray screen documented in Chapter 5. Further analysis of this data may reveal other novel miRNAs with potential roles in hESC-EC differentiation. Although identification of miRNAs involved is relatively straightforward, using modulation studies to determine importance in a particular system, investigating exactly how miRNAs function, including their specific mRNA targets, is more challenging. Although numerous open access, easy-to-use target prediction algorithms are available, e.g. TargetScan ([http://www.targetscan.org/vert\\_70/](http://www.targetscan.org/vert_70/)) and miRWalk (Dweep et al., 2015), these programmes can often generate lists of thousands of predicted mRNA targets, based purely on matching of the miRNA seed sequence to a region in the 3'UTR of mRNAs. Alternatively, miRTarBase (Hsu et al., 2014) generates lists of experimentally validated miRNA targets; however, this also has disadvantages, as novel targets may be missed, particularly important as targets can be tissue and system specific. In order to

overcome these challenges a number of strategies can be used. Firstly, mRNA microarray analysis of samples where miRNAs have been modulated may provide an insight into mRNAs dysregulated after miRNA silencing or overexpression. Any potential targets identified using this technology may then be confirmed using luciferase reporter assays. As miRNA can function by either targeting of specific mRNAs for degradation, or by inhibition of mRNA translation, analysis of mRNA levels may miss targets not targeted for degradation. Therefore, proteomic screens may alternatively be used to analyse samples after miRNA modulation to identify targets. Ideally, these two technologies could be combined to generate a comprehensive list of potential targets for validation and further investigation. As well as large scale proteomic and mRNA screens, numerous studies have used RNA pull down experiments to identify specific miRNA targets. These pull downs are performed using antibodies specific for miRNA binding proteins, such as Ago2, to co-immunoprecipitate mRNA targets (Beitzinger et al., 2007), or by the use of synthetic biotinylated miRNA molecules, which can then be isolated using streptavidin beads (Orom et al., 2007). For even higher sensitivity, these two methods can be combined, to identify bona fide mRNA targets, where both the specific miRNA and RISC are bound.

As research progresses, our understanding of how gene expression is regulated is becoming increasingly complex. The field of non-coding RNAs is ever expanding and, most recently, lncRNAs have been implicated in the differentiation of hESCs, specifically toward mesodermal, endothelial and other cardiovascular lineages (Klattenhoff et al., 2013, Kurian et al., 2015). An RNA-Seq experiment has recently been performed within our laboratory, on samples taken from direct hESC-EC differentiation, from similar time points as those run on the miRNA microarray screen in the present study (H9 d0 pluripotent cells, d3 MPs, d3 NCF, d7 CD31<sup>+</sup>CD144<sup>+</sup> hESC-ECs). These newly collected data will be combined with that collected from the microarray screen to generate a comprehensive data set, which will allow for a better understanding of the roles of non-coding RNAs in this hESC-EC differentiation system.

In terms of hESC-ECs, there is much work still to be done in order to gain a deeper understanding of phenotype, function, and mechanisms which drive pluripotent cells toward this lineage. One major area for future investigation is the maturity of cells generated using hESCs and hiPSCs. Phenotypic analysis has

demonstrated that cells derived from hESCs and hiPSCs have characteristics which more closely resemble those seen in foetal cells, than in adults (Qiu et al., 2008, Baxter et al., 2015). For example, Chang and colleagues demonstrated that erythroid cells derived from H1 hESCs coexpressed high levels of embryonic and foetal globins, with almost no cells expressing adult globin (Chang et al., 2006). The generation of cells possessing foetal characteristics is logical, given the short time scales required to generate these cells *in vitro* and the relative stability of foetal cells *in vivo*. Research is now focusing on whether these cells can be driven from their current foetal phenotypes toward a more adult-like cell, and factors and mechanisms which may be involved in this switch (Chun et al., 2015). In the context of the presented study, investigation into the maturity of produced hESC-ECs must be performed. Studies may be performed to assess whether d7 hESC-ECs possess a foetal phenotype, and whether any maturation of cells occurs by d14, after purification and further culture of CD144<sup>+</sup> ECs. If d14 cells also possess a foetal phenotype, studies surrounding the switching of cells to an adult phenotype may be designed and performed. This could involve further culture of cells, or screening of small molecules and other factors which may be involved, including miRNAs and other non-coding RNAs. In terms of clinical relevance, hESC-generated cells such as cardiomyocytes and erythroid cells must possess an adult phenotype, due to differences in conduction velocity and oxygen affinity respectively. For hESC-ECs, however, it is not known whether cells possessing a foetal phenotype could be used therapeutically and, therefore, this is another aspect which must be investigated. To date, there have been no published studies which extensively investigate characteristic and phenotypic differences between foetal and adult ECs, although comparisons between foetal ECs isolated from different organs have been performed (Invernici et al., 2005). As no obvious differences exist, for example in size or structure, it may be that the maturity of these cells would have no implications for their use in the clinic. Furthermore, with this in mind, it may be suggested that the use of adult EC types, such as HUVECs, as a positive control in hESC-EC studies may be misrepresentative, and foetal ECs would be a more relevant comparison (Baxter et al., 2015).

Moreover, if generated hESC-ECs do possess a foetal-like phenotype, studies could be performed to attempt to drive these immature cells toward a specific

adult EC phenotype e.g. venous, arterial or lymphatic ECs. The ability to produce specific EC types would potentially allow for the development of specialised cell therapies for different ischemic diseases, for example arterial ECs for the treatment of PAD and CLI. Generation of fluorescent reporter hESC lines, whereby a reporter gene, such as GFP or mCherry, is under the control of a promoter associated with arterial, venous or lymphatic specification would allow for large scale, high-throughput screening experiments to identify small molecules or growth factors which drive cells towards each specific lineage. These data could then be used to optimise hESC-EC differentiations to produce ECs with specific phenotypes and characteristics.

Ultimately, it is hoped hPSC-ECs will provide a potentially unlimited source of functional, transplantable cells for the treatment of ischemic diseases. Overall, however, hPSC-derived cell therapies still have a number of obstacles to overcome if they are to make it into routine clinical practice, including safety concerns in terms of tumourgenicity and immune rejection. While the presented studies have focused on the use of hESCs in the generation of ECs, it is hiPSCs, generated from the reprogramming of terminally differentiated somatic cells (Takahashi et al., 2007), which are thought to have the greatest potential in terms of both cell therapies and *in vitro* disease modelling. Therefore, further experiments should be performed to determine whether the presented direct and indirect hESC-EC differentiation protocols are transferrable to hiPSC lines. Theoretically, the use of patient-specific iPSCs would overcome the problem of immune rejection as transplantation would be autologous, however, some studies have suggested that, despite this, these cells may also elicit specific immune responses (Fu, 2014).

Furthermore, standardisation of hPSC culture conditions and differentiation systems, as well as the standardisation of assays used to characterise both pluripotent and generated cells, represents one major hurdle in the development of cell therapies. Although some efforts have been made to standardise conditions (Denning et al., 2006), differences existing between hESC and hiPSC lines, possibly caused due to differences in derivation techniques, mean that often differentiation and culture systems are non-transferrable. For example, differences were observed in hESC-EC differentiation efficiencies between H1 and H9 hESC lines, both generated in the same laboratory, during

studies shown in Chapter 3. If, as stated previously, patient-specific iPSCs were to be generated for the development of personalised medicine, standardised protocols would be required in order to ensure that differentiation was possible for all hiPSCs derived from any patient. Standardisation of differentiation conditions is also important for the investigation of specific mechanisms involved. This is evident from data presented in Chapter 6 of this study, whereby miR-200c and miR-150, previously shown to be upregulated in an alternative hESC-EC differentiation system (Luo et al., 2013), were downregulated and undetected during the described direct hESC-EC differentiation, respectively.

Although studying miRNA functions during hESC differentiation and commitment is a useful tool to understand exact mechanisms and signalling pathways involved during these complex processes, it would be difficult to translate this clinically. Manipulation of miRNA expression levels is a commonly used technique *in vitro* in order to increase hESC differentiation efficiencies, however, the majority of techniques used, including lentiviral vectors and Cas9/CRISPR technology, involves either random or targeted modification of the genome. Clinical use of cells containing genetic modifications may be an issue. Therefore, instead of using miRNA modulation to directly increase differentiation efficiency, it may be preferable to use small molecules, growth factors or inhibitors to target the same signalling pathways. These factors could be easily added to a differentiation system to drive hESC-EC production, or the production of other PSC-derived cell types. Alternatively, investigation of miRNA and their functions during hESC-EC differentiation could also be used to directly stimulate endogenous repair and regeneration mechanisms *in vivo*. Factors directly targeting pathways and mechanisms, affected by the changes in miRNA expression during *in vitro* differentiation, could possibly be directly administered to a patient in order to stimulate angiogenesis in an ischemic limb, therefore, circumventing numerous problems associated with cellular-based therapies. It is, therefore, imperative that improvements are made in technologies used to elucidate miRNA targets and mechanisms.

Finally, research has also begun to focus on the development of transdifferentiation techniques, as a new approach for the generation of a variety of specific cell types for transplantation or use in various cell therapies. Briefly, transdifferentiation involves the direct conversion of one terminally

differentiated or multipotent adult stem cell type to another, different, cell type. Although the mechanisms governing transdifferentiation are relatively unknown, a number of studies have achieved success via the overexpression of specific TFs (Wang et al., 2015). More recently, it has been demonstrated that, much like during iPSC generation and reprogramming, miRNAs can be used during *in vitro* transdifferentiation. Originally, Yoo et al. demonstrated that lentivirus mediated delivery of the miR-9 stem loop (containing both -3p and -5p strands) and miR-124 to human fibroblasts induced expression of the neuron-specific marker Map2 (Yoo et al., 2011a). Furthermore, when these miRNAs were used alongside the neurogenic TF Neurod-2, the efficiency of the conversion was increased. Leading on from this, Jayawardena and colleagues used only miRNAs to directly reprogramme fibroblasts to cardiomyocyte-like cells (Jayawardena et al., 2012). In this study, they showed that transient transfection of miR-1, -133, -208 and -499 in combination resulted in this switch in cell fate, demonstrated by the expression of mature cardiomyocyte markers, sarcomeric organisation and exhibition of spontaneous calcium flux characteristics. From this, it may be hypothesised that any miRNA involved in commitment of cells to the endothelial lineage, as well as those involved during the later stages of differentiation, could be used during transdifferentiation of cells to an endothelial fate. Additional knowledge of the roles of specific miRNAs during the generation of hESC-ECs may, therefore, be valuable in the production of vascular cells for cellular therapy via direct reprogramming.

### 6.3 Concluding remarks

In summary, the findings presented in this thesis confirm vast changes in global miRNA expression profiles during hESC-EC differentiation via two distinct routes; one direct and one indirect. Although investigations into the functions of miR-483 and the miR-143/145 cluster during hESC-EC differentiation were inconclusive, it is clear that regulation of the system by miRNAs and other non-coding RNAs is crucial. Further work is required determine whether miR-483 and miR-143/145 upregulation is a critical process during hESC-EC differentiation, or whether it is merely a consequence of this change in phenotype. Additionally, studies should be performed to identify other novel miRNAs, using the microarray data set generate in this thesis, with potential roles in hESC-EC

differentiation and commitment, and to pinpoint their exact mechanisms and functions.



## List of References

- ABEYTA, M. J., CLARK, A. T., RODRIGUEZ, R. T., BODNAR, M. S., PERA, R. A. & FIRPO, M. T. 2004. Unique gene expression signatures of independently-derived human embryonic stem cell lines. *Hum Mol Genet*, 13, 601-8.
- ADACHI, K., SUEMORI, H., YASUDA, S. Y., NAKATSUJI, N. & KAWASE, E. 2010. Role of SOX2 in maintaining pluripotency of human embryonic stem cells. *Genes Cells*, 15, 455-70.
- AIRD, W. C. 2007. Phenotypic heterogeneity of the endothelium: I. Structure, function, and mechanisms. *Circ Res*, 100, 158-73.
- ALBELDA, S. M., OLIVER, P. D., ROMER, L. H. & BUCK, C. A. 1990. EndoCAM: a novel endothelial cell-cell adhesion molecule. *J Cell Biol*, 110, 1227-37.
- ALLEGRUCCI, C. & YOUNG, L. E. 2007. Differences between human embryonic stem cell lines. *Human Reproduction Update*, 13, 103-120.
- ALVAREZ-VIEJO, M., MENENDEZ-MENENDEZ, Y., BLANCO-GELAZ, M. A., FERRERO-GUTIERREZ, A., FERNANDEZ-RODRIGUEZ, M. A., GALA, J. & OTERO-HERNANDEZ, J. 2013. Quantifying Mesenchymal Stem Cells in the Mononuclear Cell Fraction of Bone Marrow Samples Obtained for Cell Therapy. *Transplantation Proceedings*, 45, 434-439.
- ANKRUM, J. & KARP, J. M. 2010. Mesenchymal stem cell therapy: Two steps forward, one step back. *Trends Mol Med*, 16, 203-9.
- ASAHARA, T., MUROHARA, T., SULLIVAN, A., SILVER, M., VAN DER ZEE, R., LI, T., WITZENBICHLER, B., SCHATTEMAN, G. & ISNER, J. M. 1997. Isolation of putative progenitor endothelial cells for angiogenesis. *Science*, 275, 964-7.
- AVILION, A. A., NICOLIS, S. K., PEVNY, L. H., PEREZ, L., VIVIAN, N. & LOVELL-BADGE, R. 2003. Multipotent cell lineages in early mouse development depend on SOX2 function. *Genes Dev*, 17, 126-40.
- AZZONI, E., CONTI, V., CAMPANA, L., DELLAVALLE, A., ADAMS, R., COSSU, G. & BRUNELLI, S. 2013. Hemogenic Endothelium Generates Mesoangioblasts That Contribute to Several Mesodermal Lineages in Vivo. *Experimental Hematology*, 41, S24-S24.
- BABAIE, Y., HERWIG, R., GREBER, B., BRINK, T. C., WRUCK, W., GROTH, D., LEHRACH, H., BURDON, T. & ADJAYE, J. 2007. Analysis of Oct4-dependent transcriptional networks regulating self-renewal and pluripotency in human embryonic stem cells. *Stem Cells*, 25, 500-10.
- BAO, X., LIAN, X., DUNN, K. K., SHI, M., HAN, T., QIAN, T., BHUTE, V. J., CANFIELD, S. G. & PALECEK, S. P. 2015. Chemically-defined albumin-free differentiation of human pluripotent stem cells to endothelial progenitor cells. *Stem Cell Res*, 15, 122-9.
- BAR, M., WYMAN, S. K., FRITZ, B. R., QI, J., GARG, K. S., PARKIN, R. K., KROH, E. M., BENDORAITE, A., MITCHELL, P. S., NELSON, A. M., RUZZO, W. L., WARE, C., RADICH, J. P., GENTLEMAN, R., RUOHOLA-BAKER, H. & TEWARI, M. 2008. MicroRNA discovery and profiling in human embryonic stem cells by deep sequencing of small RNA libraries. *Stem Cells*, 26, 2496-505.
- BARNES, R. M., FIRULLI, B. A., CONWAY, S. J., VINCENTZ, J. W. & FIRULLI, A. B. 2010. Analysis of the Hand1 cell lineage reveals novel contributions to cardiovascular, neural crest, extra-embryonic, and lateral mesoderm derivatives. *Dev Dyn*, 239, 3086-97.
- BARTEL, D. P. 2004. MicroRNAs: Genomics, biogenesis, mechanism, and function. *Cell*, 116, 281-297.

- BASKERVILLE, S. & BARTEL, D. P. 2005. Microarray profiling of microRNAs reveals frequent coexpression with neighboring miRNAs and host genes. *RNA*, 11, 241-7.
- BAUMANN, C. I., BAILEY, A. S., LI, W. M., FERKOWICZ, M. J., YODER, M. C. & FLEMING, W. H. 2004. PECAM-1 is expressed on hematopoietic stem cells throughout ontogeny and identifies a population of erythroid progenitors. *Blood*, 104, 1010-1016.
- BAUMGARTNER, I., PIECZEK, A., MANOR, O., BLAIR, R., KEARNEY, M., WALSH, K. & ISNER, J. M. 1998. Constitutive expression of phVEGF165 after intramuscular gene transfer promotes collateral vessel development in patients with critical limb ischemia. *Circulation*, 97, 1114-23.
- BAUWENS, C. L., PEERANI, R., NIEBRUEGGE, S., WOODHOUSE, K. A., KUMACHEVA, E., HUSAIN, M. & ZANDSTRA, P. W. 2008. Control of human embryonic stem cell colony and aggregate size heterogeneity influences differentiation trajectories. *Stem Cells*, 26, 2300-10.
- BAXTER, M., WITHEY, S., HARRISON, S., SEGERITZ, C. P., ZHANG, F., ATKINSON-DELL, R., ROWE, C., GERRARD, D. T., SISON-YOUNG, R., JENKINS, R., HENRY, J., BERRY, A. A., MOHAMET, L., BEST, M., FENWICK, S. W., MALIK, H., KITTINGHAM, N. R., GOLDRING, C. E., HANLEY, K. P., VALLIER, L. & HANLEY, N. A. 2015. Phenotypic and functional analyses show stem cell-derived hepatocyte-like cells better mimic fetal rather than adult hepatocytes. *Journal of Hepatology*, 62, 581-589.
- BEHM-ANSMANT, I., REHWINKEL, J., DOERKS, T., STARK, A., BORK, P. & IZAURRALDE, E. 2006. mRNA degradation by miRNAs and GW182 requires both CCR4 : NOT deadenylase and DCP1 : DCP2 decapping complexes. *Genes & Development*, 20, 1885-1898.
- BEHRENS, A. N., ZIEROLD, C., SHI, X. Z., REN, Y., KOYANO-NAKAGAWA, N., GARRY, D. J. & MARTIN, C. M. 2014. Sox7 Is Regulated by ETV2 During Cardiovascular Development. *Stem Cells and Development*, 23, 2004-2013.
- BEITZINGER, M., PETERS, L., ZHU, J. Y., KREMMER, E. & MEISTER, G. 2007. Identification of human microRNA targets from isolated argonaute protein complexes. *RNA Biol*, 4, 76-84.
- BELCH, J., HIATT, W. R., BAUMGARTNER, I., DRIVER, I. V., NIKOL, S., NORNGREN, L., VAN BELLE, E. & INVESTIGATORS, T. C. 2011. Effect of fibroblast growth factor NV1FGF on amputation and death: a randomised placebo-controlled trial of gene therapy in critical limb ischaemia. *Lancet*, 377, 1929-1937.
- BEN-HAIM, N., LU, C., GUZMAN-AYALA, M., PESCATORE, L., MESNARD, D., BISCHOFBERGER, M., NAEF, F., ROBERTSON, E. J. & CONSTAM, D. B. 2006. The nodal precursor acting via activin receptors induces mesoderm by maintaining a source of its convertases and BMP4. *Dev Cell*, 11, 313-23.
- BENDERMACHER, B. L. W., WILLIGENDAEL, E. M., TEIJINK, J. A. W. & PRINS, M. H. 2005. Medical management of peripheral arterial disease. *Journal of Thrombosis and Haemostasis*, 3, 1628-1637.
- BERNSTEIN, E., CAUDY, A. A., HAMMOND, S. M. & HANNON, G. J. 2001. Role for a bidentate ribonuclease in the initiation step of RNA interference. *Nature*, 409, 363-6.
- BERNSTEIN, E., KIM, S. Y., CARMELL, M. A., MURCHISON, E. P., ALCORN, H., LI, M. Z., MILLS, A. A., ELLEDGE, S. J., ANDERSON, K. V. & HANNON, G. J. 2003. Dicer is essential for mouse development. *Nature Genetics*, 35, 215-217.

- BERTRAND, J. Y., CHI, N. C., SANTOSO, B., TENG, S., STAINIER, D. Y. & TRAVER, D. 2010. Haematopoietic stem cells derive directly from aortic endothelium during development. *Nature*, 464, 108-11.
- BETHUNE, J., ARTUS-REVEL, C. G. & FILIPOWICZ, W. 2012. Kinetic analysis reveals successive steps leading to miRNA-mediated silencing in mammalian cells. *EMBO Rep*, 13, 716-23.
- BHAYA, D., DAVISON, M. & BARRANGOU, R. 2011. CRISPR-Cas systems in bacteria and archaea: versatile small RNAs for adaptive defense and regulation. *Annu Rev Genet*, 45, 273-97.
- BHF 2014. British Heart Foundation Cardiovascular disease statistics 2014.
- BOHNSACK, M. T., CZAPLINSKI, K. & GORLICH, D. 2004. Exportin 5 is a RanGTP-dependent dsRNA-binding protein that mediates nuclear export of pre-miRNAs. *Rna-a Publication of the Rna Society*, 10, 185-191.
- BOISSET, J. C., VAN CAPPELLEN, W., ANDRIEU-SOLER, C., GALJART, N., DZIERZAK, E. & ROBIN, C. 2010. In vivo imaging of haematopoietic cells emerging from the mouse aortic endothelium. *Nature*, 464, 116-20.
- BONAUER, A., CARMONA, G., IWASAKI, M., MIONE, M., KOYANAGI, M., FISCHER, A., BURCHFIELD, J., FOX, H., DOEBELE, C., OHTANI, K., CHAVAKIS, E., POTENTE, M., TJWA, M., URBICH, C., ZEIHNER, A. M. & DIMMELER, S. 2009. MicroRNA-92a controls angiogenesis and functional recovery of ischemic tissues in mice. *Science*, 324, 1710-3.
- BOYER, L. A., LEE, T. I., COLE, M. F., JOHNSTONE, S. E., LEVINE, S. S., ZUCKER, J. P., GUENTHER, M. G., KUMAR, R. M., MURRAY, H. L., JENNER, R. G., GIFFORD, D. K., MELTON, D. A., JAENISCH, R. & YOUNG, R. A. 2005. Core transcriptional regulatory circuitry in human embryonic stem cells. *Cell*, 122, 947-56.
- BRADBURY, A. W., ADAM, D. J., BELL, J., FORBES, J. F., FOWKES, F. G., GILLESPIE, I., RUCKLEY, C. V., RAAB, G. M. & PARTICIPANTS, B. T. 2010. Bypass versus Angioplasty in Severe Ischaemia of the Leg (BASIL) trial: An intention-to-treat analysis of amputation-free and overall survival in patients randomized to a bypass surgery-first or a balloon angioplasty-first revascularization strategy. *J Vasc Surg*, 51, 5S-17S.
- BREIER, G., BREVIARIO, F., CAVEDA, L., BERTHIER, R., SCHNURCH, H., GOTSCH, U., VESTWEBER, D., RISAU, W. & DEJANA, E. 1996. Molecular cloning and expression of murine vascular endothelial-cadherin in early stage development of cardiovascular system. *Blood*, 87, 630-41.
- BROUDY, V. C. 1997. Stem cell factor and hematopoiesis. *Blood*, 90, 1345-64.
- BROUDY, V. C., LIN, N. L., BUHRING, H. J., KOMATSU, N. & KAVANAGH, T. J. 1998. Analysis of c-kit receptor dimerization by fluorescence resonance energy transfer. *Blood*, 91, 898-906.
- BUCHSCHACHER, G. L., JR. & WONG-STAAAL, F. 2000. Development of lentiviral vectors for gene therapy for human diseases. *Blood*, 95, 2499-504.
- BURRIDGE, P. W., ANDERSON, D., PRIDDLE, H., BARBADILLO MUNOZ, M. D., CHAMBERLAIN, S., ALLEGRUCCI, C., YOUNG, L. E. & DENNING, C. 2007. Improved human embryonic stem cell embryoid body homogeneity and cardiomyocyte differentiation from a novel V-96 plate aggregation system highlights interline variability. *Stem Cells*, 25, 929-38.
- BUTLER, S. L., HANSEN, M. S. T. & BUSHMAN, F. D. 2001. A quantitative assay for HIV DNA integration in vivo. *Nature Medicine*, 7, 631-634.
- CAI, W., ALBINI, S., WEI, K., WILLEMS, E., GUZZO, R. M., TSUDA, M., GIORDANI, L., SPIERING, S., KURIAN, L., YEO, G. W., PURI, P. L. & MERCOLA, M. 2013. Coordinate Nodal and BMP inhibition directs Baf60c-dependent cardiomyocyte commitment. *Genes Dev*, 27, 2332-44.

- CAI, X., HAGEDORN, C. H. & CULLEN, B. R. 2004. Human microRNAs are processed from capped, polyadenylated transcripts that can also function as mRNAs. *RNA*, 10, 1957-66.
- CARD, D. A., HEBBAR, P. B., LI, L., TROTTER, K. W., KOMATSU, Y., MISHINA, Y. & ARCHER, T. K. 2008. Oct4/Sox2-regulated miR-302 targets cyclin D1 in human embryonic stem cells. *Mol Cell Biol*, 28, 6426-38.
- CARPENTER, M. K., ROSLER, E. S., FISK, G. J., BRANDENBERGER, R., ARES, X., MIURA, T., LUCERO, M. & RAO, M. S. 2004. Properties of four human embryonic stem cell lines maintained in a feeder-free culture system. *Dev Dyn*, 229, 243-58.
- CARRIERI, C., CIMATTI, L., BIAGIOLI, M., BEUGNET, A., ZUCHELLI, S., FEDELE, S., PESCE, E., FERRER, I., COLLAVIN, L., SANTORO, C., FORREST, A. R., CARNINCI, P., BIFFO, S., STUPKA, E. & GUSTINCICH, S. 2012. Long non-coding antisense RNA controls Uchl1 translation through an embedded SINEB2 repeat. *Nature*, 491, 454-7.
- CASE, J., MEAD, L. E., BESSLER, W. K., PRATER, D., WHITE, H. A., SAADATZADEH, M. R., BHAVSAR, J. R., YODER, M. C., HANELINE, L. S. & INGRAM, D. A. 2007. Human CD34+AC133+VEGFR-2+ cells are not endothelial progenitor cells but distinct, primitive hematopoietic progenitors. *Exp Hematol*, 35, 1109-18.
- CASE, J., MEAD, L. E., WHITE, H. A., YODER, M. C., SAADATZADEH, R., HANELINE, L. & INGRAM, D. A. 2006. CD34(+)AC133(+)VEGFR-2(+) cells are primitive hematopoietic progenitors, not functional endothelial progenitor cells. *Experimental Hematology*, 34, 58-58.
- CERDAN, C., MCINTYRE, B. A. S., MECHAEL, R., LEVADOUX-MARTIN, M., YANG, J. B., LEE, J. B. & BHATIA, M. 2012. Activin A Promotes Hematopoietic Fated Mesoderm Development Through Upregulation of Brachyury in Human Embryonic Stem Cells. *Stem Cells and Development*, 21, 2866-2877.
- CHANG, K. H., NELSON, A. M., CAO, H., WANG, L. L., NAKAMOTO, B., WARE, C. B. & PAPAYANNOPOULOU, T. 2006. Definitive-like erythroid cells derived from human embryonic stem cells coexpress high levels of embryonic and fetal globins with little or no adult globin. *Blood*, 108, 1515-1523.
- CHASIS, J. A. & MOHANDAS, N. 1992. Red blood cell glycoporphins. *Blood*, 80, 1869-79.
- CHELOUFI, S., DOS SANTOS, C. O., CHONG, M. M. W. & HANNON, G. J. 2010. A Dicer-independent miRNA biogenesis pathway that requires Ago catalysis. *Nature*, 465, 584-U76.
- CHEN, M. J., YOKOMIZO, T., ZEIGLER, B. M., DZIERZAK, E. & SPECK, N. A. 2009a. Runx1 is required for the endothelial to haematopoietic cell transition but not thereafter. *Nature*, 457, 887-891.
- CHEN, M. Y., LIE, P. C., LI, Z. L. & WEI, X. 2009b. Endothelial differentiation of Wharton's jelly-derived mesenchymal stem cells in comparison with bone marrow-derived mesenchymal stem cells. *Exp Hematol*, 37, 629-40.
- CHEN, X., BA, Y., MA, L., CAI, X., YIN, Y., WANG, K., GUO, J., ZHANG, Y., CHEN, J., GUO, X., LI, Q., LI, X., WANG, W., ZHANG, Y., WANG, J., JIANG, X., XIANG, Y., XU, C., ZHENG, P., ZHANG, J., LI, R., ZHANG, H., SHANG, X., GONG, T., NING, G., WANG, J., ZEN, K., ZHANG, J. & ZHANG, C. Y. 2008a. Characterization of microRNAs in serum: a novel class of biomarkers for diagnosis of cancer and other diseases. *Cell Res*, 18, 997-1006.
- CHEN, Y., BANDA, M., SPEYER, C. L., SMITH, J. S., RABSON, A. B. & GORSKI, D. H. 2010. Regulation of the expression and activity of the antiangiogenic

- homeobox gene GAX/MEOX2 by ZEB2 and microRNA-221. *Mol Cell Biol*, 30, 3902-13.
- CHEN, Y. & GORSKI, D. H. 2008b. Regulation of angiogenesis through a microRNA (miR-130a) that down-regulates antiangiogenic homeobox genes GAX and HOXA5. *Blood*, 111, 1217-26.
- CHENDRIMADA, T. P., GREGORY, R. I., KUMARASWAMY, E., NORMAN, J., COOCH, N., NISHIKURA, K. & SHIEKHATTAR, R. 2005. TRBP recruits the Dicer complex to Ago2 for microRNA processing and gene silencing. *Nature*, 436, 740-4.
- CHEUNG, C. & SINHA, S. 2011. Human embryonic stem cell-derived vascular smooth muscle cells in therapeutic neovascularisation. *J Mol Cell Cardiol*, 51, 651-64.
- CHOI, K. D., VODYANIK, M. A., TOGARRATI, P. P., SUKNUNTHA, K., KUMAR, A., SAMARJEET, F., PROBASCO, M. D., TIAN, S., STEWART, R., THOMSON, J. A. & SLUKVIN, I. 2012. Identification of the hemogenic endothelial progenitor and its direct precursor in human pluripotent stem cell differentiation cultures. *Cell Rep*, 2, 553-67.
- CHOI, K. D., YU, J., SMUGA-OTTO, K., SALVAGIOTTO, G., REHRAUER, W., VODYANIK, M., THOMSON, J. & SLUKVIN, I. 2009. Hematopoietic and endothelial differentiation of human induced pluripotent stem cells. *Stem Cells*, 27, 559-67.
- CHUN, Y. W., BALIKOV, D. A., FEASTER, T. K., WILLIAMS, C. H., SHENG, C. C., LEE, J. B., BOIRE, T. C., NEELY, M. D., BELLAN, L. M., ESS, K. C., BOWMAN, A. B., SUNG, H. J. & HONG, C. C. 2015. Combinatorial polymer matrices enhance in vitro maturation of human induced pluripotent stem cell-derived cardiomyocytes. *Biomaterials*, 67, 52-64.
- CIFUENTES, D., XUE, H., TAYLOR, D. W., PATNODE, H., MISHIMA, Y., CHELOUFI, S., MA, E., MANE, S., HANNON, G. J., LAWSON, N. D., WOLFE, S. A. & GIRALDEZ, A. J. 2010. A novel miRNA processing pathway independent of Dicer requires Argonaute2 catalytic activity. *Science*, 328, 1694-8.
- CIRUNA, B. & ROSSANT, J. 2001. FGF signaling regulates mesoderm cell fate specification and morphogenetic movement at the primitive streak. *Developmental Cell*, 1, 37-49.
- CIVIN, C. I., STRAUSS, L. C., BROVALL, C., FACKLER, M. J., SCHWARTZ, J. F. & SHAPER, J. H. 1984. Antigenic analysis of hematopoiesis. III. A hematopoietic progenitor cell surface antigen defined by a monoclonal antibody raised against KG-1a cells. *J Immunol*, 133, 157-65.
- COMEROTA, A. J., THROM, R. C., MILLER, K. A., HENRY, T., CHRONOS, N., LAIRD, J., SEQUEIRA, R., KENT, C. K., BACCHETTA, M., GOLDMAN, C., SALENIUS, J. P., SCHMIEDER, F. A. & PILSUDSKI, R. 2002. Naked plasmid DNA encoding fibroblast growth factor type 1 for the treatment of end-stage unreconstructible lower extremity ischemia: preliminary results of a phase I trial. *J Vasc Surg*, 35, 930-6.
- COSTA, G., MAZAN, A., GANDILLET, A., PEARSON, S., LACAUD, G. & KOUSKOFF, V. 2012. SOX7 regulates the expression of VE-cadherin in the haemogenic endothelium at the onset of haematopoietic development. *Development*, 139, 1587-1598.
- COSTA, M., SOURRIS, K., LIM, S. M., YU, Q. C., HIRST, C. E., PARKINGTON, H. C., JOKUBAITIS, V. J., DEAR, A. E., LIU, H. B., MICALLEF, S. J., KOUTSIS, K., ELEFANTY, A. G. & STANLEY, E. G. 2013. Derivation of endothelial cells from human embryonic stem cells in fully defined medium enables identification of lysophosphatidic acid and platelet activating factor as regulators of eNOS localization. *Stem Cell Research*, 10, 103-117.

- COULTAS, L., CHAWENGSAKSOPHAK, K. & ROSSANT, J. 2005. Endothelial cells and VEGF in vascular development. *Nature*, 438, 937-45.
- CREAGER, M. A., OLIN, J. W., BELCH, J. J., MONETA, G. L., HENRY, T. D., RAJAGOPALAN, S., ANNEX, B. H. & HIATT, W. R. 2011. Effect of hypoxia-inducible factor-1alpha gene therapy on walking performance in patients with intermittent claudication. *Circulation*, 124, 1765-73.
- DE UGARTE, D. A., MORIZONO, K., ELBARBARY, A., ALFONSO, Z., ZUK, P. A., ZHU, M., DRAGOO, J. L., ASHJIAN, P., THOMAS, B., BENHAIM, P., CHEN, I., FRASER, J. & HEDRICK, M. H. 2003. Comparison of multi-lineage cells from human adipose tissue and bone marrow. *Cells Tissues Organs*, 174, 101-9.
- DE VRIES, S. O. & HUNINK, M. G. 1997. Results of aortic bifurcation grafts for aortoiliac occlusive disease: a meta-analysis. *J Vasc Surg*, 26, 558-69.
- DE WERT, G. & MUMMERY, C. 2003. Human embryonic stem cells: research, ethics and policy. *Hum Reprod*, 18, 672-82.
- DEJANA, E., TADDEI, A. & RANDI, A. M. 2007. Foxs and Ets in the transcriptional regulation of endothelial cell differentiation and angiogenesis. *Biochim Biophys Acta*, 1775, 298-312.
- DEKELVER, R. C., CHOI, V. M., MOEHLE, E. A., PASCHON, D. E., HOCKEMEYER, D., MEIJSING, S. H., SANCAK, Y., CUI, X. X., STEINE, E. L. J., MILLER, J. C., TAM, P., BARTSEVICH, V. V., MENG, X. D., RUPNIEWSKI, I., GOPALAN, S. M., SUN, H. C., PITZ, K. J., ROCK, J. M., ZHANG, L., DAVIS, G. D., REBAR, E. J., CHEESEMAN, I. M., YAMAMOTO, K. R., SABATINI, D. M., JAENISCH, R., GREGORY, P. D. & URNOV, F. D. 2010. Functional genomics, proteomics, and regulatory DNA analysis in isogenic settings using zinc finger nuclease-driven transgenesis into a safe harbor locus in the human genome. *Genome Research*, 20, 1133-1142.
- DEMAISON, C., PARSLEY, K., BROUNS, G., SCHERR, M., BATTMER, K., KINNON, C., GREZ, M. & THRASHER, A. J. 2002. High-level transduction and gene expression in hematopoietic repopulating cells using a human immunodeficiency [correction of imunodeficiency] virus type 1-based lentiviral vector containing an internal spleen focus forming virus promoter. *Hum Gene Ther*, 13, 803-13.
- DENNING, C., ALLEGRUCCI, C., PRIDDLE, H., BARBADILLO-MUNOZ, M. D., ANDERSON, D., SELF, T., SMITH, N. M., PARKIN, C. T. & YOUNG, L. E. 2006. Common culture conditions for maintenance and cardiomyocyte differentiation of the human embryonic stem cell lines, BG01 and HUES-7. *Int J Dev Biol*, 50, 27-37.
- DERRIEN, T., JOHNSON, R., BUSSOTTI, G., TANZER, A., DJEBALI, S., TILGNER, H., GUERNEC, G., MARTIN, D., MERKEL, A., KNOWLES, D. G., LAGARDE, J., VEERAVALLI, L., RUAN, X., RUAN, Y., LASSMANN, T., CARNINCI, P., BROWN, J. B., LIPOVICH, L., GONZALEZ, J. M., THOMAS, M., DAVIS, C. A., SHIEKHATTAR, R., GINGERAS, T. R., HUBBARD, T. J., NOTREDAME, C., HARROW, J. & GUIGO, R. 2012. The GENCODE v7 catalog of human long noncoding RNAs: analysis of their gene structure, evolution, and expression. *Genome Res*, 22, 1775-89.
- DESCAMPS, B. & EMANUELI, C. 2012. Vascular differentiation from embryonic stem cells: novel technologies and therapeutic promises. *Vascul Pharmacol*, 56, 267-79.
- DEWS, M., HOMAYOUNI, A., YU, D., MURPHY, D., SEVIGNANI, C., WENTZEL, E., FURTH, E. E., LEE, W. M., ENDERS, G. H., MENDELL, J. T. & THOMAS-TIKHONENKO, A. 2006. Augmentation of tumor angiogenesis by a Myc-activated microRNA cluster. *Nat Genet*, 38, 1060-5.

- DHARA, S. K. & STICE, S. L. 2008. Neural differentiation of human embryonic stem cells. *J Cell Biochem*, 105, 633-40.
- DI BERNARDINI, E., CAMPAGNOLO, P., MARGARITI, A., ZAMPETAKI, A., KARAMARITI, E., HU, Y. & XU, Q. 2014. Endothelial lineage differentiation from induced pluripotent stem cells is regulated by microRNA-21 and transforming growth factor beta2 (TGF-beta2) pathways. *J Biol Chem*, 289, 3383-93.
- DITADI, A., STURGEON, C. M., TOBER, J., AWONG, G., KENNEDY, M., YZAGUIRRE, A. D., AZZOLA, L., NG, E. S., STANLEY, E. G., FRENCH, D. L., CHENG, X., GADUE, P., SPECK, N. A., ELEFANTY, A. G. & KELLER, G. 2015. Human definitive haemogenic endothelium and arterial vascular endothelium represent distinct lineages. *Nat Cell Biol*, 17, 580-91.
- DOEBELE, C., BONAUER, A., FISCHER, A., SCHOLZ, A., REISS, Y., URBICH, C., HOFMANN, W. K., ZEIHNER, A. M. & DIMMELER, S. 2010. Members of the microRNA-17-92 cluster exhibit a cell-intrinsic antiangiogenic function in endothelial cells. *Blood*, 115, 4944-50.
- DORE, L. C., AMIGO, J. D., DOS SANTOS, C. O., ZHANG, Z., GAI, X., TOBIAS, J. W., YU, D., KLEIN, A. M., DORMAN, C., WU, W., HARDISON, R. C., PAW, B. H. & WEISS, M. J. 2008. A GATA-1-regulated microRNA locus essential for erythropoiesis. *Proc Natl Acad Sci U S A*, 105, 3333-8.
- DRUKKER, M., KATCHMAN, H., KATZ, G., EVEN-TOV FRIEDMAN, S., SHEZEN, E., HORNSTEIN, E., MANDELBOIM, O., REISNER, Y. & BENVENISTY, N. 2006. Human embryonic stem cells and their differentiated derivatives are less susceptible to immune rejection than adult cells. *Stem Cells*, 24, 221-9.
- DRUKKER, M., TANG, C., ARDEHALI, R., RINKEVICH, Y., SEITA, J., LEE, A. S., MOSLEY, A. R., WEISSMAN, I. L. & SOEN, Y. 2012. Isolation of primitive endoderm, mesoderm, vascular endothelial and trophoblast progenitors from human pluripotent stem cells. *Nat Biotechnol*, 30, 531-42.
- DWEEP, H. & GRETZ, N. 2015. miRWalk2.0: a comprehensive atlas of microRNA-target interactions. *Nat Methods*, 12, 697.
- DYSON, S. & GURDON, J. B. 1997. Activin signalling has a necessary function in *Xenopus* early development. *Current Biology*, 7, 81-84.
- EGGERMANN, J., KLICHE, S., JARMY, G., HOFFMANN, K., MAYR-BEYRLE, U., DEBATIN, K. M., WALTENBERGER, J. & BELTINGER, C. 2003. Endothelial progenitor cell culture and differentiation in vitro: a methodological comparison using human umbilical cord blood. *Cardiovascular Research*, 58, 478-486.
- EILKEN, H. M., NISHIKAWA, S. & SCHROEDER, T. 2009. Continuous single-cell imaging of blood generation from haemogenic endothelium. *Nature*, 457, 896-900.
- EVANS, M. J. & KAUFMAN, M. H. 1981. Establishment in culture of pluripotential cells from mouse embryos. *Nature*, 292, 154-6.
- EVSEENKO, D., ZHU, Y., SCHENKE-LAYLAND, K., KUO, J., LATOUR, B., GE, S., SCHOLE, J., DRAVID, G., LI, X., MACLELLAN, W. R. & CROOKS, G. M. 2010. Mapping the first stages of mesoderm commitment during differentiation of human embryonic stem cells. *Proc Natl Acad Sci U S A*, 107, 13742-7.
- EWAN, L. C., JOPLING, H. M., JIA, H., MITTAR, S., BAGHERZADEH, A., HOWELL, G. J., WALKER, J. H., ZACHARY, I. C. & PONNAMBALAM, S. 2006. Intrinsic tyrosine kinase activity is required for vascular endothelial growth factor receptor 2 ubiquitination, sorting and degradation in endothelial cells. *Traffic*, 7, 1270-82.

- FABIAN, M. R., MATHONNET, G., SUNDERMEIER, T., MATHYS, H., ZIPPRICH, J. T., SVITKIN, Y. V., RIVAS, F., JINEK, M., WOHLSCHLEGEL, J., DOUDNA, J. A., CHEN, C. Y., SHYU, A. B., YATES, J. R., 3RD, HANNON, G. J., FILIPOWICZ, W., DUCHAINE, T. F. & SONENBERG, N. 2009. Mammalian miRNA RISC recruits CAF1 and PABP to affect PABP-dependent deadenylation. *Mol Cell*, 35, 868-80.
- FASANARO, P., D'ALESSANDRA, Y., DI STEFANO, V., MELCHIONNA, R., ROMANI, S., POMPILIO, G., CAPOGROSSI, M. C. & MARTELLI, F. 2008. MicroRNA-210 modulates endothelial cell response to hypoxia and inhibits the receptor tyrosine kinase ligand Ephrin-A3. *J Biol Chem*, 283, 15878-83.
- FENG, Y., ZHANG, X., GRAVES, P. & ZENG, Y. 2012. A comprehensive analysis of precursor microRNA cleavage by human Dicer. *RNA*, 18, 2083-92.
- FICHTLSCHERER, S., DE ROSA, S., FOX, H., SCHWIETZ, T., FISCHER, A., LIEBETRAU, C., WEBER, M., HAMM, C. W., ROXE, T., MULLER-ARDOGAN, M., BONAUER, A., ZEIHNER, A. M. & DIMMELER, S. 2010. Circulating microRNAs in patients with coronary artery disease. *Circ Res*, 107, 677-84.
- FINA, L., MOLGAARD, H. V., ROBERTSON, D., BRADLEY, N. J., MONAGHAN, P., DELIA, D., SUTHERLAND, D. R., BAKER, M. A. & GREAVES, M. F. 1990. Expression of the CD34 gene in vascular endothelial cells. *Blood*, 75, 2417-26.
- FISCHER, A., SCHUMACHER, N., MAIER, M., SENDTNER, M. & GESSLER, M. 2004. The Notch target genes Hey1 and Hey2 are required for embryonic vascular development. *Genes Dev*, 18, 901-11.
- FISH, J. E., SANTORO, M. M., MORTON, S. U., YU, S., YEH, R. F., WYTHE, J. D., IVEY, K. N., BRUNEAU, B. G., STAINIER, D. Y. & SRIVASTAVA, D. 2008. miR-126 regulates angiogenic signaling and vascular integrity. *Dev Cell*, 15, 272-84.
- FONG, H., HOHENSTEIN, K. A. & DONOVAN, P. J. 2008. Regulation of self-renewal and pluripotency by Sox2 in human embryonic stem cells. *Stem Cells*, 26, 1931-8.
- FOSHAY, K. M. & GALLICANO, G. I. 2009. miR-17 family miRNAs are expressed during early mammalian development and regulate stem cell differentiation. *Dev Biol*, 326, 431-43.
- FU, X. 2014. The immunogenicity of cells derived from induced pluripotent stem cells. *Cell Mol Immunol*, 11, 14-6.
- GANSBACHER, B. & EUROPEAN SOCIETY OF GENE THERAPY, T. 2003. Report of a second serious adverse event in a clinical trial of gene therapy for X-linked severe combined immune deficiency (X-SCID). Position of the European Society of Gene Therapy (ESGT). *J Gene Med*, 5, 261-2.
- GEHLING, U. M., ERGUN, S., SCHUMACHER, U., WAGENER, C., PANTEL, K., OTTE, M., SCHUCH, G., SCHAFHAUSEN, P., MENDE, T., KILIC, N., KLUGE, K., SCHAFER, B., HOSSFELD, D. K. & FIEDLER, W. 2000. In vitro differentiation of endothelial cells from AC133-positive progenitor cells. *Blood*, 95, 3106-12.
- GORSKI, D. H., LEPAGE, D. F., PATEL, C. V., COPELAND, N. G., JENKINS, N. A. & WALSH, K. 1993. Molecular cloning of a diverged homeobox gene that is rapidly down-regulated during the G0/G1 transition in vascular smooth muscle cells. *Mol Cell Biol*, 13, 3722-33.
- GRANT, J. S., WHITE, K., MACLEAN, M. R. & BAKER, A. H. 2013. MicroRNAs in pulmonary arterial remodeling. *Cell Mol Life Sci*, 70, 4479-94.
- GREGORY, R. I., YAN, K. P., AMUTHAN, G., CHENDRIMADA, T., DORATOTAJ, B., COOCH, N. & SHIEKHATTAR, R. 2004. The Microprocessor complex mediates the genesis of microRNAs. *Nature*, 432, 235-240.



- GRISHOK, A., PASQUINELLI, A. E., CONTE, D., LI, N., PARRISH, S., HA, I., BAILLIE, D. L., FIRE, A., RUVKUN, G. & MELLO, C. C. 2001. Genes and mechanisms related to RNA interference regulate expression of the small temporal RNAs that control *C. elegans* developmental timing. *Cell*, 106, 23-34.
- GROSSMAN, P. M., MENDELSON, F., HENRY, T. D., HERMILLER, J. B., LITT, M., SAUCEDO, J. F., WEISS, R. J., KANDZARI, D. E., KLEIMAN, N., ANDERSON, R. D., GOTTLIEB, D., KARLSBERG, R., SNELL, J. & ROCHA-SINGH, K. 2007. Results from a phase II multicenter, double-blind placebo-controlled study of Del-1 (VLTS-589) for intermittent claudication in subjects with peripheral arterial disease. *Am Heart J*, 153, 874-80.
- GRUNDMANN, S., HANS, F. P., KINNIRY, S., HEINKE, J., HELBING, T., BLUHM, F., SLUIJTER, J. P., HOEFER, I., PASTERKAMP, G., BODE, C. & MOSER, M. 2011. MicroRNA-100 regulates neovascularization by suppression of mammalian target of rapamycin in endothelial and vascular smooth muscle cells. *Circulation*, 123, 999-1009.
- GUO, H., INGOLIA, N. T., WEISSMAN, J. S. & BARTEL, D. P. 2010. Mammalian microRNAs predominantly act to decrease target mRNA levels. *Nature*, 466, 835-40.
- GUTTMAN, M., AMIT, I., GARBER, M., FRENCH, C., LIN, M. F., FELDSEER, D., HUARTE, M., ZUK, O., CAREY, B. W., CASSADY, J. P., CABILI, M. N., JAENISCH, R., MIKKELSEN, T. S., JACKS, T., HACOEN, N., BERNSTEIN, B. E., KELLIS, M., REGEV, A., RINN, J. L. & LANDER, E. S. 2009. Chromatin signature reveals over a thousand highly conserved large non-coding RNAs in mammals. *Nature*, 458, 223-7.
- HAN, J., LEE, Y., YEOM, K. H., KIM, Y. K., JIN, H. & KIM, V. N. 2004. The Drosha-DGCR8 complex in primary microRNA processing. *Genes Dev*, 18, 3016-27.
- HAN, J., LEE, Y., YEOM, K. H., NAM, J. W., HEO, I., RHEE, J. K., SOHN, S. Y., CHO, Y., ZHANG, B. T. & KIM, V. N. 2006. Molecular basis for the recognition of primary microRNAs by the Drosha-DGCR8 complex. *Cell*, 125, 887-901.
- HANNAN, N. R., SEGERITZ, C. P., TOUBOUL, T. & VALLIER, L. 2013. Production of hepatocyte-like cells from human pluripotent stem cells. *Nat Protoc*, 8, 430-7.
- HARRIS, T. A., YAMAKUCHI, M., FERLITO, M., MENDELL, J. T. & LOWENSTEIN, C. J. 2008. MicroRNA-126 regulates endothelial expression of vascular cell adhesion molecule 1. *Proc Natl Acad Sci U S A*, 105, 1516-21.
- HARRIS, T. A., YAMAKUCHI, M., KONDO, M., OETTGEN, P. & LOWENSTEIN, C. J. 2010. Ets-1 and Ets-2 regulate the expression of microRNA-126 in endothelial cells. *Arterioscler Thromb Vasc Biol*, 30, 1990-7.
- HASSEL, D., CHENG, P., WHITE, M. P., IVEY, K. N., KROLL, J., AUGUSTIN, H. G., KATUS, H. A., STAINIER, D. Y. & SRIVASTAVA, D. 2012. miR-10 Regulates the Angiogenic Behavior of Zebrafish and Human Endothelial Cells by Promoting VEGF Signaling. *Circ Res*.
- HAY, D. C., SUTHERLAND, L., CLARK, J. & BURDON, T. 2004. Oct-4 knockdown induces similar patterns of endoderm and trophoblast differentiation markers in human and mouse embryonic stem cells. *Stem Cells*, 22, 225-35.
- HAYASHITA, Y., OSADA, H., TATEMATSU, Y., YAMADA, H., YANAGISAWA, K., TOMIDA, S., YATABE, Y., KAWAHARA, K., SEKIDO, Y. & TAKAHASHI, T. 2005. A polycistronic microRNA cluster, miR-17-92, is overexpressed in human lung cancers and enhances cell proliferation. *Cancer Research*, 65, 9628-9632.

- HENRY, T. D., ANNEX, B. H., MCKENDALL, G. R., AZRIN, M. A., LOPEZ, J. J., GIORDANO, F. J., SHAH, P. K., WILLERSON, J. T., BENZA, R. L., BERMAN, D. S., GIBSON, C. M., BAJAMONDE, A., RUNDLE, A. C., FINE, J., MCCLUSKEY, E. R. & INVESTIGATORS, V. 2003. The VIVA trial: Vascular endothelial growth factor in Ischemia for Vascular Angiogenesis. *Circulation*, 107, 1359-65.
- HERZOG, Y., KALCHEIM, C., KAHANE, N., RESHEF, R. & NEUFELD, G. 2001. Differential expression of neuropilin-1 and neuropilin-2 in arteries and veins. *Mech Dev*, 109, 115-9.
- HOFFMAN, L. M. & CARPENTER, M. K. 2005. Characterization and culture of human embryonic stem cells. *Nat Biotechnol*, 23, 699-708.
- HOUBAVIY, H. B., MURRAY, M. F. & SHARP, P. A. 2003. Embryonic stem cell-specific MicroRNAs. *Dev Cell*, 5, 351-8.
- HOWE, S. J., MANSOUR, M. R., SCHWARZWAELDER, K., BARTHOLOMAE, C., HUBANK, M., KEMPSKI, H., BRUGMAN, M. H., PIKE-OVERZET, K., CHATTERS, S. J., DE RIDDER, D., GILMOUR, K. C., ADAMS, S., THORNHILL, S. I., PARSLEY, K. L., STAAL, F. J., GALE, R. E., LINCH, D. C., BAYFORD, J., BROWN, L., QUAYE, M., KINNON, C., ANCLIFF, P., WEBB, D. K., SCHMIDT, M., VON KALLE, C., GASPAR, H. B. & THRASHER, A. J. 2008. Insertional mutagenesis combined with acquired somatic mutations causes leukemogenesis following gene therapy of SCID-X1 patients. *J Clin Invest*, 118, 3143-50.
- HSU, S. D., TSENG, Y. T., SHRESTHA, S., LIN, Y. L., KHALEEL, A., CHOU, C. H., CHU, C. F., HUANG, H. Y., LIN, C. M., HO, S. Y., JIAN, T. Y., LIN, F. M., CHANG, T. H., WENG, S. L., LIAO, K. W., LIAO, I. E., LIU, C. C. & HUANG, H. D. 2014. miRTarBase update 2014: an information resource for experimentally validated miRNA-target interactions. *Nucleic Acids Res*, 42, D78-85.
- HU, S., WILSON, K. D., GHOSH, Z., HAN, L., WANG, Y., LAN, F., RANSOHOFF, K. J., BURRIDGE, P. & WU, J. C. 2013. MicroRNA-302 increases reprogramming efficiency via repression of NR2F2. *Stem Cells*, 31, 259-68.
- HUA, Z., LV, Q., YE, W., WONG, C. K., CAI, G., GU, D., JI, Y., ZHAO, C., WANG, J., YANG, B. B. & ZHANG, Y. 2006. MiRNA-directed regulation of VEGF and other angiogenic factors under hypoxia. *PLoS One*, 1, e116.
- HUMAR, R., KIEFER, F. N., BERNS, H., RESINK, T. J. & BATTEGAY, E. J. 2002. Hypoxia enhances vascular cell proliferation and angiogenesis in vitro via rapamycin (mTOR)-dependent signaling. *FASEB J*, 16, 771-80.
- HUTVAGNER, G., MCLACHLAN, J., PASQUINELLI, A. E., BALINT, E., TUSCHL, T. & ZAMORE, P. D. 2001. A cellular function for the RNA-interference enzyme Dicer in the maturation of the let-7 small temporal RNA. *Science*, 293, 834-8.
- HYSLOP, L., STOJKOVIC, M., ARMSTRONG, L., WALTER, T., STOJKOVIC, P., PRZYBORSKI, S., HERBERT, M., MURDOCH, A., STRACHAN, T. & LAKO, M. 2005. Downregulation of NANOG induces differentiation of human embryonic stem cells to extraembryonic lineages. *Stem Cells*, 23, 1035-43.
- INVERNICI, G., PONTI, D., CORSINI, E., CRISTINI, S., FRIGERIO, S., COLOMBO, A., PARATI, E. & ALESSANDRI, G. 2005. Human microvascular endothelial cells from different fetal organs demonstrate organ-specific CAM expression. *Exp Cell Res*, 308, 273-82.
- IORIO, M. V. & CROCE, C. M. 2012. MicroRNA dysregulation in cancer: diagnostics, monitoring and therapeutics. A comprehensive review. *EMBO Mol Med*, 4, 143-59.

- ISNER, J. M., PIECZEK, A., SCHAINFELD, R., BLAIR, R., HALEY, L., ASAHARA, T., ROSENFELD, K., RAZVI, S., WALSH, K. & SYMES, J. F. 1996. Clinical evidence of angiogenesis after arterial gene transfer of phVEGF165 in patient with ischaemic limb. *Lancet*, 348, 370-4.
- ITSKOVITZ-ELDOR, J., SCHULDINER, M., KARSENTI, D., EDEN, A., YANUKA, O., AMIT, M., SOREQ, H. & BENVENISTY, N. 2000. Differentiation of human embryonic stem cells into embryoid bodies comprising the three embryonic germ layers. *Molecular Medicine*, 6, 88-95.
- ITZHAKI, I., MAIZELS, L., HUBER, I., ZWI-DANTSIS, L., CASPI, O., WINTERSTERN, A., FELDMAN, O., GEPSTEIN, A., ARBEL, G., HAMMERMAN, H., BOULOS, M. & GEPSTEIN, L. 2011. Modelling the long QT syndrome with induced pluripotent stem cells. *Nature*, 471, 225-9.
- IVEY, K. N., MUTH, A., ARNOLD, J., KING, F. W., YEH, R. F., FISH, J. E., HSIAO, E. C., SCHWARTZ, R. J., CONKLIN, B. R., BERNSTEIN, H. S. & SRIVASTAVA, D. 2008. MicroRNA regulation of cell lineages in mouse and human embryonic stem cells. *Cell Stem Cell*, 2, 219-29.
- IWASAKI, S., KOBAYASHI, M., YODA, M., SAKAGUCHI, Y., KATSUMA, S., SUZUKI, T. & TOMARI, Y. 2010. Hsc70/Hsp90 chaperone machinery mediates ATP-dependent RISC loading of small RNA duplexes. *Mol Cell*, 39, 292-9.
- JACQUET, L., STEPHENSON, E., COLLINS, R., PATEL, H., TRUSSLER, J., AL-BEDAERY, R., RENWICK, P., OGILVIE, C., VAUGHAN, R. & ILIC, D. 2013. Strategy for the creation of clinical grade hESC line banks that HLA-match a target population. *Embo Molecular Medicine*, 5, 10-17.
- JAFFREDO, T., GAUTIER, R., BRAJEUL, V. & DIETERLEN-LIEVRE, F. 2000. Tracing the progeny of the aortic hemangioblast in the avian embryo. *Dev Biol*, 224, 204-14.
- JAFFREDO, T., GAUTIER, R., EICHMANN, A. & DIETERLEN-LIEVRE, F. 1998. Intraaortic hemopoietic cells are derived from endothelial cells during ontogeny. *Development*, 125, 4575-83.
- JAHN, T., SEIPEL, P., COUTINHO, S., URSCHEL, S., SCHWARZ, K., MIETHING, C., SERVE, H., PESCHEL, C. & DUYSER, J. 2002. Analysing c-kit internalization using a functional c-kit-EGFP chimera containing the fluorochrome within the extracellular domain. *Oncogene*, 21, 4508-4520.
- JAKOB, P. & LANDMESSER, U. 2012. Role of microRNAs in stem/progenitor cells and cardiovascular repair. *Cardiovasc Res*, 93, 614-22.
- JANKOWSKI, R. J., DEASY, B. M. & HUARD, J. 2002. Muscle-derived stem cells. *Gene Ther*, 9, 642-7.
- JAYAWARDENA, T. M., EGEMNAZAROV, B., FINCH, E. A., ZHANG, L., PAYNE, J. A., PANDYA, K., ZHANG, Z., ROSENBERG, P., MIROTSOU, M. & DZAU, V. J. 2012. MicroRNA-mediated in vitro and in vivo direct reprogramming of cardiac fibroblasts to cardiomyocytes. *Circ Res*, 110, 1465-73.
- JOHNSTON, M., GEOFFROY, M. C., SOBALA, A., HAY, R. & HUTVAGNER, G. 2010. HSP90 protein stabilizes unloaded argonaute complexes and microscopic P-bodies in human cells. *Mol Biol Cell*, 21, 1462-9.
- JONES, W. S., DOLOR, R. J., HASSELBLAD, V., VEMULAPALLI, S., SUBHERWAL, S., SCHMIT, K., HEIDENFELDER, B. & PATEL, M. R. 2014. Comparative effectiveness of endovascular and surgical revascularization for patients with peripheral artery disease and critical limb ischemia: systematic review of revascularization in critical limb ischemia. *Am Heart J*, 167, 489-498 e7.
- JORDAN, H. E. 1916. Evidence of hemogenic capacity of endothelium. *Anatomical Record*, 10, 417-420.

- KALBAUGH, C. A., TAYLOR, S. M., BLACKHURST, D. W., DELLINGER, M. B., TRENT, E. A. & YOUKEY, J. R. 2006. One-year prospective quality-of-life outcomes in patients treated with angioplasty for symptomatic peripheral arterial disease. *J Vasc Surg*, 44, 296-302; discussion 302-3.
- KALKA, C., MASUDA, H., TAKAHASHI, T., KALKA-MOLL, W. M., SILVER, M., KEARNEY, M., LI, T., ISNER, J. M. & ASAHARA, T. 2000. Transplantation of ex vivo expanded endothelial progenitor cells for therapeutic neovascularization. *Proceedings of the National Academy of Sciences of the United States of America*, 97, 3422-3427.
- KALUZA, D., KROLL, J., GESIERICH, S., MANAVSKI, Y., BOECKEL, J. N., DOEBELE, C., ZELENT, A., ROSSIG, L., ZEIHNER, A. M., AUGUSTIN, H. G., URBICH, C. & DIMMELER, S. 2013. Histone deacetylase 9 promotes angiogenesis by targeting the antiangiogenic microRNA-17-92 cluster in endothelial cells. *Arterioscler Thromb Vasc Biol*, 33, 533-43.
- KANE, N. M., HOWARD, L., DESCAMPS, B., MELONI, M., MCCLURE, J., LU, R., MCCAHILL, A., BREEN, C., MACKENZIE, R. M., DELLES, C., MOUNTFORD, J. C., MILLIGAN, G., EMANUELI, C. & BAKER, A. H. 2012. Role of microRNAs 99b, 181a, and 181b in the differentiation of human embryonic stem cells to vascular endothelial cells. *Stem Cells*, 30, 643-54.
- KANE, N. M., MELONI, M., SPENCER, H. L., CRAIG, M. A., STREHL, R., MILLIGAN, G., HOUSLAY, M. D., MOUNTFORD, J. C., EMANUELI, C. & BAKER, A. H. 2010. Derivation of endothelial cells from human embryonic stem cells by directed differentiation: analysis of microRNA and angiogenesis in vitro and in vivo. *Arterioscler Thromb Vasc Biol*, 30, 1389-97.
- KANELLOPOULOU, C., MULJO, S. A., KUNG, A. L., GANESAN, S., DRAPKIN, R., JENUWEIN, T., LIVINGSTON, D. M. & RAJEWSKY, K. 2005. Dicer-deficient mouse embryonic stem cells are defective in differentiation and centromeric silencing. *Genes Dev*, 19, 489-501.
- KANG, Y., PARK, C., KIM, D., SEONG, C. M., KWON, K. & CHOI, C. 2010. Unsorted human adipose tissue-derived stem cells promote angiogenesis and myogenesis in murine ischemic hindlimb model. *Microvasc Res*, 80, 310-6.
- KAUPISCH, A., KENNEDY, L., STELMANIS, V., TYE, B., KANE, N. M., MOUNTFORD, J. C., COURTNEY, A. & BAKER, A. H. 2012. Derivation of vascular endothelial cells from human embryonic stem cells under GMP-compliant conditions: towards clinical studies in ischaemic disease. *J Cardiovasc Transl Res*, 5, 605-17.
- KAWANISHI, Y., NAKASA, T., SHOJI, T., HAMANISHI, M., SHIMIZU, R., KAMEI, N., USMAN, M. A. & OCHI, M. 2014. Intra-articular injection of synthetic microRNA-210 accelerates avascular meniscal healing in rat medial meniscal injured model. *Arthritis Res Ther*, 16, 488.
- KAZENWADEL, J., MICHAEL, M. Z. & HARVEY, N. L. 2010. Prox1 expression is negatively regulated by miR-181 in endothelial cells. *Blood*, 116, 2395-401.
- KEMLER, R., HIERHOLZER, A., KANZLER, B., KUPPIG, S., HANSEN, K., TAKETO, M. M., DE VRIES, W. N., KNOWLES, B. B. & SOLTER, D. 2004. Stabilization of beta-catenin in the mouse zygote leads to premature epithelial-mesenchymal transition in the epiblast. *Development*, 131, 5817-24.
- KENNEDY, M., AWONG, G., STURGEON, C. M., DITADI, A., LAMOTTE-MOHS, R., ZUNIGA-PFLUCKER, J. C. & KELLER, G. 2012. T lymphocyte potential marks the emergence of definitive hematopoietic progenitors in human pluripotent stem cell differentiation cultures. *Cell Rep*, 2, 1722-35.
- KHVOROVA, A., REYNOLDS, A. & JAYASENA, S. D. 2003. Functional siRNAs and miRNAs exhibit strand bias. *Cell*, 115, 209-16.

- KINNAIRD, T., STABILE, E., BURNETT, M. S., LEE, C. W., BARR, S., FUCHS, S. & EPSTEIN, S. E. 2004. Marrow-derived stromal cells express genes encoding a broad spectrum of arteriogenic cytokines and promote in vitro and in vivo arteriogenesis through paracrine mechanisms. *Circulation Research*, 94, 678-685.
- KIRANA, S., STRATMANN, B., PRANTE, C., PROHASKA, W., KOERPERICH, H., LAMMERS, D., GASTENS, M. H., QUAST, T., NEGREAN, M., STIRBAN, O. A., NANDREAN, S. G., GOTTING, C., MINARTZ, P., KLEESIEK, K. & TSCHOEPE, D. 2012. Autologous stem cell therapy in the treatment of limb ischaemia induced chronic tissue ulcers of diabetic foot patients. *Int J Clin Pract*, 66, 384-93.
- KISSA, K. & HERBOMEL, P. 2010. Blood stem cells emerge from aortic endothelium by a novel type of cell transition. *Nature*, 464, 112-5.
- KLATTENHOFF, C. A., SCHEUERMANN, J. C., SURFACE, L. E., BRADLEY, R. K., FIELDS, P. A., STEINHAUSER, M. L., DING, H., BUTTY, V. L., TORREY, L., HAAS, S., ABO, R., TABEBORDBAR, M., LEE, R. T., BURGE, C. B. & BOYER, L. A. 2013. Braveheart, a long noncoding RNA required for cardiovascular lineage commitment. *Cell*, 152, 570-83.
- KNIGHT, S. W. & BASS, B. L. 2001. A role for the RNase III enzyme DCR-1 in RNA interference and germ line development in *Caenorhabditis elegans*. *Science*, 293, 2269-71.
- KOH, W., STRATMAN, A. N., SACHARIDOU, A. & DAVIS, G. E. 2008. In vitro three dimensional collagen matrix models of endothelial lumen formation during vasculogenesis and angiogenesis. *Methods Enzymol*, 443, 83-101.
- KORTEN, S., BRUNSEN, C., POITZ, D. M., GROSSKLAUS, S., BRUX, M., SCHNITTLER, H. J., STRASSER, R. H., BORNSTEIN, S. R., MORAWIETZ, H. & GOETTSCHE, W. 2013. Impact of Hey2 and COUP-TFII on genes involved in arteriovenous differentiation in primary human arterial and venous endothelial cells. *Basic Res Cardiol*, 108, 362.
- KOZOMARA, A. & GRIFFITHS-JONES, S. 2014. miRBase: annotating high confidence microRNAs using deep sequencing data. *Nucleic Acids Research*, 42, D68-D73.
- KRIEGEL, A. J., BAKER, M. A., LIU, Y., LIU, P., COWLEY, A. W., JR. & LIANG, M. 2015. Endogenous MicroRNAs in Human Microvascular Endothelial Cells Regulate mRNAs Encoded by Hypertension-Related Genes. *Hypertension*.
- KUEHBACHER, A., URBICH, C., ZEIHNER, A. M. & DIMMELER, S. 2007. Role of Dicer and Drosha for endothelial microRNA expression and angiogenesis. *Circ Res*, 101, 59-68.
- KURIAN, L., AGUIRRE, A., SANCHO-MARTINEZ, I., BENNER, C., HISHIDA, T., NGUYEN, T. B., REDDY, P., NIVET, E., KRAUSE, M. N., NELLES, D. A., RODRIGUEZ ESTEBAN, C., CAMPISTOL, J. M., YEO, G. W. & IZPISUA BELMONTE, J. C. 2015. Identification of Novel Long Non-Coding RNAs Underlying Vertebrate Cardiovascular Development. *Circulation*.
- KWAK, P. B. & TOMARI, Y. 2012. The N domain of Argonaute drives duplex unwinding during RISC assembly. *Nat Struct Mol Biol*, 19, 145-51.
- LAGOS-QUINTANA, M., RAUHUT, R., YALCIN, A., MEYER, J., LENDECKEL, W. & TUSCHL, T. 2002. Identification of tissue-specific microRNAs from mouse. *Curr Biol*, 12, 735-9.
- LANCRIN, C., SROCZYNSKA, P., STEPHENSON, C., ALLEN, T., KOUSKOFF, V. & LACAUD, G. 2009. The haemangioblast generates haematopoietic cells through a haemogenic endothelium stage. *Nature*, 457, 892-5.
- LANDER, E. S., CONSORTIUM, I. H. G. S., LINTON, L. M., BIRREN, B., NUSBAUM, C., ZODY, M. C., BALDWIN, J., DEVON, K., DEWAR, K., DOYLE, M.,

- FITZHUGH, W., FUNKE, R., GAGE, D., HARRIS, K., HEAFORD, A., HOWLAND, J., KANN, L., LEHOCZKY, J., LEVINE, R., MCEWAN, P., MCKERNAN, K., MELDRIM, J., MESIROV, J. P., MIRANDA, C., MORRIS, W., NAYLOR, J., RAYMOND, C., ROSETTI, M., SANTOS, R., SHERIDAN, A., SOUGNEZ, C., STANGE-THOMANN, N., STOJANOVIC, N., SUBRAMANIAN, A., WYMAN, D., ROGERS, J., SULSTON, J., AINSCOUGH, R., BECK, S., BENTLEY, D., BURTON, J., CLEE, C., CARTER, N., COULSON, A., DEADMAN, R., DELOUKAS, P., DUNHAM, A., DUNHAM, I., DURBIN, R., FRENCH, L., GRAFHAM, D., GREGORY, S., HUBBARD, T., HUMPHRAY, S., HUNT, A., JONES, M., LLOYD, C., MCMURRAY, A., MATTHEWS, L., MERCER, S., MILNE, S., MULLIKIN, J. C., MUNGALL, A., PLUMB, R., ROSS, M., SHOWNKEEN, R., SIMS, S., WATERSTON, R. H., WILSON, R. K., HILLIER, L. W., MCPHERSON, J. D., MARRA, M. A., MARDIS, E. R., FULTON, L. A., CHINWALLA, A. T., PEPIN, K. H., GISH, W. R., CHISSOE, S. L., WENDL, M. C., DELEHAUNTY, K. D., MINER, T. L., DELEHAUNTY, A., KRAMER, J. B., COOK, L. L., FULTON, R. S., JOHNSON, D. L., MINX, P. J., CLIFTON, S. W., HAWKINS, T., BRANSCOMB, E., PREDKI, P., RICHARDSON, P., WENNING, S., SLEZAK, T., DOGGETT, N., CHENG, J. F., OLSEN, A., LUCAS, S., ELKIN, C., UBERBACHER, E., et al. 2001. Initial sequencing and analysis of the human genome. *Nature*, 409, 860-921.
- LANDTHALER, M., YALCIN, A. & TUSCHL, T. 2004. The human DiGeorge syndrome critical region gene 8 and its D. melanogaster homolog are required for miRNA biogenesis. *Curr Biol*, 14, 2162-7.
- LAURENT, L. C., CHEN, J., ULITSKY, I., MUELLER, F. J., LU, C., SHAMIR, R., FAN, J. B. & LORING, J. F. 2008. Comprehensive microRNA profiling reveals a unique human embryonic stem cell signature dominated by a single seed sequence. *Stem Cells*, 26, 1506-16.
- LEDERMAN, R. J., MENDELSON, F. O., ANDERSON, R. D., SAUCEDO, J. F., TENAGLIA, A. N., HERMILLER, J. B., HILLEGASS, W. B., ROCHA-SINGH, K., MOON, T. E., WHITEHOUSE, M. J., ANNEX, B. H. & INVESTIGATORS, T. 2002. Therapeutic angiogenesis with recombinant fibroblast growth factor-2 for intermittent claudication (the TRAFFIC study): a randomised trial. *Lancet*, 359, 2053-8.
- LEE, D. Y., DENG, Z., WANG, C. H. & YANG, B. B. 2007. MicroRNA-378 promotes cell survival, tumor growth, and angiogenesis by targeting SuFu and Fus-1 expression. *Proc Natl Acad Sci U S A*, 104, 20350-5.
- LEE, H. C., AN, S. G., LEE, H. W., PARK, J. S., CHA, K. S., HONG, T. J., PARK, J. H., LEE, S. Y., KIM, S. P., KIM, Y. D., CHUNG, S. W., BAE, Y. C., SHIN, Y. B., KIM, J. I. & JUNG, J. S. 2012. Safety and effect of adipose tissue-derived stem cell implantation in patients with critical limb ischemia: a pilot study. *Circ J*, 76, 1750-60.
- LEE, R. C. & AMBROS, V. 2001. An extensive class of small RNAs in *Caenorhabditis elegans*. *Science*, 294, 862-4.
- LEE, R. C., FEINBAUM, R. L. & AMBROS, V. 1993. The *C. elegans* heterochronic gene *lin-4* encodes small RNAs with antisense complementarity to *lin-14*. *Cell*, 75, 843-54.
- LEE, Y., AHN, C., HAN, J., CHOI, H., KIM, J., YIM, J., LEE, J., PROVOST, P., RADMARK, O., KIM, S. & KIM, V. N. 2003. The nuclear RNase III Drosha initiates microRNA processing. *Nature*, 425, 415-9.
- LEE, Y., HUR, I., PARK, S. Y., KIM, Y. K., SUH, M. R. & KIM, V. N. 2006. The role of PACT in the RNA silencing pathway. *EMBO J*, 25, 522-32.
- LEE, Y., JEON, K., LEE, J. T., KIM, S. & KIM, V. N. 2002. MicroRNA maturation: stepwise processing and subcellular localization. *EMBO J*, 21, 4663-70.

- LEE, Y., KIM, M., HAN, J., YEOM, K. H., LEE, S., BAEK, S. H. & KIM, V. N. 2004. MicroRNA genes are transcribed by RNA polymerase II. *EMBO J*, 23, 4051-60.
- LEHEMBRE, F., YILMAZ, M., WICKI, A., SCHOMBER, T., STRITTMATTER, K., ZIEGLER, D., KREN, A., WENT, P., DERKSEN, P. W. B., BERNIS, A., JONKERS, J. & CHRISTOFORI, G. 2008. NCAM-induced focal adhesion assembly: a functional switch upon loss of E-cadherin. *Embo Journal*, 27, 2603-2615.
- LENNARTSSON, J. & RONNSTRAND, L. 2012. Stem cell factor receptor/c-Kit: from basic science to clinical implications. *Physiol Rev*, 92, 1619-49.
- LEONHARDT, F., GRUNDMANN, S., BEHE, M., BLUHM, F., DUMONT, R. A., BRAUN, F., FANI, M., RIESNER, K., PRINZ, G., HECHINGER, A. K., GERLACH, U. V., DIERBACH, H., PENACK, O., SCHMITT-GRAFF, A., FINKE, J., WEBER, W. A. & ZEISER, R. 2013. Inflammatory neovascularization during graft-versus-host disease is regulated by alphav integrin and miR-100. *Blood*, 121, 3307-18.
- LEVENBERG, S., GOLUB, J. S., AMIT, M., ITSKOVITZ-ELDOR, J. & LANGER, R. 2002. Endothelial cells derived from human embryonic stem cells. *Proc Natl Acad Sci U S A*, 99, 4391-6.
- LEWIS, B. P., SHIH, I. H., JONES-RHOADES, M. W., BARTEL, D. P. & BURGE, C. B. 2003. Prediction of mammalian microRNA targets. *Cell*, 115, 787-98.
- LI, L., BAROJA, M. L., MAJUMDAR, A., CHADWICK, K., ROULEAU, A., GALLACHER, L., FERBER, I., LEBKOWSKI, J., MARTIN, T., MADRENAS, J. & BHATIA, M. 2004. Human embryonic stem cells possess immune-privileged properties. *Stem Cells*, 22, 448-56.
- LIAN, Q., ZHANG, Y., ZHANG, J., ZHANG, H. K., WU, X., ZHANG, Y., LAM, F. F., KANG, S., XIA, J. C., LAI, W. H., AU, K. W., CHOW, Y. Y., SIU, C. W., LEE, C. N. & TSE, H. F. 2010. Functional mesenchymal stem cells derived from human induced pluripotent stem cells attenuate limb ischemia in mice. *Circulation*, 121, 1113-23.
- LIANG, X., DING, Y., ZHANG, Y., TSE, H. F. & LIAN, Q. 2014. Paracrine mechanisms of mesenchymal stem cell-based therapy: current status and perspectives. *Cell Transplant*, 23, 1045-59.
- LIEW, A. & O'BRIEN, T. 2012. Therapeutic potential for mesenchymal stem cell transplantation in critical limb ischemia. *Stem Cell Res Ther*, 3, 28.
- LIN, N., CHANG, K. Y., LI, Z., GATES, K., RANA, Z. A., DANG, J., ZHANG, D., HAN, T., YANG, C. S., CUNNINGHAM, T. J., HEAD, S. R., DUESTER, G., DONG, P. D. & RANA, T. M. 2014. An evolutionarily conserved long noncoding RNA TUNA controls pluripotency and neural lineage commitment. *Mol Cell*, 53, 1005-19.
- LIN, S. L., CHANG, D. C., CHANG-LIN, S., LIN, C. H., WU, D. T., CHEN, D. T. & YING, S. Y. 2008. Mir-302 reprograms human skin cancer cells into a pluripotent ES-cell-like state. *RNA*, 14, 2115-24.
- LINDSLEY, R. C., GILL, J. G., KYBA, M., MURPHY, T. L. & MURPHY, K. M. 2006. Canonical Wnt signaling is required for development of embryonic stem cell-derived mesoderm. *Development*, 133, 3787-3796.
- LIU, C. G., CALIN, G. A., MELOON, B., GAMLIEL, N., SEVIGNANI, C., FERRACIN, M., DUMITRU, C. D., SHIMIZU, M., ZUPO, S., DONO, M., ALDER, H., BULLRICH, F., NEGRINI, M. & CROCE, C. M. 2004. An oligonucleotide microchip for genome-wide microRNA profiling in human and mouse tissues. *Proc Natl Acad Sci U S A*, 101, 9740-4.
- LIU, C. G., CALIN, G. A., VOLINIA, S. & CROCE, C. M. 2008. MicroRNA expression profiling using microarrays. *Nature Protocols*, 3, 563-578.

- LIU, F. P., DONG, J. J., SUN, S. J., GAO, W. Y., ZHANG, Z. W., ZHOU, X. J., YANG, L., ZHAO, J. Y., YAO, J. M., LIU, M. & LIAO, L. 2012. Autologous bone marrow stem cell transplantation in critical limb ischemia: a meta-analysis of randomized controlled trials. *Chin Med J (Engl)*, 125, 4296-300.
- LIU, P. T., WAKAMIYA, M., SHEA, M. J., ALBRECHT, U., BEHRINGER, R. R. & BRADLEY, A. 1999. Requirement for Wnt3 in vertebrate axis formation. *Nature Genetics*, 22, 361-365.
- LIU, Y., KANEDA, R., LEJA, T. W., SUBKHANKULOVA, T., TOLMACHOV, O., MINCHIOTTI, G., SCHWARTZ, R. J., BARAHONA, M. & SCHNEIDER, M. D. 2014. Hhex and Cer1 mediate the Sox17 pathway for cardiac mesoderm formation in embryonic stem cells. *Stem Cells*, 32, 1515-26.
- LIU, Y. M., XU, Y. Y., FANG, F., ZHANG, J. T., GUO, L. & WENG, Z. 2015. Therapeutic Efficacy of Stem Cell-based Therapy in Peripheral Arterial Disease: A Meta-Analysis. *Plos One*, 10.
- LIVAK, K. J. & SCHMITTGEN, T. D. 2001. Analysis of relative gene expression data using real-time quantitative PCR and the 2(-Delta Delta C(T)) Method. *Methods*, 25, 402-8.
- LOEWER, S., CABILI, M. N., GUTTMAN, M., LOH, Y. H., THOMAS, K., PARK, I. H., GARBER, M., CURRAN, M., ONDER, T., AGARWAL, S., MANOS, P. D., DATTA, S., LANDER, E. S., SCHLAEGER, T. M., DALEY, G. Q. & RINN, J. L. 2010. Large intergenic non-coding RNA-RoR modulates reprogramming of human induced pluripotent stem cells. *Nat Genet*, 42, 1113-7.
- LOPEZ-ROMERO, P. 2011. Pre-processing and differential expression analysis of Agilent microRNA arrays using the AgiMicroRna Bioconductor library. *BMC Genomics*, 12, 64.
- LOSORDO, D. W., KIBBE, M. R., MENDELSON, F., MARSTON, W., DRIVER, V. R., SHARAFUDDIN, M., TEODORESCU, V., WIECHMANN, B. N., THOMPSON, C., KRAISS, L., CARMAN, T., DOHAD, S., HUANG, P., JUNGE, C. E., STORY, K., WEISTROFFER, T., THORNE, T. M., MILLAY, M., RUNYON, J. P., SCHAINFELD, R. & AUTOLOGOUS, C. D. C. T. F. C. L. I. I. 2012. A randomized, controlled pilot study of autologous CD34+ cell therapy for critical limb ischemia. *Circ Cardiovasc Interv*, 5, 821-30.
- LOU, Y. L., GUO, F., LIU, F., GAO, F. L., ZHANG, P. Q., NIU, X., GUO, S. C., YIN, J. H., WANG, Y. & DENG, Z. F. 2012. miR-210 activates notch signaling pathway in angiogenesis induced by cerebral ischemia. *Mol Cell Biochem*.
- LU, D. B., CHEN, B., LIANG, Z. W., DENG, W. Q., JIANG, Y. Z., LI, S. F., XU, J., WU, Q. N., ZHANG, Z. H., XIE, B. & CHEN, S. H. 2011. Comparison of bone marrow mesenchymal stem cells with bone marrow-derived mononuclear cells for treatment of diabetic critical limb ischemia and foot ulcer: A double-blind, randomized, controlled trial. *Diabetes Research and Clinical Practice*, 92, 26-36.
- LU, J., GETZ, G., MISKA, E. A., ALVAREZ-SAAVEDRA, E., LAMB, J., PECK, D., SWEET-CORDERO, A., EBERT, B. L., MAK, R. H., FERRANDO, A. A., DOWNING, J. R., JACKS, T., HORVITZ, H. R. & GOLUB, T. R. 2005. MicroRNA expression profiles classify human cancers. *Nature*, 435, 834-8.
- LU, T. Y., LU, R. M., LIAO, M. Y., YU, J., CHUNG, C. H., KAO, C. F. & WU, H. C. 2010. Epithelial Cell Adhesion Molecule Regulation Is Associated with the Maintenance of the Undifferentiated Phenotype of Human Embryonic Stem Cells. *Journal of Biological Chemistry*, 285, 8719-8732.
- LUND, E., GUTTINGER, S., CALADO, A., DAHLBERG, J. E. & KUTAY, U. 2004. Nuclear export of microRNA precursors. *Science*, 303, 95-8.
- LUO, Z., WEN, G., WANG, G., PU, X., YE, S., XU, Q., WANG, W. & XIAO, Q. 2013. MicroRNA-200C and -150 Play an Important Role in Endothelial Cell



- Differentiation and Vasculogenesis by Targeting Transcription Repressor ZEB1. *Stem Cells*.
- LV, F. J., TUAN, R. S., CHEUNG, K. M. & LEUNG, V. Y. 2014. Concise review: the surface markers and identity of human mesenchymal stem cells. *Stem Cells*, 32, 1408-19.
- LYTLE, J. R., YARIO, T. A. & STEITZ, J. A. 2007. Target mRNAs are repressed as efficiently by microRNA-binding sites in the 5' UTR as in the 3' UTR. *Proceedings of the National Academy of Sciences of the United States of America*, 104, 9667-9672.
- MACRAE, I. J., MA, E., ZHOU, M., ROBINSON, C. V. & DOUDNA, J. A. 2008. In vitro reconstitution of the human RISC-loading complex. *Proc Natl Acad Sci U S A*, 105, 512-7.
- MADARIC, J., KLEPANEC, A., MISTRİK, M., ALTANER, C. & VULEV, I. 2013. Intra-arterial autologous bone marrow cell transplantation in a patient with upper-extremity critical limb ischemia. *Cardiovasc Intervent Radiol*, 36, 545-8.
- MAH, S. M., BUSKE, C., HUMPHRIES, R. K. & KUCHENBAUER, F. 2010. miRNA\*: a passenger stranded in RNA-induced silencing complex? *Crit Rev Eukaryot Gene Expr*, 20, 141-8.
- MALI, P., YANG, L., ESVELT, K. M., AACH, J., GUELL, M., DICARLO, J. E., NORVILLE, J. E. & CHURCH, G. M. 2013. RNA-guided human genome engineering via Cas9. *Science*, 339, 823-6.
- MARSEE, D. K., PINKUS, G. S. & YU, H. 2010. CD71 (transferrin receptor): an effective marker for erythroid precursors in bone marrow biopsy specimens. *Am J Clin Pathol*, 134, 429-35.
- MARSHALL, E. 1999. Gene therapy death prompts review of adenovirus vector. *Science*, 286, 2244-5.
- MARTIN, G. R. 1980. Teratocarcinomas and mammalian embryogenesis. *Science*, 209, 768-76.
- MARTIN, G. R. 1981. Isolation of a pluripotent cell line from early mouse embryos cultured in medium conditioned by teratocarcinoma stem cells. *Proc Natl Acad Sci U S A*, 78, 7634-8.
- MASAKI, I., YONEMITSU, Y., YAMASHITA, A., SATA, S., TANII, M., KOMORI, K., NAKAGAWA, K., HOU, X., NAGAI, Y., HASEGAWA, M., SUGIMACHI, K. & SUEISHI, K. 2002. Angiogenic gene therapy for experimental critical limb ischemia: acceleration of limb loss by overexpression of vascular endothelial growth factor 165 but not of fibroblast growth factor-2. *Circ Res*, 90, 966-73.
- MASKA, E. L., CSERJESI, P., HUA, L. L., GARSTKA, M. E., BRODY, H. M. & MORIKAWA, Y. 2010. A Tlx2-Cre mouse line uncovers essential roles for hand1 in extraembryonic and lateral mesoderm. *Genesis*, 48, 479-84.
- MATIN, M. M., WALSH, J. R., GOKHALE, P. J., DRAPER, J. S., BAHRAMI, A. R., MORTON, I., MOORE, H. D. & ANDREWS, P. W. 2004. Specific knockdown of Oct4 and beta2-microglobulin expression by RNA interference in human embryonic stem cells and embryonic carcinoma cells. *Stem Cells*, 22, 659-68.
- MATOBA, S., TATSUMI, T., MUROHARA, T., IMAIZUMI, T., KATSUDA, Y., ITO, M., SAITO, Y., UEMURA, S., SUZUKI, H., FUKUMOTO, S., YAMAMOTO, Y., ONODERA, R., TERAMUKAI, S., FUKUSHIMA, M. & MATSUBARA, H. 2008. Long-term clinical outcome after intramuscular implantation of bone marrow mononuclear cells (Therapeutic Angiogenesis by Cell Transplantation [TACT] trial) in patients with chronic limb ischemia. *Am Heart J*, 156, 1010-8.

- MATRANGA, C., TOMARI, Y., SHIN, C., BARTEL, D. P. & ZAMORE, P. D. 2005. Passenger-strand cleavage facilitates assembly of siRNA into Ago2-containing RNAi enzyme complexes. *Cell*, 123, 607-620.
- MATSA, E., RAJAMOHAN, D., DICK, E., YOUNG, L., MELLOR, I., STANIFORTH, A. & DENNING, C. 2011. Drug evaluation in cardiomyocytes derived from human induced pluripotent stem cells carrying a long QT syndrome type 2 mutation. *Eur Heart J*, 32, 952-62.
- MATSUI, J., WAKABAYASHI, T., ASADA, M., YOSHIMATSU, K. & OKADA, M. 2004. Stem cell factor/c-kit signaling promotes the survival, migration, and capillary tube formation of human umbilical vein endothelial cells. *J Biol Chem*, 279, 18600-7.
- MEDVINSKY, A. & DZIERZAK, E. 1996. Definitive hematopoiesis is autonomously initiated by the AGM region. *Cell*, 86, 897-906.
- MEDVINSKY, A., RYBTSOV, S. & TAOUDI, S. 2011. Embryonic origin of the adult hematopoietic system: advances and questions. *Development*, 138, 1017-31.
- MEISTER, G., LANDTHALER, M., PETERS, L., CHEN, P. Y., URLAUB, H., LUHRMANN, R. & TUSCHL, T. 2005. Identification of novel argonaute-associated proteins. *Curr Biol*, 15, 2149-55.
- MINENO, J., OKAMOTO, S., ANDO, T., SATO, M., CHONO, H., IZU, H., TAKAYAMA, M., ASADA, K., MIROCHNITCHENKO, O., INOUE, M. & KATO, I. 2006. The expression profile of microRNAs in mouse embryos. *Nucleic Acids Res*, 34, 1765-71.
- MITRA, R., LIN, C. C., EISCHEN, C. M., BANDYOPADHYAY, S. & ZHAO, Z. 2015. Concordant dysregulation of miR-5p and miR-3p arms of the same precursor microRNA may be a mechanism in inducing cell proliferation and tumorigenesis: a lung cancer study. *RNA*.
- MITSUI, K., TOKUZAWA, Y., ITOH, H., SEGAWA, K., MURAKAMI, M., TAKAHASHI, K., MARUYAMA, M., MAEDA, M. & YAMANAKA, S. 2003. The homeoprotein Nanog is required for maintenance of pluripotency in mouse epiblast and ES cells. *Cell*, 113, 631-642.
- MIYOSHI, N., ISHII, H., NAGANO, H., HARAGUCHI, N., DEWI, D. L., KANO, Y., NISHIKAWA, S., TANEMURA, M., MIMORI, K., TANAKA, F., SAITO, T., NISHIMURA, J., TAKEMASA, I., MIZUSHIMA, T., IKEDA, M., YAMAMOTO, H., SEKIMOTO, M., DOKI, Y. & MORI, M. 2011. Reprogramming of mouse and human cells to pluripotency using mature microRNAs. *Cell Stem Cell*, 8, 633-8.
- MORETTI, F., KAISER, C., ZDANOWICZ-SPECHT, A. & HENTZE, M. W. 2012. PABP and the poly(A) tail augment microRNA repression by facilitated miRISC binding. *Nat Struct Mol Biol*, 19, 603-8.
- MOURELATOS, Z., DOSTIE, J., PAUSHKIN, S., SHARMA, A., CHARROUX, B., ABEL, L., RAPPSILBER, J., MANN, M. & DREYFUSS, G. 2002. miRNPs: a novel class of ribonucleoproteins containing numerous microRNAs. *Genes Dev*, 16, 720-8.
- MULLER, S., RAULEFS, S., BRUNS, P., AFONSO-GRUNZ, F., PLOTNER, A., THERMANN, R., JAGER, C., SCHLITZER, A. M., KONG, B., REGEL, I., ROTH, W. K., ROTTER, B., HOFFMEIER, K., KAHL, G., KOCH, I., THEIS, F. J., KLEEFF, J., WINTER, P. & MICHALSKI, C. W. 2015. Next-generation sequencing reveals novel differentially regulated mRNAs, lncRNAs, miRNAs, sdrRNAs and a piRNA in pancreatic cancer. *Mol Cancer*, 14, 94.
- MULLER, W. A., RATTI, C. M., MCDONNELL, S. L. & COHN, Z. A. 1989. A human endothelial cell-restricted, externally disposed plasmalemmal protein enriched in intercellular junctions. *J Exp Med*, 170, 399-414.

- MUMMERY, C. L., ZHANG, J., NG, E. S., ELLIOTT, D. A., ELEFANTY, A. G. & KAMP, T. J. 2012. Differentiation of human embryonic stem cells and induced pluripotent stem cells to cardiomyocytes: a methods overview. *Circ Res*, 111, 344-58.
- MUONA, K., MAKINEN, K., HEDMAN, M., MANNINEN, H. & YLA-HERTTUALA, S. 2012. 10-year safety follow-up in patients with local VEGF gene transfer to ischemic lower limb. *Gene Ther*, 19, 392-5.
- MURAKAMI, M. & SIMONS, M. 2008. Fibroblast growth factor regulation of neovascularization. *Curr Opin Hematol*, 15, 215-20.
- MURCHISON, E. P., PARTRIDGE, J. F., TAM, O. H., CHELOUFI, S. & HANNON, G. J. 2005. Characterization of Dicer-deficient murine embryonic stem cells. *Proc Natl Acad Sci U S A*, 102, 12135-40.
- MURPHY, M. P., LAWSON, J. H., RAPP, B. M., DALRING, M. C., KLEIN, J., WILSON, M. G., HUTCHINS, G. D. & MARCH, K. L. 2011. Autologous bone marrow mononuclear cell therapy is safe and promotes amputation-free survival in patients with critical limb ischemia. *Journal of Vascular Surgery*, 53, 1565-1574.
- MUTIRANGURA, P., RUANGSETAKIT, C., WONGWANIT, C., CHINSAKCHAI, K., PORAT, Y., BELLELI, A. & CZEIGER, D. 2009. Enhancing limb salvage by non-mobilized peripheral blood angiogenic cell precursors therapy in patients with critical limb ischemia. *J Med Assoc Thai*, 92, 320-7.
- NAKAYA, Y. & SHENG, G. 2008. Epithelial to mesenchymal transition during gastrulation: an embryological view. *Dev Growth Differ*, 50, 755-66.
- NALDINI, L., BLOMER, U., GAGE, F. H., TRONO, D. & VERMA, I. M. 1996a. Efficient transfer, integration, and sustained long-term expression of the transgene in adult rat brains injected with a lentiviral vector. *Proc Natl Acad Sci U S A*, 93, 11382-8.
- NALDINI, L., BLOMER, U., GALLAY, P., ORY, D., MULLIGAN, R., GAGE, F. H., VERMA, I. M. & TRONO, D. 1996b. In vivo gene delivery and stable transduction of nondividing cells by a lentiviral vector. *Science*, 272, 263-7.
- NG, C. E., YOKOMIZO, T., YAMASHITA, N., CIROVIC, B., JIN, H., WEN, Z., ITO, Y. & OSATO, M. 2010a. A Runx1 intronic enhancer marks hemogenic endothelial cells and hematopoietic stem cells. *Stem Cells*, 28, 1869-81.
- NG, E. S., DAVIS, R. P., AZZOLA, L., STANLEY, E. G. & ELEFANTY, A. G. 2005. Forced aggregation of defined numbers of human embryonic stem cells into embryoid bodies fosters robust, reproducible hematopoietic differentiation. *Blood*, 106, 1601-1603.
- NG, V. Y., ANG, S. N., CHAN, J. X. & CHOO, A. B. H. 2010b. Characterization of Epithelial Cell Adhesion Molecule as a Surface Marker on Undifferentiated Human Embryonic Stem Cells. *Stem Cells*, 28, 29-35.
- NHSCHOICES. 2012. *Peripheral Arterial Disease - complications* [Online]. Available: <http://www.nhs.uk/Conditions/peripheralarterialdisease/Pages/Complications.aspx> [Accessed 10 Jun 2014].
- NICHOLS, J., ZEVIK, B., ANASTASSIADIS, K., NIWA, H., KLEWE-NEBENIUS, D., CHAMBERS, I., SCHOLER, H. & SMITH, A. 1998. Formation of pluripotent stem cells in the mammalian embryo depends on the POU transcription factor Oct4. *Cell*, 95, 379-91.
- NIH, N. H., LUNG AND BLOOD INSTITUTE. 2014. *What Is Atherosclerosis?* [Online]. <http://www.nhlbi.nih.gov/health/health-topics/topics/atherosclerosis>. Available: <http://www.nhlbi.nih.gov/health/health-topics/topics/atherosclerosis>.

- NISHIKAWA, S. I., NISHIKAWA, S., HIRASHIMA, M., MATSUYOSHI, N. & KODAMA, H. 1998. Progressive lineage analysis by cell sorting and culture identifies FLK1+VE-cadherin+ cells at a diverging point of endothelial and hemopoietic lineages. *Development*, 125, 1747-57.
- NIWA, H., MIYAZAKI, J. & SMITH, A. G. 2000. Quantitative expression of Oct-3/4 defines differentiation, dedifferentiation or self-renewal of ES cells. *Nat Genet*, 24, 372-6.
- NORGREN, L., HIATT, W. R., DORMANDY, J. A., NEHLER, M. R., HARRIS, K. A., FOWKES, F. G. & GROUP, T. I. W. 2007. Inter-Society Consensus for the Management of Peripheral Arterial Disease (TASC II). *J Vasc Surg*, 45 Suppl S, S5-67.
- NOURSE, M. B., HALPIN, D. E., SCATENA, M., MORTISEN, D. J., TULLOCH, N. L., HAUCH, K. D., TOROK-STORB, B., RATNER, B. D., PABON, L. & MURRY, C. E. 2010. VEGF induces differentiation of functional endothelium from human embryonic stem cells: implications for tissue engineering. *Arterioscler Thromb Vasc Biol*, 30, 80-9.
- O'DONNELL, K. A., WENTZEL, E. A., ZELLER, K. I., DANG, C. V. & MENDELL, J. T. 2005. c-Myc-regulated microRNAs modulate E2F1 expression. *Nature*, 435, 839-43.
- OGAWA, M., MATSUZAKI, Y., NISHIKAWA, S., HAYASHI, S., KUNISADA, T., SUDO, T., KINA, T., NAKAUCHI, H. & NISHIKAWA, S. 1991. Expression and function of c-kit in hemopoietic progenitor cells. *J Exp Med*, 174, 63-71.
- OKAMOTO, K., OKAZAWA, H., OKUDA, A., SAKAI, M., MURAMATSU, M. & HAMADA, H. 1990. A Novel Octamer Binding Transcription Factor Is Differentially Expressed in Mouse Embryonic-Cells. *Cell*, 60, 461-472.
- ONO, K., KUWABARA, Y. & HAN, J. 2011. MicroRNAs and cardiovascular diseases. *FEBS J*, 278, 1619-33.
- ORLOVA, V. V., DRABSCH, Y., FREUND, C., PETRUS-REURER, S., VAN DEN HIL, F. E., MUENTHAISON, S., DIJKE, P. T. & MUMMERY, C. L. 2014a. Functionality of endothelial cells and pericytes from human pluripotent stem cells demonstrated in cultured vascular plexus and zebrafish xenografts. *Arterioscler Thromb Vasc Biol*, 34, 177-86.
- ORLOVA, V. V., DRABSCH, Y., TEN DIJKE, P. & MUMMERY, C. L. 2014b. Assessment of functional competence of endothelial cells from human pluripotent stem cells in zebrafish embryos. *Methods Mol Biol*, 1213, 107-19.
- ORLOVA, V. V., VAN DEN HIL, F. E., PETRUS-REURER, S., DRABSCH, Y., TEN DIJKE, P. & MUMMERY, C. L. 2014c. Generation, expansion and functional analysis of endothelial cells and pericytes derived from human pluripotent stem cells. *Nat Protoc*, 9, 1514-31.
- OROM, U. A. & LUND, A. H. 2007. Isolation of microRNA targets using biotinylated synthetic microRNAs. *Methods*, 43, 162-165.
- OROM, U. A., NIELSEN, F. C. & LUND, A. H. 2008. MicroRNA-10a binds the 5' UTR of ribosomal protein mRNAs and enhances their translation. *Molecular Cell*, 30, 460-471.
- OSAFUNE, K., CARON, L., BOROWIAK, M., MARTINEZ, R. J., FITZ-GERALD, C. S., SATO, Y., COWAN, C. A., CHIEN, K. R. & MELTON, D. A. 2008. Marked differences in differentiation propensity among human embryonic stem cell lines. *Nat Biotechnol*, 26, 313-5.
- PARK, J. E., HEO, I., TIAN, Y., SIMANSHU, D. K., CHANG, H., JEE, D., PATEL, D. J. & KIM, V. N. 2011. Dicer recognizes the 5' end of RNA for efficient and accurate processing. *Nature*, 475, 201-5.

- PATRICK, D. M., ZHANG, C. C., TAO, Y., YAO, H., QI, X., SCHWARTZ, R. J., JUNSHEN HUANG, L. & OLSON, E. N. 2010. Defective erythroid differentiation in miR-451 mutant mice mediated by 14-3-3zeta. *Genes Dev*, 24, 1614-9.
- PATSCH, C., CHALLET-MEYLAN, L., THOMA, E. C., URICH, E., HECKEL, T., O'SULLIVAN, J. F., GRAINGER, S. J., KAPP, F. G., SUN, L., CHRISTENSEN, K., XIA, Y., FLORIDO, M. H., HE, W., PAN, W., PRUMMER, M., WARREN, C. R., JAKOB-ROETNE, R., CERTA, U., JAGASIA, R., FRESKGDARD, P. O., ADATTO, I., KLING, D., HUANG, P., ZON, L. I., CHAIKOF, E. L., GERSZTEN, R. E., GRAF, M., IACONE, R. & COWAN, C. A. 2015. Generation of vascular endothelial and smooth muscle cells from human pluripotent stem cells. *Nat Cell Biol*, 17, 994-1003.
- PEICHEV, M., NAIYER, A. J., PEREIRA, D., ZHU, Z., LANE, W. J., WILLIAMS, M., OZ, M. C., HICKLIN, D. J., WITTE, L., MOORE, M. A. & RAFII, S. 2000. Expression of VEGFR-2 and AC133 by circulating human CD34(+) cells identifies a population of functional endothelial precursors. *Blood*, 95, 952-8.
- PERIN, E. C., SILVA, G., GAHREMANPOUR, A., CANALES, J., ZHENG, Y., CABREIRA-HANSEN, M. G., MENDELSON, F., CHRONOS, N., HALEY, R., WILLERSON, J. T. & ANNEX, B. H. 2011. A randomized, controlled study of autologous therapy with bone marrow-derived aldehyde dehydrogenase bright cells in patients with critical limb ischemia. *Catheter Cardiovasc Interv*, 78, 1060-7.
- PESCE, M., WANG, X., WOLGEMUTH, D. J. & SCHOLER, H. 1998. Differential expression of the Oct-4 transcription factor during mouse germ cell differentiation. *Mech Dev*, 71, 89-98.
- PIAO, X., ZHANG, X., WU, L. & BELASCO, J. G. 2010. CCR4-NOT deadenylates mRNA associated with RNA-induced silencing complexes in human cells. *Mol Cell Biol*, 30, 1486-94.
- POLISENO, L., SALMENA, L., ZHANG, J., CARVER, B., HAVEMAN, W. J. & PANDOLFI, P. P. 2010. A coding-independent function of gene and pseudogene mRNAs regulates tumour biology. *Nature*, 465, 1033-8.
- POLISENO, L., TUCCOLI, A., MARIANI, L., EVANGELISTA, M., CITTI, L., WOODS, K., MERCATANTI, A., HAMMOND, S. & RAINALDI, G. 2006. MicroRNAs modulate the angiogenic properties of HUVECs. *Blood*, 108, 3068-71.
- POWELL, R. J. 2012. Update on clinical trials evaluating the effect of biologic therapy in patients with critical limb ischemia. *J Vasc Surg*, 56, 264-6.
- POWELL, R. J., GOODNEY, P., MENDELSON, F. O., MOEN, E. K., ANNEX, B. H. & INVESTIGATORS, H. G. F. T. 2010. Safety and efficacy of patient specific intramuscular injection of HGF plasmid gene therapy on limb perfusion and wound healing in patients with ischemic lower extremity ulceration: results of the HGF-0205 trial. *J Vasc Surg*, 52, 1525-30.
- PROCHAZKA, V., GUMULEC, J., JALUVKA, F., SALOUNOVA, D., JONSZTA, T., CZERNY, D., KRAJCA, J., URBANEC, R., KLEMENT, P., MARTINEK, J. & KLEMENT, G. L. 2010. Cell therapy, a new standard in management of chronic critical limb ischemia and foot ulcer. *Cell Transplant*, 19, 1413-24.
- QIU, C., OLIVIER, E. N., VELHO, M. & BOUHASSIRA, E. E. 2008. Globin switches in yolk sac-like primitive and fetal-like definitive red blood cells produced from human embryonic stem cells. *Blood*, 111, 2400-8.
- QUICK-CLEVELAND, J., JACOB, J. P., WEITZ, S. H., SHOFFNER, G., SENTURIA, R. & GUO, F. 2014. The DGCR8 RNA-binding heme domain recognizes primary microRNAs by clamping the hairpin. *Cell Rep*, 7, 1994-2005.

- RAJAGOPALAN, S., TRACHTENBERG, J., MOHLER, E., OLIN, J., MCBRIDE, S., PAK, R., RASMUSSEN, H. & CRYSTAL, R. 2002. Phase I study of direct administration of a replication deficient adenovirus vector containing the vascular endothelial growth factor cDNA (CI-1023) to patients with claudication. *Am J Cardiol*, 90, 512-6.
- RAMALINGAM, P., PALANICHAMY, J. K., SINGH, A., DAS, P., BHAGAT, M., KASSAB, M. A., SINHA, S. & CHATTOPADHYAY, P. 2014. Biogenesis of intronic miRNAs located in clusters by independent transcription and alternative splicing. *RNA*, 20, 76-87.
- RAN, F. A., HSU, P. D., WRIGHT, J., AGARWALA, V., SCOTT, D. A. & ZHANG, F. 2013. Genome engineering using the CRISPR-Cas9 system. *Nature Protocols*, 8, 2281-2308.
- RAVAL, Z. & LOSORDO, D. W. 2013. Cell therapy of peripheral arterial disease: from experimental findings to clinical trials. *Circ Res*, 112, 1288-302.
- ROBINSON, H. C. & BAKER, A. H. 2012. How do microRNAs affect vascular smooth muscle cell biology? *Current Opinion in Lipidology*, 23, 405-411.
- RODDA, D. J., CHEW, J. L., LIM, L. H., LOH, Y. H., WANG, B., NG, H. H. & ROBSON, P. 2005. Transcriptional regulation of nanog by OCT4 and SOX2. *J Biol Chem*, 280, 24731-7.
- RODRIGUEZ, R. T., VELKEY, J. M., LUTZKO, C., SEERKE, R., KOHN, D. B., O'SHEA, K. S. & FIRPO, M. T. 2007. Manipulation of OCT4 levels in human embryonic stem cells results in induction of differential cell types. *Exp Biol Med (Maywood)*, 232, 1368-80.
- RONG, Z. L., ZHU, S. Y., XU, Y. & FU, X. M. 2014. Homologous recombination in human embryonic stem cells using CRISPR/Cas9 nickase and a long DNA donor template. *Protein & Cell*, 5, 258-260.
- ROSA, A. & BRIVANLOU, A. H. 2011. A regulatory circuitry comprised of miR-302 and the transcription factors OCT4 and NR2F2 regulates human embryonic stem cell differentiation. *EMBO J*, 30, 237-48.
- ROSNER, M. H., VIGANO, M. A., OZATO, K., TIMMONS, P. M., POIRIER, F., RIGBY, P. W. & STAUDT, L. M. 1990. A POU-domain transcription factor in early stem cells and germ cells of the mammalian embryo. *Nature*, 345, 686-92.
- ROTTIERS, V. & NAAR, A. M. 2012. MicroRNAs in metabolism and metabolic disorders. *Nat Rev Mol Cell Biol*, 13, 239-50.
- RUFAlHAH, A. J., HUANG, N. F., JAME, S., LEE, J. C., NGUYEN, H. N., BYERS, B., DE, A., OKOGBAA, J., ROLLINS, M., REIJO-PERA, R., GAMBHIR, S. S. & COOKE, J. P. 2011. Endothelial cells derived from human iPSCs increase capillary density and improve perfusion in a mouse model of peripheral arterial disease. *Arterioscler Thromb Vasc Biol*, 31, e72-9.
- SAFLEY, D. M., HOUSE, J. A., LASTER, S. B., DANIEL, W. C., SPERTUS, J. A. & MARSO, S. P. 2007. Quantifying improvement in symptoms, functioning, and quality of life after peripheral endovascular revascularization. *Circulation*, 115, 569-75.
- SCHWARTZ, S. D., REGILLO, C. D., LAM, B. L., ELIOTT, D., ROSENFELD, P. J., GREGORI, N. Z., HUBSCHMAN, J. P., DAVIS, J. L., HEILWELL, G., SPIRN, M., MAGUIRE, J., GAY, R., BATEMAN, J., OSTRICK, R. M., MORRIS, D., VINCENT, M., ANGLADE, E., DEL PRIORE, L. V. & LANZA, R. 2015. Human embryonic stem cell-derived retinal pigment epithelium in patients with age-related macular degeneration and Stargardt's macular dystrophy: follow-up of two open-label phase 1/2 studies. *Lancet*, 385, 509-16.
- SCOTT, E., LOYA, K., MOUNTFORD, J., MILLIGAN, G. & BAKER, A. H. 2013. MicroRNA regulation of endothelial homeostasis and commitment-

- implications for vascular regeneration strategies using stem cell therapies. *Free Radical Biology and Medicine*, 64, 52-60.
- SESSA, R., SEANO, G., DI BLASIO, L., GAGLIARDI, P. A., ISELLA, C., MEDICO, E., COTELLI, F., BUSSOLINO, F. & PRIMO, L. 2012. The miR-126 regulates angiopoietin-1 signaling and vessel maturation by targeting p85beta. *Biochim Biophys Acta*, 1823, 1925-35.
- SHAN, S. W., FANG, L., SHATSEVA, T., RUTNAM, Z. J., YANG, X., DU, W., LU, W. Y., XUAN, J. W., DENG, Z. & YANG, B. B. 2013. Mature miR-17-5p and passenger miR-17-3p induce hepatocellular carcinoma by targeting PTEN, GalNT7 and vimentin in different signal pathways. *J Cell Sci*, 126, 1517-30.
- SHEIK MOHAMED, J., GAUGHWIN, P. M., LIM, B., ROBSON, P. & LIPOVICH, L. 2010. Conserved long noncoding RNAs transcriptionally regulated by Oct4 and Nanog modulate pluripotency in mouse embryonic stem cells. *RNA*, 16, 324-37.
- SHEN, B., ZHANG, W. S., ZHANG, J., ZHOU, J. K., WANG, J. Y., CHEN, L., WANG, L., HODGKINS, A., IYER, V., HUANG, X. X. & SKARNES, W. C. 2014. Efficient genome modification by CRISPR-Cas9 nickase with minimal off-target effects. *Nature Methods*, 11, 399-+.
- SHEN, X., FANG, J., LV, X., PEI, Z., WANG, Y., JIANG, S. & DING, K. 2011. Heparin impairs angiogenesis through inhibition of microRNA-10b. *J Biol Chem*, 286, 26616-27.
- SHI, Q., RAFII, S., WU, M. H., WIJELATH, E. S., YU, C., ISHIDA, A., FUJITA, Y., KOTHARI, S., MOHLE, R., SAUVAGE, L. R., MOORE, M. A., STORB, R. F. & HAMMOND, W. P. 1998. Evidence for circulating bone marrow-derived endothelial cells. *Blood*, 92, 362-7.
- SIMONS, M., ALITALO, K., ANNEX, B. H., AUGUSTIN, H. G., BEAM, C., BERK, B. C., BYZOVA, T., CARMELIET, P., CHILIAN, W., COOKE, J. P., DAVIS, G. E., EICHMANN, A., IRUELA-ARISPE, M. L., KESHET, E., SINUSAS, A. J., RUHRBERG, C., WOO, Y. J., DIMMELER, S., AMERICAN HEART ASSOCIATION COUNCIL ON BASIC CARDIOVASCULAR, S., COUNCIL ON CARDIOVASCULAR, S. & ANESTHESIA 2015. State-of-the-Art Methods for Evaluation of Angiogenesis and Tissue Vascularization: A Scientific Statement From the American Heart Association. *Circ Res*, 116, e99-132.
- SKORA, J., PUPKA, A., JANCZAK, D., BARC, P., DAWISKIBA, T., KORTA, K., BACZYNSKA, D., MASTALERZ-MIGAS, A. & GARCAREK, J. 2015. Combined autologous bone marrow mononuclear cell and gene therapy as the last resort for patients with critical limb ischemia. *Archives of Medical Science*, 11, 325-331.
- SLOVUT, D. P. & SULLIVAN, T. M. 2008. Critical limb ischemia: medical and surgical management. *Vasc Med*, 13, 281-91.
- SMITH, J. R., MAGUIRE, S., DAVIS, L. A., ALEXANDER, M., YANG, F. T., CHANDRAN, S., FFRENCH-CONSTANT, C. & PEDERSEN, R. A. 2008. Robust, persistent transgene expression in human embryonic stem cells is achieved with AAVS1-targeted integration. *Stem Cells*, 26, 496-504.
- SMITH, K. N., SINGH, A. M. & DALTON, S. 2010. Myc represses primitive endoderm differentiation in pluripotent stem cells. *Cell Stem Cell*, 7, 343-54.
- STADLER, B., IVANOVSKA, I., MEHTA, K., SONG, S., NELSON, A., TAN, Y., MATHIEU, J., DARBY, C., BLAU, C. A., WARE, C., PETERS, G., MILLER, D. G., SHEN, L., CLEARY, M. A. & RUOHOLA-BAKER, H. 2010. Characterization of microRNAs involved in embryonic stem cell states. *Stem Cells Dev*, 19, 935-50.

- SUAREZ, Y., FERNANDEZ-HERNANDO, C., POBER, J. S. & SESSA, W. C. 2007. Dicer dependent microRNAs regulate gene expression and functions in human endothelial cells. *Circ Res*, 100, 1164-73.
- SUAREZ, Y., FERNANDEZ-HERNANDO, C., YU, J., GERBER, S. A., HARRISON, K. D., POBER, J. S., IRUELA-ARISPE, M. L., MERKENSCHLAGER, M. & SESSA, W. C. 2008. Dicer-dependent endothelial microRNAs are necessary for postnatal angiogenesis. *Proc Natl Acad Sci U S A*, 105, 14082-7.
- SUBHERWAL, S., PATEL, M. R., KOBER, L., PETERSON, E. D., BHATT, D. L., GISLASON, G. H., OLSEN, A. M. S., JONES, W. S., TORP-PEDERSEN, C. & FOSBOL, E. L. 2015. Peripheral artery disease is a coronary heart disease risk equivalent among both men and women: results from a nationwide study. *European Journal of Preventive Cardiology*, 22, 317-325.
- SUH, M. R., LEE, Y., KIM, J. Y., KIM, S. K., MOON, S. H., LEE, J. Y., CHA, K. Y., CHUNG, H. M., YOON, H. S., MOON, S. Y., KIM, V. N. & KIM, K. S. 2004. Human embryonic stem cells express a unique set of microRNAs. *Dev Biol*, 270, 488-98.
- SUI, X., KRANTZ, S. B. & ZHAO, Z. J. 2000. Stem cell factor and erythropoietin inhibit apoptosis of human erythroid progenitor cells through different signalling pathways. *Br J Haematol*, 110, 63-70.
- SUN, C. Y., SHE, X. M., QIN, Y., CHU, Z. B., CHEN, L., AI, L. S., ZHANG, L. & HU, Y. 2013. miR-15a and miR-16 affect the angiogenesis of multiple myeloma by targeting VEGF. *Carcinogenesis*, 34, 426-35.
- SUN, X., ICLI, B., WARA, A. K., BELKIN, N., HE, S., KOBZIK, L., HUNNINGHAKE, G. M., VERA, M. P., BLACKWELL, T. S., BARON, R. M. & FEINBERG, M. W. 2012. MicroRNA-181b regulates NF-kappaB-mediated vascular inflammation. *J Clin Invest*, 122, 1973-90.
- TADA, S., ERA, T., FURUSAWA, C., SAKURAI, H., NISHIKAWA, S., KINOSHITA, M., NAKAO, K., CHIBA, T. & NISHIKAWA, S. 2005. Characterization of mesendoderm: a diverging point of the definitive endoderm and mesoderm in embryonic stem cell differentiation culture. *Development*, 132, 4363-74.
- TAKAHASHI, K., TANABE, K., OHNUKI, M., NARITA, M., ICHISAKA, T., TOMODA, K. & YAMANAKA, S. 2007. Induction of pluripotent stem cells from adult human fibroblasts by defined factors. *Cell*, 131, 861-72.
- TAKAHASHI, K. & YAMANAKA, S. 2006. Induction of pluripotent stem cells from mouse embryonic and adult fibroblast cultures by defined factors. *Cell*, 126, 663-76.
- TAKATA, H., KATO, M., DENDA, K. & KITAMURA, N. 2000. A hrs binding protein having a Src homology 3 domain is involved in intracellular degradation of growth factors and their receptors. *Genes Cells*, 5, 57-69.
- TAOUDI, S. & MEDVINSKY, A. 2007. Functional identification of the hematopoietic stem cell niche in the ventral domain of the embryonic dorsal aorta. *Proc Natl Acad Sci U S A*, 104, 9399-403.
- TAVIAN, M., COULOMBEL, L., LUTON, D., CLEMENTE, H. S., DIETERLEN-LIEVRE, F. & PEAULT, B. 1996. Aorta-associated CD34+ hematopoietic cells in the early human embryo. *Blood*, 87, 67-72.
- TAY, F. C., TAN, W. K., GOH, S. L., RAMACHANDRA, C. J. A., LAU, C. H., ZHU, H. B., CHEN, C., DU, S. H., PHANG, R. Z., SHAHBAZI, M., FAN, W. M. & WANG, S. 2013. Targeted transgene insertion into the AAVS1 locus driven by baculoviral vector-mediated zinc finger nuclease expression in human-induced pluripotent stem cells. *Journal of Gene Medicine*, 15, 384-395.
- TAYLOR, C. J., BOLTON, E. M., POCOCK, S., SHARPLES, L. D., PEDERSEN, R. A. & BRADLEY, J. A. 2005. Banking on human embryonic stem cells: estimating



- the number of donor cell lines needed for HLA matching. *Lancet*, 366, 2019-25.
- TERAA, M., SPRENGERS, R. W., SCHUTGENS, R. E., SLAPER-CORTENBACH, I. C., VAN DER GRAAF, Y., ALGRA, A., VAN DER TWEEL, I., DOEVENDANS, P. A., MALI, W. P., MOLL, F. L. & VERHAAR, M. C. 2015. Effect of Repetitive Intra-Arterial Infusion of Bone Marrow Mononuclear Cells in Patients With No-Option Limb Ischemia: The Randomized, Double-Blind, Placebo-Controlled Rejuvenating Endothelial Progenitor Cells via Transcutaneous Intra-arterial Supplementation (JUVENTAS) Trial. *Circulation*, 131, 851-60.
- THOMSON, J. A., ITSKOVITZ-ELDOR, J., SHAPIRO, S. S., WAKNITZ, M. A., SWIERGIEL, J. J., MARSHALL, V. S. & JONES, J. M. 1998. Embryonic stem cell lines derived from human blastocysts. *Science*, 282, 1145-7.
- THOMSON, J. A., KALISHMAN, J., GOLOS, T. G., DURNING, M., HARRIS, C. P., BECKER, R. A. & HEARN, J. P. 1995. Isolation of a primate embryonic stem cell line. *Proc Natl Acad Sci U S A*, 92, 7844-8.
- THOMSON, J. M., PARKER, J., PEROU, C. M. & HAMMOND, S. M. 2004. A custom microarray platform for analysis of microRNA gene expression. *Nat Methods*, 1, 47-53.
- THOMSON, L. F., RUEDI, J. M., GLASS, A., MOLDENHAUER, G., MOLLER, P., LOW, M. G., KLEMENS, M. R., MASSAIA, M. & LUCAS, A. H. 1990. Production and characterization of monoclonal antibodies to the glycosyl phosphatidylinositol-anchored lymphocyte differentiation antigen ecto-5'-nucleotidase (CD73). *Tissue Antigens*, 35, 9-19.
- THUKKANI, A. K. & KINLAY, S. 2015. Endovascular Intervention for Peripheral Artery Disease. *Circulation Research*, 116, 1599-1613.
- TREGUER, K., HEINRICH, E. M., OHTANI, K., BONAUER, A. & DIMMELER, S. 2012. Role of the MicroRNA-17-92 Cluster in the Endothelial Differentiation of Stem Cells. *J Vasc Res*, 49, 447-60.
- TZUR, G., LEVY, A., MEIRI, E., BARAD, O., SPECTOR, Y., BENTWICH, Z., MIZRAHI, L., KATZENELLENBOGEN, M., BEN-SHUSHAN, E., REUBINOFF, B. E. & GALUN, E. 2008. MicroRNA expression patterns and function in endodermal differentiation of human embryonic stem cells. *PLoS One*, 3, e3726.
- UEKI, K., FRUMAN, D. A., YBALLE, C. M., FASSHAUER, M., KLEIN, J., ASANO, T., CANTLEY, L. C. & KAHN, C. R. 2003. Positive and negative roles of p85 alpha and p85 beta regulatory subunits of phosphoinositide 3-kinase in insulin signaling. *J Biol Chem*, 278, 48453-66.
- UNGRIN, M. D., JOSHI, C., NICA, A., BAUWENS, C. & ZANDSTRA, P. W. 2008. Reproducible, ultra high-throughput formation of multicellular organization from single cell suspension-derived human embryonic stem cell aggregates. *PLoS One*, 3, e1565.
- URBICH, C. & DIMMELER, S. 2004. Endothelial progenitor cells: characterization and role in vascular biology. *Circ Res*, 95, 343-53.
- USMAN, M. A., NAKASA, T., SHOJI, T., KATO, T., KAWANISHI, Y., HAMANISHI, M., KAMEI, N. & OCHI, M. 2015. The effect of administration of double stranded MicroRNA-210 on acceleration of Achilles tendon healing in a rat model. *J Orthop Sci*, 20, 538-46.
- VAN GRUNSVEN, L. A., MICHIELS, C., VAN DE PUTTE, T., NELLES, L., WUYTENS, G., VERSCHUEREN, K. & HUYLEBROECK, D. 2003. Interaction between Smad-interacting protein-1 and the corepressor C-terminal binding protein is dispensable for transcriptional repression of E-cadherin. *J Biol Chem*, 278, 26135-45.

- VENDITTI, A., BATTAGLIA, A., DEL POETA, G., BUCCISANO, F., MAURILLO, L., TAMBURINI, A., DEL MORO, B., EPICENO, A. M., MARTIRADONNA, M., CARAVITA, T., SANTINELLI, S., ADORNO, G., PICARDI, A., ZINNO, F., LANTI, A., BRUNO, A., SUPPO, G., FRANCHI, A., FRANCONI, G. & AMADORI, S. 1999. Enumeration of CD34+ hematopoietic progenitor cells for clinical transplantation: comparison of three different methods. *Bone Marrow Transplant*, 24, 1019-27.
- VILLA-DIAZ, L. G., GARCIA-PEREZ, J. L. & KREBSBACH, P. H. 2010. Enhanced transfection efficiency of human embryonic stem cells by the incorporation of DNA liposomes in extracellular matrix. *Stem Cells Dev*, 19, 1949-57.
- VODYANIK, M. A., THOMSON, J. A. & SLUKVIN, II 2006. Leukosialin (CD43) defines hematopoietic progenitors in human embryonic stem cell differentiation cultures. *Blood*, 108, 2095-105.
- WAKIOKA, T., SASAKI, A., KATO, R., SHOUDA, T., MATSUMOTO, A., MIYOSHI, K., TSUNEOKA, M., KOMIYA, S., BARON, R. & YOSHIMURA, A. 2001. Sprouty is a Sprouty-related suppressor of Ras signalling. *Nature*, 412, 647-51.
- WALSH, J. & ANDREWS, P. W. 2003. Expression of Wnt and Notch pathway genes in a pluripotent human embryonic carcinoma cell line and embryonic stem cells. *Apmis*, 111, 197-211.
- WANG, F. Z., WEBER, F., CROCE, C., LIU, C. G., LIAO, X. & PELLETT, P. E. 2008a. Human cytomegalovirus infection alters the expression of cellular microRNA species that affect its replication. *J Virol*, 82, 9065-74.
- WANG, H., LI, X., GAO, S., SUN, X. & FANG, H. 2015. Transdifferentiation via transcription factors or microRNAs: Current status and perspective. *Differentiation*.
- WANG, H. U., CHEN, Z. F. & ANDERSON, D. J. 1998. Molecular distinction and angiogenic interaction between embryonic arteries and veins revealed by ephrin-B2 and its receptor Eph-B4. *Cell*, 93, 741-753.
- WANG, P., RODRIGUEZ, R. T., WANG, J., GHODASARA, A. & KIM, S. K. 2011. Targeting SOX17 in human embryonic stem cells creates unique strategies for isolating and analyzing developing endoderm. *Cell Stem Cell*, 8, 335-46.
- WANG, Q., LI, Y. C., WANG, J., KONG, J., QI, Y., QUIGG, R. J. & LI, X. 2008b. miR-17-92 cluster accelerates adipocyte differentiation by negatively regulating tumor-suppressor Rb2/p130. *Proc Natl Acad Sci U S A*, 105, 2889-94.
- WANG, S., AURORA, A. B., JOHNSON, B. A., QI, X., MCANALLY, J., HILL, J. A., RICHARDSON, J. A., BASSEL-DUBY, R. & OLSON, E. N. 2008c. The endothelial-specific microRNA miR-126 governs vascular integrity and angiogenesis. *Dev Cell*, 15, 261-71.
- WANG, Y., XU, Z., JIANG, J., XU, C., KANG, J., XIAO, L., WU, M., XIONG, J., GUO, X. & LIU, H. 2013. Endogenous miRNA sponge lincRNA-RoR regulates Oct4, Nanog, and Sox2 in human embryonic stem cell self-renewal. *Dev Cell*, 25, 69-80.
- WANG, Z., GERSTEIN, M. & SNYDER, M. 2009. RNA-Seq: a revolutionary tool for transcriptomics. *Nature Reviews Genetics*, 10, 57-63.
- WANG, Z. Z., AU, P., CHEN, T., SHAO, Y., DAHERON, L. M., BAI, H., ARZIGIAN, M., FUKUMURA, D., JAIN, R. K. & SCADDEN, D. T. 2007. Endothelial cells derived from human embryonic stem cells form durable blood vessels in vivo. *Nat Biotechnol*, 25, 317-8.
- WATANABE, K., UENO, M., KAMIYA, D., NISHIYAMA, A., MATSUMURA, M., WATAYA, T., TAKAHASHI, J. B., NISHIKAWA, S., NISHIKAWA, S.,

- MUGURUMA, K. & SASAI, Y. 2007. A ROCK inhibitor permits survival of dissociated human embryonic stem cells. *Nat Biotechnol*, 25, 681-6.
- WEI, Y., LI, L., WANG, D., ZHANG, C. Y. & ZEN, K. 2014. Importin 8 regulates the transport of mature microRNAs into the cell nucleus. *J Biol Chem*, 289, 10270-5.
- WEINMANN, L., HOCK, J., IVACEVIC, T., OHRT, T., MUTZE, J., SCHWILLE, P., KREMMER, E., BENES, V., URLAUB, H. & MEISTER, G. 2009. Importin 8 Is a Gene Silencing Factor that Targets Argonaute Proteins to Distinct mRNAs. *Cell*, 136, 496-507.
- WHITE, M. P., RUFAlHAH, A. J., LIU, L., GHEBREMARIAM, Y. T., IVEY, K. N., COOKE, J. P. & SRIVASTAVA, D. 2013. Limited gene expression variation in human embryonic stem cell and induced pluripotent stem cell-derived endothelial cells. *Stem Cells*, 31, 92-103.
- WIEDENHEFT, B., STERNBERG, S. H. & DOUDNA, J. A. 2012. RNA-guided genetic silencing systems in bacteria and archaea. *Nature*, 482, 331-8.
- WIENHOLDS, E., KLOOSTERMAN, W. P., MISKA, E., ALVAREZ-SAAVEDRA, E., BEREZIKOV, E., DE BRUIJN, E., HORVITZ, H. R., KAUPPINEN, S. & PLASTERK, R. H. 2005. MicroRNA expression in zebrafish embryonic development. *Science*, 309, 310-1.
- WIENHOLDS, E., KOUDIJS, M. J., VAN EEDEN, F. J. M., CUPPEN, E. & PLASTERK, R. H. A. 2003. The microRNA-producing enzyme Dicer1 is essential for zebrafish development. *Nature Genetics*, 35, 217-218.
- WIGHTMAN, B., HA, I. & RUVKUN, G. 1993. Posttranscriptional regulation of the heterochronic gene *lin-14* by *lin-4* mediates temporal pattern formation in *C. elegans*. *Cell*, 75, 855-62.
- WILLIAMS, R. L., HILTON, D. J., PEASE, S., WILLSON, T. A., STEWART, C. L., GEARING, D. P., WAGNER, E. F., METCALF, D., NICOLA, N. A. & GOUGH, N. M. 1988. Myeloid leukaemia inhibitory factor maintains the developmental potential of embryonic stem cells. *Nature*, 336, 684-7.
- WILSON, K. D., HU, S., VENKATASUBRAHMANYAM, S., FU, J. D., SUN, N., ABILEZ, O. J., BAUGH, J. J., JIA, F., GHOSH, Z., LI, R. A., BUTTE, A. J. & WU, J. C. 2010. Dynamic microRNA expression programs during cardiac differentiation of human embryonic stem cells: role for miR-499. *Circ Cardiovasc Genet*, 3, 426-35.
- WILSON, K. D., VENKATASUBRAHMANYAM, S., JIA, F., SUN, N., BUTTE, A. J. & WU, J. C. 2009. MicroRNA profiling of human-induced pluripotent stem cells. *Stem Cells Dev*, 18, 749-58.
- WINNIER, G., BLESSING, M., LABOSKY, P. A. & HOGAN, B. L. M. 1995. Bone Morphogenetic Protein-4 Is Required for Mesoderm Formation and Patterning in the Mouse. *Genes & Development*, 9, 2105-2116.
- WU, H., XU, J., PANG, Z. P., GE, W., KIM, K. J., BLANCHI, B., CHEN, C., SUDHOF, T. C. & SUN, Y. E. 2007. Integrative genomic and functional analyses reveal neuronal subtype differentiation bias in human embryonic stem cell lines. *Proc Natl Acad Sci U S A*, 104, 13821-6.
- WU, L., FAN, J. & BELASCO, J. G. 2006. MicroRNAs direct rapid deadenylation of mRNA. *Proc Natl Acad Sci U S A*, 103, 4034-9.
- WURDINGER, T., TANNOUS, B. A., SAYDAM, O., SKOG, J., GRAU, S., SOUTSCHEK, J., WEISSLEDER, R., BREAKFIELD, X. O. & KRICHEVSKY, A. M. 2008. miR-296 regulates growth factor receptor overexpression in angiogenic endothelial cells. *Cancer Cell*, 14, 382-93.
- XU, C., INOKUMA, M. S., DENHAM, J., GOLDS, K., KUNDU, P., GOLD, J. D. & CARPENTER, M. K. 2001. Feeder-free growth of undifferentiated human embryonic stem cells. *Nat Biotechnol*, 19, 971-4.

- XU, C., ROSLER, E., JIANG, J., LEBKOWSKI, J. S., GOLD, J. D., O'SULLIVAN, C., DELAVAN-BOORSMA, K., MOK, M., BRONSTEIN, A. & CARPENTER, M. K. 2005. Basic fibroblast growth factor supports undifferentiated human embryonic stem cell growth without conditioned medium. *Stem Cells*, 23, 315-23.
- XU, N., PAPAGIANNAKOPOULOS, T., PAN, G., THOMSON, J. A. & KOSIK, K. S. 2009. MicroRNA-145 regulates OCT4, SOX2, and KLF4 and represses pluripotency in human embryonic stem cells. *Cell*, 137, 647-58.
- XUE, G., RESTUCCIA, D. F., LAN, Q., HYNX, D., DIRNHOFER, S., HESS, D., RUEGG, C. & HEMMINGS, B. A. 2012. Akt/PKB-mediated phosphorylation of Twist1 promotes tumor metastasis via mediating cross-talk between PI3K/Akt and TGF-beta signaling axes. *Cancer Discov*, 2, 248-59.
- XUE, G., YAN, H. L., ZHANG, Y., HAO, L. Q., ZHU, X. T., MEI, Q. & SUN, S. H. 2015. c-Myc-mediated repression of miR-15-16 in hypoxia is induced by increased HIF-2alpha and promotes tumor angiogenesis and metastasis by upregulating FGF2. *Oncogene*, 34, 1393-406.
- YANG, J. S., MAURIN, T., ROBINE, N., RASMUSSEN, K. D., JEFFREY, K. L., CHANDWANI, R., PAPAPETROU, E. P., SADELAIN, M., O'CARROLL, D. & LAI, E. C. 2010. Conserved vertebrate mir-451 provides a platform for Dicer-independent, Ago2-mediated microRNA biogenesis. *Proc Natl Acad Sci U S A*, 107, 15163-8.
- YANG, J. S., PHILLIPS, M. D., BETEL, D., MU, P., VENTURA, A., SIEPEL, A. C., CHEN, K. C. & LAI, E. C. 2011. Widespread regulatory activity of vertebrate microRNA\* species. *RNA*, 17, 312-26.
- YANG, X. L., DU, W. W., LI, H. R., LIU, F. Q., KHORSHIDI, A., RUTNAM, Z. J. & YANG, B. B. 2013. Both mature miR-17-5p and passenger strand miR-17-3p target TIMP3 and induce prostate tumor growth and invasion. *Nucleic Acids Research*, 41, 9688-9704.
- YI, R., QIN, Y., MACARA, I. G. & CULLEN, B. R. 2003. Exportin-5 mediates the nuclear export of pre-microRNAs and short hairpin RNAs. *Genes & Development*, 17, 3011-3016.
- YI, T., ARTHANARI, H., AKABAYOV, B., SONG, H., PAPADOPOULOS, E., QI, H. H., JEDRYCHOWSKI, M., GUTTLER, T., GUO, C., LUNA, R. E., GYGI, S. P., HUANG, S. A. & WAGNER, G. 2015. eIF1A augments Ago2-mediated Dicer-independent miRNA biogenesis and RNA interference. *Nat Commun*, 6, 7194.
- YONEMITSU, Y., MATSUMOTO, T., ITOH, H., OKAZAKI, J., UCHIYAMA, M., YOSHIDA, K., ONIMARU, M., ONOHARA, T., INOBUCHI, H., KYURAGI, R., SHIMOKAWA, M., BAN, H., TANAKA, M., INOUE, M., SHU, T., HASEGAWA, M., NAKANISHI, Y. & MAEHARA, Y. 2013. DVC1-0101 to treat peripheral arterial disease: a Phase I/IIa open-label dose-escalation clinical trial. *Mol Ther*, 21, 707-14.
- YOO, A. S., SUN, A. X., LI, L., SHCHEGLOVITOV, A., PORTMANN, T., LI, Y., LEE-MESSER, C., DOLMETSCH, R. E., TSIEN, R. W. & CRABTREE, G. R. 2011a. MicroRNA-mediated conversion of human fibroblasts to neurons. *Nature*, 476, 228-31.
- YOO, J. K., JUNG, H. Y., KIM, C. H., SON, W. S. & KIM, J. K. 2013. miR-7641 modulates the expression of CXCL1 during endothelial differentiation derived from human embryonic stem cells. *Arch Pharm Res*, 36, 353-8.
- YOO, J. K., KIM, J., CHOI, S. J., KIM, C. H., LEE, D. R., CHUNG, H. M. & KIM, J. K. 2011b. The hsa-miR-5739 modulates the endoglin network in endothelial cells derived from human embryonic stem cells. *Biochem Biophys Res Commun*, 415, 258-62.

- YOO, J. K., KIM, J., CHOI, S. J., NOH, H. M., KWON, Y. D., YOO, H., YI, H. S., CHUNG, H. M. & KIM, J. K. 2012. Discovery and characterization of novel microRNAs during endothelial differentiation of human embryonic stem cells. *Stem Cells Dev*, 21, 2049-57.
- YOON, J. H., ABDELMOHSEN, K., SRIKANTAN, S., YANG, X., MARTINDALE, J. L., DE, S., HUARTE, M., ZHAN, M., BECKER, K. G. & GOROSPE, M. 2012. LincRNA-p21 suppresses target mRNA translation. *Mol Cell*, 47, 648-55.
- YOU, L. R., LIN, F. J., LEE, C. T., DEMAYO, F. J., TSAI, M. J. & TSAI, S. Y. 2005. Suppression of Notch signalling by the COUP-TFII transcription factor regulates vein identity. *Nature*, 435, 98-104.
- ZEKRI, L., HUNTZINGER, E., HEIMSTADT, S. & IZAURRALDE, E. 2009. The Silencing Domain of GW182 Interacts with PABPC1 To Promote Translational Repression and Degradation of MicroRNA Targets and Is Required for Target Release. *Molecular and Cellular Biology*, 29, 6220-6231.
- ZENG, L., HE, X., WANG, Y., TANG, Y., ZHENG, C., CAI, H., LIU, J., WANG, Y., FU, Y. & YANG, G. Y. 2014. MicroRNA-210 overexpression induces angiogenesis and neurogenesis in the normal adult mouse brain. *Gene Ther*, 21, 37-43.
- ZENG, Y. & CULLEN, B. R. 2005. Efficient processing of primary microRNA hairpins by Drosha requires flanking nonstructured RNA sequences. *J Biol Chem*, 280, 27595-603.
- ZHANG, P., LI, J., TAN, Z., WANG, C., LIU, T., CHEN, L., YONG, J., JIANG, W., SUN, X., DU, L., DING, M. & DENG, H. 2008. Short-term BMP-4 treatment initiates mesoderm induction in human embryonic stem cells. *Blood*, 111, 1933-41.
- ZHANG, Z., HONG, Y., XIANG, D., ZHU, P., WU, E., LI, W., MOSENSON, J. & WU, W. S. 2015. MicroRNA-302/367 cluster governs hESC self-renewal by dually regulating cell cycle and apoptosis pathways. *Stem Cell Reports*, 4, 645-57.
- ZHAO, Y., SAMAL, E. & SRIVASTAVA, D. 2005. Serum response factor regulates a muscle-specific microRNA that targets Hand2 during cardiogenesis. *Nature*, 436, 214-220.
- ZOVEIN, A. C., HOFMANN, J. J., LYNCH, M., FRENCH, W. J., TURLO, K. A., YANG, Y., BECKER, M. S., ZANETTA, L., DEJANA, E., GASSON, J. C., TALLQUIST, M. D. & IRUELA-ARISPE, M. L. 2008. Fate tracing reveals the endothelial origin of hematopoietic stem cells. *Cell Stem Cell*, 3, 625-36.